HISTONE DEACETYLASE (HDAC) INHIBITORS AND FBXL20 IN BREAST CANCER

Thesis submitted by

Alexandra Vassiliki Stavropoulou

To

The University of London

For the degree of

Doctor of Philosophy

Imperial College University, London
Department of Oncology
Division of SORA
Hammersmith Hospital
Du Cane Road
London W12 0NN

BIBL. LONDON UNIV.

DECLARATION OF ORIGINALITY

Unless otherwise stated in the text, this thesis is the result of my own work.

ABSTRACT

Research performed over the last decade has highlighted the role of HDAC inhibitors (HDACi) as modulators of transcriptional activity and as a potential new class of therapeutic agents against many types of malignacies including breast cancer. These drugs inhibit histone deacetylases, leading to derepression of transcription of various genes that are important for cell cycle arrest and cell death. Trichostatin A (TSA) is one of the best established HDAC inhibitors and has been shown to exhibit potent differentiating and anti-proliferative properties. My data demonstrated that treatment of the MCF-7 breast cancer cell line with TSA causes G_2/M phase cell cycle arrest. I characterised the novel F-Box protein called FBXL20 and identified it as an important target of TSA. This protein is part of a novel E3 ligase complex as it binds Skp1, CUL-1 and ROC-1 and forms a classical SCF complex that is responsible for ubiquitination and targeting proteins for degradation by the 26S proteasome. I further studied the differences between FBXL20 in human cells and its isoform in rat cells. My data showed that FBXL20 is localised in the cytoplasm concentrated around the nucleus and plays a role in the TSA-induced effects in MCF-7 cells, through regulating the pro-apoptotic protein Bim. Silencing *FBXL20* abolished the G_2/M arrest caused by TSA treatment. Although FBXL20 is a similar protein to Skp2 they are regulated by different proteins and exert different functions. These findings provide novel data to demonstrate that known and novel HDACi induce G2/M arrest followed by cell death and that this arrest is dependent on the novel FBXL20 protein in breast cancer cells. Using these newly defined properties of HDACi, I screened a panel of potential HDACi and identified at least one to be more potent than SAHA, which is currently used in the clinical setting, and showed that it is able to inhibit proliferation, cause cell cycle arrest and cell death of breast cancer cells.

PUBLICATIONS

- Takano M, Lu Z, Goto T, Fusi L, Higham J, Francis J, Withey A, Hardt J, Cloke B, Stavropoulou AV, Ishihara O, Lam EW, Unterman TG, Brosens JJ, Kim JJ. (2007) Transcriptional cross talk between the forkhead transcription factor forkhead box O1A and the progesterone receptor coordinates cell cycle regulation and differentiation in human endometrial stromal cells, *Mol Endocrinol, 21(10):2334-49*

- Stavropoulou AV*, Alao JP*, Lam EW, Coombes RC (2006) Role of glycogen synthase kinase 3 beta (GSK3beta) in mediating the cytotoxic effects of the histone deacetylase inhibitor trichostatin A (TSA) in MCF-7 breast cancer cells, *Mol Cancer., 3;5:40.*

  * contributed equally

- Leyton J, Alao JP, Da Costa M, Stavropoulou AV, Latigo JR, Perumal M, Pillai R, He Q, Atadja P, Lam EW, Workman P, Vigushin DM, Aboagye EO (2006) In vivo biological activity of the histone deacetylase inhibitor LAQ824 is detectable with 3'-deoxy-3'-[18F]fluorothymidine positron emission tomography, *Cancer Res., 1;66(15):7621-9.*

- Alao JP, Stavropoulou AV, Lam EW, Coombes RC, Vigushin DM (2006) Histone deacetylase inhibitor, trichostatin A induces ubiquitin-dependent cyclin D1 degradation in MCF-7 breast cancer cells, *Molecular Cancer., 20;5:8*

- Alao JP, Gamble SC, Stavropoulou AV, Pomeranz KM, Lam EW, Coombes RC, Vigushin DM.(2006)The cyclin D1 proto-oncogene is sequestered in the cytoplasm of mammalian cancer cell lines, *Molecular Cancer, 17;5:7*

- Alao JP, Lam EW, Ali S, Buluwela L, Bordogna W, Lockey P, Varshochi R, Stavropoulou AV, Coombes RC, Vigushin DM. (2004) Histone deacetylase inhibitor trichostatin A represses estrogen receptor alpha-dependent transcription and promotes proteasomal degradation of cyclin D1 in human breast carcinoma cell lines, *Clinical Cancer Research 10(23):8094-104.*

ACKNOWLEDGEMENTS

I would like to express my gratitude to my supervisor Prof. Eric Lam for his guidance and support that were the driving force for the completion of my PhD.

I must also acknowledge Prof. Charles Coombes for being my supervisor.

I would also like to thank Dr. John Patrick Alao for his help during the time we were working together.

I am especially grateful to Dr. David Vigushin for getting me started on the journey and for hid advice and support during the time we were working together.

I am very much grateful to my colleagues Barrie Peck for his help with using the fluorimeter and Dr. Giolanta Kogianni for helping me with the fluorescence microscope.

I would also like to thank Dr. Ka Kei Ho and Dr. Richard Francis for their valuable help in the lab and during the writing of the thesis.

Many thanks go to my good friends Smaragda and Ursula for their support and help during the writing of the thesis and for being there every step of the way.

Team members, past and present, colleagues from other labs, by now good friends, thank you for all the help and advice, but more importantly, for making the Cyclotron Building a happier place to be in.

I would like to thank my parents, my brother Costas and my sister Natasa for their support that was crucial in bringing this journey to an end.

Many thanks go to "The Mandeville trust" for the financial assistance they offered me.

TABLE OF CONTENTS

ABSTRACT 3

PUBLICATIONS 4

ACKNOWLEDGEMENTS 5

TABLE OF CONTENTS 6

LIST OF FIGURES 9

ABBREVIATIONS 11

CHAPTER I
INTRODUCTION 14

I.1 Cancer 15

I.2 Breast cancer 16

Breast cancer treatment 19

I.3 Cell cycle 23

Cell cycle regulation 23

I.4 Cell death and senescence 26

I.5 Bim 30

I.6 Epigenetics 32

I.7 HDACs 36

HDAC inhibitors (HDACi) 41

Clinical potential of HDAC inhibitors 46

I.8 Trichostatin A 49

I.9 F-Box proteins 53

I.10 Ubiquitin-dependent proteasomal degradation pathway 54

E3 ligases 57

I.11 The Forkhead box M1 transcription factor (FoxM1) 64

Project aims 66

CHAPTER II
MATERIALS AND METHODS 67

Data bank analyses 68

Cell culture 68

Chemicals 69
PCR 69
Production of recombinant vector 71
Transfection of plasmid DNA 76
Western Blotting or SDS-PAGE 77
Antibodies 79
Immunoprecipitation 80
Sulphorhodamine B (SRB) assay 80
Rapid amplification of 5' and 3' cDNA ends PCR (RACE-PCR) 81
RNA interference 82
RNA extraction 84
Real-time Quantitative PCR (RT-QPCR) 85
Propidium Iodide (PI) staining and FACS (cell cycle) analysis 87
Sub-cellular fractionation 88
Fluorescence microscopy 89
Immunofluorescent cytochemical staining 89
HDAC flurimetric assay 90
Statistical tests 91

CHAPTER III
CHARACTERISATION OF FBXL20 92

III.1 BACKGROUND AND OBJECTIVES 93
III.2 RESULTS 94
Analysis of the *FBXL20* DNA sequence 94
FBXL20 is expressed in many cancer cell types 100
FBXL20 is expressed at higher levels in growth arrested 100
FBXL20 is localised in the cytoplasm of MCF-7 cells concentrated mainly around the nucleus. 103
FBXL20 part of a SCF complex 106
Silencing *FBXL20* induces Skp2 expression 108
FoxM1 does not regulate the transcription of *FBXL20* 111
III.3 DISCUSSION 113

CHAPTER IV
TSA AND FBXL20 117

IV.1 BACKGROUND AND OBJECTIVES 118

IV.2 RESULTS 119

TSA causes a G_2/M arrest at high concentrations 119

TSA induces the expression of FBXL20 mRNA 121

TSA does not affect the localisation of FBXL20 123

Silencing *FBXL20* increases the proliferation and abrogates the G_2/M arrest induced by TSA 125

Silencing FBXL20 abrogates the G_2/M arrest induced by SAHA and SBHA. 129

Silencing HDAC2 leads to upregulation of FBXL20 mRNA levels 132

FBXL20 regulates Bim protein levels 134

IV.3 DISCUSSION 142

CHAPTER V
ANALYSIS OF NOVEL HDAC INHIBITORS 149

V.1 BACKGROUND AND OBJECTIVES 150

V.2 RESULTS 152

Compounds 201, 202, 203, 204, 205, 207, 208, 209, 211, 212, 213, 216, 217, 218, 219 do not have a significant effect on MCF-7 cell proliferation 152

Compounds 214, 215, 220, 221 inhibit proliferation of MCF-7 cells 157

Compounds 214, 215, 220, 221 induce expression of Ac-H3, Bim and $p21^{Cip1}$ 160

Compound 220 inhibits HDACs 164

V.3 DISCUSSION 166

CHAPTER VI
DISCUSSION 171

REFERENCES 182

LIST OF FIGURES

Figure 1.1 New cancer cases in 2005 16

Figure 1.2 Cell cycle profile and regulators..... 26

Figure 1.3 Apoptosis versus necrosis 30

Figure1.4 Effects of HDACi 41

Figure 1.5 HDACi inhibit HDACs that target the chromatin or other proteins directly, leading to cell cycle arrest, apoptosis etc..... 43

Figure 1.6 Chemical structure of trichostatin A 50

Figure 1.7 Ubiquitin-dependent proteasome degradation pathway..... 56

Figure 3.1 FBXL20 gene organisation 96

Figure 3.2 Comparison of FBXL20 protein sequence between species and with Skp2 97

Figure 3.3 FBXL20 consists of 12 LRR repeats..... 98

Figure 3.4 Sequence of the Rat FBL2..... 99

Figure 3.5 FBXL20 is expressed in a variety of cancer cell lines 101

Figure 3.6 FBXL20 is expressed at higher levels in growth arrested cells compared to proliferating cells..... 102

Figure 3.7 FBXL20 is localised in the cytoplasm of MCF-7 cells, concentrated mainly around the nuclei..... 104

Figure 3.8 FBXL20 is part of a SCF complex..... 107

Figure 3.9 Knockdown of FBXL20 induces the protein expression of Skp2..... 109

Figure 3.10 Silencing Skp2 does not significantly induce the expression of FBXL20 mRNA..... 110

Figure 3.11 FoxM1 regulates Skp2 but not FBXL20 mRNA levels 112

Figure 4.1 TSA causes G_2/M arrest. ..... .120

Figure 4.2 TSA directly induces the expression of FBXL20 mRNA in MCF-7 cells.122

Figure 4.3 TSA does not alter the localisation of FBXL20 in MCF-7 cells..... 124

Figure 4.4 siRNA-mediated *FBXL20* knockdown causes a non-significant change in the cell cycle progression of MCF-7 cells ..... .126

Figure 4.5 Overexpression of Flag-FBXL20 increases the cell death induced by TSA..... **127**

Figure 4.6 Specific knockdown of FBXL20 attenuates the cytotoxic effect of TSA on MCF-7 cells **128**

Figure 4.7 Effect of SBHA and SAHA on the proliferation of MCF-7 cells **130**

Figure 4.8 siRNA-mediated FBXL20 knockdown attenuates the cytotoxic effect of SBHA and SAHA on the cell cycle progression of MCF-7 cells..... **131**

Figure 4.9 Specific knockdown of HDAC2 induces expression of FBXL20 mRNA. **133**

Figure 4.10 TSA induces the expression of Bim mRNA and protein.Error! Bookmark not defined.

Figure 4.11 Silencing FBXL20 leads to downregulation of Bim protein levels. **137**

Figure 4.12 Silencing FBXL20 does not affect Bim mRNA levels **138**

Figure 4.13 Overexpression of FBXL20 leads to upregulation of Bim protein levels. **139**

Figure 4.14 FBXL20 binds Bim. **140**

Figure 4.15 siRNA-mediated FBXL20 and Bim knockdown on the cell cycle progression of MCF-7 cells treated with TSA..... **141**

Figure 4.16 Schematic to represent the role of FBXL20 and in the TSA-induced cell cycle arrest and apoptosis..... **147**

Figure 5.1 Representation of the chemical structures of the compounds synthesized in this study..... **153**

Figure 5.2 Compounds do not affect the proliferation of MCF-7 cells. **156**

Figure 5.3 The effect of 214,215,220,221 on MCF-7 cell proliferation..... **158**

Figure 5.4 IC_{50} of 214, 215, 220 and 221..... **159**

Figure 5.5 214, 215, 220, 221 induce expression of acetylated H3 (Ac-H3), Bim_{EL} and $p21^{Cip1}$ **161**

Figure 5.6 Cell cycle profiles of cells treated with 214, 215, 220, 221 ..... **162**

Figure 5.7 Compound 220 inhibits HDACs. **165**

Figure 6.1 Schematic to represent the role of FBXL20 and Skp2 in TSA-induced cell cycle arrest and apoptosis..... **175**

ABBREVIATIONS

Abbreviations used in Materials and Methods

APS	Ammonium persulphate
BSA	Bovine Serum Albumin
ddH_20	double distilled water
DNA	Deoxyribonucleic acid
DTT	Dithiothreitol
ECL	Enhanced Chemi-Luminescence
EDTA	ethylenediamine tetra-acetic acid
FACS	Fluorescence activated cell sorting (Flow cytometry)
FCS	Foetal calf serum
HRP	Horseradish peroxidase
LB broth	Luria-Bertrani broth
NaF	sodium fluoride
Na_3VO_4	sodium orthovanadate
NSC siRNA	Non-specific siRNA
PAGE	Polyacryalmide gel electrophoresis
PBS	Phosphate buffered saline
PCR	Polymerase chain reaction
RPM	Revolutions per minute
RT	Room temperature
SDS	Sodium dodecyl sulphate
TBS	Tris buffered saline
TBS-T	Tris buffered saline-Tween
TEMED	N,N,N,'N-tetramethylethylenediamine
TCA	Trichloroacetic acid
Tris	Tris (hydroxymethyl) aminomethane
Tween 20	polyoxyethylene-sorbitan monolaurate

Abbreviations used for units of measurement

h	hour
μ	micro
M	Molar
min	minutes
n	nano
s	seconds
v/v	volume:volume ratio
w/v	weight:volume ratio

Abbreviations of molecules, drugs etc.

APC/C	anaphase promoting complex
CBP	CREB binding protein
CDK	cyclin dependent kinase
CENPA	centromere protein A
CDKI	cyclin-dependent kinase inhibitor
Cks1	cdc kinase subunit 1
CMF	cyclophosphamide, methotrexate and fluorouracil
CUL-1	cullin-1
DLC	dynein light chain
EGFR	epidermal growth factor receptor
ERα	oestrogen receptor α
ERβ	oestrogen receptor β
ERK	extracellular signal-regulated kinase (MAPK)
FBXL20	F-Box leucine rich repeat 20
HAT	histone acetyltransferase
HCV	hepatitis C virus
HDAC	histone deacetylase
HDACi	histone deacetylase inhibitor (s)
HDLP	histone deacetylase- like protein
Id1	Inhibitor of differentiation 1
JNK	c-Jun NH2-terminal kinase

LRR	leucine-rich repeats
NES	nuclear export signal
NLS	nuclear localisation signal
PP1	protein phosphatase 1
Rb	retinoblastoma protein
ROS	reactive oxygen species
SAHA	suberoylanilide hydroxamic acid
SD	standard deviation
SBHA	suberic bishydroxamate
Skp1	S-phase kinase associated protein 1
Skp2	S-phase kinase associated protein 2
STAT3	signal transducer and activator of transcription 3
SUMO	small ubiquitin-like modifier
TSA	trichostatin A

CHAPTER I

INTRODUCTION

I.1 Cancer

Cancer is one of the leading causes of death in the UK. Every year, around 280,000 people are diagnosed with cancer. Overall, it is estimated that more than one in three people will develop some forms of cancer during their lifetime and about 25% will die from it. From 1993 to 2002, the incidence rate for cancer has increased by 3% in females and has not change a lot in males.

Although cancer affects people of all ages, the risk increases with age. It most commonly occurs in people aged 65 or over, while a small percent occurs in children. In UK, the risk of cancer diagnosed in a child less than 15 years of age is 1 in 500 individuals. Between 1975 and 1990 childhood cancers increased 19%. Of course, apart from people, cancer may affect animals and plants (Statistics obtained from the Cancer Research UK Website). There are more than 200 different types of cancer, but the most common ones are breast, prostate, lung and colorectal cancer (Fig.1.1).

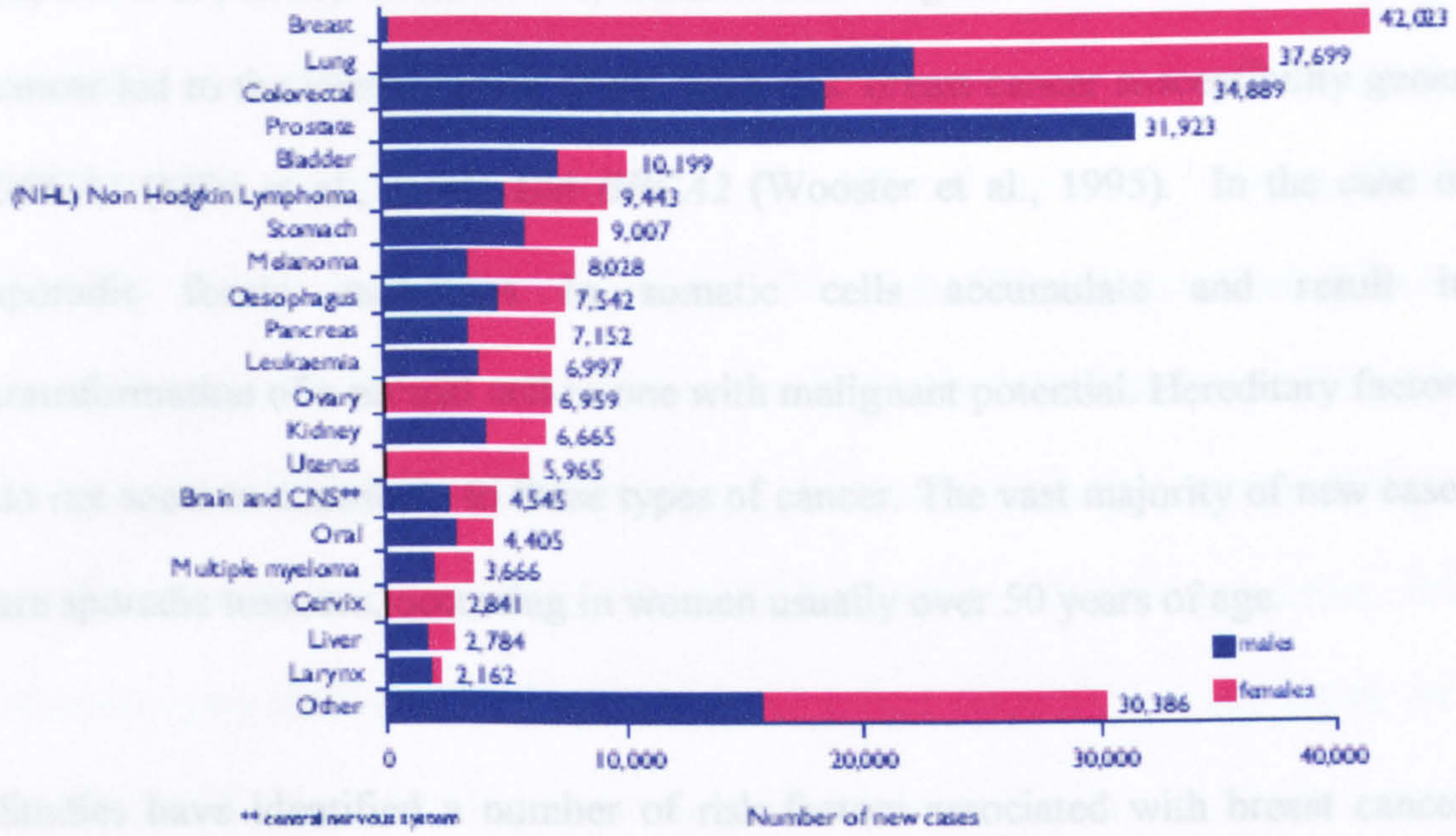


Figure 1.1 New cancer cases in 2005 (Cancer Research UK website)

There are many references that attempt to define cancer but perhaps the simplest one is 'a group of diseases characterized by uncontrolled growth and spread of abnormal cells'. If the spread is not controlled, it can result in death (American Cancer Society website).

I.2 Breast cancer

Breast cancer is one of the most commonly diagnosed malignancies and one of the main causes of cancer death among women (Ferlay, 2007). Breast cancer can occur in sporadic and hereditary forms. In hereditary forms, a mutation in a specific gene predisposes individuals to cancer. However, unlike typical genetic diseases in which mutations in a single gene is responsible for the disease, it is rather the mutations in several genes that lead to carcinogenesis. Hereditary breast cancer is suspected when there is a strong family history of breast cancer. Hereditary breast cancer accounts for as much as 10% of breast cancer cases

(Lynch et al., 2008). In the 1990s, research into the genetic basis of familial breast cancer led to the identification of the 'high risk' breast cancer susceptibility genes *BRCA1* (Miki et al., 1994) and *BRCA2* (Wooster et al., 1995). In the case of sporadic forms, mutations in somatic cells accumulate and result in transformation of a normal cell to one with malignant potential. Hereditary factors do not seem to contribute to these types of cancer. The vast majority of new cases are sporadic tumours, occurring in women usually over 50 years of age.

Studies have identified a number of risk factors associated with breast cancer. They include family history, individual history of breast diseases, age, late menopause, early menarche, excess ionizing radiation exposure, not having children and hormone replacement therapy.

Breast cancer is heterogeneous in its clinical, genetic, and biochemical profile. Overall there are more than 50,000 deaths from breast cancer every year in the United States alone. Breast cancer accounts for 30% of all female cancers diagnosed in the UK and in 2002 41,000 women were diagnosed with breast cancer. A woman's risk of developing breast cancer by the age of 65 is less than 6% but the overall lifetime risk is 11% (Statistics obtained from the Cancer Research UK Website). Due to screening, improved treatment options and the intensive research over the past decades, there has been a 15% fall in mortality from breast cancer in the UK.

The most important regulators of breast cancer growth are the oestrogens, the most abundant of which is 17β estradiol. Oestrogens are steroid hormones

synthesised mainly by the ovary and placenta. They act through the nuclear oestrogen receptors ERα and ERβ that control gene expression by recruiting transcriptional co-factors (Paruthiyil et al., 2004; Sommer and Fuqua, 2001). Although these receptors are very similar, they exert different functions. ERα has a proliferative role and changes in its expression and activity can cause deregulation of various cellular processes, eventually leading to cancer (Sommer and Fuqua, 2001). In contrast to ERα, ERβ has anti-proliferative properties. Both receptors play distinct roles in breast development (Paruthiyil et al., 2004). ERα knockout mice have primitive mammary development (Couse and Korach, 1999), whereas ERβ knockout mice develop normal mammary glands (Krege et al., 1998). Therefore, only ERα is required for growth and differentiation of the mouse mammary gland. Studies indicate that ERβ may function as a tumour suppressor and its loss promotes breast carcinogenesis (Jarvinen et al., 2000; Roger et al., 2001; Skliris et al., 2001); however, the exact role of ERβ remains unknown.

Oestrogens and the oestrogen receptors are important in the regulation of many physiological conditions such as the growth and function of the female reproductive organs, determination of the mineral density of bones and maintenance of the cardiovascular and central nervous system. Nuclear, cytoplasmic (Pietras and Szego, 1977) and the more recently discovered membrane-localised oestrogen receptors (Razandi et al., 1999) exhibit distinct protein interactions, signalling mechanisms and cellular functions which are implicated in the initiation and development of breast cancer (Aranda and

Pascual, 2001). The connection between oestrogens and cancer was established more than 100 years ago by George Beatson.

High levels of oestrogen and its metabolites are associated with both the initiation and progression of breast cancer. Oestrogens can induce the formation of reactive oxygen and nitrogen species and through different cellular signalling pathways can lead to genotoxic damage, cell apoptosis, or cell growth (Roy et al., 2007). However, no study has yet definitively demonstrated that oestrogen metabolites contribute to human breast cancer.

Breast cancer treatment

Systemic treatment for breast cancer can be given after (adjuvant) or before (neoadjuvant) locoregional treatment. Adjuvant therapy has been shown to improve survival and reduce the risk of recurrent breast cancer and is now the standard of care in the treatment of early stage breast cancer. With neo-adjuvant therapy, about 50-70% of the patients will have enough tumour regression that mastectomy will be avoided. The choice of adjuvant treatment depends on the risk of relapse, oestrogen receptor status, patient performance status and acceptability of treatment. The current treatment for breast cancer involves multimodality therapy including surgery, chemotherapy, radiotherapy, endocrine treatment and molecular therapy (Smith and Chua, 2006).

Over the past twenty years, the most common endocrine therapy used for the treatment of breast cancer is tamoxifen (Howell and Dowsett, 1997), which is a member of the selective oestrogen receptor modulators (SERMs) (they can

function as both agonists and antagonists) (Ali and Coombes, 2002). Tamoxifen is an anti-oestrogen that blocks the binding of oestrogen to its receptor. ERα is therefore a well-established predictive marker of hormone sensitivity in breast cancer as only ER(α)-positive tumours can be treated with tamoxifen (Hayes, 2004). In contrast to normal breast cells, most breast cancer cells overexpress ERα and are hormone-dependent and thus when oestrogen is removed, tumours shrink. Tamoxifen has antagonistic functions but also agonistic actions on the endometrium and bone. It also causes an increase risk of thromboembolism. Another disadvantage of this treatment is that after a period of time, patients become resistant to tamoxifen. Tamoxifen is effective in both pre- and postmenopausal women in all age groups and has been shown to be more effective when given after chemotherapy rather than concurrently (Smith and Chua, 2006a; Smith and Chua, 2006b; Smith and Chua, 2006c; Smith and Chua, 2006d). Breast cancer patients who become resistant to tamoxifen are sometimes responsive to ICI182,780 (also called faslodex), which is a pure anti-oestrogen. In contrast to tamoxifen, it has no agonistic activities as it degrades the ER protein and can therefore target ER dependent tumours that are resistant to endocrine therapy (Horwitz and McGuire, 1980). Research is now focused in understanding the mechanisms that underlie endocrine resistance and the discovery of novel agents for the treatment of breast cancer.

Various clinical trials have shown that aromatase inhibitors are also suitable for the treatment of breast cancer (Buzdar et al., 2007). These agents act by inhibiting oestrogen synthesis and include the non-steroidal anastrozole and letrozole and the steroidal compound exemestane. They are effective only in post-menopausal

women and have been shown to improve disease free and metastatic free survival when compared to tamoxifen alone (ATAC trial) (Forbes et al., 2008). Nowadays, patients are switched to an aromatase inhibitor after two or three years of tamoxifen, as it has been shown that sequential treatment with tamoxifen followed by an aromatase inhibitor improves long term survival and reduces the risk of recurrent breast cancer (Dutta and Pant, 2007).

When chemotherapy is used as an adjuvant treatment, younger women tend to have the greatest benefit, particularly when they are lymph node positive and ER negative. The side effects usually include hair loss, fatigue, lethargy, oral mucositis, haematological toxicity and ovarian suppression with potential loss of fertility. The most common chemotherapeutic agents used currently are the anthracyclines doxorubicin and epirubicin. These drugs have been shown to be more effective than the traditionally used cyclophosphamide, methotrexate and fluorouracil (CMF) chemotherapy combination (Smith and Chua, 2006). Furthermore, evidence indicates that the addition of the newer class of chemotherapeutic agents, the taxanes, (paclitaxel and docetaxel) may improve survival in high risk patients. Clinical trials are ongoing to establish the most effective chemotherapy combination for use in early stage breast cancer. Many of these drugs have already proven efficacy in women with metastatic breast cancer (Friedrichs et al., 2002).

Presence of growth factor receptors has been correlated with poor disease-free survival and resistance to endocrine therapy and chemotherapy and therefore inhibitors of growth factor activity have attracted increasing interest in the

treatment of breast cancer (Spigel and Burstein, 2002). Anti-receptor antibodies and tyrosine kinase inhibitors are some of the strategies used to develop drugs to target the epidermal growth factor receptor (EGFR) and the related ErbB2/HER-2/neu. One of these inhibitors is the recently discovered Herceptin or trastuzumab (Slamon et al., 2001). Herceptin is a novel humanized monoclonal antibody that is directed against the external domain of the HER2 receptor. HER2 is over-expressed in 20% of breast cancers (Stern, 2000). Results have shown that this inhibitor reduces the risk of recurrence by about 50% when given with or after chemotherapy for a year in women across all ages with early stage breast cancer (Engel and Kaklamani, 2007). Clinical trials have also shown that herceptin improves survival when given in combination with paclitaxel or docetaxel in patients with metastatic disease (Azambuja et al., 2008). However, there is an increased risk of cardiotoxicity when given with the anthracyclines; hence Herceptin is given after chemotherapy and not concurrently (Sengupta et al., 2008). Furthermore, because Herceptin only targets one protein, it is limited in the range of patients it can reach.

Recent studies reveal that the novel tyrosine kinase inhibitor lapatinib may also play a role in the treatment of breast cancer. It targets both the epidermal growth factor receptor (EGFR) and HER2 receptor and has recently been approved by the US Food and Drug Administration (FDA) (Bilancia et al., 2007). Lapatinib prevents tumour growth by inhibiting intracellular tyrosine kinase activity and in contrast to other EGFR tyrosine kinase inhibitors, such as erlotinib and gefitinib, it binds the inactive form of the receptor and therefore dissociates at a slower rate

from the receptor resulting in a greater duration of effect on the target site (Wood et al., 2004).

I.3 Cell cycle

The growth and development of organisms is based on a fundamental process known as the 'cell cycle', in which cells reproduce by duplicating their contents and dividing into two daughter cells. A complex set of cellular events have to be coordinated with one another during this process, so that normal cell growth is maintained. Loss of regulation of the cell cycle can result in unrestrained cell division leading to proliferative diseases such as cancer. The cell cycle consists of four phases. The first phase, G_1 phase, is the most variable of the cycle phases and is the period in which future commitment to division, differentiation or death is made. It is a growth period during which RNA and proteins are synthesized. Following the G_1 phase is the S phase, where synthesis of DNA occurs. During this phase the total content of DNA increases from the diploid value of 2N to the fully replicated value of 4N. The period from the end of S phase until mitosis is another gap phase like G_1 called the G_2 phase. During this period, the cell ensures that DNA replication is complete before it enters mitosis. During M phase, the replicated chromosomes segregate into separate nuclei by mitosis and the cell splits into two daughter cells (Schafer, 1998); Alberts et al., 1994).

Cell cycle regulation

Tight regulation is needed for the series of events during the cell cycle. The cell cycle transitions, entry and exit from S and M phases, are the major points of regulation. With regard to cellular transformation, the two most important

transitions are the transition through the restriction point (R) and the transition from a quiescent state (G_0) to an actively dividing state. When a cell enters the G_0 phase, it cannot enter the S phase and can remain there for a long period of time before starting to proliferate again. Reentry into the cell cycle from G_0 is triggered by extracellular growth factors. The restriction point is the point beyond which the cells are no longer dependent on growth factors but continued growth factor stimulation is required for cells to reach this point. If cells progress through the restriction point they can complete the cell cycle. Many proto-oncogenes (genes that when mutated or over-expressed lead to cancer) deregulate the G_0-G_1 transition, while many tumour suppressor genes (genes that protect cells by inhibiting tumour cell growth) regulate passage through the restriction point (Lewin et al., 2000;Vermeulen et al., 2003).

Other points of regulation of the cell cycle are the checkpoints, which occur in the different cell cycle phases. In each checkpoint the cells ensure that the initiation of one event in the cell cycle depends on the successful completion of an earlier event. The G_1/S checkpoint ensures that damaged DNA is not replicated. The S phase checkpoint prevents the replication of damaged DNA that has not been repaired in G_1 phase or DNA that was damaged early at S phase. The G_2 checkpoint prevents damaged DNA being segregated into daughter cells and also it allows repair of DNA that was damaged in late S phase. The M checkpoint controls mitotic spindle and metaphase-anaphase transition (Skorski, 2002).

The cell cycle is regulated by a complex of two types of proteins the cyclin-dependent protein kinases (CDK) and the cyclins. CDKs phosphorylate target

proteins on serines and threonines. They are inactive on their own because their catalytic sites, which bind ATP and substrate, are blocked by their C-terminal tails. When cyclins bind CDKs, a conformational change is induced that allows access to the catalytic site and activation of CDK kinase activity. There are two classes of cyclins: the mitotic cyclins, which bind to CDK molecules during the G_2 phase and are required for entry into mitosis and the G_1 cyclins which bind to CDK molecules during the G_1 phase and are required for entry into the S phase. Each of the different cyclins is activated at different cell cycle phases. Cyclin E-A-B levels and activity are highest in late G_1, G_2 and M respectively (Schafer, 1998; Vermeulen *et al.* 2003). Cyclin D rises early in mid-G_1 and remains constant thereafter (Baldin et al., 1993). CDK4 and CDK6 in combination with cyclin D are responsible for cell progression through G_1 phase, CDK2 and cyclin E are responsible for progression from G_1 phase to S phase, CDK2 and cyclin A for progression through S phase, and a complex of CDK1(cdc2) and cyclin B for mitosis (Fig.1.2) (Vermeulen et al., 2003).

Finally, the cyclin-CDK complexes are in turn controlled by another family of regulatory proteins known as the cycle-dependent kinase inhibitors (CKIs). The most well known inhibitors of the cell cycle are the CKIs which regulate the G_1 checkpoint. One group made up of members of the inhibitor of cyclin-dependent kinase 4 (INK4) family, which associate with CDK4 and CDK6, therefore preventing binding of the D-type cyclins. CKIs include $p15^{INK4b}$, $p16^{INK4a}$, $p18^{INK4c}$, $p19^{INK4d}$ (Guan et al., 1994). The other CKIs, called Cip/Kip, family members of which are the proteins $p21^{Cip1}$, $p27^{Kip1}$, $p57^{Kip2}$, bind to cyclin-CDK complexes, rather than the CDK alone. Interactions between cyclins, CKIs and

CDKs regulate the checkpoints of the cell cycle (Barnes and Gillett, 1998; Schafer, 1998).

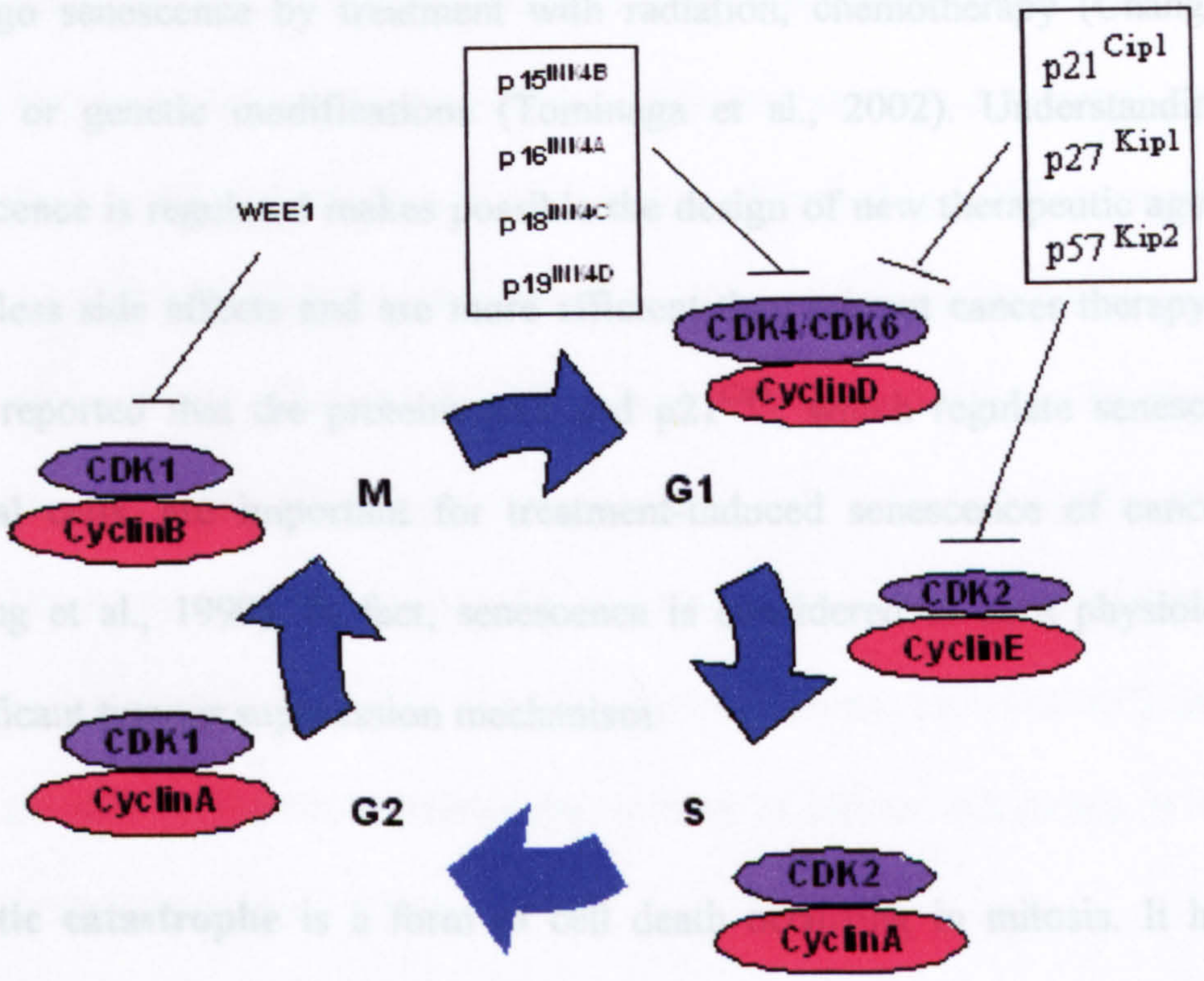


Figure 1.2 Cell cycle profile and regulators

I.4 Cell death and senescence

It has been increasingly noted that chemotherapeutic agents induce apoptosis or other forms of cell death such as necrosis and autophagy, but they also cause irreversible cell cycle arrest called senescence.

Senescence is the process where cells stop dividing after a finite number of division cycles (about 50). During this terminal growth arrest, cells cannot divide even if stimulated by mitogens, but they remain metabolically and synthetically active. Senescent cells show changes in morphology, such as enlarged, flattened cell shape and increased granularity (Roninson, 2003). The rate of senescence in

some cells depends on the cell's environment, such as the concentration of growth factors in the medium (Alberts et al, 1994). Cancer cells can be induced to undergo senescence by treatment with radiation, chemotherapy (Chang et al., 1999) or genetic modifications (Tominaga et al., 2002). Understanding how senescence is regulated makes possible the design of new therapeutic agents that have less side effects and are more efficient than current cancer therapy. It has been reported that the proteins p53 and $p21^{Cip1}$, which regulate senescence in normal cells, are important for treatment-induced senescence of cancer cells (Chang et al., 1999). In fact, senescence is considered to be a physiologically significant tumour suppression mechanism.

Mitotic catastrophe is a form of cell death occurring in mitosis. It has been proposed that it results due to cellular damage and the deficiency of cell cycle checkpoints. It is controlled by many proteins that are important for the cell cycle such as cyclin B1, polo-like kinases (PLK) and Aurora kinases but it is also controlled by p53, other checkpoint proteins, caspases and members of the Bcl-2 family of cell death regulators (Castedo et al., 2004). Mitotic catastrophe, like apoptosis, results in cell death by caspase-dependent and caspase-independent mechanisms (Mansilla et al., 2006). Mitotic catastrophe is usually assayed by visualization of multinucleated cells.

Autophagy is a protein degradation system in which proteins and organelles in a cell are sequestered then transported to lysosomes, before being digested by lysosomal hydrolases. In normal cells, unnecessary proteins and damaged organelles are removed by autophagy so that homeostasis is maintained and

therefore autophagy functions to protect cells. However, it is still unknown if autophagy in cancer cells plays the same role. In order to detect autophagic cell death, electron microscopy is usually used to visualize the autophagosomes in cells. The autophagosome-associated protein microtubule-associated protein 1 light chain 3 (LC3) is also used as a marker of autophagy. When autophagy is induced, LC3 is localised in the autophagosome membrane, whereas when it is not activated it is localised homogeneously in the cytoplasm. In contrast to apoptosis where the phagosome eats the dying cell, cells undergoing autophagy digest themselves by formation of autophagosomes (Kondo and Kondo, 2006). Various anticancer therapies like the histone deacetylase (HDAC) inhibitors Butyrate and SAHA have been demonstrated to induce autophagy in different cancer cells (Shao et al., 2004).

Necrosis (derived from the Greek "nekros" for dead) is a form of cell death characterized by swelling of cell organelles, random DNA degradation and loss of membrane integrity. Necrosis has been know to occur during the accidental cell death caused by physical or chemical agents; so it results from events outside the cell and leads to the release of the cellular components and an inflammatory tissue response (Zong et al., 2004). Many insults induce apoptosis at lower doses and necrosis at higher doses (Majno and Joris, 1995). Chemotherapeutic agents, such as alkylating DNA-damaging agents, have been shown to cause necrosis instead of apoptosis in cancer cells (Zong and Thompson, 2006).

Apoptosis is a genetically programmed mechanism for cell death that is known to play a role in both normal breast epithelial cell development and breast

carcinogenesis (Kinloch et al., 1999; Song and Steller, 1999). Characteristics of apoptotic cell death include chromatin condensation, membrane blebbing, breakdown of cytoplasmic and nuclear skeletons, DNA fragmentation, and formation of "apoptotic bodies", which are phagocytozed by neighboring cells (Fig.1.3) (Kerr, 2002; Kerr et al., 1972). Apoptosis is a highly regulated process, being controlled by various ligands and signalling pathways (Kinloch et al., 1999; Song and Steller, 1999). A trigger for apoptosis can be an external signals e.g. nutrient deprivation, accumulation of toxic metabolites, hypoxia or excessive formation of reactive oxygen species (Barber, 2000). Nowadays, detection of apoptosis can be done by many methods including Annexin V staining and caspase activation assays.

Inappropriate control of cell death has been implicated in the pathogenesis of diseases ranging from neurodegenerative disorders to tumour development Deregulation of apoptosis is associated with diseases including cancer, AIDS, various neurodegenerative diseases, etc. (Thompson, 1995). Inhibition of apoptosis in tumour cells is thought to play a critical role in breast cancer pathogenesis as well as resistance to chemotherapy. In the adult human breast, multiple endocrine and paracrine signals keep the balance between epithelial cell proliferation and apoptotic cell death during pregnancy, lactation and the menstrual cycle.

Two major apoptotic pathways exist and they are: the extrinsic death receptor and the intrinsic mitochondria-initiated pathways. The former is activated by interaction of cell surface death receptors with their ligands. The mitochondrial

apoptotic pathway involves the permeabilisation of the outer mitochondrial membrane and subsequent release of several pro-apoptotic factors into the cytosol. Both of these two major systems lead to the activation of the executioners of apoptosis named caspases. Caspases form a family of cysteine proteases that exist within the cell as inactive proenzymes which are cleaved to form active enzymes that then induce apoptosis (Thornberry and Lazebnik, 1998). However, it has been reported that it is possible for caspase-independent apoptosis to occur (Broker et al., 2005).

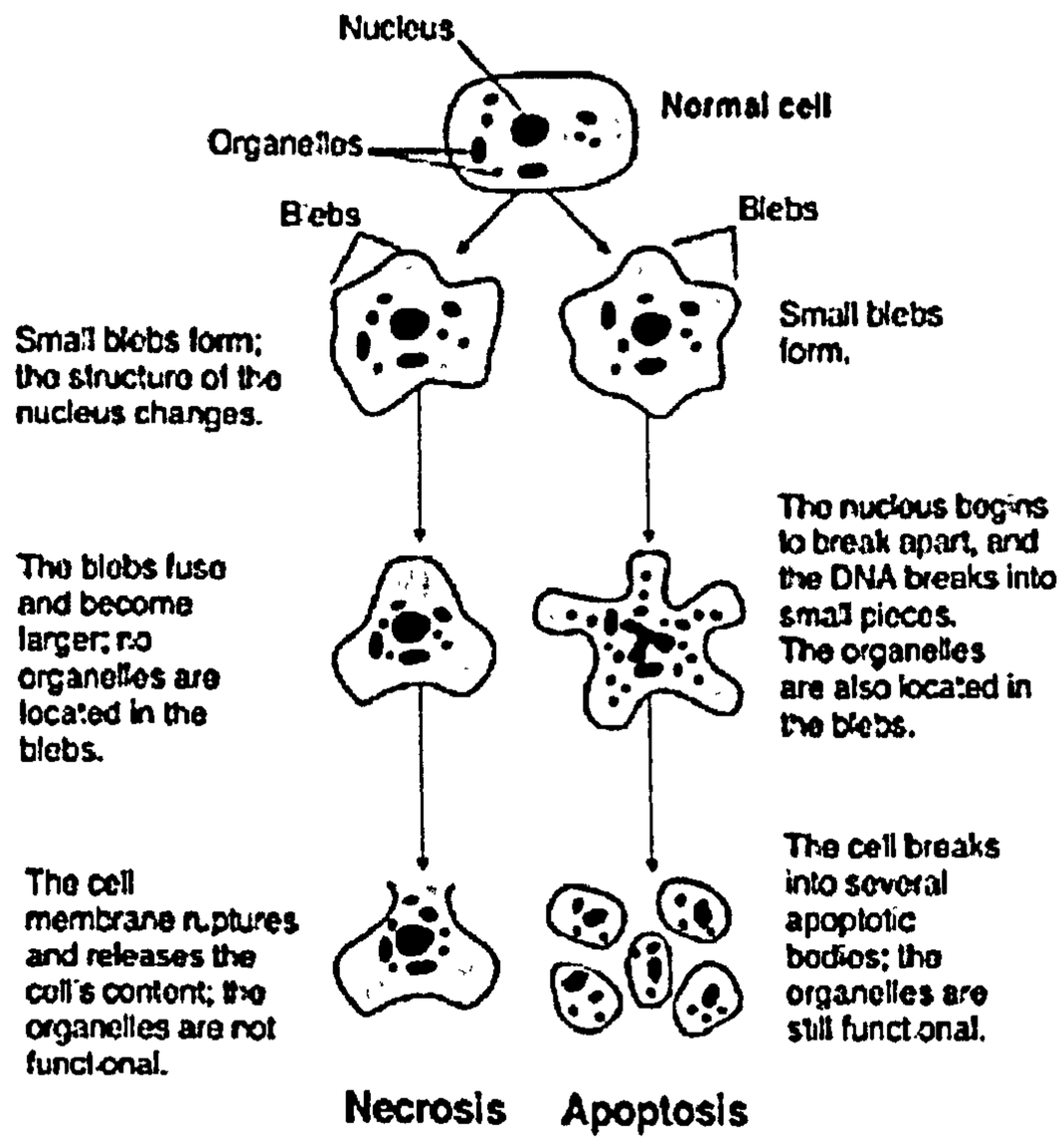


Figure 1.3 Apoptosis versus necrosis (Goodlett and Horn, 2001)

I.5 Bim

The bcl-2 protein family is known to regulate cell death. One group of this family includes anti-apoptotic proteins such as Bcl-2, Bcl-X_L, MCL1 which are required for cell survival and the other group, includes pro-apoptotic proteins such as

Bax/Bak-like proteins and BH3-only proteins. Bcl-2 proteins have four homology domains: BH-1, BH-2, BH-3 and BH-4 that are characteristics of this family of proteins (Gross et al., 1999). Not all members contain all of these domains, as there are pro-apoptotic proteins that only contain one. An important member of this type of pro-apoptotic Bcl-2 family is Bim (Bcl-2 interacting mediator of cell death). It is a member of the BH3-only proteins as it only contains the BH-3 domain. There are three Bim isoforms: Bim_{EL} (the largest), Bim_S and Bim_L. Bim causes release of cytochrome *c* from mitochondria into the cytosol, which then leads to apoptosis. Cell death is regulated through interaction between pro-survival and pro-apoptotic members of the Bcl-2 family of proteins (Coultas and Strasser, 2003). In order for the BH3-only proteins such as Bim to initiate apoptosis they have to bind the pro-survival Bcl-2 family members. This binding occurs between the helix formed by the BH3 region of the BH3-only proteins and the hydrophobic cleft formed on the surface of the pro-survival proteins by the combination of their BH1, BH2 and BH3 regions (Fesik, 2000).

Bim_L and Bim_{EL} are expressed in normal cells, but they cannot induce apoptosis because of their binding to the dynein motor complex via an interaction with dynein light chain (DLC)1 (Song et al., 1999). Bim_S does not have the domain that binds DLC1 and therefore it is a much more potent inducer of apoptosis (Puthalakath et al., 2001). The MAP kinase related stress activated c-Jun NH2-terminal kinase (JNK) induces apoptosis through phosphorylation of Bim in this DLC1 binding domain and enhances its pro-apoptotic activity (Lei et al., 2002).

The most abundant of all Bim isoforms, Bim_{EL}, is degraded by the ubiquitin-dependent proteasome pathway following phosphorylation by the extracellular signal-regulated kinase (ERK1/2) pathway (Ley et al., 2003). The exon 3 of *BIM_{EL}* contains the ERK1/2 phosphorylation sites and provides an ERK1/2 docking domain, which is not only important for its proteasomal degradation but also impairs its binding to Bax, thereby inhibiting its pro-apoptotic activity (Ley et al, 2003). When ERK1/2 is inactivated, these regions encoded by exon 3 are crucial for the stabilisation and activation of Bim. Furthermore, although it was previously thought that the E3 ubiquitin ligase c-Cbl is required for the ERK1/2 dependent degradation of Bim, it has now been proved that this is not necessarily true as Bim_{EL} degradation has also been demonstrated to be c-Cbl independent (Wiggins et al., 2007). However, the E3 ligase responsible for its degradation remains unknown.

Inhibition of the PI3 kinase pathway and subsequent inactivation of Akt leads to the dephosphorylation and nuclear translocation of the Forkhead transcription factor FOXO3α (Greer and Brunet, 2005). FOXO3α regulates *Bim* at the transcription level and thereby controls its mRNA expression (Sunters et al., 2003). This regulation has been demonstrated to control apoptosis in paclitaxel-treated breast cancer cells (Sunters et al., 2003).

I.6 Epigenetics

Genetic as well as epigenetic events play a key role in carcinogenesis and cancer progression. Epigenetic is a term used to describe changes in gene expression that are not due to changes in the DNA sequence and are inheritable from one

generation to the next (Bird, 2002). Unlike genetic changes, epigenetic alterations are reversible. Some of the epigenetic events include: acetylation, methylation, ubiquitination, phosphorylation, sumoylation and glycosylation.

Methylation occurs on DNA and histones. DNA methylation is used for long-term silencing of gene expression. DNA is methylated in the 5' position of the cytosine ring, most commonly located in CpG islands within the promoter regions of genes, and is mediated by enzymes called DNA methyltransferases (Takai and Jones, 2002; Yoo and Jones, 2006). Lack of DNA methylation activates gene expression (Fujita et al., 1999). The methylation pattern is established during development. Methylation can maintain differential gene expression patterns in a developmental-stage specific and in a tissue-specific manner. Genome-wide decrease in methylation leads to chromosomal instability and carcinogenesis (Yoo and Jones, 2006). Histone methylation occurs on lysine and arginine residues by specific enzymes called histone lysine methyltransferases and protein arginine methyltransferases respectively (Yoo and Jones, 2006).

Acetylation is a chemical modification involving the transfer of an acetyl group from the acetyl co-enzyme to the ε-amino group of lysines in target proteins (Lin et al., 2006). Acetylation can occur in histones as well as other proteins and can have many effects. Histone acetylation affects histone structure by destabilizing nucleosomes leading to their dissociation or by inhibiting their stacking into the solenoid structure. Therefore acetylation leads to a less compact structure that allows access of transcription factors and other molecules such as RNA polymerase to the DNA and thus stimulate transcription of genes (Cress and Seto,

2000). Acetylation of a protein affects protein stability as acetylation and ubiquitination occur on lysine residues and so there are cross-talks between these two modifications (Caron et al., 2005). The stability of many known proteins, such as p53 and p73, has been shown to increase after lysine acetylation. The same lysines in these proteins are subject to ubiquitination and acetylation, therefore when acetylation occurs ubiquitination is prevented and stability of these proteins is increased (Caron et al., 2005; Ito et al., 2002; Jin et al., 2004). In other cases acetylation is needed to stimulate degradation, such as in the case of the Hypoxia-induced factor 1 (Hif-1), where its degradation occurs after binding to pVHL which then mediates its ubiquitination. Acetylation of one of the subunits of Hif-1, Hif-1a, enhances its binding to pVHL and therefore its degradation (Lee et al., 2004). More complex and indirect processes connecting ubiquitination and acetylation other than just through competition have also been reported (Caron et al., 2005).

In addition, acetylation plays a role in protein-protein interactions and localization (Minucci and Pelicci, 2006). For example, acetylation of the transcription factor signal transducer and activator of transcription 3 (STAT3) induces its dimerization and translocation into the nucleus (Yuan et al., 2005) (Minucci and Pelicci, 2006).

Phosphorylation is one of the most common protein modifications that occur in animal cells. It was originally discovered in the mid-1950s and is important for the regulation of many cellular processes such as protein-protein interactions, protein degradation, and enzyme activity inhibition and also for the biological

thermodynamics of energy-requiring reactions. Phosphorylation is mediated through the addition of phosphate to a molecule. Reversible phosphorylation results in conformational changes in the structure of many enzymes and receptors, causing them to become activated or deactivated. The enzymes that phosphorylate proteins are termed kinases and those that remove phosphates are termed phosphatases. The common amino acids phosphorylated in animal cells are serine, threonine and tyrosine (Pawson, 2005) the most common of which are serines and threonines. Tyrosine phosphorylation occurs less frequently but is very important for many cellular functions in eukaryotes and bacteria (Grangeasse, 2007). An important epigenetic event is the phosphorylation of histone H3 at Ser10, which is implicated in both transcriptional and mitotic regulation.

Ubiquitination, is the process by which ubiquitin is attached through Lys48 to target proteins. Ubiquitination regulates target proteins in many ways. The most common use of ubiquitination is for targeting proteins for degradation as it will be discussed later on. However, besides this, ubiquitination also plays a role in protein-protein interaction, transcription, intracellular trafficking and activation of protein kinases (Pines and Lindon, 2005). Moreover, mono-ubiquitination has also been shown to regulate histones, the endocytosis of membrane receptors and retroviral budding from the plasma membrane (Hicke, 2001).

Sumoylation is the modification where small ubiquitin-like modifier (SUMO) proteins covalently attach to their targets. SUMO is a small protein that mechanistically acts similar to ubiquitin but they do not always have similar sequence similarity and also they exert different functions. Both ubiquitin and

SUMO bind lycine residues of substrates. SUMO competes with ubiquitin for the conjugation of the same protein on the same time and thus proteins can be stabilized from ubiquitin-dependent proteasomal degradation (Ulrich, 2005). Sumoylation plays many important roles, such as in regulating protein stability and function, DNA damage repair, cell cycle regulation, nucleo-cytoplasmic trafficking, transcriptional regulation, apoptosis, maintaining genome stability and thus participates in maintaining cellular homeostasis (Kim et al., 2006).

Glycosylation is a highly conserved post-translational modification. Three types of glycosylation occur: N-linked glycosylation of asparagine residues of proteins within the consensus sequence Asn-Xaa-Ser/Thr, O-linked glycosylation of serine or threonine, and glycosylphosphatidyl inositol derivatization of the carboxyl-terminal carboxyl groups. N-glycosylation is very important as it has been to shown to be crucial for viability. It plays a role in cell cycle regulation, protein folding and stability and cell-matrix and cell-cell interactions (Kukuruzinska and Lennon, 1998). H1 histone and core histones have also been shown to be glycosylated. This modification probably plays a role in the regulation of cell proliferation and protein-DNA interactions, but further studies need to be done to examine its role and significance.

I.7 HDACs

Genomic DNA is wrapped around 8 histones to form nucleosomes, which is the fundamental unit of chromatin. Chromatin contains five types of histones: H1, H2A, H2B, H3, and H4. The nucleosome consists of an octamer of four core histones i.e. two H2A/H2B dimmers and an H3/H4 tetramer, surrounded by

146bp of DNA (Yoo and Jones, 2006). H1 histone lies on the outer portion of the nucleosome and occurs in chromatin in about half the amount of the other types of chromatin. There is also the H5 histone that has similar functions to H1 (Marks et al., 2000). The amino-terminal and the carboxyl-terminal tails of histones protrude out of the nucleosomes and are subject to post-translational modifications that regulate gene expression. Studies on the impact of these modifications in cellular processes are fast growing areas of research. Such a modification is the acetylation of histones by histone acetyltransferases (HATs) and deacetylation by histone deacetylases (HDACs). Acetylation is correlated with an open chromatin structure, allowing transcription factors to access the promoters of target genes, therefore activating transcription (Nelson et al., 2007). Acetylation is involved in the regulation of DNA replication, repair and recombination (Masumoto et al., 2005; Yang and Seto, 2007). Disordered HAT or HDAC activity has been linked to cancer. The fact that acetylation plays a very important role in the regulation of gene expression has lead to the extensive study of HDACs in relation to cancer (Vigushin and Coombes, 2002).

HATs acetylate histones leading to an open chromatin structure where transcription factors can easily reach the DNA and as a result transcriptional activity is induced. There are four families of HATs. The prototype family related to the yeast GCN5 includes human GCN5 and P/CAF (p300/CREB binding protein associating factor). The second family includes CREB binding protein (CBP) and p300 which mainly function as co-activators for many transcription factors. The third family includes the TAF250 protein which is part of the TFIID transcription factor complex that binds the TATA box and finally the fourth

family, including SRC-1 and ACTR, function as co-activators for ligand-activated nuclear receptors. Other splice variants or related proteins exist that have HAT activity (Kouzarides, 1999).

HDACs deacetylate histones leading to a very compact chromatin structure where transcription factors and other regulatory complexes cannot access the DNA, thereby gene transcription is repressed. HDACs usually interact as constituents of large protein complexes that downregulate genes through association with co-repressors (NcoR, SMRT), transcription factors (ER, p53, Mad/Max), cell cycle specific regulators (Rb, E2F), but they can also bind their target directly (Cress and Seto, 2000) (Fig.5). For example, a decade ago the non-histone tumour suppressor p53 protein was shown to be acetylated by the recruitment of coactivators/HATs, a process very crucial for p53 function and activation of transcription of target genes (Gu and Roeder, 1997; Barlev et al., 2001). Another example is the thyroid hormone receptor that activates transcription, upon binding of a ligand, by associating with the p300/PCAF histone acetyltransferases (Cress and Seto 2000). The proteins NCoR (Horlein et al., 1995; Kurokawa et al., 1995; Zamir et al., 1996), SMRT (Chen and Evans, 1995), Sin3 and histone deacetylases (Alland et al., 1997; Heinzel et al., 1997) are part of this complex which is usually referred to as the Sin3 complex. Many proteins interact with HDACs directly or through other yet unidentified proteins (Brehm et al., 1998; Chen et al., 1999; Luo et al., 1998; Yang et al., 1996).

Dependent on sequence similarity and cofactor dependency, HDACs are grouped into two families: the classical HDAC family and the Sirtuin family of NAD^+-

dependent HDACs. Members of the classical HDAC family are divided in three classes. Class I HDACs include HDAC1, 2, 3, 8 and resemble the RPD3 trascriptional regulator in yeast, class II include 4, 5, 6, 7, 9, 10 HDACS and resemble the yeast HDA1 deacetylase and class IV includes HDAC11. Classes I, II, IV have a similar sequence and are dependent on Zinc for their deacetylase activity. Class I is expressed in most cell types, while class II expression is more restricted. For this reason class II HDACS are thought to be involved in developmental processes and differentiation (de Ruijter et al., 2003). The newly discovered HDAC 11 has conserved regions in the catalytic core region shared by both class I and II HDACs (Gao et al., 2002). Most HDACs contain a nuclear localisation signal (NLS) that targets them to the nucleus where most their substrates locate. Other HDACs can be cytosolic depending on other regulatory domains (de Ruijter et al., 2003). For example HDAC3 has both a NLS and a nuclear export signal (NES) suggesting that it can be also located in the cytoplasm (Yang et al., 2002). In most studies, HDAC3 is localized in the nucleus but this can be cell type specific. Class II HDACs shuttle between nucleus and cytoplasm depending on the signals they receive, while HDAC1 and HDAC2 are always in the nucleus as they lack a NES (Bertos et al., 2001).

Functional HDACs are never found as single polypeptides but, with the exception of HDAC8, they form parts of multiprotein complexes along with other chromatin modifying enzymes or specific co-regulators. Both class I and class II HDACs play roles as transcriptional co-repressors by forming complexes with other DNA binding proteins and target the promoters of genes (Kumar et al., 2005). Although class I and II HDACs have a very similar catalytic site, they have differences in

the entrance region of the active site and the outer charge transfer relay system (Finnin et al., 1999; Hildmann et al., 2006; Nielsen et al., 2005; Somoza et al., 2004; Vannini et al., 2004). Many class II HDACs are subject to posttranslational modifications such as sumoylation as it has been shown with HDAC4 where it is sumoylated at lysine 559 (Kirsh et al., 2002). HDAC 7 has been shown to act as a mitochondrial protein playing a role in apoptosis, as it translocates from the mitochondrial membrane to the cytoplasm in response to apoptotic signals (Bakin and Jung, 2004). Class II HDACs are able to bind directly and inactivate some transcription factors leading to their transcriptional repression, therefore HDAC biological function are not strictly dependent on their enzymatic activity (Gallinari et al., 2007).

The class III HDAC family called the sirtuin family includes seven members SIRT1-7. There are no sequence similarities amongst members and they require NAD^+ as the cofactor important for their enzymatic activity (Nelson et al., 2007).

It was recently shown that the mutational status of HDACs is very important in future pharmacogenetic treatment of cancer patients. Frameshift mutations in HDAC2 causing its loss of expression were seen in sporadic carcinomas with microsatellite instability and in cancer patients with hereditary non polyposis colorectal cancer syndrome. This loss of HDAC2 expression leads to tumours being less sensitive to the anti-cancer effects of HDACi (Ropero et al., 2006).

HDAC inhibitors (HDACi)

It has become apparent that imbalances of histone acetylation play a significant role in cancer development and progression. Cancer cells target chromatin-remodeling pathways in order to disrupt transcriptional regulation. Research performed over the last decade has highlighted the role of HDACi as modulators of transcriptional activity and as a potential new class of therapeutic agents. HDAC inhibitors have been shown to inhibit proliferation, cause cell cycle arrest, promote differentiation, induce mitotic cell death, senescence and reactive oxygen species-induced cell death (Fig.1.4, 1.5) (Johnstone et al., 2002; Narlikar et al., 2002). Part of the reason why HDACi have anti-cancer properties is that they suppress cancer cell migration, invasion, metastasis *in vitro* (Dyer et al., 2002; Eyupoglu et al., 2005; Kim et al., 2004; McGarry et al., 2004) and *in vivo* (Coradini et al., 2004; Tang et al., 2004) and also suppress angiogenesis (Kwon et al., 2002a; Sasakawa et al., 2003; Zgouras et al., 2004; Zgouras et al., 2003).

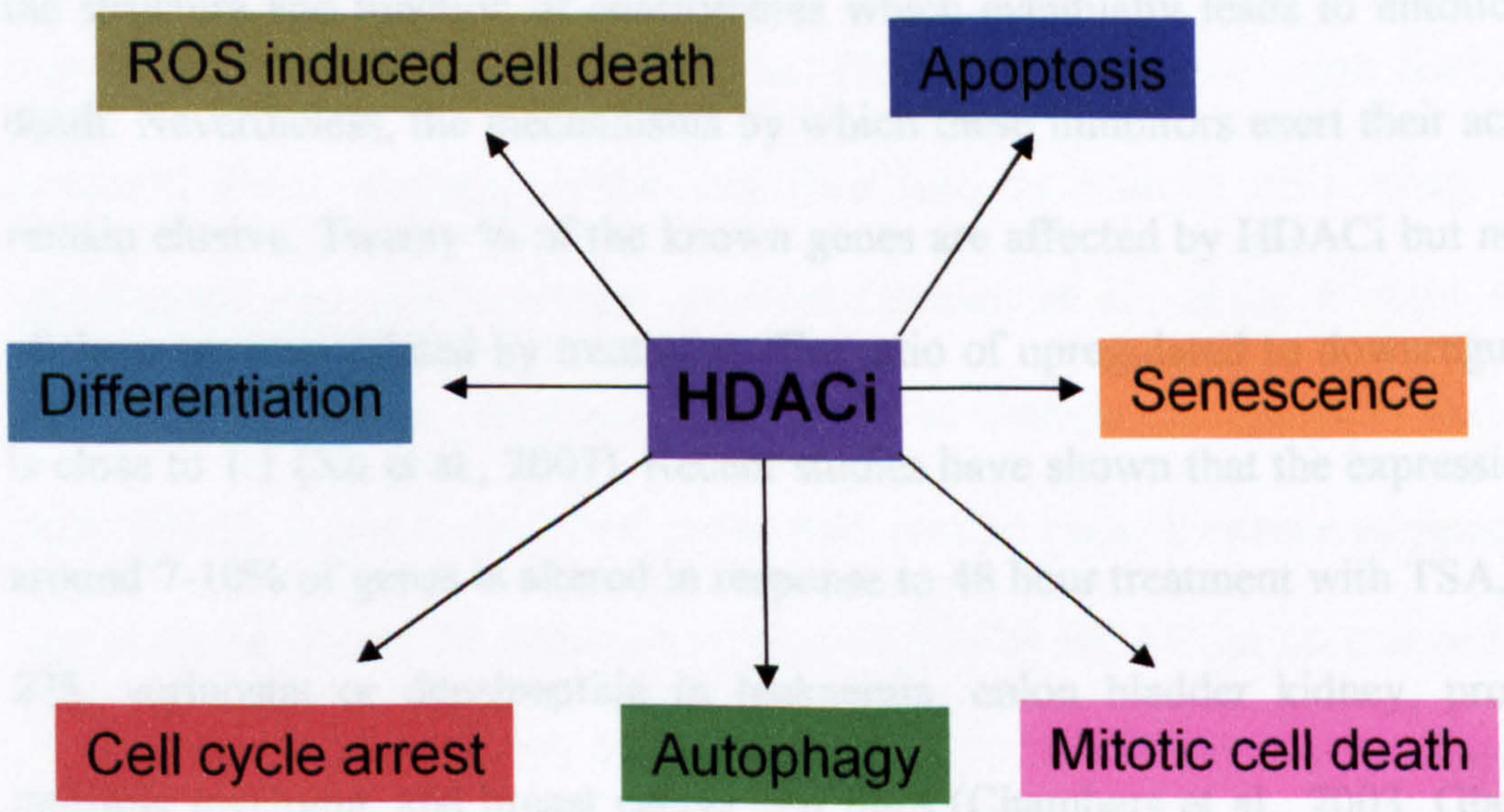


Figure 1.4 Effects of HDACi

Low concentrations of HDACi usually induce G_1 arrest while higher concentrations induce both G_1 and G_2/M arrest. G_1 arrest is predominantly caused by the increase in the expression of the $p21^{Cip1}$ cell cycle inhibitor (Richon et al., 2000). However, cells without $p21^{Cip1}$ have been seen to arrest in response to HDACi treatment by the induction of the $p15^{INK4b}$ cell cycle inhibitor (Hitomi et al., 2003). HDACi have been shown to activate intrinsic apoptotic pathways which are mediated by the mitochondria, by inducing the expression of pro-apoptotic proteins such as Bad, Bim, caspase 3, Apaf-1 and repress the expression of anti-apoptotic proteins like Bcl-2, XIAP and Bcl-XL (Liu et al., 2006). They also activate extrinsic apoptotic pathways initiated by death receptors like Fas (Kwon et al., 2002b) and TRAIL (Nebbioso et al., 2005) by upregulating their expression. Compounds such as MS-275, TSA, vorinostat and butyrate induced cell death by generation of reactive oxygen species (ROS) (Rosato et al., 2003; Ruefli et al., 2001; Ungerstedt et al., 2005; Xu et al., 2006). Also, HDACi disrupt the structure and function of centromeres which eventually leads to mitotic cell death. Nevertheless, the mechanisms by which these inhibitors exert their actions remain elusive. Twenty % of the known genes are affected by HDACi but not all of them are upregulated by treatment. The ratio of upregulated to downregulated is close to 1:1 (Xu et al., 2007). Recent studies have shown that the expression of around 7-10% of genes is altered in response to 48 hour treatment with TSA, MS-275, vorinostat or depsipeptide in leukaemia, colon bladder kidney, prostate, multiple myeloma, and breast cancer cell lines (Chambers et al., 2003; Glaser et al., 2003; Mitsiades et al., 2004; Peart et al., 2005; Sasakawa et al., 2005). Some of these changes are caused by direct effects of the inhibitor on specific gene promoters while other effects are secondary. Of course, a different mumber of

genes have variations in their expression when using a different concentration of drugs and for a different length of time.

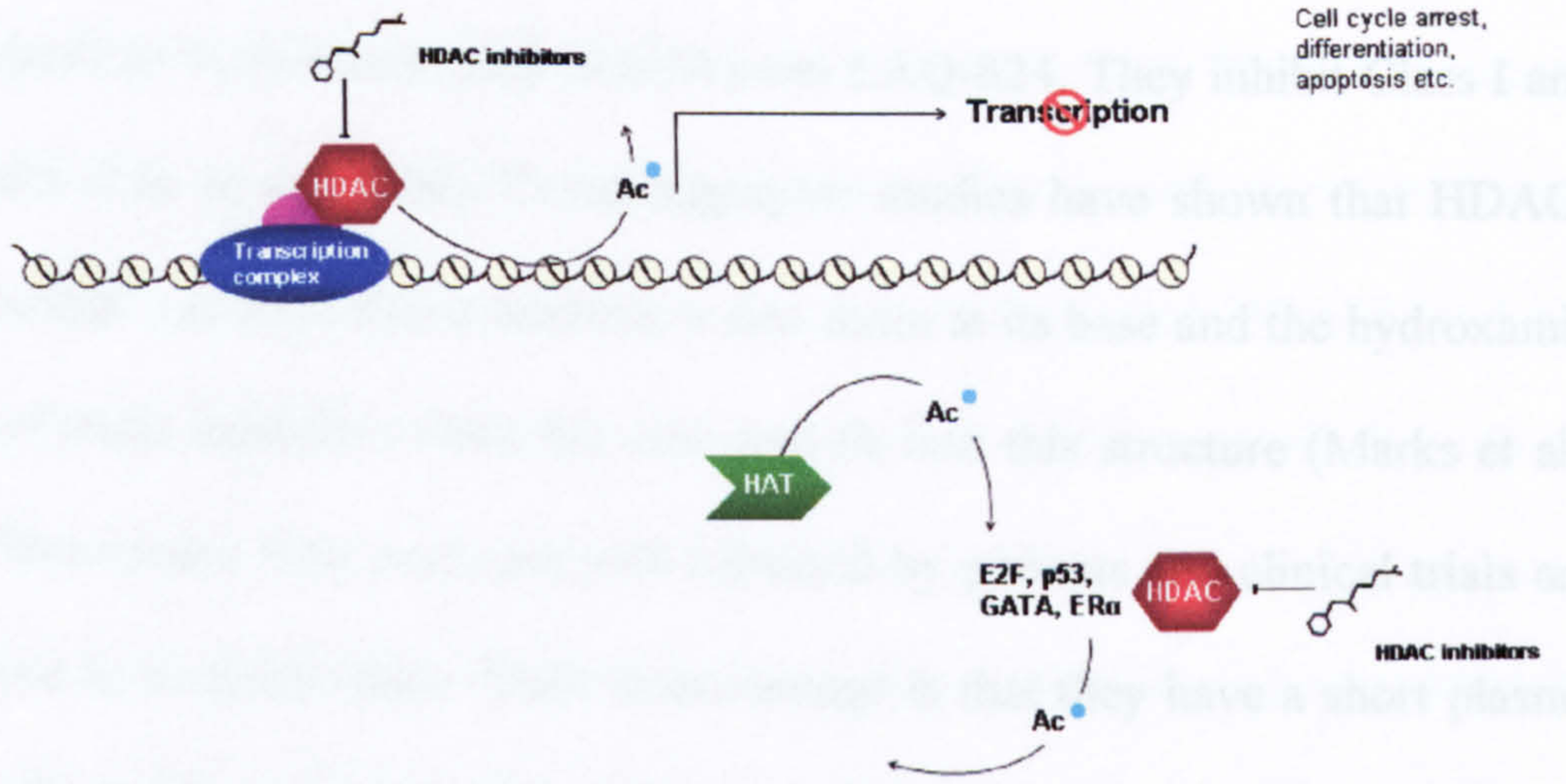


Figure 1.5 HDACi inhibit HDACs that target the chromatin or other proteins directly, leading to cell cycle arrest, apoptosis etc.

Noteworthy, HDACi not only influence transcription but also other processes, such as DNA repair. In a few cell lines, HDACi inhibit DNA repair leading to increased DNA damage, which can then lead to tumour cells being more radiotherapy and chemotherapy sensitive (Bolden et al., 2006; Munshi et al., 2006). An important advantage of HDACi as therapeutic agents is that they preferentially target transformed rather than normal cells. Evidence suggests that this might be due to the induction of thioredoxin by HDACi in normal cells, but not in transformed (Ungerstedt et al., 2005). Thioredoxin is a ubiquitous oxidoreductase enzyme that acts as an antioxidant by facilitating the reduction of other proteins. Another advantage of using HDACi as a treatment is that in contrast to anti-estrogens, HDACi can act in both ER positive and negative cells.

A number of HDACi have been developed, several of which are in clinical trials. HDACi are classified into four categories: hydroxamic acids, short-chain fatty acids, benzamide derivatives, and cyclic peptides. The very potent hydroxamic acids include compounds such as the well known Trichostatin A (TSA), suberoylanilide hydroxamic acid (SAHA) and LAQ-824. They inhibit Class I and II HDACs (Lin et al., 2006). Crystallographic studies have shown that HDACs have a tubular catalytic site containing a zinc atom at its base and the hydroxamic moiety of these inhibitors bind this zinc and fit into this structure (Marks et al., 2000). Short-chain fatty acids are well tolerated by patients and clinical trials are carried out to evaluate them. Their disadvantage is that they have a short plasma half-life due to the rapid rate of metabolism and their non-specific mode of action, as well as the high doses needed for therapeutic effects. Agents like this are Valproate, Butyrate and Phenylbutyrate. On the other hand, benzamides inhibit HDACs at μM concentrations. These agents include MS-274 and CI-944 which are currently under clinical evaluation. Lastly, cyclic peptides, like depsipeptide and apicidin A, are the most structurally complex class of HDACi. Depsipeptide was pulled out from clinical trials due to its cardiovascular toxicity (Lin et al., 2006).

Very few HDACi developed can only inhibit a specific HDAC. For example, tubacin selectivily inhibits HDAC6 but does not inhibit proliferation and causes accumulation of acetylated α-tubulin. Also, the novel compounds SK7041 and SK7068 target only HDAC1 and 2 and have been shown to inhibit the proliferation of cancer cell lines (Haggarty et al., 2003; Kim et al., 2003a). The

anti-proliferative effects of selective HDACi towards cancer cells, remains undetermined.

HDACi have been demonstrated to induce apoptotic and autophagic cell death *in vitro* and *in vivo* (Hess-Stumpp, 2005; Minucci and Pelicci, 2006; Shao et al., 2004). Induction of autophagic cell death has clear clinical implications in treating cancers with apoptotic defects. Butyrate, a short fatty-acid HDACi, and the hydroxamic acid SAHA, induced caspase-3 activation and apoptosis through the mitochondria/cytochrome *c*-mediated apoptotic pathway in many cancer cell lines. However, cell death was also induced without caspases and resembled the features of autophagic cell death. Therefore, HDAC inhibitors can induce both mitochondria-mediated apoptosis and caspase-independent autophagic cell death (Shao et al., 2004).

While the primary action of HDACi is attributed to histone remodelling, other targets are also responsible for their anti-tumour properties. For example, treatment with HDACi leads to the dephosphorylation of Akt (also called protein kinase B/PKB) resulting in its inactivation. This occurs through the dissociation of protein phosphatase 1 (PP1) from HDACs, leading to an increased association of PP1 with Akt. Akt enhances cellular survival through the phosphorylation-dependent inhibition of several proapoptotic proteins (Datta et al., 1999; Woodgett, 2005). Mutation of negative regulators of Akt and the deregulated expression or activation of Akt has been demonstrated in several cancers (Samuels et al., 2005).

It is important to mention that HDACi can also cause non-desired effects in cancer cells since they are also able to induce proliferation and differentiation and abrogate apoptosis (Minucci and Pelicci, 2006). An example is the retinoblastoma protein (Rb) that recruits HDACs to E2F transcription factor target genes, thereby controlling the G_1 to S transition. HDACi should therefore induce Rb targets but only a subset of these is dependent on HDAC recruitment. RB regulation of cell cycle would therefore continue to be unaffected by HDACi and can therefore induce proliferation of cancer cells (Siddiqui et al., 2003).

Clinical potential of HDAC inhibitors

HDACi are being heralded as the first anti-cancer drugs targeting the epigenome. They have entered clinical trials for both blood cancers and solid tumours. Generally, HDACi have a favourable outcome in clinic trials so far. SAHA is now approved by the Food and Drug Administation (FDA) for the treatment of cutaneous T-cell lymphoma and can be administrated to patients intravenously or orally and is well tolerated by patients (Kelly et al., 2005; Kelly et al., 2003). It has also been proven to inhibit the growth of pancreatic cancer cells causing G_2/M arrest, differentiation and apoptosis (Kumagai et al., 2007). Similarly depsipeptide is advancing in clinical trials but it has not shown much activity in solid tumours. On the other hand cutaneous T-cell lymphoma has again been proven to be responsive to depsipeptide (Piekarz et al., 2001). The reason why this cancer is responsive both to SAHA and depsipeptide remains unclear. FK-228 or romidepsin has been reported to induce apoptosis in colon cancer, chronic myelogenous leukemia, and non small cell lung carcinoma. It is well tolerated and has a similar toxicity profile as SAHA. As it is not a hydroxamic acid as SAHA it

is a more selective inhibitor of the class I HDACs (Choudhary and Wang, 2007; Radhakrishnan et al., 2007; Yu et al., 2007). In addition, the benzamide MS-275 has been shown to induce apoptosis in B-chronic lymhocytic leukaemia cells, prostate cancer cells and Jurkat lymphoblastic cells and is used in clinical trials in combination with other agents (Lucas et al., 2004; Maggio et al., 2004; Pan et al., 2007; Qian et al., 2007). It is however anticipated that inhibitors targeted against specific HDACs may potentially have a greater therapeutic effect than all these non-specific drugs.

Furthermore, it appears that HDACi will have better clinical efficacy when used in combination with other drugs. There are many ongoing phase II trials in which this is investigated. Combination of HDACi with other chemotherapeutic agents has shown to reduce side effects and morbidity in patients. For example, depsipeptide in combination with the nitrogen mustard derivative melphalan, has been reported to be more cytotoxic in multiple myeloma cells (Khan et al., 2004). Also, clinical trials are now testing the combined effect of anthracyclines with an HDAC inhibitor in leukaemia. The novel hydroxamic acid Belinostat has been reported to have additive or synergistic activity when combined with carboplatin and paclitaxel in ovarian cancer models (Karagiannis and El-Osta, 2006). Inhibition of HDACs with compounds like valproic acid has been reported to enhance the anti-proliferative action of anti-oestrogens in breast cancer cells and block tamoxifen-induced proliferation of uterine cells (Hodges-Gallagher et al., 2007).

Pre-incubation of cancer cell lines with TSA or SAHA increases the cell death efficiency induced by the DNA cross-linking agent cisplatin, the DNA intercalator doxorubicin and the topoisomerase II inhibitor VD-16. This is probably caused because HDACi make the DNA more accessible for the other DNA binding drugs. However, this in not true for all the DNA binding drugs since cyclophosphamide induced cell death was not increased by pre-incubation with SAHA (Kim et al., 2003a; Zhang et al., 2004). It has also been proved that HDACi sensitize cells to ionizing radiation.

Suberic bishydroxamate (SBHA) has proved to be effective on inducing apoptosis on a panel of human melanoma cell lines but not in melanocytes and fibroblasts. It induced caspase-dependent apoptosis and down-regulated anti-apoptotic Bcl-2 family proteins, Bcl-XL and Mcl-1, while inducing the expression of pro-apoptotic Bim, Bax, and Bak. Bim was particularly important in the SBHA induced apoptosis (Zhang et al., 2004).

Besides cancer, HDACi are also used for the treatment of other diseases. For example, some HDACi can reduce graft-versus-host disease in patients that have had bone marrow transplantation by the suppression of pro-inflammatory cytokines. HDACis affect proteins such as STAT1, STAT3 and NFkB that regulate immune cell function (Leng et al., 2006). Moreover, they activate latent viruses like HIV. When the virus is in latent stage activation by HDACi causes it to be more susceptible to treatment with targeted anti-viral-therapy. The combination of valproic acid and highly active retroviral therapy caused resting cell infection declined significantly in 3 out of 4 patients (Ylisastigui et al., 2004).

HDACi have also been useful for the treatment of strokes and other neurodegenerative diseases as they increase the expression of neuroprotective proteins, like Hsp70 and Bcl-2, in the ischemic brain. Valproic acid has been found to be a very efficient anti-epileptic drug. Although, it is well tolerated by patients, it can cause birth defects, like neural tube defects, during early pregnancy (Nau et al., 1991). HDACi have also proved to be important for the therapy of Huntington's disease (Sadri-Vakili and Cha, 2006).

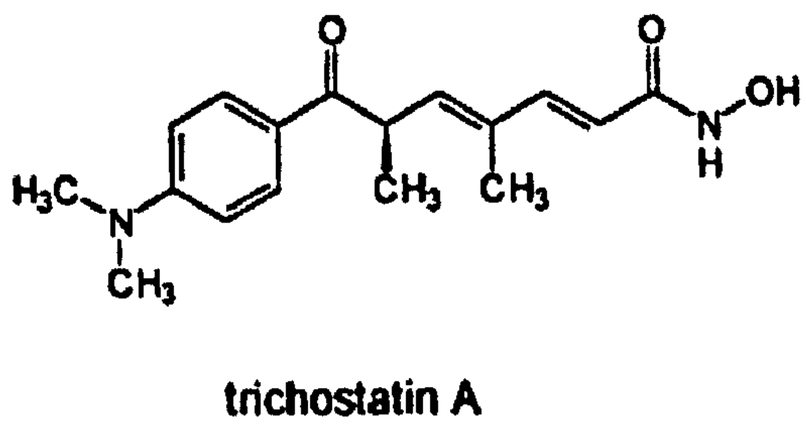
However, some HDAC inhibitors have very toxic side effects at high doses and therefore, are of limited therapeutic use. Other HDACi, such as butyrate and phenylbutyrate, degrade rapidly, therefore patients will require high dose administration (Warrell et al., 1998). Another disadvantage of these compounds is that they are not specific. They not only inhibit HDACs but they also inhibit other processes like the phosphorylation and methylation of proteins as well as DNA (Newmark and Young, 1995).

I.8 Trichostatin A

The natural product Trichostatin A (Fig.1.6), was first isolated from the culture broth of *Streptomyces hygroscopicus* as an antifungal antibiotic active against *Trichophyton* species. Now it has been shown to exhibit potent differentiating and anti-proliferative properties (Vigushin and Coombes, 2002). TSA consists of a Zn motif that has a chelating function, a conjugated, aliphatic chain that acts as a linker and finally a polar cap group. All these motifs interact with the enzyme pocket. The HDAC catalytic domain consists of a tube like pocket and Zn is located at the bottom of this. X-ray crystallographic analysis of the bacterial

BIBL. LONDON UNIV.

HDAC histone deacetylase- like protein (HDLP) has revealed how inhibitors like TSA mediate enzyme inhibition. A distinct protein-ligand interaction occurs where TSA is docked into the active site pocket of HDLP following energy minimization (Lin et al., 2006).



trichostatin A

Figure 1.6 Chemical structure of trichostatin A (Vigushin *et al.* 2002)

TSA induces different types of cell death, differentiation and cell cycle arrest (Yoshida et al., 1990). In cancer cells, TSA induces apoptosis, whereas in normal cells it arrests cell cycle progression. Generally, TSA has been shown to induce the expression of the $p21^{Cip1}$ cell cycle inhibitor, increase the acetylation of H4 and cause arrest in G_1/S and G_2/M in many cancer cell lines (Kim et al., 1999; Li et al., 2006; Rokhlin et al., 2006; Sowa et al., 1999; Yamashita et al., 2003). Studies have also shown that TSA inhibits the growth of non-small-cell lung cancer cells (Mukhopadhyay et al., 2006) and small-cell lung cancer cells (Platta et al., 2007).

In the A2780 ovarian cells TSA caused differentiation and inhibited cell proliferation by inducing $p21^{Cip1}$, reducing the phosphorylation of the cell cycle regulator retinoblastoma protein (Rb), decreasing Id1 expression (Inhibitor of differentiation 1), while not affecting Id2 levels (Strait et al., 2002). Furthermore, TSA not only has been demonstrated to induce caspase-dependent apoptosis but it

is also able to induce caspase-independent apoptosis in human gastric cancer cells through regulating apoptosis-related genes, such as *Bcl-2*, *Bax* and *surviving* (Wu et al., 2007). TSA has also been seen to inactivate the mitotic spindle checkpoint, suggesting that it can increase the cell death caused by microtubule-disrupting agents like the taxanes (Dowling et al., 2005).

TSA treatment also modulates the radiation-induced DNA damage repair process in human squamous carcinoma cells SQ-20B. This was partly due to TSA induced suppression of the *BRCA1* gene expression, suggesting that BRCA1 is one of the molecular targets of TSA (Zhang et al., 2007). Recently, it was shown that TSA also inhibits the telomerase activity in brain cancer cell lines and may therefore be used as a telomerase inhibitor in cancer therapy (Khaw et al., 2007).

TSA has also proved to inhibit angiogenesis. TSA treatment reduced the expression of VEGF-D in U251MG glioblastoma cells suggesting that HDACi modulate the expression of VEGF family members, and therefore may inhibit angiogenesis (Sawa et al., 2002). Also, combination of TSA and alpha-interferon (IFNalpha) therapy reduced tumour angiogenesis in neuroblastoma-bearing transgenic mice (Kuljaca et al., 2007).

TSA increases the agonist activity of anti-estrogens, by a mechanism dependent on the reduction of ERα expression (Margueron et al., 2003). ERα positive cell lines are more sensitive than ERα negative cell lines to the antiproliferative effects of TSA. This was shown to be due to the fact that in ER+ breast cancer

cells the *p21*^{Cip1} gene was expressed at higher levels and it was more sensitive to TSA regulation (Margueron et al., 2003).

Recently, TSA has been shown to sensitize ERα-negative (MDA-MB-231 and Hs578T), endocrine resistant breast cancer cells to tamoxifen possibly by upregulating ERβ activity (Jang et al., 2004). Studies in our lab have also shown that TSA represses the transcription of *ERα* and *cyclin D1* in the MCF-7 breast cancer cells and induces ubiquitin-dependent proteasome degradation of cyclin D1 in both ERα- positive and ERα-negative cell lines. Cyclin D1 is known to activate ERα, independent of CDK and estrogen binding, and therefore can stimulate cancer cell growth. The inhibition of this effect by TSA provides a potential tool in overcoming resistance to endocrine therapy (Alao et al., 2004).

TSA is also thought to provide an important treatment of cancer by combining its activity with other chemotherapeutic agents or radiation. Studies are now being done on the link of TSA and radiation, some of them reporting that TSA enhances the radiosensitivity in some human cancer cell lines (Akimoto, 2004).

Besides the fact that TSA is toxic, another disadvantage is its high biotransformation. Research on the biotransformation pathways of TSA in rat hepatocytes and human liver microsomes showed that TSA undergoes a high phase I biotransformation. The hydroxamic acid was converted to its corresponding metabolites after only 20min of exposure therefore causing a very short exposure to the pharmacologically active parent compound. This has important consequences for its potential development as an anti-cancer drug, as

exposure to a complex mixture of metabolites is usually not desired (Elaut et al., 2002).

Clearly, an understanding of the mechanism of action of HDAC inhibitors like TSA is very important for their potential use as cancer therapeutic agents. However, although there is a high volume of research going on regarding TSA, targets of this drug are still unknown. In this study I characterized the regulation and function of an important target of TSA.

I.9 F-Box proteins

At present little is known about the genes encoding F-Box proteins and their functions. F-box proteins contain an approximately 50 amino acid domain called F-box that functions as a site of protein-protein interaction. The name F-Box proteins was quoted by Bai *et al.* in 1996, (Bai et al., 1996) because it was first identified in cyclin F. F-Box proteins are present in all eukaryotes; 11 members of the F-Box family have been found in budding yeast, 22 in *Drosophila*, 326 predicted in *Caenorhabditis elegans*, and 38 in humans but none known in prokaryotes. The interestingly high number of F-Box proteins in *C. elegans* makes it the fourth most common protein domain in *C. elegans*. The F-Box domain is usually found in the N-terminal region of proteins. A small number of studies have been carried out to analyze the subcellular localisation of F-Box proteins and showed F-box proteins to be distributed both in the cytoplasm and nucleus. No information is available on their expression patterns and tissue specificities. Furthermore, mutating the F-Box domain has been shown not to be

important for determining their localisation in the cell (Kipreos and Pagano, 2000).

F-box proteins are also characterised by their carboxyl-terminal motifs capable of protein-protein interaction; the most common motifs being WD repeats and leucine-rich repeats (LRRs). They are also shown to contain other secondary motifs, eg. cyclin domains, zing fingers, the diversity of which suggests that F-Box motifs must have been transferred into existing proteins many times during evolution (Ilyin et al., 2002). The F-box proteins containing LRRs are named FBXL, those with WD40 repeats are denoted FBXW and those with no or another motif are called FBXO. F-Box proteins have been shown to play an important role in the ubiquitin-mediated degradation of many cellular proteins.

I.10 Ubiquitin-dependent proteasomal degradation pathway

The ubiquitin-dependent proteasomal degradation pathway (Fig.1.7) plays a very important role in the post-translational regulation of proteins. It involves the generation of a polyubiquitin chain covalently conjugated to the protein substrate followed by degradation of the conjugated protein by the 26S proteasome. Ubiquitin is a 76-amino acid globular protein that its covalent conjugation to other proteins — ubiquitination — is essential for their degradation. This process involves the action of three enzymes: the ubiquitin activating enzyme E1, the ubiquitin-conjugating enzyme E2 and the ubiquitin ligase E3 (Ciechanover et al., 2000; Weissman, 2001).

In detail, free ubiquitin is activated by the E1 enzyme to form a thiol- ester bond between glycine 76 and cysteine in an ATP-dependent reaction. The ubiquitin molecule is then transferred to the active cysteine of one of several E2 enzymes. There are approximately 13 E2s in vertebrates and yeast. Then, E3 enzymes facilitate the transfer of ubiquitin from E2s onto a lysine residue on specific substrate proteins or onto Lys-48 of a substrate bound multi-ubiquitin chain. Following 26S proteasomal degradation, free ubiquitin is released back into the cellular ubiquitin pool. In certain instances, the E3 may itself be tagged with ubiquitin and targeted for degradation. The 26S proteasome is an abundant 5'-triphosphate-dependent protease complex consisting of a cylindrical 20S core particle flanked by two 19S regulatory particles regulating substrate access on both ends of the 20S core (Ciechanover et al., 2000; Jackson et al., 2000; Weissman, 2001). Furthermore, proteasomes are present in eukaryotic cells both in the cytoplasm and nucleus and are more active and abundant in transformed compared to non-transformed cell lines.

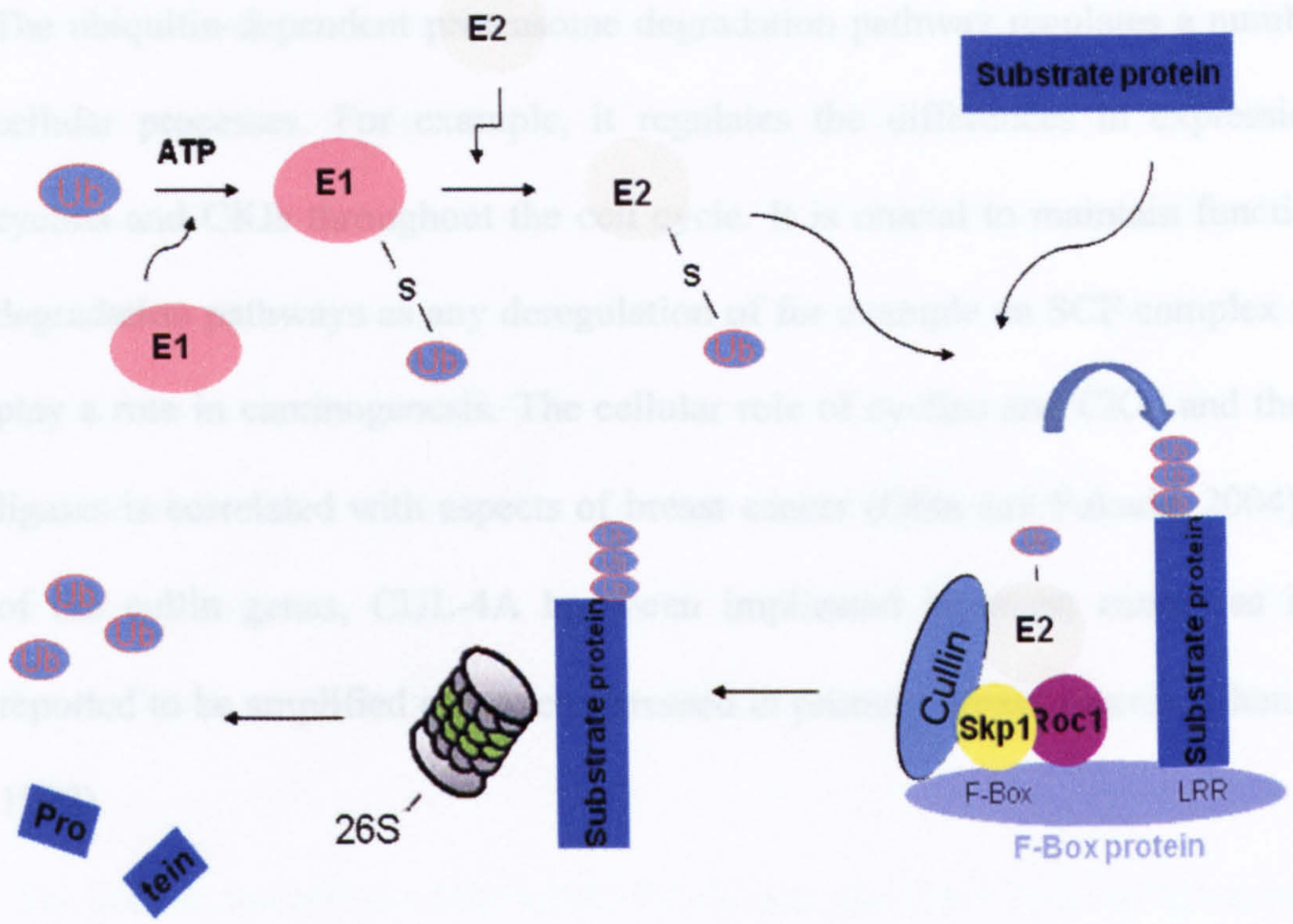


Figure 1.7 Ubiquitin-dependent proteasome degradation pathway

Although some proteins are quite unstable and this degradation by the ubiquitin-proteasome system occurs most of the time, some proteins are only degraded at a particular time, in response to a particular event or at particular locations. For example, the anaphase promoting complex (APC/C) E3 ligase gets phosphorylated and activated upon entry into mitosis. The APC/C mediated degradation of the cyclin B1 protein is spatially controlled as proteolysis seems to occur in the mitotic spindle. Other times a protein has to be modified by processes like glycosylation or phosphorylation, in order for the E3 ligase to recognise it and target it for proteolysis. Controlling when proteins are degraded is important for enhancing the specificity and timing of ubiquitin-proteasome degradation (Pines and Lindon, 2005).

The ubiquitin-dependent proteasome degradation pathway regulates a number of cellular processes. For example, it regulates the differences in expression of cyclins and CKIs throughout the cell cycle. It is crucial to maintain functioning degradation pathways as any deregulation of for example an SCF complex might play a role in carcinogenesis. The cellular role of cyclins and CKIs and their E3 ligases is correlated with aspects of breast cancer (Ohta and Fukuda, 2004). One of the cullin genes, CUL-4A has been implicated in breast cancer as it was reported to be amplified and overexpressed in primary breast cancers (Chen et al., 1998).

Inhibition of the 26S proteasome results in cell cycle arrest and apoptosis. Therefore dysregulation of this system may result in carcinogenesis and drug resistance, making the proteasome a novel target in cancer therapy. Indeed clinical trials are on going with the proteasome inhibitor Bortezomib. Bortezomib is a boronic acid dipeptide that is quite specific for the proteasome. It was approved by the FDA for the treatment of advanced multiple myeloma in patients who had relapsed after at least two prior treatments and were resistant to the previous treatment (Rajkumar et al., 2005). It has been reported to activate c-Jun N-terminal kinase activation and inhibit nuclear factor-kappa B leading to apoptosis (Mitsiades et al., 2002a; Mitsiades et al., 2002b).

E3 ligases

E3 ligases are the most varied proteins of the pathway. They are responsible for the direct substrate recognition and are classified into Ring-H2-finger domain, HECT domain and U-box domain families (Ang and Wade Harper, 2005). These

three families differ in the way they transfer ubiquitin to their substrates. With E3 ligases containing the HECT domain, ubiquitin is first transferred to the HECT E3 ligase and then to the substrate whereas the RING E3 ligases transfer ubiquitin directly from the E2 enzymes onto the target proteins (Ho et al., 2006). U-box E3 ligases mediate polyubiquitination in the presence of enzymes E1 and E2. In the absence of E3 U-box proteins they catalyse polyubiquitination by targeting lysine residues of ubiquitin other than lysine 48, which is utilized by HECT and RING finger E3 enzymes (Hatakeyama et al., 2001).

The best characterized of the RING E3 ligase is the SCF ubiquitin ligase which is composed of S-phase kinase associated protein 1 (Skp1) (Bai et al., 1996; Zhang et al., 1995), Cdc53/CUL-1 (Lisztwan et al., 1998; Lyapina et al., 1998), the Roc1/Rbx1 ring finger protein (Kamura et al., 1999; Ohta et al., 1999; Tan et al., 1999) and one of many F-Box proteins. Other domains may also be part of the SCF complex but are probably not important for its ubiquitinating activity. Cdc53/CUL-1 binds Skp1 through its N-terminal domain while the C-terminal of cullin binds Roc1/Rbx1. CUL-1 is a member of the cullin family (containing CUL-1-CUL-5 and Apc2), and their function is to recruit E2 enzyme into the E3 ubiquitin ligase complex and they also organize and activate the ubiquitin ligase complex. Some cullins, like CUL-3, has been shown to control the stability of cyclin E. Roc1/Rbx1 is essential for the ubiquitinating activity of the SCF complex. It also associates CUL-1 with the E2 enzyme. The role of F-Box proteins is to ensure specific substrate recognition and many of the F-Box subunits facilitate the ubiquitination of various substrates. The F-Box binds Skp1, which is the subunit facilitating ubiquitination by spatially orientating the SCF

subunits and the substrate proteins (Ang and Wade Harper, 2005). Substrate recognition by F-Box proteins is usually dependent upon certain modifications of the substrate proteins like phosphorylation or glycosylation (Feldman et al., 1997; Nash et al., 2001; Orlicky et al., 2003; Skowyra et al., 1997). Phosphorylation also allows regulation of the degradation of the substrate when SCF complexes are active throughout the cell cycle. The SCF complex itself can also be subject to post-translational modifications. The winged-helix B domain of the cullin subunit can undergo neddylation, in which the ubiquitin-like Nedd8-α protein binds a lysine residue on a substrate protein (Lammer et al., 1998).

E3 ligases can also be important to determine a person's predisposition to cancer. The N-terminal RING finger domain of BRCA1 has a ubiquitin ligase activity when bound to the RING finger protein BARD1. This ubiquitin ligase activity of BRCA1-BARD1 can be abolished by mutations in this RING finger domain of BRCA1 found in many familial breast cancers. Analysis of those mutations are important for the determination of the effect they have on biological function of BRCA1 and its role as a tumour suppressor as well as to predict an individuals predispotion to cancer (Hashizume et al., 2001; Ohta and Fukuda, 2004). Mutations have also been found in the *BRAD1* gene in breast and ovarian cancer patients (Thai et al., 1998). In recent years, a series of studies have focused on elucidating ubiquitination-related mechanisms in carcinogenesis.

Another, very well studied E3 ligase is the anaphase promoting complex/cyclosome or APC/C. Like SCF it is also a member of the Ring-H2-finger-containg E3 ubiquitin-ligase family but whereas SCF is functional

throughout the cell cycle, APC/C functions during mitosis and G_1 phase. APC/C mediates the ubiquitin dependent degradation of mitotic cyclins and anaphase inhibitors. It also contains a similar ring finger protein to Roc1/Rbx1 named Apc11 (Ohta et al., 1999).

The importance of determining the functions of F-Box proteins and their involvement in cancer is very well illustrated by the F-Box protein Fbw7, which has been shown to catalyse the ubiquitination of the oncogene c-Myc, cyclin E, c-jun and Notch. Fbw7 was originally shown to be linked to the degradation of Notch/LIN-12 in *C elegans*. Its frequent loss in cancer cells is linked to the activation of c-Myc, a transcription factor regulating proliferation, differentiation and apoptosis (Welcker et al., 2004; Yada et al., 2004). c-Myc degradation by Fbw7 occurs by phosphorylation by GSK3β at Thr-58 (Ang and Wade Harper, 2005). Its knockdown in U2OS osteosarcoma cells has been shown to increase cell size, consistent with its ability to regulate c-myc levels in the nucleolus (Welcker et al., 2004). Therefore, *Fbw7* acts as a tumour suppressor gene. Fbw7 knockout mice die at approximately 10 days of gestation with many defects in heart, vascular and haematopoietic development. Furthermore, colon cancer cell lines lacking *Fbw7* have increased levels of cyclin E, overexpression of which leads to genomic instability (Ang and Wade Harper, 2005).

Another well-characterised F-Box protein is the Skp2 (Fbl1). It is an important regulator of cell proliferation and has C-terminal leucine-rich repeats that are important for protein-protein interactions. Skp2 also binds Skp1 forming an E3 ligase complex mediating the ubiquitination of cyclin E and the CDK inhibitor

$p27^{Kip1}$ (Carrano et al., 1999; Sutterluty et al., 1999; Zhang et al., 1995). Skp2 recognises $p27^{Kip1}$ in a phosphorylation-dependent manner (Carrano et al., 1999). It also binds the cyclin A-CDK2 complex making it very important for S phase entry.

The cell regulates the activity of Skp2 primarily by regulating its levels throughout the cell cycle. Its levels vary during the cell cycle, being first detectable at the G_1-S transition point, accumulating at S and G_2 and decreasing at mitosis (Ang and Wade Harper, 2005). Levels of Skp2 are being regulated by the ubiquitin-mediated protein degradation pathway. It is degraded by the anaphase-promoting complex (APC^{CDH1})(Wei et al., 2004). Moreover, Skp2 is subject to degradation through autoubiquitination which is known to be negatively regulated by the cdc kinase subunit 1 (Cks1). Cks1 binds Skp2 and plays a very important role in the ubiquitination of $p27^{Kip1}$. Upon phosphorylation of threonine-187, $p27^{Kip1}$ binds to Cks1 and Skp2, both of which are being degraded by APC^{cdh1} (Wang et al., 2004).

Skp2 has been shown to exert oncogenic potential in breast epithelial cells and is overexpressed in many breast carcinomas (Signoretti et al., 2002). It has also been shown to ubiquitinate and lead to the degradation of the Forkhead transcription factor FOXO1, an action dependent upon AKT phosphorylation at Ser-256. Skp2 abolishes the inhibitory role of FOXO1 in proliferation and survival, showing again the importance of Skp2 in tumorigenesis (Huang et al., 2005). Skp2 also influences c-Myc stability and has been shown to play a role in promoting *c-Myc*

transcriptional activation but also overexpression of Skp2 promotes c-Myc ubiquitination (Kim et al., 2003b).

Some F-Box proteins have functions not directly related to the SCF complexes. For example, in budding yeast, three F-Box proteins were bound to Skp1 but they were not part of an SCF complex. Skp1 here plays a critical structural role in the CBF-3 protein complex assembly by activating the Ctf13 F-Box protein. CBF-3 is composed of p110 (Ndc10), p64 (Cep3), p58 (Ctf13) and Skp1 and plays a role in the kinetochore. The mechanism of activation is independent of SCF. Skp1's associated F-box protein interacts with other proteins in a way reminiscent of the SCF (Bouck and Bloom, 2005; Kitagawa et al., 1999).

Furthermore, some F-box proteins function independently of their F-box motif or their interaction with Skp1. Some times, an F-Box protein associates with Skp1 and the SCF complex to regulate its own degradation or even others (Hermand, 2006). For example, the APC inhibitor Rca1/Emi1 prevents premature cyclin degradation. The F-box of Rca1 is not important for its inhibitory effect on the APC, but along with its interaction with components of the SCF, is required for an unknown function at the G_1 -S transition (Zielke et al., 2006).

Noteworthy is the existence of the F-Box protein Fbx2 that has been proved to bind Skp1 but not the other parts of the complex, cullin-1 and ROC-1. This protein bound to Skp1 is thought to form a novel heterodimeric complex and may form a non traditional complex that has a different function (Nelson et al., 2007).

Previous research in our laboratory has shown that Skp2 is involved in the degradation of cyclin D1 in the MCF-7 breast cancer cell line. Interest in finding proteins related to Skp2 that may be involved in cyclin D1 regulation, led to the identification of the novel FBXL20 F-Box protein. Like Skp2, the FBXL20 protein has an F-box domain and C-terminal LRR repeats. FBXL20 has been shown to interact with Skp1 suggesting a possible role for FBXL20 in the ubiquitin dependent proteasomal degradation of target proteins. In contrast to Skp2, FBXL20 was found to localise in the cytoplasm of rat liver epithelial cells and its expression increased in growth-arrested cells, indicating that although both proteins bind Skp1 and are structurally related, they probably have different cellular functions (Ilyin et al., 1999).

Recently, a very similar protein to FBXL20, FBL2 was shown to have a geranylgeranylation site, CAAX (CVIL), in the very end of the coding sequence that is important for binding the hepatitis C virus (HCV) nonstructural protein 5A (NS5A). The binding of NS5A to FBL2 doesn't require the F-Box. Experimental observations like, siRNA-mediated knockdown of FBL2 in Huh7-HP cells reduced HCV RNA by 65%, lead to the conclusion that geranylgeranylated FBL2 binding to NS5A plays an important role in HCV RNA replication (Wang et al., 2005a).

I.11 The Forkhead box M1 transcription factor (FoxM1)

FoxM1 is part of the mammalian Forkhead box transcription factor family that includes at least 50 proteins (Costa, 2005). This family is characterized by a winged-helix DNA-binding motif. FoxM1 is the only Forkhead transcription factor shown to exhibit proliferation-dependent expression and it is one of the most important regulators of the G_1/S and G_2/M transitions. The levels of FoxM1 increase at the onset of S-phase and persist until the end of mitosis (Laoukili et al., 2005). The G_1/S transition is controlled by FoxM1 by decreasing the nuclear levels of the cyclin- dependent kinase inhibitors $p21^{Cip1}$ and $p27^{Kip1}$. Inhibition of these two CDK inhibitors has been linked to a FoxM1-induced transcriptional increase in the expression of Skp2 and Cks1 (Wang et al., 2005b). At the G_1/S phase FoxM1 also increases the levels of the Cdc25A phosphatase which activates Cdk2-cyclin E activity.

For progression through the G_2/M transition FoxM1 has been shown to be important for the transcription of a number of proteins including, cyclin B1, Cdc25B, Polo-like kinase 1 (PLK1), survivin, Aurora B kinase, the centromere protein A (CENPA) and CENPB (Wang et al., 2005b). Cdc25B and Cdc25C phosphatases dephosphorylate and activate Cdk1 leading to activation of the cyclin B1-Cdk1 complex and progression through the G_2/M phase of the cell cycle. PLK1 phosphorylates and activates these phosphatases. PLK1 is also very important for centrosome duplication and along with Aurora B kinase facilitate attachment of spindle microtubules to the kinetochore complex on the centrosomes (Meraldi et al., 2004). Aurora B kinase is important for cytokinesis and chromosome segregation (Meraldi et al., 2004). Furthermore, FoxM1 is very

important for chromosome stability. FoxM1 depleted cells show a high degree of polyploidy, abnormal chromosome segregation and a significantly reduced G_2/M progression (Laoukili et al., 2005).

Additionally, translocation of FoxM1 to the nucleus, just before entry into the G_2/M phase, requires the activity of the c-raf/MEK/MAPK pathway (Ma et al., 2005). Furthermore, the activity of FoxM1 regulated genes is suppressed when the RAF/MEK/MAPK pathway is inhibited by the specific MEK-1 inhibitor UO126. In cells treated with UO126, synchronized S-phase cells become arrested in the following G_2 phase with a concomitant decrease in cyclin B-CDK1 kinase activity (Roberts et al., 2002; Wright et al., 1999). All these reports have demonstrated that there is a link between the RAF/MEK/MAPK pathway and FoxM1 in regulating G_2/M transition (Ma et al., 2005).

PROJECT AIMS

This project aims to lead to a better understanding of the mechanism of action of HDACi, using the well known hydroxamic acid TSA as a model of HDACi. This will be done by examining the role of TSA on one of its novel targets, the protein FBXL20, in the MCF-7 breast cancer cell line. Since FBXL20 has not been characterized in human cells this project will firstly aim to chracterize this protein in breast cancer cells. The effect of this protein on the TSA-induced inhibition of proliferation and the induction of cell cycle arrest and cell death will then be examined. Lastly this work also aims to identify a novel HDACi that is more potent but less toxic than the HDACi SAHA, currently used in the clinical setting. Using the structure of SAHA, novel HDACi will be developed and analysed for their ability to inhibit HDACS and the proliferation of breast cancer cells.

CHAPTER II

MATERIALS AND METHODS

Data bank analyses

The NCBI databases and blast programmes were used for DNA and protein sequence analysis.

Cell culture

The MCF-7 breast cancer cell line was used for the experiments. They were maintained in Dulbecco's modified eagle medium (DMEM) (Life Technologies Gibco/BRL, Paisley, UK) supplemented with 10% foetal calf serum and L-Glutamine-Penicillin-Streptomycin solution (2mM L-glutamine, 100U/ml penicillin and 100μg/ml streptomycin). Cultures were maintained at 37°C, in 10% CO_2 humidified atmosphere. For oestrogen depleted conditions, cells were grown in phenol red-free DMEM supplemented with 5% (v/v) dextran-coated charcoal-stripped fetal calf serum, 2mmol/L L-glutamine, 100units/mL penicillin, and 100μg/ml streptomycin.

Cell line maintenance

Cells were split 1:5 twice a week. Media was aspirated and cells were washed once in PBS followed by washing once with trypsin. After cells were detached by the addition of trypsin, they were resuspended in the appropriate media and seeded into new plates. Cells were cultured for approximately 35 passages before discarding.

Chemicals

Cycloheximide (Sigma-Aldrich, Dorset, UK) was dissolved in DMSO and stored at -20°C at a concentration of 10mg/µl. **TSA** (Sigma-Aldrich, Dorset, UK) was dissolved in ethanol at 10mM concentration and stored at -20°C. **SBHA** (Sigma-Aldrich, Dorset, UK) was dissolved in DMSO at 10mM concentration and stored at -20°C. **SAHA** and the **novel HDAC inhibitors** (provided by Prof. Marson) were dissolved in DMSO at 10mM concentration and stored at -20°C.

PCR

PCR amplification was performed using a Taq DNA polymerase Kit (West Sussex, Qiagen). Reaction solutions contained DNA template (1µg), 0.5µM of forward primer, 0.5µM reverse primer, 1x PCR buffer, 1x Q solution, 0.2nM dNTP, 0.5U Taq polymerase and ddH_20 to a final volume of 50µl. cDNA was denatured at 94°C for 3min, followed by 22-35 cycles of annealing and a final 10min extension at 72°C. PCR reactions were carried out using a DNAEngine Peltier Thermal Cycler (BIO-RAD) using the following programme: A initial denaturation step for 3min at 94 °C, followed by 22-35 cycles of denaturation for 1min at 94 °C, annealing for 1min at 50-68°C depending on the oligonucleotides utilised, extension at 72°C for 1min/kb DNA followed by a final extension for 10min at 72 °C.

The FailSafe PCR PreMix Selection Kit and defined oligonucleotide primers were used to amplify the complete *FBXL20* cDNA. The kit contains a FailSafe PCR enzyme mix containing a 3' to 5' proofreading DNA polymerase and a set of twelve reaction premixes containing a buffered salt solution with all four dNTPs

and various amounts of $MgCl_2$ and FailSafe PCR enhancer (with betaine). PCR mix contained: 25µl of each FailSafe PCR 2X Premix, 0.5µl of *FBXL20* forward primer (100pmol/µl), 0.5µl *FBXL20* reverse primer (100pmol/µl), DNA template and ddH_20 in a 50µl final volume. 35 cycles were performed and the annealing temperature was 58°C. For a control reaction, DNA was substituted with the equivalent amount of ddH_20. After amplification, PCR products were separated and visualized on an ethidium bromide-stained 1% agarose gel, using a 100bp molecular marker.

Primer	**Sequence**	**Gene**	**Annealing Temp °C**
FBL20RF2-F	5'-catgaggagggacgtgaacg-3'	*FBXL20*	*58*°C
FBL20RF-R	5'-aaggttgaccacctccattg-3'	*FBXL20*	*58*°C
FBL2-R	5'-tggcatctgtgatgttggag-3'	*FBXL20*	*58*°C
FBL2-F	5'-tgagtgagggatgtccactg-3'	*FBXL20*	*58*°C
FBL2BamH1	5'-ccggatcctaggatggatgcagc-3'	*FBXL20*	*58*°C
FBL2xhoI	5'-ccgctcgagaggagggacgtgaac-3'	*FBXL20*	*58* °C
GAPDH-F	5'-tcccatcaccatcttcca-3'	*GAPDH*	23 °C
GAPDH-R	5'-catcacgccacagtttcc-3'	*GAPDH*	23 °C
ACTIN-F	5'-tctggcaccacaccttctacaatgagctgcg-3'	*Actin*	23 °C
ACTIN-R	5'-cgtcatactcctgcttgctgatccacatctgc-3'	*Actin*	23 °C

Table 2.1 Primers used for PCR and RT-PCR in human cell lines.

It is sometimes necessary to re-amplify the PCR product by a second step PCR. This form of PCR is described as 'Semi-Nested' or 'Nested PCR' depending on whether either primer or both primers are substituted in the second reaction. All reactions were carried out using the same conditions as for normal PCR except that 2µl of the first step PCR was used as the template.

Production of recombinant vector

FBXL20 cDNA (1200bp) (GenBank accession number: BC007557) was amplified from human breast carcinoma MCF-7 cDNA using the forward primer FBL2xhoI and the reverse FBL2BamH1 that contain restriction sites. PCR products were digested and cloned into the X*hoI* and *BamHI* sites of the PSG5 vector (4.7kb) containing a Flag-tag. Genes cloned into the multiple cloning sites of vectors will be expressed as fusions to the C-terminus of *Flag* if they are in the same reading frame as the Flag epitope and there are no intervening stop codons.

Digestion

The *FBXL20* cDNA and vector DNA were digested with the appropriate restriction enzymes in a 20µl reaction mixture containing up to 5µg DNA, 2µl 10x Buffer, 1.0µl (10units) of *BamHI* and X*hoI* enzymes, and ddH_20. Incubation for 1-3h at the appropriate temperature was followed in incubators or PCR cyclers with heated leads to minimize evaporation of the sample. Aliquots of each sample where then mixed with 5x agarose gel loading buffer containing bromophenol blue and run on agarose gels to ensure complete digestion and verify the sizes of the fragments.

Calf intestine alkaline phosphatase treatment

In order to prevent self-ligation of vector plasmids with compatible sticky ends, calf intestine alkalike phosphatase treatment (CIAP) treatment was carried out as follows: after restriction enzyme digestion and DNA purification, linearised plasmids were eluted in 20µl of sterile distilled water. 16µl of the elutant, was mixed with 20 units of CIAP (Fermentas) and 2µl of the 10x dephosphorylation

buffer supplied by the manufacturer in a 20µl reaction mixture. The mixture was incubated for 2h at 37°C, followed by agarose gel electrophoresis and DNA purification as described above.

Agarose gel electrophoresis

One % (w/v) agarose gels were made up with 1x Tris-acetate buffer (40mM Tris-acetate, 1mM EDTA, pH 8.0) and 1µg of ethidium bromide. Samples were electrophoresed by applying a constant current (100V) through the gel. Separated DNA fragments were visualised using a UV transilluminator. Where required, the DNA fragment from the gel was cut out using a razor blade for subsequent purification.

DNA extraction from agarose gel

DNA restriction fragments separated on agarose gels were purified using the QIAquick Gel Extraction Kit (Qiagen), according to the manufacturer's instructions. After agarose separation DNA was viewed with a long wavelength ultraviolet emission (UV) transilluminator and the required band cut out using a scalpel and transferred to an eppendorf tube. The gel fragment was dissolved by adding 3 volumes (per weight of gel slice) of QG buffer (QIAquick spin kit, Qiagen) and incubating at 50°C for 10min. The sample was then transferred to a QIAquick spin column and microcentrifuged for 1min, after which the DNA in the column was washed with 0.75ml of PE buffer (QIAquick spin kit, Qiagen). Residual wash buffer was removed by centrifugation for 1min at full speed. DNA was eluted in a microcentrifuge tube by adding 30µl of ddH_2O and centrifugation for 1min.

Ligation

Ligation of FBXL20 with the PSG5 vector was performed using T4 DNA ligase. This enzyme catalyses the formation of a phosphodiester bond between juxtaposed 5' phosphate and 3' hydroxyl termini in duplex DNA or RNA. Vector is treated with alkaline phosphatase to remove 5' terminal phosphates so to prevent vector from self-ligating. The ligation reaction included 1.0µl 10x T4 DNA ligase buffer (1x = 50mM Tris-HCl,10mM $MgCl_2$, 10mM DTT, 1mM ATP, 25µg/ml BSA, pH 7.5), 1.0µl T4 DNA ligase, 1:3 vector/DNA ratio and ddH_20 to a final volume of 10µl. Samples were incubated at 4°C overnight or for few hours at room temperature.

Transformation

Sub-cloning efficiency DH5α competent cells (Invitrogen LT, Paisley, UK) were used according to manufacturer's protocol. DH5α competent cells were removed from -70 °C freezer and defrosted on wet ice. Required number of autoclaved 1.5ml microcentrifuge tubes was placed on wet ice. 100µl of competent cells was used for each reaction. 5µl of the DNA ligation reaction was added and the mixture was incubated on ice for 30min. Cells were then heat-shocked for 45s at 37°C and then tubes were placed on ice for 2min. 900µl of room temperature LB Broth was added in each tube and then incubated with shaking at 225rpm for 1h at 37°C to express kanamycin or ampicillin resistance. Centrifugation at 6000rpm for 5min in a microcentrifuge was followed. 900µl of the reaction mixture was removed and pellet was resuspended with 100µl LB and spread on LB agar plates. Plates were incubated overnight at 37°C.

Media and maintenance

Bacterial Competent cells were grown in either Luria-Bertani (LB) broth or LB Agar. LB Agar was made by mixing 37g/L of LB agar pellets (Miller) with deionized water and LB Broth was made by mixing 20g/L of LB broth powder (Sigma) with deionized water. Autoclaving for 20min at 120°C was folllowed.

Preparation of plasmid DNA

- Minipreps

Individual colonies were picked from the plate using a sterile loop and inoculated in 2ml of selective media containing kanamycin or ampicillin. Further treatment varied according to the scale of the plasmid preparation. For "minipreps" (up to 20μg DNA) the minicultures were incubated overnight at 37°C in a bacterial shaker. The QIAprep Spin Miniprep Kit protocol (Qiagen Ltd.) was used according to the manufacturer's protocol. 1.5ml of culture was then transferred to an eppendorf tube and centrifuged at 5000rpm for 5min in bench top microfuge. Pelleted bacterial cells were resuspended in 250μl Buffer P1 (50mM Tris-HCl pH 8.0, 10mM EDTA, 100μg/ml RNAse A). 250μl of buffer P2 (200mM NaOH, 1% SDS) was then added and solution was gently inverted 4-6 times to mix. 350μl Buffer N3 (3.0M sodium acetate, pH 5.5) was added and tube was again inverted gently 4-6 times. Centrifugation for 10min at 13,000rpm formed a compact white pellet. Supernatant was transferred to QIAprep Spin Columns and centrifuged for 30-60s. Flow-through was discarded and column was washed by adding 0.5ml Buffer PE and centrifuging for 30-60s. Flow-through was discarded and centrifugation step was repeated to remove residual wash buffer. The QIAprep column was then placed in a clean 1.5ml microcentrifuge tube and the DNA was

eluted with 50µl of ddH_2O.

- **Maxipreps**

For Maxipreps the Qiagen Hi speed plasmid maxi kit was used. 250ml of LB containing 100µg/ml ampicillin or kanamycin was inoculated with 1ml of an 8h bacteria culture. Cultures were incubated at 37°C overnight with vigorous shaking. Bacterial cells were then harvested by centrifugation at 6000x g for 15min at 4°C. Pellet was resuspended in 10ml Buffer P1(50mM Tris-HCl pH 8.0, 10mM EDTA, 100µg/ml RNAse A) followed by addition of 10ml of Buffer P2 (200mM NaOH, 1% SDS) and 10ml of Buffer P3 (3mM potassium acetate pH 5.5). The solutions were mixed and lysates were poured into the barrel of the QIAfilter Cartridge followed by incubation at room temperature for 10min. The solution was added to a previously equilibrated HiSpeed Maxi Tip (by addition of 10ml Buffer QBT), washed with 60ml Buffer QC (1M NaCl, 50mM MOPS pH 7.0, 15% ethanol) and DNA was eluted with 15ml Buffer QF (1.25M NaCl, 50mM Tris-HCl pH 8.5, 15% Ethanol). DNA was precipitated by adding 10.5ml isopropanol and incubated at room temperature for 5min. The eluate/isopropanol was filtered through a syringe that was attached to QIAprecipitator Maxi Module, 70% ethanol is added and the QIAprecipitator is removed from the syringe and the plunger was removed. Qiaprecipitator was then attached again and the plunger was inserted and by pressing air through the QIAprecipitator the membrane was dried. QIAprecipitator was then attached to a 5ml syringe and 1ml of buffer TE (10mM Tris-HCl, 1mM EDTA, pH 8) was added to elute DNA into a collection tube.

DNA quantification

The concentration of DNA was measured using a BioRad spectrophotometer (Bio-rad Smart Spec^{TM}3000 Spectrophotometer) by measuring the optical density (OD) of the samples at 260nm. The formula used to calculate DNA concentration was: 1 OD unit at 260nm = 50μg/ml ddDNA

DNA sequencing

Each sequencing reaction was prepared using 3.2pmol of a forward primer or reverse primer and 1μg DNA in a total volume of 10μl made up with ddH_2O. Prepared samples were sent to MRC Genomics Core Laboratory at Imperial College London (Hammersmith Hospital Campus) for sequencing.

Transfection of plasmid DNA

Transfection is the general process of bringing foreign DNA into cells and monitoring protein expression. A liposome-mediated transfection method was performed using the Fugene 6 transfection reagent which complexes and transports DNA into the cells. Fugene 6 is a proprietary blend of lipids and other components supplied in 80% ethanol, sterile filtered and packaged in polypropylene tubes. Twenty four hours prior to transfection, 2-3 x 10^5 cells per well of a 6-well plate were plated so that they reached 50-80% confluency on the day of transfection.

For transfection in 6-well plates, containing a monolayer of cells that is 50-80% confluent, transfection was made using Fugene 6 (μl) to DNA (μg) amounts of 3:1 respectively. Before Fugene 6 Reagent:DNA complex was added, wells are

washed with PBS and medium replaced. Complexes were added directly to cells growing in 2ml media (DMEM 10%FCS) and incubated for 5h after which cells were washed again with PBS buffer and fresh medium added.

Western Blotting or SDS-PAGE

Cells where harvested and then lysed with Hepes lysis buffer (50.0mM Hepes buffer (pH 7.5), 10mM NaCl, 1% Triton-x 100, 1% glycerol, 5mM $MgCl_2$, 1mM EDTA in dH_20) containing protease inhibitors [Pepstatin, Leupeptin, Trypsin inhibitor, Aprotinin, Na_2VO_3 (200mM), PMSF (100mM)] for 30min on ice followed by centrifugation for 10min at 4°C. Pellets were discarded and supernatants transferred in clean tubes. 20µg of protein was mixed with 4x Nupage LDS sample and 1µl of 1M DTT. Samples were then boiled for 2min at 100 °C followed by centirfugation at 8000rpm for 30s. 20µl of each sample and 5µl of marker are loaded on 4-12% gels and transferred onto nitrocellulose or PVDF membranes (Hybond P; Amersham Biosciences UK Limited, Little Chalfont, UK). Electrophoresis is carried out according to standard protocols. Gels were made of a lower resolving gel [0.375M Tris pH8.8, acrylamide, 0.1% (w/v) SDS, 0.1% (w/v) APS, 0.1% (v/v) TEMED] and an upper stacking gel [0.126M Tris pH6.8, acrylamide, 0.1% (w/v) SDS, 0.1% (w/v) APS, TEMED] according to Table 2.2. Samples were run at a constant current of 100V in running buffer (25mM Tris-base, 250mM Glycine, 0.1% (w/v) SDS). Then gel and apparatus were assembled in the blotting apparatus (Bio-Rad Laboratories Trans-Blot cell) and the proteins transfered to the membrane electrophoretically at 400mA for 1h in transfer buffer (24mM Tris, 193mM glycine, 20% v/v methanol). Afterwards, non-specific sites were blocked for 1h with blocking buffer [5% (w/v) non-fat dried milk (Marvel, Premier Brands) in 136 mM NaCl,

120 mM Tris (pH 7.6) with 0.05% (v/v) Tween 20 (TBS-T)] at room temperature with shaking. Blots were incubated with primary antibody overnight. Membranes were washed four times with TBS-T for 15min each and then incubated with secondary antibody for 20min with shaking at room temperature. After washing again with TBS-T, bands were visualized by enhanced chemiluminescence (Supersignal West Pico; Perbio Science UK Ltd., Cheshire, UK). Membranes were incubated for 5min with Luminol enhancer solution and then placed in a plastic membrane protector, all air bubbles are removed between the blot and the surface of the membrane protector before exposure to autoradiography film (Kodak BioMax ML-light or MR-1).

	Resolving gel				**Stacking gel**
	7%	**10%**	**12%**	**14%**	**5%**
dH_20-ml	5.02	4.02	3.35	2.68	3.67
1.5M Tris pH8.8	2.5	2.5	2.5	2.5	-
1.5M Tris pH 6.8	-	-	-	-	0.42
30%Acrylamide/ 0.8% Bis mix (37.5:1)	2.33	3.33	4.00	4.67	0.83
10% SDS -µl	100	100	100	100	50
25% APS -µl	40	40	40	40	20
TEMED-µl	10	10	10	10	10
Total-ml	10	10	10	10	5

Table 2.2 SDS-PAGE gels

Determination of protein concentration

Protein concentration was determined using the Bio-Rad D_c protein assay (Bio-Rad Laboratories), as instructed by the manufacturer. The reaction between protein and copper in the alkaline solution and the Folin reagent reduced by the copper-treated protein leads to color development. 20µl of reagent S was added to 1 ml of reagent A. 100µl of this mixture were added to 2µl of protein solution and subsequently mixed with 800µl of reagent B. After 15min incubation, absorbance was read at 750nm for each of the experimental samples, with protein concentrations ranging from 200 µg/ml to 1.0 mg/ml. Protein concentrations were determined by the equation absorbance x 25 = µg/µl.

Antibodies

The antibodies used were:

mouse-monoclonal anti-SP1 (sc-420, Santa Cruz Biotechnology, Santa Cruz, CA)

rabbit polyclonal anti- α tubulin (sc-5546 Santa Cruz Biotechnology, Santa Cruz, CA)

goat polyclonal anti-actin (sc-1615, Santa Cruz Biotechnology, Santa Cruz, CA)

rabbit polyclonal anti-FoxM1 (sc-502, Santa Cruz Biotechnology, Santa Cruz, CA)

mouse monoclonal anti-$p45^{Skp2}$ (32-3300, Zymed S.San Francisco,California,USA)

rabbit polyclonal anti-HDAC1 (ab7028; Abcam Ltd., Cambridge, U.K.)

goat polyclonal anti-HDAC2 (sc-6296, Santa Cruz Biotechnology, Santa Cruz, CA)

rabbit polyclonal anti-CUL-1 (ab2964, Abcam Ltd., Cambridge, U.K.)

rabbit polyclonal anti-ROC-1 (RB-9287-P0, NeoMarkers, Fremont, CA)

mouse monoclonal anti-$p19^{Skp1}$ (P46020, BD Biosciences, Oxford, U.K.)

mouse monoclonal anti-FLAG (M2 antibody, F1804, Sigma-Aldrich, Dorset, U.K.)

rabbit polyclonal anti-Bim [Y36] (ab32158-100, Abcam Ltd., Cambridge, U.K.)

rabbit anti-acetylated-histone 3 (AcH3) (ab9045-50, Abcam Ltd., Cambridge, U.K.)

mouse monoclonal anti-$p21^{Cip1}$ (sc-6246, Santa Cruz Biotechnology, Santa Cruz, CA)

rabbit polyclonal anti-Bad (#9292, New England Biolabs, Hitchin, Herts, U.K.)

rabbit polyclonal anti-Bax (sc-493, Santa Cruz Biotechnology, Santa Cruz, CA)

Immunoprecipitation

Cells were plated in 10cm plates and grown to 60% confluency in the appropriate medium and growth conditions. 24h after transfection of the specified recombinant vector, cells were harvested and lysed in 1ml lysis buffer (50mM Tris HCl, pH7.4, 150mM NaCl, 1mM EDTA, 1% Triton x 100 containing protease inhibitors) as descibed above. One tenth of solution was kept and loaded as a control. The lysate was incubated with the indicated antibody for 3h at 4°C on an orbital shaker. 30µl of the 50% protein G sepharose slurry, which was previously washed four times in lysis buffer, was then added to the cell lysate/antibody mix and the samples were incubated at 4°C overnight on an orbital shaker. Following incubation, the beads were collected by centrifugation at 4°C for 30s at 1000rpm in a microcentrifuge and washed 4 times with 1ml of lysis buffer. The beads were then re-suspended in 20µl of loading buffer and boiled for 5min to dissociate the immuno-complexes from the beads. The beads were separated from the loading buffer by centrifugation and the supernatant was then loaded onto SDS-PAGE gels for protein fractionation.

Sulphorhodamine B (SRB) assay

SRB is a water-soluble dye that binds to the basic amino acids of cellular proteins. Thus, colorimetric measurement of the bound dye provides an estimate of the total protein mass that is related to the cell number. In this assay, cells were seeded in

96 well plates and incubated overnight. The cell number was such that the cells reach confluency on the last day of the assay. In this study, 3,000 cells per well were used. On the day of harvesting 100µl of ice cold 40% trichloroacetic acid (TCA) was added to each well for 1h at 4 °C. The plate was then washed five times with tap water. 100µl of 0.4% SRB in 1% acetic acid was then added to each well for 1h at room temperature. The plate was washed five times with 1% acetic acid and left to air dry at room temperature. On the day of reading the plates, bound dye was solubilised by adding 100µl of 10mM Tris base and placed on a plate shaker for 30min. Absorbance was read on an Anthos 2001 plate reader at 492nm.

Rapid amplification of 5' and 3' cDNA ends PCR (RACE-PCR)

The GeneRacer kit (Invitrogen LT), which provides a method to obtain unknown full-length 5' and 3' ends of genes, was used in this study, according to the manufacturer's protocol. It is based on RNA ligase-mediated rapid amplification of 5' and 3' cDNA ends (RLM-RACE) and oligo-capping rapid amplification of cDNA ends (RACE) methods. The 3' RACE method was used in this work to obtain the 3' end of the rat FBL2.

For amplification of the 3' ends of genes, mRNA was converted to cDNA by reverse transcription, using an oligo-dT adapter primer, binding the poly(A)tail of mRNAs. Specific cDNAs could then be amplified by using a 5' gene specific primer that anneals to known regions of exons and a 3' adapter primer that targets the poly(A)tail. A reverse transcription reaction is performed using the Superscript III first-strand synthesis system for RT-PCR according to the

manufacturer's protocol (Invitrogen LT). In detail, 10nM dNTP, sterile water and primers were first mixed and incubated at 65 °C for 5min. This was then mixed with 4µl of 5x first strand buffer, 1µl 0.1M DTT, 1µl RNaseOut (40U/µl) and 1µl SuperScript III RT (200U/µl) to a final volume of 20µl per reaction. The samples were incubated at 50°C for 60min followed by a 15min at 70°C inactivation step. 1µl RNase H (2U) was then added and the reaction mix was incubated at 37°C for 20min. Solutions were stored at –20°C or used directly for PCR amplification. PCR products were then purified and sent for DNA sequencing. Samples were sent for sequencing to MRC Genomics Core Laboratory at Imperial College London (Hammersmith Hospital Campus). Each sequencing reaction was prepared using 3.2pmol of primer, 30-90ng/1kb DNA in a total volume of 10µl made up with ddH_2O.

RNA interference

RNA interference (RNAi) is a post-transcriptional process leading to the silencing of genes. It is triggered by double-stranded RNA molecules that cause sequence-specific mRNA degradation of homologous single-stranded target RNAs and the translated products (Tuschl and Borkhardt, 2002). RNAi is initiated by the conversion of dsRNA into 21-23 nucleotide fragments by the RNase III enzyme, Dicer. These short RNAs are called small interfering RNAs (siRNAs), containing two nucleotide single-stranded overhangs at the 3' end and bearing 5'-monophosphate and 3'- hydroxyl groups which are crucial for the degradation of target RNAs complementary to the siRNA sequence. siRNAs are incorporated into the RNA-induced silencing complex (RISC), in an ATP-dependent step or series of steps during which the siRNA duplex is unwound into single strands.

The resulting single-stranded siRNA is proposed to guide the RISC to recognize and cleave the target RNA without requirement of other nucleotide cofactors (Schwarz et al., 2002).

In this study, genes were silenced using the SMARTpool TM Product Insert-Version 2.0 (DHARMACON, RNA technologies). The SMARTpool siRNAs used were: siFBXL20 (M-015029-00), siFoxM1 (M-009762-00), siSkp2 (M-003324-04), siHDAC1 (M-003493-02), siHDAC2 (M-003495-02), siBim (M-004383-02). Oligofectamine (Invitrogen LT) was used as the transfection reagent. 200,000 cells per well of a 6-well plate, were plated 24h prior to transfection. For each well, 70µl of OPTIMEN, was mixed with 5µl oligofectamine and incubated at room temperature for 10min. This solution was then mixed with 250µl Optimem and 7.5µl (50nM final concentration) siRNA oligos specific for each gene. After 25min incubation, 160µl OPTIMEM was added to each mixture, reaching a final volume of 500µl, which was then added to the wells that have been previously washed with warmed PBS. The final concentration of siRNA oligos in each well was 50nM. After 4h of incubation 2ml of DMEM containing 10%FCS was added to each well.

As a control reaction for the experiment, cells were subjected to transfection with the 1x Universal Buffer (Mock) (without any siRNA added), in order to detect cellular effects caused by the transfection event or delivery process. As another control, cells were also transfected with a non-specific (NSC) siRNA (D-001210-01-05, Dharmacon) in order to detect off-target effects caused by the introduction of any siRNA. These siRNAs have an impaired ability to be processed by RISC

and share little or no homology with known mRNA targets in the cell. It is a more biologically relevant control than the Mock transfection control, as NSC siRNAs are expected to have similar properties such as charge density and molecular weight. Their effects in the cell, if any, may be through non-RNAi pathways and for this reason may be used to check for general side effects associated with siRNA delivery.

RNA extraction

Total RNA was prepared by harvesting cells and extracted by guanidine isothiocyanate lysis followed by silica gel membrane purification (RNeasy kit, Qiagen Ltd., West Sussex, U.K.). Cells were disrupted by adding buffer RLT (Qiagen) containing 10% β-mercaptoethanol. Samples were homogenized, and 1 volume of 70% ethanol was added. 700µl of the sample was added to an RNeasy mini-column placed in a 2ml collection tube and centrifuged at 10,000rpm for 15s in a microcentrifuge. Flow-through was discarded and 700µl of buffer RW1 (Qiagen) was added followed by centrifugation for 15s at 10,000rpm. Flow-through was again discarded. The RNeasy column was transferred to a new collection tube and 500µl RPE (Qiagen) buffer was added. The centrifugation step was repeated again. Another 500µl RPE was added followed by centrifugation at 10,000rpm for 2min. The RNeasy column was then transferred to a new collection tube, 50µl RNase free water was added and centrifuged at 10,000rpm for 1min to elute RNA. The concentration and purity of RNA were determined by measuring the spectrophotometric absorption at 260nm and 280nm.

Real-time Quantitative PCR (RT-QPCR)

Total RNA from samples was extracted using the RNeasy kit as explained above. RNA was then converted to cDNA using the Superscript III First-strand synthesis system for RT-PCR (Invitrogen LT) as described above. Real time PCR was performed with ABI PRISMÒ 7700 Sequence Detection System using 2x SYBR Green Mastermix (Applied Biosystems) according to manufacturer's instructions. One minute annealing at 60°C was used for 40 cycles. Gene-specific primer pairs were designed using the ABI Primer Express software. Primers were designed so that they produce a fragment of 50-150bp. When possible, primers spanned intron/exon boundaries to avoid amplification of contaminating genomic DNA. The primers used are listed in Table 2.3. Analysis was performed using the relative standard curve method. For the standard curve, 1-2µg cDNA from each sample was mixed and diluted 1:2 and then 1:4 for four serial dilutions. As a control, primers for the L19 ribosomal housekeeping protein were used to normalize input RNA. The samples were diluted 1 in 4 and 2µl from each was used per reaction. The reaction mix also contained 23µl of SYBR Master Mix and the appropriate amount of primers which have been previously optimized, to a final volume of 25µl. All measurements were performed in triplicates. The TAQMAN 7700 Real-time PCR machine was used. Efficiency of PCR was obtained from the slope of the standard curve (Eff = 10(-1/slope) -1). 90-110% was expected with optimal primers with slope between -3.1 and -3.6.

Primer optimisation

Each primer set was optimized with 10ng cDNA standard to determine the minimum concentration required for maximum yield and minimum non-specific

amplification. Dilutions of 50-900nM forward and reverse primers (table 2.4) were tested with different combination (table 2.3). The concentration that gave the lowest Ct value with standard DNA and highest with water was used in further experiments. Specificity of PCR product was confirmed by agarose gel electrophoresis. The concentrations of primers used to amplify FoxM1 and L19 were optimized by Dr. Rosaline Hui and Dr. Demetra Constantinidou.

	Forward Primer		
Reverse primer	**50nM**	**300nM**	**900nM**
50nM	50/50	300/50	900/50
300nM	50/300	300/300	900/300
900nM	50/900	300/900	900/900

Table 2.3 Combination of different primer concentrations

The concentrations of primers used were:

For *L19*: 900nM Forward primer /300nM Reverse primer

For *FoxM1*: 300nM Forward primer /900nM Reverse primer

For *Bim*: 300nM Forward primer/900nM Reverse Primer

For *FBXL20, Skp2, HDAC1, HDAC2*: 300nM Forward primer/300nM Reverse primer.

RT-QPCR PRIMER	SEQUENCE (5'-3')	GENE
FoxM1-F	TGCAGCTAGGGATGTGAATCTTC	*FoxM1*
FoxM1-R	GGAGCCCAGTCCATCAGAACT	*FoxM1*
FBXL20-F	GGATATTGAGGGCCGAGTAGTG	*FBXL20*
FBXL20-R	AAGCCCCCACATCGTTTTG	*FBXL20*
Skp2-F	AAACCTGGGCCACCCG	Skp2
Skp2-R	TTGTCACTCCCTTTGCTCTTCA	*Skp2,*
L19-F	GCGGAAGGGTACAGCCAAT	*L19*
L19-R	GCAGCCGGCGCAAA	*L19*
Bim-F	CACAAAACCCCAAGTCCTCCTT	*Bim*
Bim-R	TTCAGCCTGCCTCATGGAA	*Bim*
HDAC1-F	CGATGAGGACGAAGACGACC	*HDAC1*
HDAC1-R	TCACAGGCAATTCGTTTGTCA	*HDAC1*
HDAC2-F	TTGGAGGAGGTGGCTACACAA	*HDAC2*
HDAC2-R	ACAATCAAGGGCAACTGCAGT	*HDAC2*

Table 2.4 RT-QPCR primer sequences

Propidium Iodide (PI) staining and FACS (cell cycle) analysis

Cells were treated as indicated. Floating and adherent cells were collected by centrifugation and washed with PBS. Cells were resuspended in 10% PBS with 90% ethanol and stored at -20°C. On the day of analysis, samples were centrifuged to remove ethanol and stained by resuspension in PBS containing propidium iodide (final concentration of PI: 50μg/ml) and RNase A (5μg/ml) for

30min at 4°C. The cell suspension was subsequently passed through a 0.6 mm bore needle in order to generate single cell suspensions and samples were then analyzed on a FACSCalibur flow cytometer (Becton Dickinson, Oxford, UK) using the FACSDiva™ (BD Biosciences) acquisition software. Graphs represent the percentage of cells (Y-axis) in each phase of the cell cycle determined by their DNA contents (X-axis). Data were acquired using a minimum of 10,000 single cells defined by a dot plot of PI width versus PI area.

Sub-cellular fractionation

The NE-PER nuclear-cytoplasmic kit (Perbio, Erembodegem, Belgium) was used to separate and prepare cytoplasmic and nuclear extracts from asynchronously growing human breast cancer cells, according to the manufacturer's instructions. Fistly, the two reagents named CERI and CERII were added to the cell pellet, causing distruption of the cell membrane and release of cytoplasmic contents. After recovering the intact nuclei from the cytoplasmic extract by centrifugation, the nuclei were lysed with another reagent named NER to yield the nuclear extract. The protease inhibitors mentioned above, were firstly added to the reagents CERI and NER before addition to the pellets.

Alternatively, cytoplasmic, membrane/organelle and nuclear fractions were prepared using a ProteoExtract® Subcellular Proteome Extraction Kit (Calbiochem, VWR International Ltd., Lutterworth, United Kingdom) according to the manufacturer's instructions.

Extracts were then used for immunoblot analysis. The purity of the cytoplasmic fraction was analysed by immunoblotting with the antibody against tubulin and the nuclear lysate with an antibody against Sp1.

Fluorescence microscopy

MCF-7 cells were plated on coverslips and transfected with FBXL20-GFP (obtained from RZPD, Berlin, Germany) or GFP alone. 24h later, coverslips were washed gently with PBS and fixed in methanol for 5min. The cells were subsequently mounted in Vectashield mounting medium containing 4', 6'-diamidino-2-phenylindole dihydrochloride (DAPI) (Vector Laboratories Ltd., Peterborough, UK) to counterstain DNA and analyzed using a fluorescence microscope.

Immunofluorescent cytochemical staining

Cells were grown on coverslips and transfected with Flag-FBXL20 with Fugene 6 as described above. 24h later cells were washed with PBS and then fixed with PBS containing 4% paraformaldehyde for 15min at room temperature (RT). Cells were then washed four times with PBS for 5min each. PBS was removed and cells were permeabilized by incubation with 0.25% Triton x-100 in PBS for 30min at RT. Cells were washed again with PBS for 10min followed by blocking by incubation with 10% BSA blocking solution for 30min at RT. Antibody for phaloidin that stains the actin filaments, in blocking solution was then added for 1h. The monoclonal anti-Flag antibody (200μg/ml), in blocking solution was then added in order to bind to the Flag-FBXL20 in the cells for 1h followed by washes with PBS. Secondary antibody anti-mouse FITC conjugate in blocking solution

was added and incubated for 45min. Cells were again washed with PBS and then stained with DAPI for 3-4 min to identify the nuclei. Coverslips were put on microscope slides and examined by fluorescent microscopy.

HDAC Fluorimetric Assay

The HDAC Fluorimetric Assay/Drug Discovery Kit (AK-500, Biomol International) was used according to the manufacturer's instructions. This assay is designed to measured HDAC activity in cells. It is based on the *Fluor de Lys* (Fluorogenic Histone deAcetylase Lysyl Substrate/Developer) substrate and developer combination. The *Fluor de Lys* substrate comprises an acetylated lysine side chain which is incubated with a sample containing HDAC activity. Deacetylation of the substrate sensitizes the substrate so that after the addition of the *Fluor de Lys* developer there is production of a fluorophore. During measurement, a microplate fluorimeter (Fluorskan Ascent FL from Thermofisher UK) was used capable of excitation at a wavelength in the range of 350-380nm and detection of emitted light in the range 440-460nm.

Firstly, compounds diluted in the provided assay buffer are added to the wells in a final volume of 10µl. The HeLa nuclear extract, which was used as the source of HDAC activity, was then added to all wells except those that were used as "no enzyme controls" in a volume of 15µl. The Fluor de Lys substrate and the samples in the plate were equilibrated to assay temperature of 25 °C. HDAC reactions were then initiated by the addition of 25µl of the diluted substrate in each well and incubated for 20min. Reactions were stopped by adding the Fluor de Lys developer (50µl) and incubated at room temperature for 10-15min. Samples were

then read in the fluorimeter. As a positive control, the HDAC inhibitor TSA was used at 1μM concentration.

Sample	Assay Buffer	HeLa Extract (Dilution)	Inhibitor (5x)	*Fluor de Lys*™ Substrate (2x)
Blank (No Enzyme)	25 µl	0	0	25 µl
Control	10 µl	15 µl	0	25 µl
Trichostatin A	0	15 µl	10 µl	25 µl
Test Sample	0	15 µl	10 µl	25 µl

Table 2.5 From Biomol Internation LT instruction manual

Statistical tests

The concentration of the compounds that inhibited cell proliferation by 50% (*IC*50)) was determined graphically in each case with nonlinear regression analysis to fit data to the appropriate dose-response curve (GraphPad Prism version 4.0; Graph- Pad Software Inc., San Diego, CA). The ***Mann-Whitney*** test, is a nonparametric test that compares sums of ranks. ***One- way ANOVA*** was followed by Dunnet's or Bonferrroni test. ***Dunnett's*** test was used when one column represented control data and wanted to compare all other columns to that control column but not to each other. ***Bonferroni test*** was used for selected pairs of columns when wanted to compare certain column pairs. A p value of less than 0.05 was considered significant.

CHAPTER III

CHARACTERISATION OF FBXL20

III.1 BACKGROUND AND OBJECTIVES

FBXL20 (F-Box/Leucine-rich repeat protein 20) belongs to the F-Box group of proteins that are mainly involved in targeting proteins for ubiquitin- dependent degradation by the proteasome. In doing so, they form part of a complex, such as the SCF complex that consists of a cullin family member of proteins, a ROC ring finger protein and the Skp1 protein. An example of a F-Box protein is the well known Skp2 protein, which has been shown to be responsible for the degradation of the cell cycle inhibitor $p27^{Kip1}$(Carrano et al., 1999). Similarly to Skp2, the N-terminal of FBXL20 contains an F-box domain that binds Skp1, whilst the C-terminus contains LRR repeats that bind target proteins. The rat FBXL20 homologue FBL2 was shown to interact with Skp1 suggesting a possible role for FBL2 in the ubiquitin-dependent proteasomal degradation of target proteins (Iliyn et al, 1999). In contrast to Skp2, FBL2 localised in the cytoplasm of rat liver epithelial cells and its expression increases in growth-arrested cells, indicating that although both proteins bind Skp1 and are structurally related, they probably have different cellular functions (Ilyin *et al.*, 1999). Additionally, Skp2 has been shown to be transcriptionally regulated by the FoxM1 transcription factor (Wang et al, 2005). The first aim of this project was to characterize the novel FBXL20 F-Box protein in human cells.

III.2 RESULTS

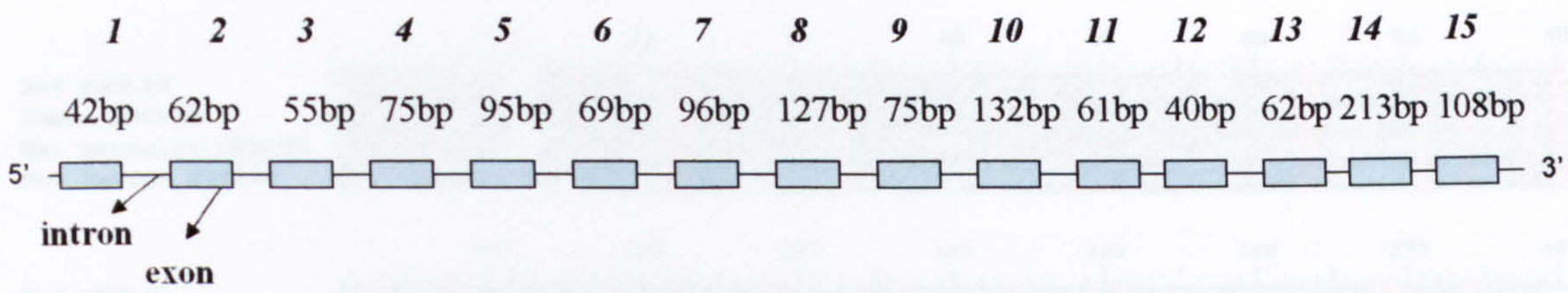
Analysis of the FBXL20 DNA sequence

A GenBank search for the gene encoding the human *FBXL20* (GenBank Accession number BC007557), revealed that this gene is located on chromosome 17. Comparison of the human *FBXL20* cDNA sequence to the human genome allowed the exon/intron organisation of the *FBXL20* gene to be determined (Fig.3.1). Ilyin *et al.* (1999) working on *FBL2* in rat hepatocyte cells performed experiments using only part of the gene observed in human cells. Comparing the sequences between different species it was observed that FBXL20 is very similar in all species (Fig.3.2A) and human FBXL20 is very similar to the human Skp2 F-Box protein (Fig.3.2B). Comparative analysis of the FBXL20 amino acid sequence showed very high levels of homology with the rat counterpart (more than 99% identity); however, mutations or polymorphisms have created a stop codon in the end of exon 10 thereby producing a truncated protein (Fig.3.1). A Blast search for the full-length human FBXL20 sequence in the rat genome revealed that the whole gene exists in the rat cells but it is not expressing a full-length protein. In order to identify the unknown 3' untranslated region of the rat *FBL2*, the 3'-Race technique was performed and sequencing results using the primers FBL216-F (5'-tttccagagggacattgagg-3') FBL721-F (5'-accatatgcagagggtgtca-3) showed that there is a poly-A-tail after the 10th exon in RAT-1 cells (Fig.3.4).

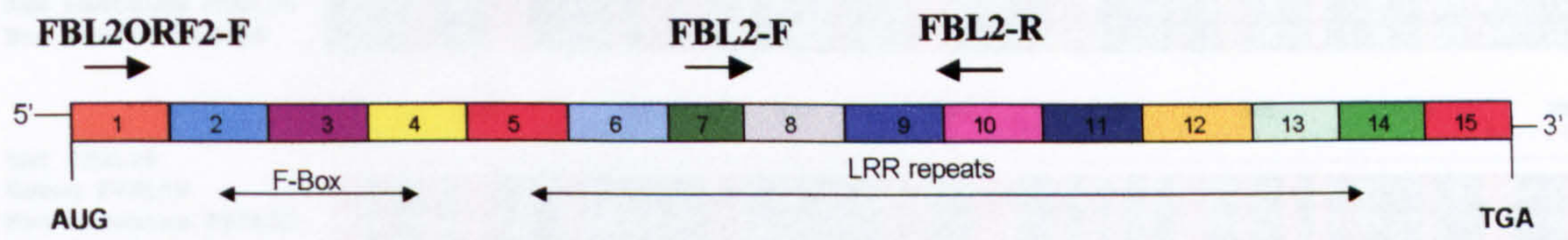
Utilising genome DNA extracted from the human MCF-7 breast cancer cell line, the full length *FBXL20* gene was amplified using the FailSafe PCR kit with the

FBL2ORF2-F and FBL2ORF-R primers. Interestingly, when using the FBL2ORF2-F forward primer and the reverse FBL2-R located in the middle of the *FBXL20* cDNA, two bands were detected on a 1% agarose gel (Fig.3.1C). Both bands were gel extracted and sequenced. Sequencing results indicated a novel splice variant of *FBXL20* lacking exon 7 exists, which was submitted to GenBank (Accession number DQ223959). When the primers FBL2-F (in exon 7) and FBL2-R were used in a PCR reaction, only the full-length FBXL20 band was detected. The forward primer FBL2-F was binding a region in exon 7 and therefore only the full length transcript can be amplified since the splice variant lacks exon 7. However, the open reading frame downstream of the deletion is the same as the full-length FBXL20 cDNA. Identification of the position of the splice donor and acceptor sites was performed using the Blast program. Analysis of the amino acid sequence showed that in addition to the F-box motif located at the N-terminal region, 12 LRR repeats (Fig.3.3) (LxxLxLxxN/CxL)(Kajava et al., 1995) were also found in the C-terminal half of the protein.

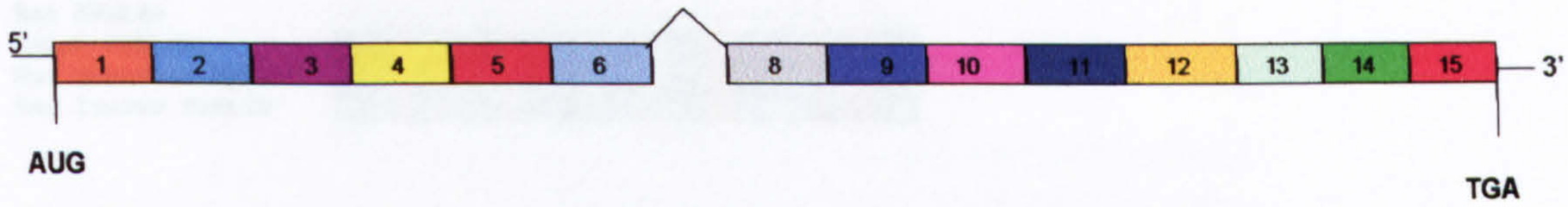
A)



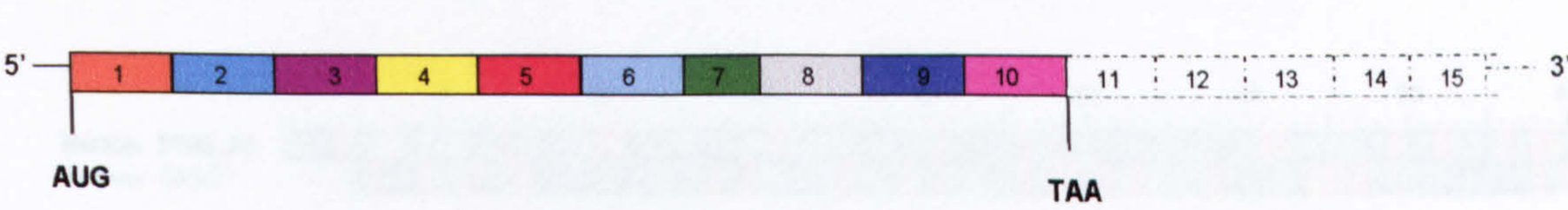
B) **Human FBXL20**



Human FBXL20 splice variant



Rat FBL2



C)

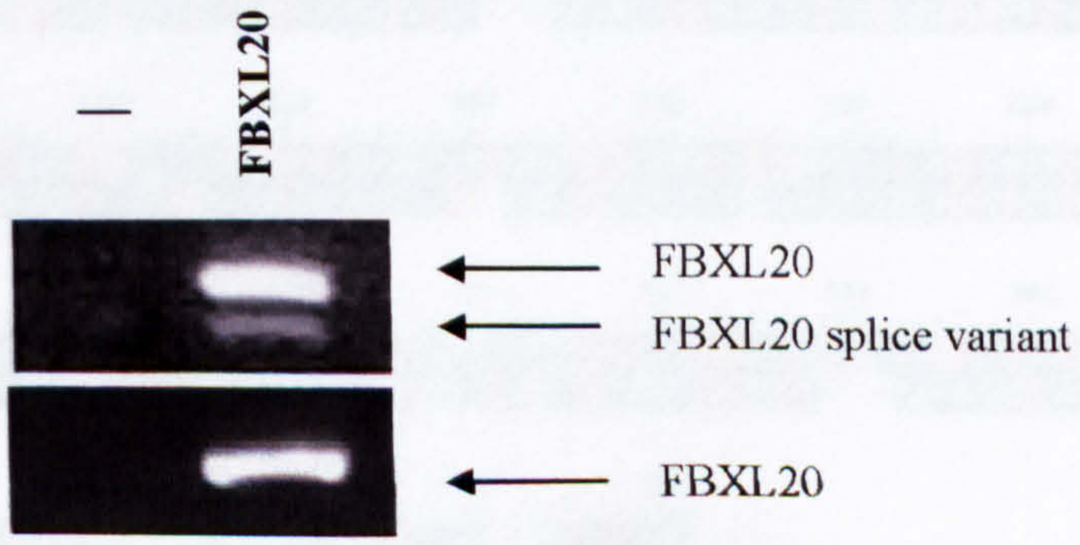
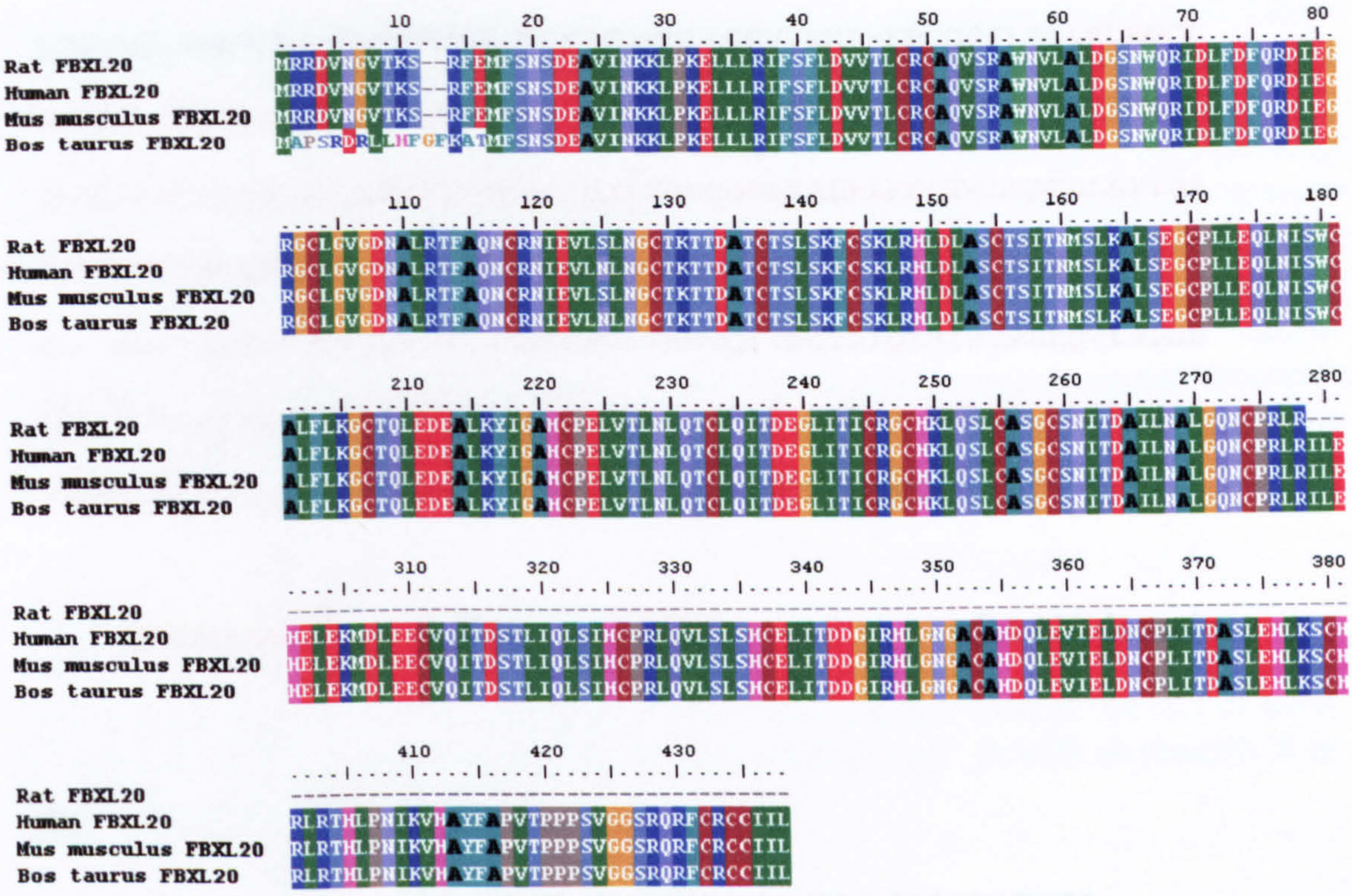


Figure 3.1 *FBXL20* gene organisation. A) Representation of the exon-intron organisation of the *FBXL20* gene. B) Representation of the full length *FBXL20* in contrast to its splice variant and the rat homolog *FBL2*. C) RNA extraction followed by RT-PCR analysis of MCF-7 cells using primers 1) FBL2ORF2-F and FBL2-R and 2) FBL2-F and FBL2-R.

A)



B)

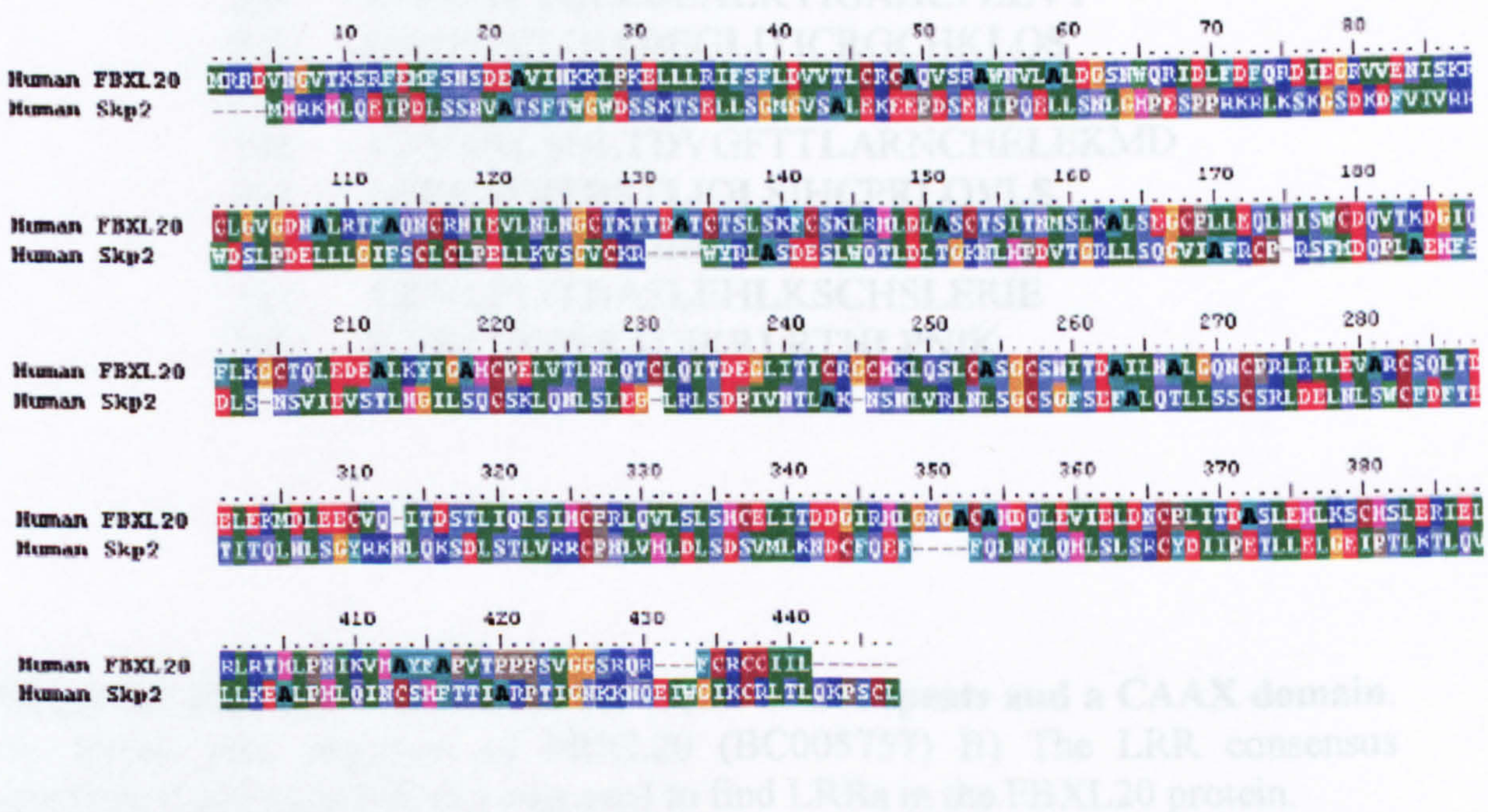


Figure 3.2 Comparison of FBXL20 protein sequences between species (A) and with Skp2 (B). Sequences were obatiend from Genbank with Accession numbers: Rat FBXL20 NM_022272, Bos Taurus FBXL20 NM_001035096, Human FBXL20 BC007557, Mus musculus FBXL20 NM_028149, Human Skp2 NM_005983. In-color alignments were compiled using the BioEdit programme.

A)

MRRDVNGVTKSRFEMFSNSDEAVINKKLPKELLLRIFSFLDVVT

LCRCAQVSRAWNVLALDGSNWQRIDLFDFQRDIEGRVVENISKRCGGFLRKLSLRGCL

GVGDNALRTFAQNCRNIEVLNLNGCTKTTDATCTSLSKFCSKLRHLDLASCTSITNMS

LKALSEGCPLLEQLNISWCDQVTKDGIQALVRGCGGLKALFLKGCTQLEDEALKYIGA

HCPELVTLNLQTCLQITDEGLITICRGCHKLQSLCASGCSNITDAILNALGQNCPRLR

ILEVARCSQLTDVGFTTLARNCHELEKMDLEECVQITDSTLIQLSIHCPRLQVLSLSH

CELITDDGIRHLGNGACAHDQLEVIELDNCPLITDASLEHLKSCHSLERIELYDCQQI

TRAGIKRLRTHLPNIKVHAYFAPVTPPPSVGGSRQRFCRCCIIL

Methionine F-Box LLR repeats CAAX domain

B)

96	LSLRGCLGVGDNALRTFAQNCRNIEV
122	LNLNGCTKTTDATCTSLSKFCSKLRH
148	LDLASCTSITNMSLKALSEGCPLLEQ
174	LNISWCDQVTKDGIQALVRGCGGLKA
200	LFLKGCTQLEDEALKYIGAHCPELVT
226	LNLQTCLQITDEGLITICRGCHKLQS
252	LCASGCSNITDAILNALGQNCPRLRI
278	LEVARCSQLTDVGFTTLARNCHELEKMD
308	LEECVQITDSTLIQLSIHCPRLQVLS
334	LSHCELITDDGIRHLGNGACAHDQLEVIE
363	LDNCPLITDASLEHLKSCHSLERIE
388	LYDCQQITRAGIKRLRTHLPNIK

Figure 3.3 FBXL20 contains an F-Box, 12 LRR repeats and a CAAX domain.
A) Amino acid sequence of FBXL20 (BC005757) B) The LRR consensus sequence (LxxLxLxxN/CxL) was used to find LRRs in the FBXL20 protein.

atgaggagggacgtgaacggagtgaccaagagcaggtttgagatgttctcaaacagtgacgaagccgtaatcaataaa
aaacttcccaaagaactcctgctaaggatattttctttcctggatgttgttacccttgtcgctgtgctcaggtctccagggcc
tggaatgtcctagctctggatggcagtaactggcaacggatagacctgttcgatttccagagggacattgagggccggg
tagtggaaaatatttctaaacgatgcggaggctttttacggaagttaagtcttcgtgggtgtctcggagtaggagacaatgc
actgaggacctttgcacaaaactgtaggaatattgaagtactaagtctcaacggatgtacaaagacgacagacgccacct
gcactagccttagcaagttctgctccaaactcaggcacctcgacctggcttcctgtacgtcaataacaaacatgtctctcaa
agctctgagtgagggctgtccactgttggagcagttgaacatctcctggtgtgaccaagtaaccaaggatggcattcaag
cactagtgagaggctgtgggggtctcaaggccttattcttaaaaggctgcactcagctagaagatgaagctctcaagtac
ataggtgcacactgccctgagctggtgactttgaacttgcaaacttgcttacaaatcacagatgaaggcctcatcaccatat
gcagagggtgtcataagttgcagtctctctgtgcctctgggtgctccaacatcacagatgccatcctgaatgctctaggtc
agaactgccctcggcttagg**taa**acgtgtttatttagctcaaaaaaaaaaaaaaaaaaaaaaaa

Figure 3.4 Sequence of the Rat *FBL2*. FBL2 has a stop codon at the end of exon 10 followed by a poly(A)tail underlined, determined by 3' RACE as described in the materials and methods section.

FBXL20 is expressed in a variety of cancer cell lines

To gain an insight into the possible role of FBXL20, a comparative expression analysis among different cancer cell lines was performed. A commercially available human cancer cell line cDNA panel (BD Biosciences), was used in a PCR amplification reaction using primers FBL2-F and FBL2-R, which detected *FBXL20* in all cell lines (Fig. 3.5).

FBXL20 is expressed at higher levels in growth arrested compared to proliferating cells

The expression of F-Box proteins similar to FBXL20, such as Skp2, has been shown to be cell cycle-dependent. In order to investigate whether the expression pattern of *FBXL20* is cell cycle-dependent, MCF-7 cells were synchronised by serum starvation overnight and then RNA extracted and analysed by RT-QPCR. Cell cycle analysis confirmed that cells were synchronised and that the cells entered S phase after 16 hours of addition of media containing serum (Fig.3.6A). Results showed that *FBXL20* mRNA expression was maximal when cells were arrested (0h) and significantly decreased upon entry into the cell cycle and remained low throughout it. Primers against FoxM1 were used as a control since FoxM1 levels are known to increase after entry into the S phase (Fig. 3.6B).

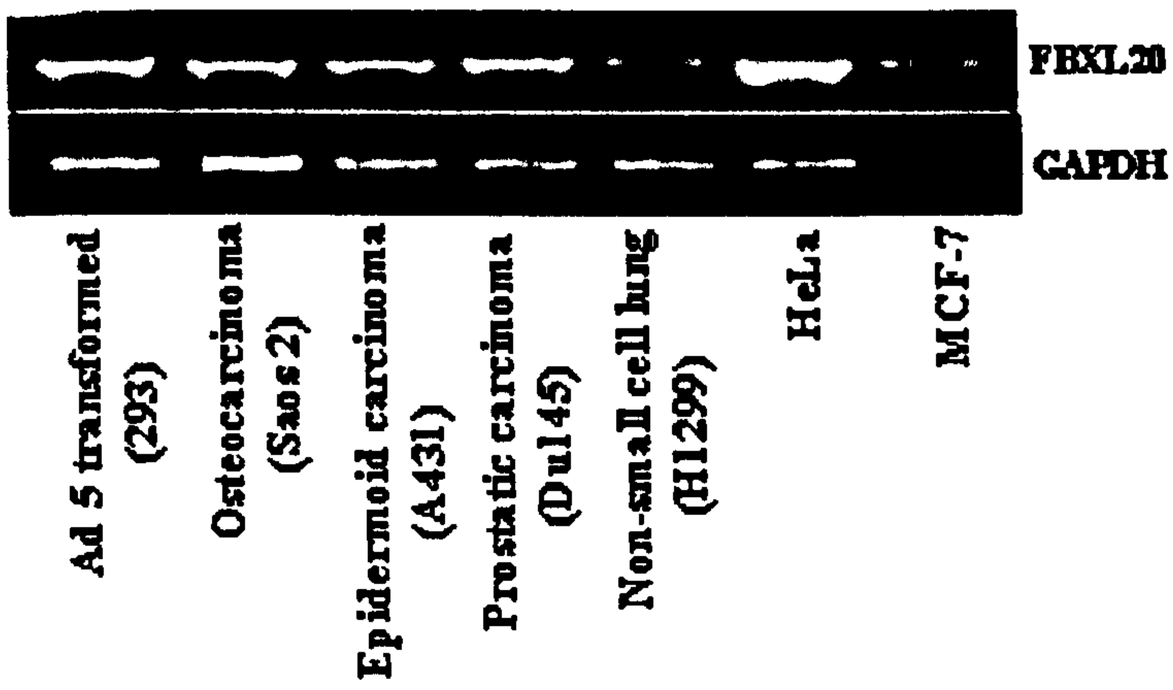
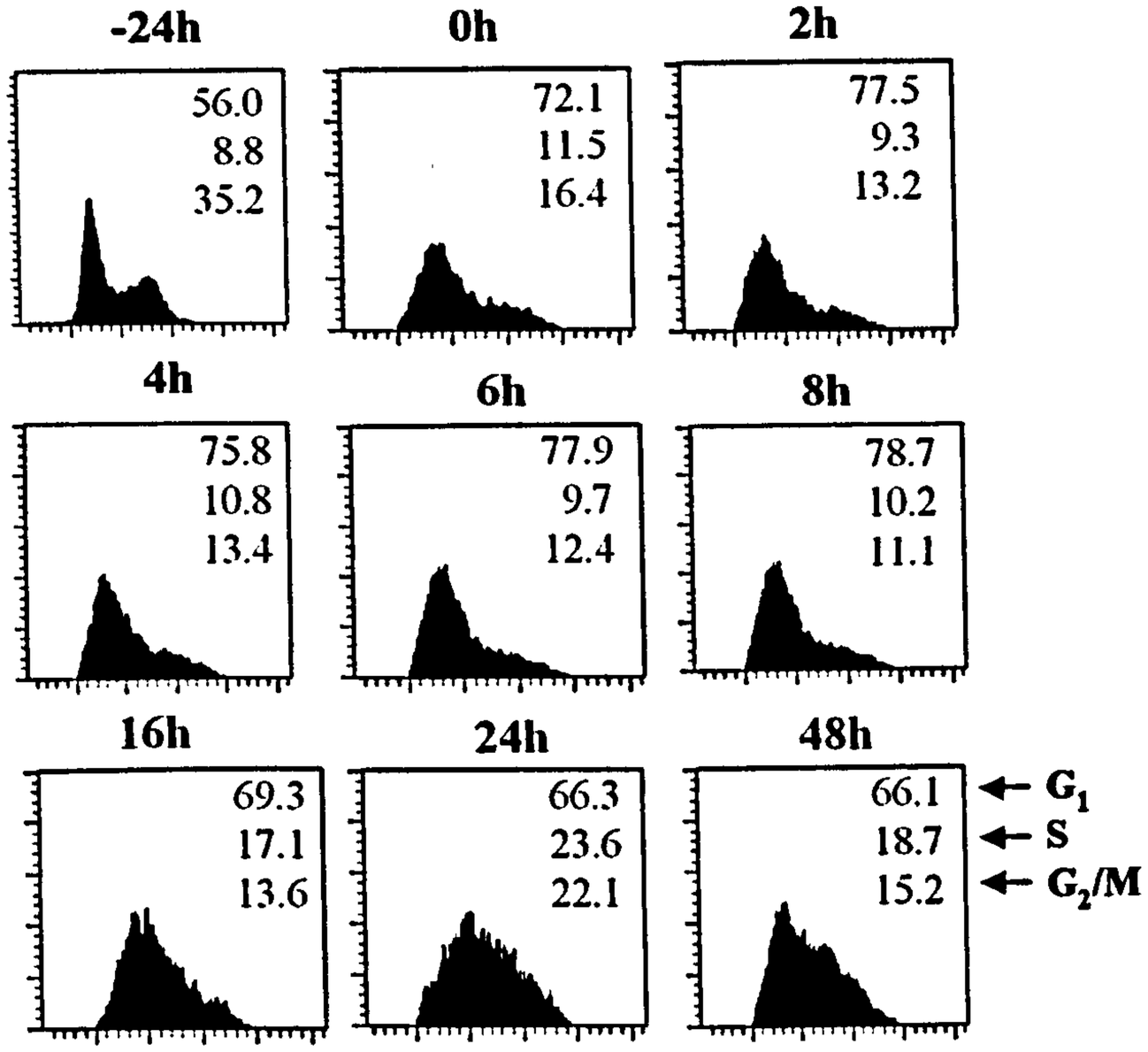


Figure 3.5 *FBXL20* is expressed in a variety of cancer cell lines. cDNA from human cancer cell lines were used in PCR reactions to amplify *FBXL20* using specific primers. *GAPDH* was used as a loading control.

A)



B)

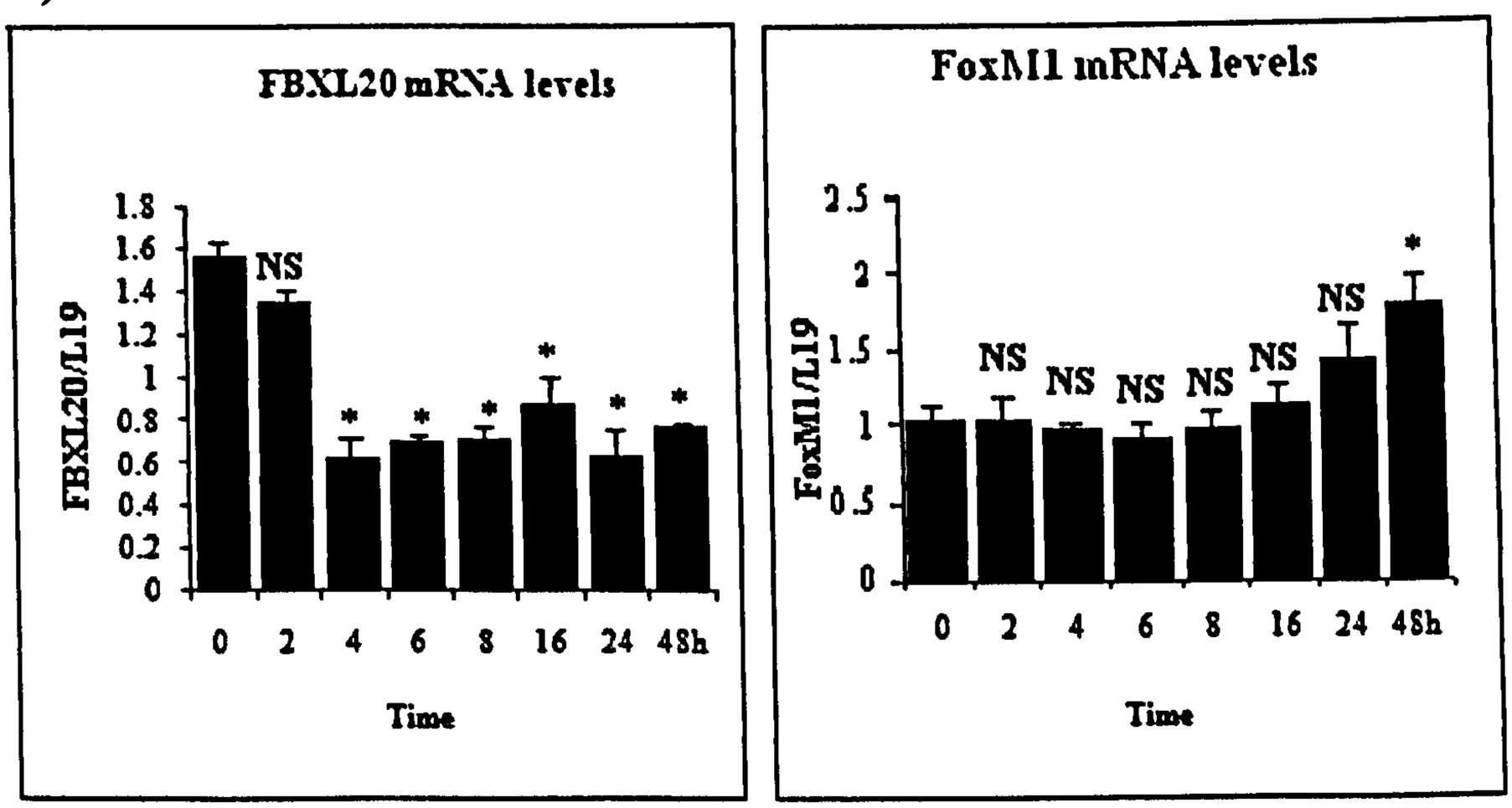


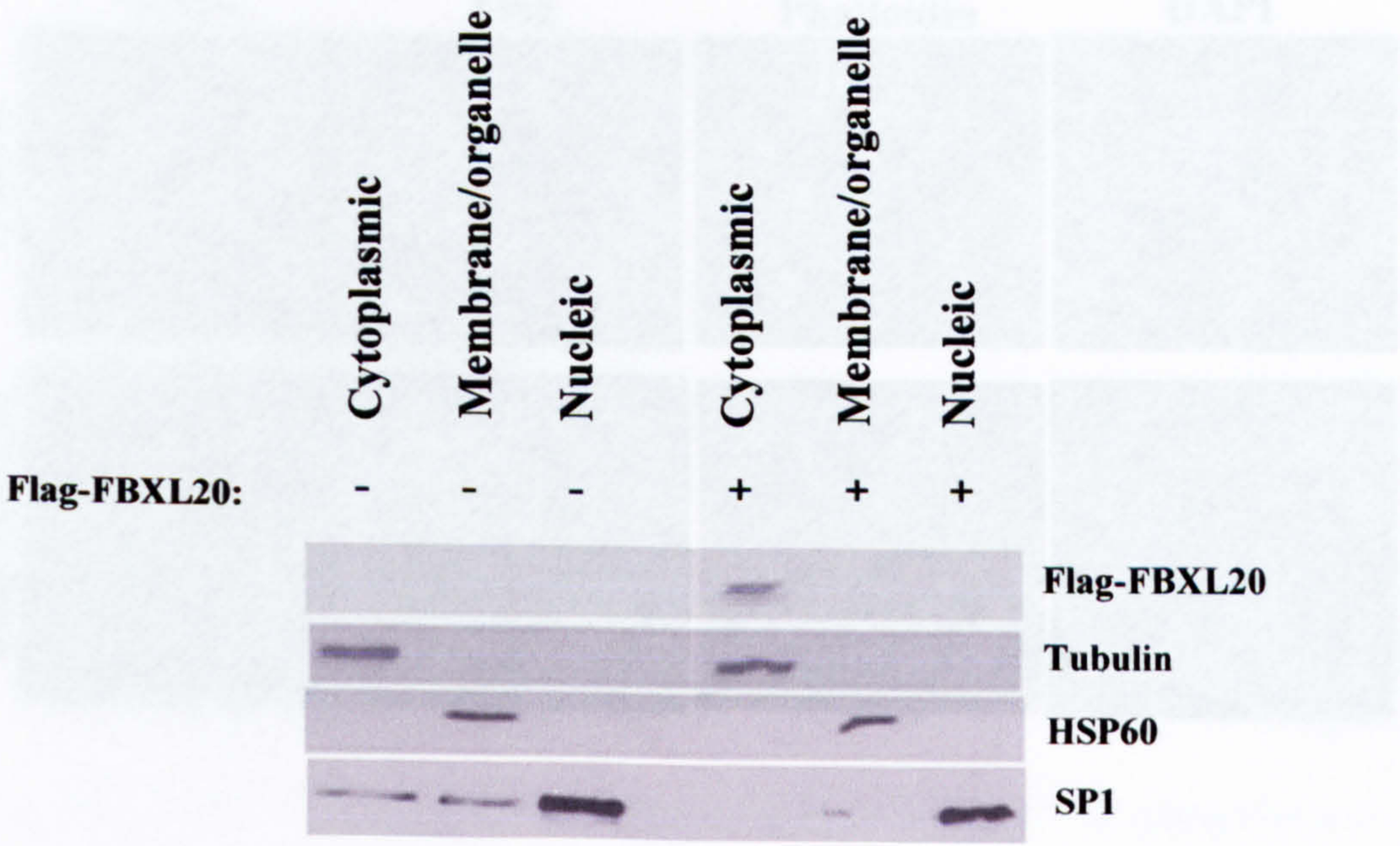
Figure 3.6 *FBXL20* mRNA expression is increased in growth arrested cells. MCF-7 cells were synchronised overnight by serum starvation in a phenol red free medium containing 0.5% DSS, followed by re-entry into the cell cycle after serum addition (0h). Cells were harvested at the indicated times for A) FACS analysis, B) RT-QPCR. Graphs show *FoxM1* mRNA levels normalised by L19 mRNA, and FBXL20 mRNA levels normalised by L19 mRNA levels. Results represent the mean ± SD of three individual experiments. Statistical analysis was performed using ANOVA with Dunnett's post-hoc analysis for all time points compared to control (0 hr) and *$p<0.05$.

FBXL20 is localised in the cytoplasm and mainly concentrated around the nucleus of MCF-7 cells

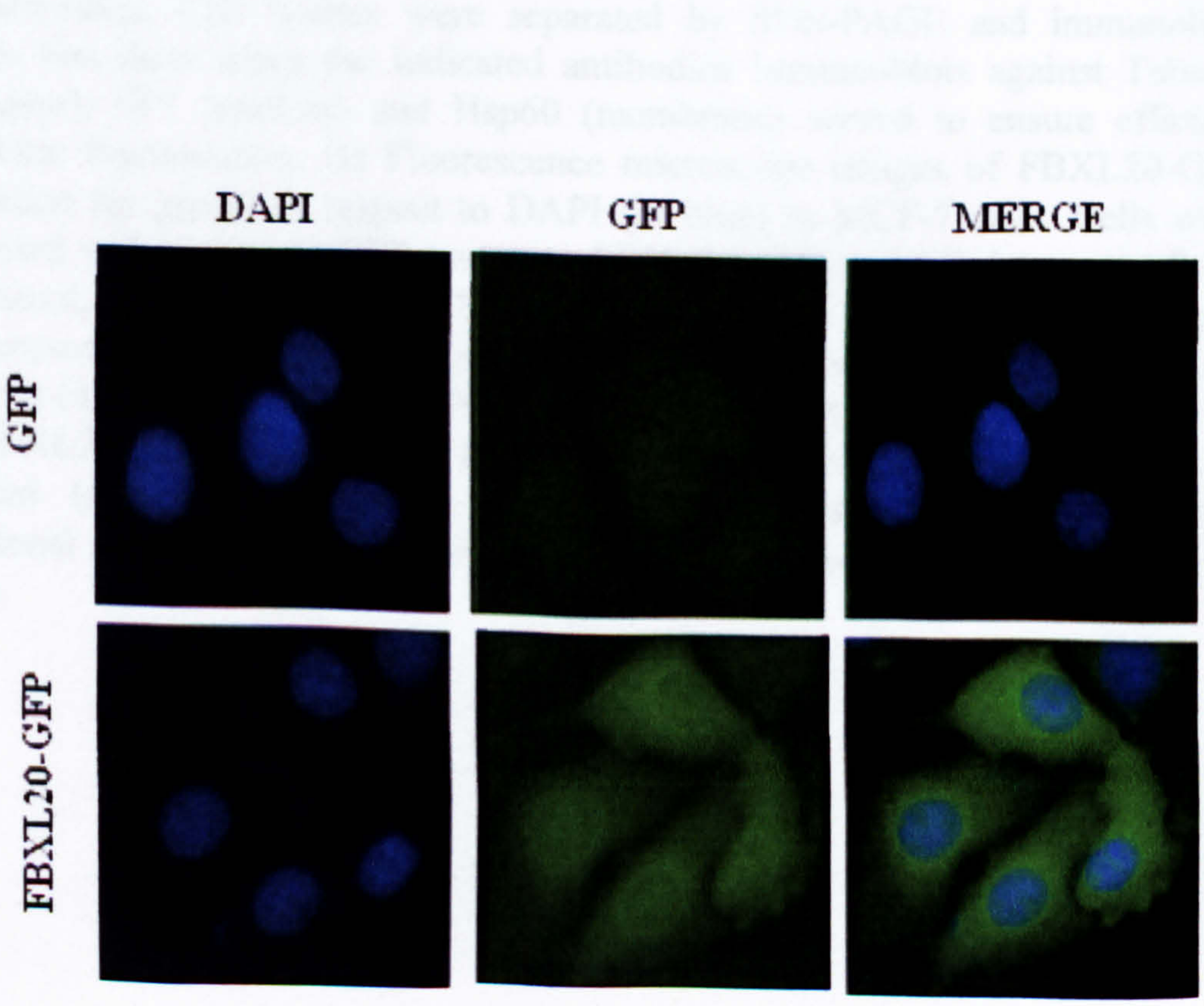
FBXL20 has a CAAX domain in its C-terminus, which has been shown to target proteins, such as FBL2, to the membrane (Wang et al. 2005). In order to test if FBXL20 is localised in the membrane, a sub-cellular fractionation kit was used to separate the nucleus, cytoplasm and membrane fractions of cells. MCF-7 cells, were transfected with Flag-FBXL20 and subsequent SDS-PAGE analysis showed that the exogenous FBXL20 was only expressed in the cytoplasmic fraction (Fig. 3.7A). In order to confirm efficient separation of fractions, antibodies against the membrane protein HSP60, the nuclear SP1 and the cytoplasmic tubulin were used. HSP60 was located in the membrane fraction, SP1 was located in the nuclear fraction and Tubulin was in the cytoplasmic fraction.

In order to examine the subcellular localisation of FBXL20 in MCF-7 cells, it was expressed as a GFP fusion protein for 24h, counterstained with DAPI (nuclear stain) and visualized by fluorescence microscopy. The control cells were transfected with pEGFP-C2 empty vector. FBXL20-GFP was localised in the cytoplasm, with higher intensity around the nuclei (Fig. 3.7B). This was also confirmed by transfecting with Flag-FBXL20 and staining with an anti-Flag antibody. Phalloidin detected the actin filaments and DAPI stained the nuclei. Consistently, fluorescence microscopy revealed Flag-FBXL20 localisation in the cytoplasm, concentrated mainly around the nuclei. Control (not transfected with Flag-FBXL20) cells display a regular distribution of F-actin, with strong staining around cell periphery and in cytoplasm (Fig. 3.7C).

A)


Cytoplasmic
Membrane/organelle
Nucleic
Cytoplasmic
Membrane/organelle
Nucleic
Flag-FBXL20: - - - + + +
Flag-FBXL20
Tubulin
HSP60
SP1

B)


DAPI
GFP
MERGE
GFP
FBXL20-GFP

C)

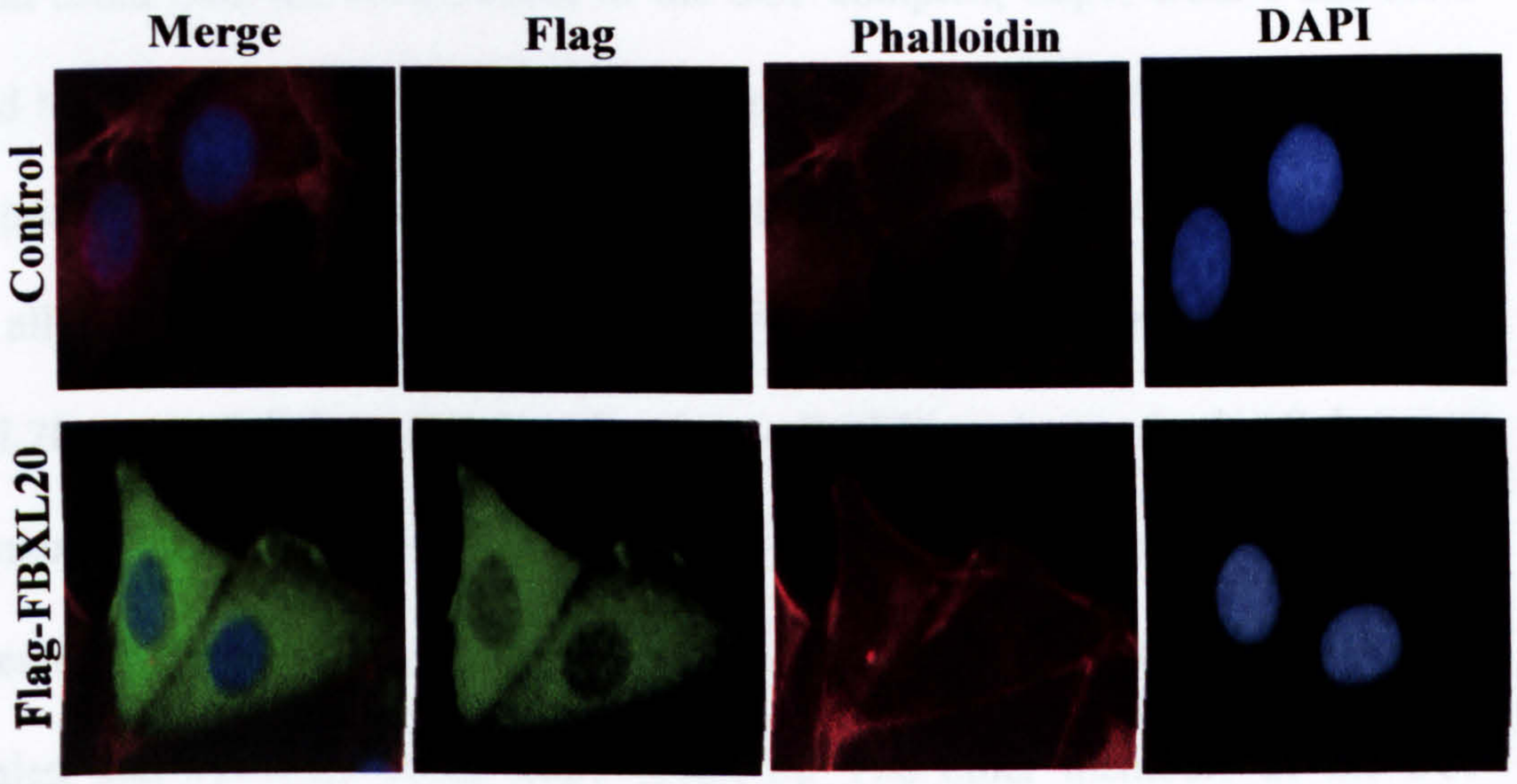


Figure 3.7 FBXL20 is localised in the cytoplasm of MCF-7 cells concentrated mainly around the nuclei. A) Nuclear, cytoplasmic and membrane fractions were separated. Cell lysates were separated by SDS-PAGE and immunoblot analysis was done using the indicated antibodies Immunoblots against Tubulin (cytoplasm), SP1 (nuclear) and Hsp60 (membrane) served to ensure efficient subcellular fractionation. B) Fluorescence microscope images of FBXL20-GFP localisation (in green) in respect to DAPI (in blue) in MCF-7 cells. Cells were transfected with an empty GFP vector or FBXL20-GFP and 24h later were fixed in methanol, counterstained with DAPI and visualised by Fluorescent microscopy. C) Fluorescence microscope images of FBXL20 localisation (in green) in respect to F-actin (in red) and DAPI (in blue) in MCF-7 cells. Cells were transfected with Flag-FBXL20 and control cells remained untransfected. 24h later, cells were subjected to immunofluorescent cytochemical staining, using an anti-Flag mococlonal antibody and phalloidin, as described in the materials and methods section.

FBXL20 is part of a SCF complex

The presence of the F-box domain in FBXL20 led me to investigate whether this protein could bind the components of the SCF complex, Skp1, CUL-1 and ROC-1, and be part of a novel SCF-complex. Similar proteins like Skp2, and other F-Box proteins such as FBXO31 (Kumar et al., 2005), have been demonstrated to bind all three components. MCF-7 cells were transiently transfected with Flag-FBXL20, myc-ROC-1 (kind gift from Prof.Xiong) or both. Subsequent immunoprecipitation (IP) with a monoclonal anti-Flag antibody, followed by sequential immunoblotting with monoclonal anti-Flag and anti-Skp1 antibodies, revealed that FBXL20 binds Skp1 (Fig.3.8). The other members of the SCF-complex, CUL-1 and ROC-1, were also shown to bind FBXL20. IP using the anti-Flag antibody in untransfected cells did not precipitate any protein (Fig. 3.8). These results together suggested that FBXL20 forms a SCF complex and is potentially a novel E3 ligase.

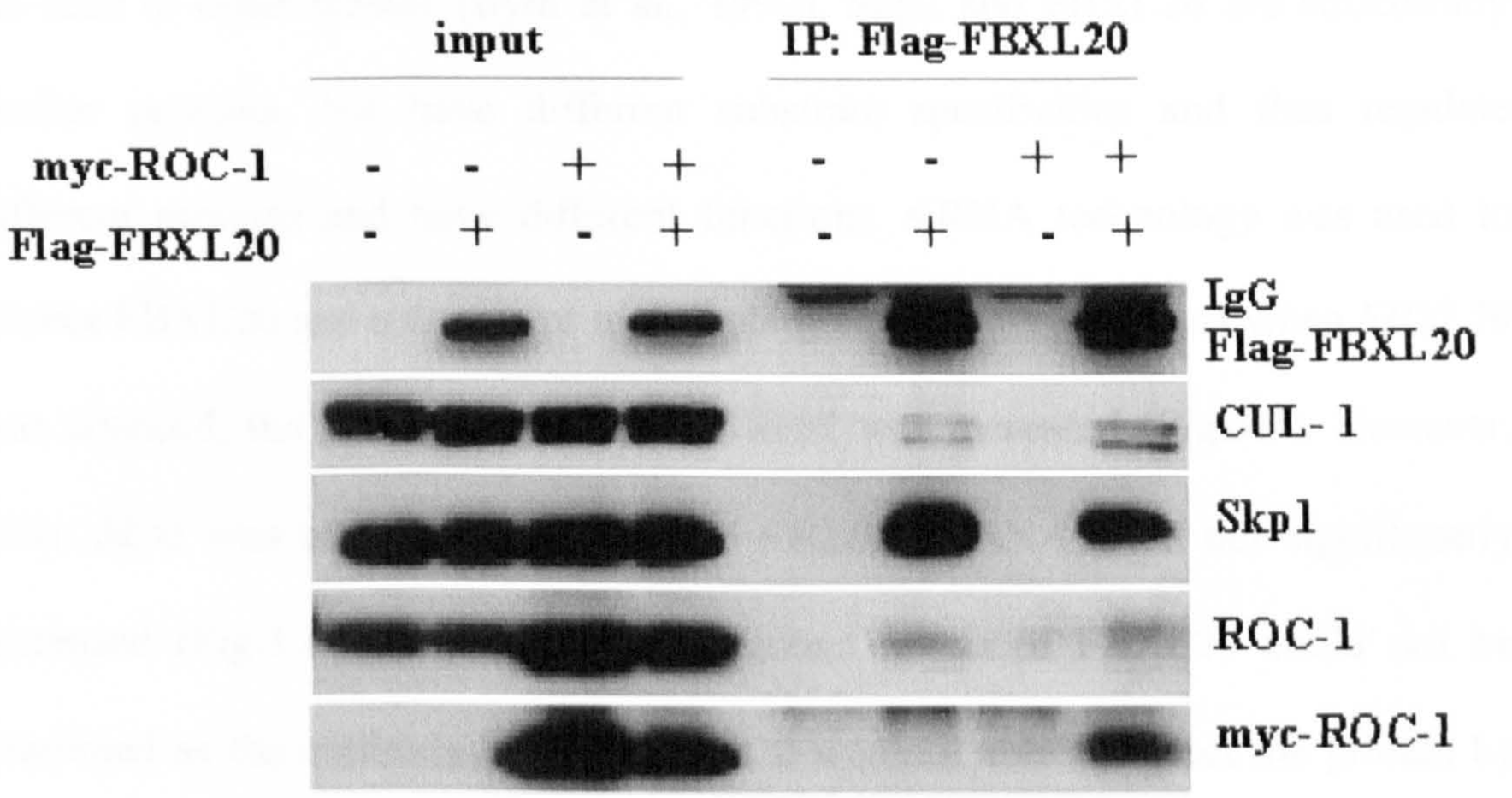
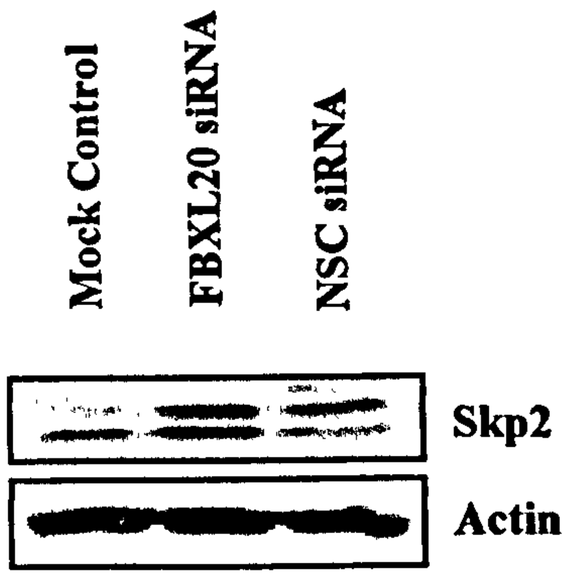


Figure 3.8 FBXL20 is part of a SCF complex. MCF-7 cells were transfected with Flag-FBXL20 or myc-ROC-1 or the combination and harvested 24h later. Whole cell extracts were prepared in lysis buffer and immuprecipitations (IP) were performed using an anti-Flag antibody as described in materials and methods. The IP samples along with samples from the whole cell lysates were then analysed by SDS-PAGE and immunoblotted with anti-Flag, anti-Skp1, anti-ROC-1 and anti-CUL-1 antibodies. Results are representative of 3 individual experiments.

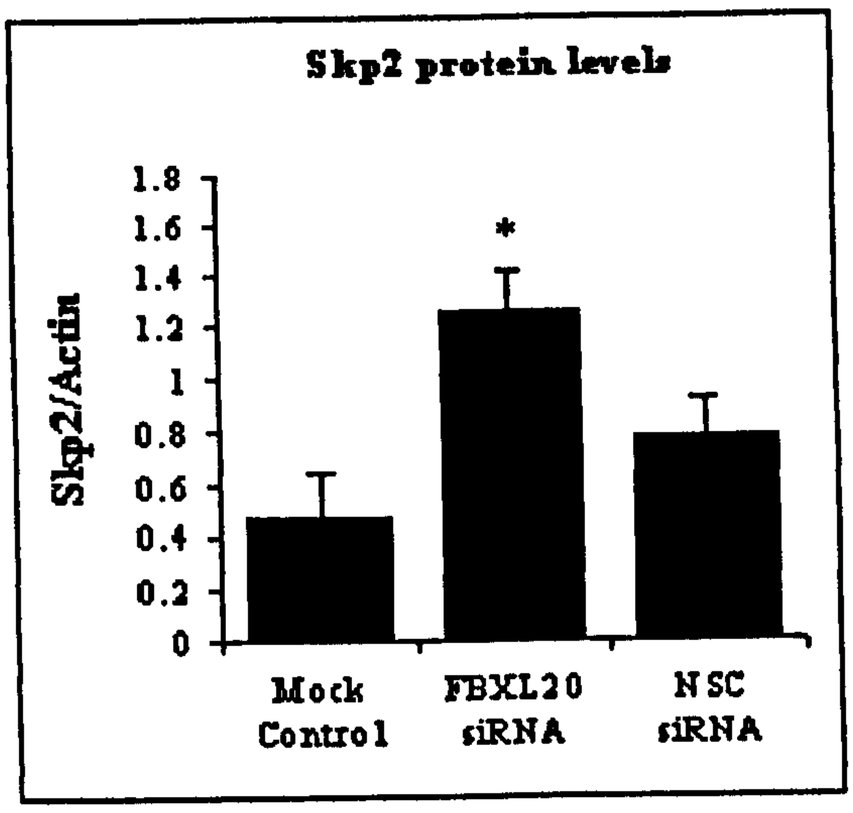
Silencing FBXL20 induces Skp2 protein expression

As seen in other studies (Ilyin et al., 1999), Skp2 and FBXL20 are structurally similar proteins, but have different substrate specificities and thus regulate different proteins and have different functions. siRNA technology was used to silence FBXL20 and subsequent immunoblot analysis revealed that when *FBXL20* was silenced, the protein expression of Skp2 was increased (Fig.3.9). However, when *Skp2* was silenced, the levels of *FBXL20* mRNA were not significantly increased (Fig.3.10). Once again the protein levels of FBXL20 could not be examined as the antibody against FBXL20 was not able to detect the protein by immunoblotting.

A)



B)



C)

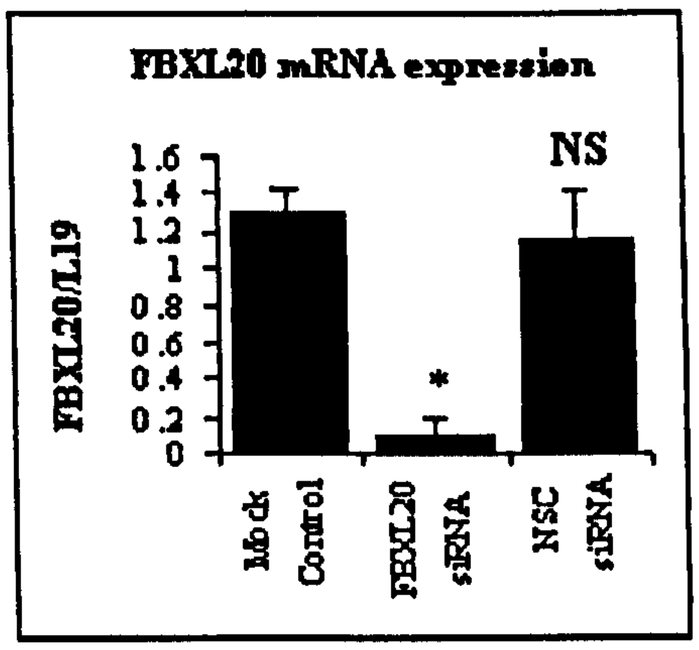


Figure 3.9 Knockdown of *FBXL20* induces the mRNA and protein expression of Skp2. Cells were transfected with siRNA against *FBXL20* and harvested 72h later. A) Lysates were analysed by SDS-PAGE. Immunoblot analysis was performed using the anti-Skp2 antibody. Actin was used as a loading control. Results are representative of three individual experiments. B) Results represent the average protein concetration of Skp2 from three individual experiments normalised by actin protein levels. Statistical analysis was performed using the Mann-Witney U test and *$p<0.05$ (NS = no significant change). C) RNA was extracted and reverse transcribed and cDNA was analysed by RT-QPCR. Results show the levels of *FBXL20* mRNA normalised by *L19* mRNA levels.

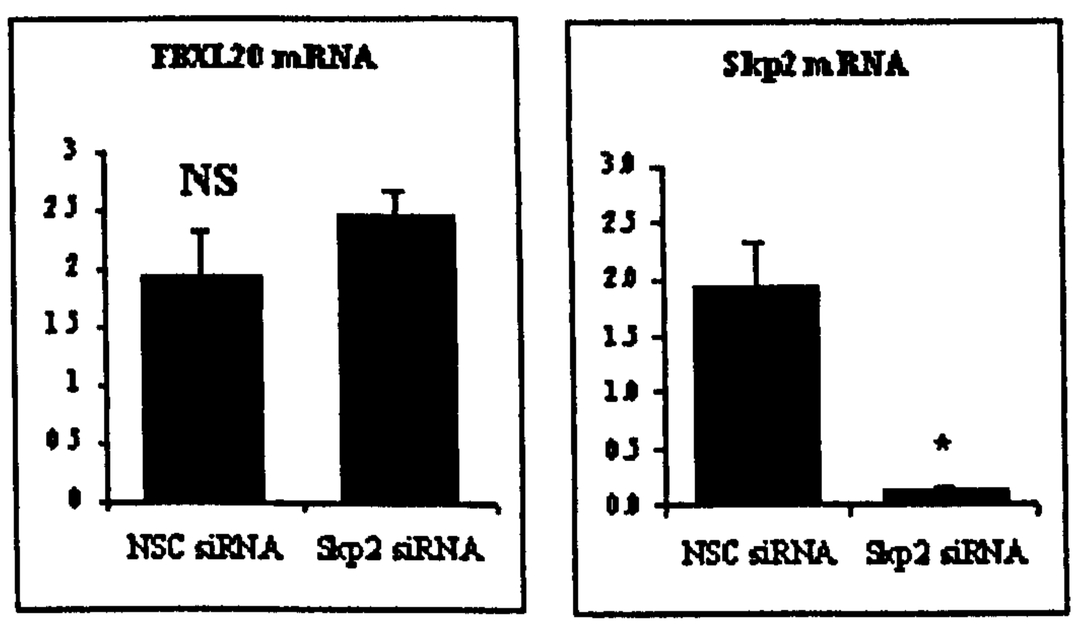
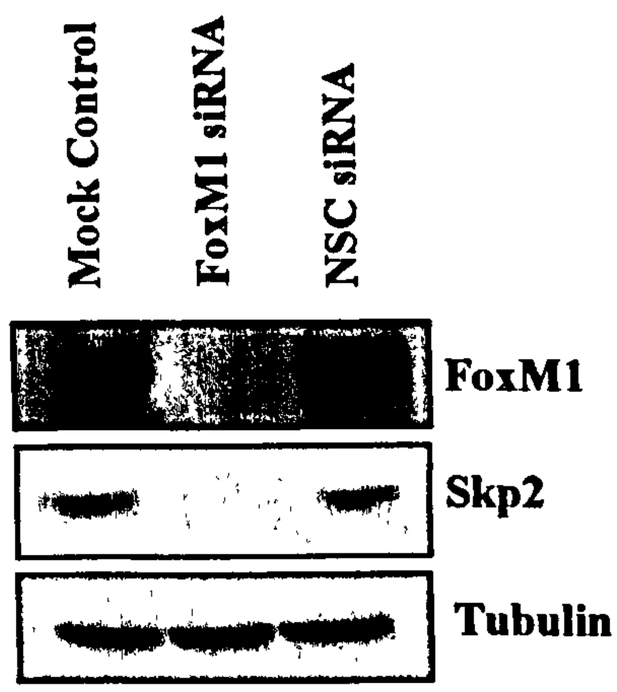


Figure 3.10 Silencing *Skp2* does not significantly induce the expression of *FBXL20* mRNA. Cells were transfected with siRNA against *Skp2* and harvested 72h later. RNA extraction and cDNA synthesis was followed and finally analysed by RT-QPCR. Graph shows the levels of *FBXL20* and *Skp2* mRNA normalised by L19 mRNA levels. Results represent the average ± SD of three independent experiments. Statistical analysis was performed using the Mann-Witney U test *$p<0.05$.

FoxM1 does not regulate the transcription of *FBXL20*

The transcription factor FoxM1 has been shown to regulate the transcription of *Skp2* (Wang et al., 2005). This suggests that the FoxM1 transcription factor may regulate the mRNA expression of FBXL20 as well. In order to test this, siRNA pools targeting *FoxM1* was used to knockdown *FoxM1* in MCF-7 cells and then protein and mRNA expression were analysed by SDS-PAGE and RT-QPCR. Immunoblot analysis confirmed the FoxM1 knockdown and revealed that Skp2 expression is decreased upon silencing FoxM1. RT-QPCR analysis showed that knockdown of *FoxM1* leads to a significant downregulation of *Skp2* mRNA levels ($p<0.05$) but does not significantly affect the *FBXL20* mRNA ($p>0.05$), suggesting that in contrast to *Skp2*, FoxM1 does not regulate the transcription of *FBXL20* (Fig. 3.11).

A)



B)

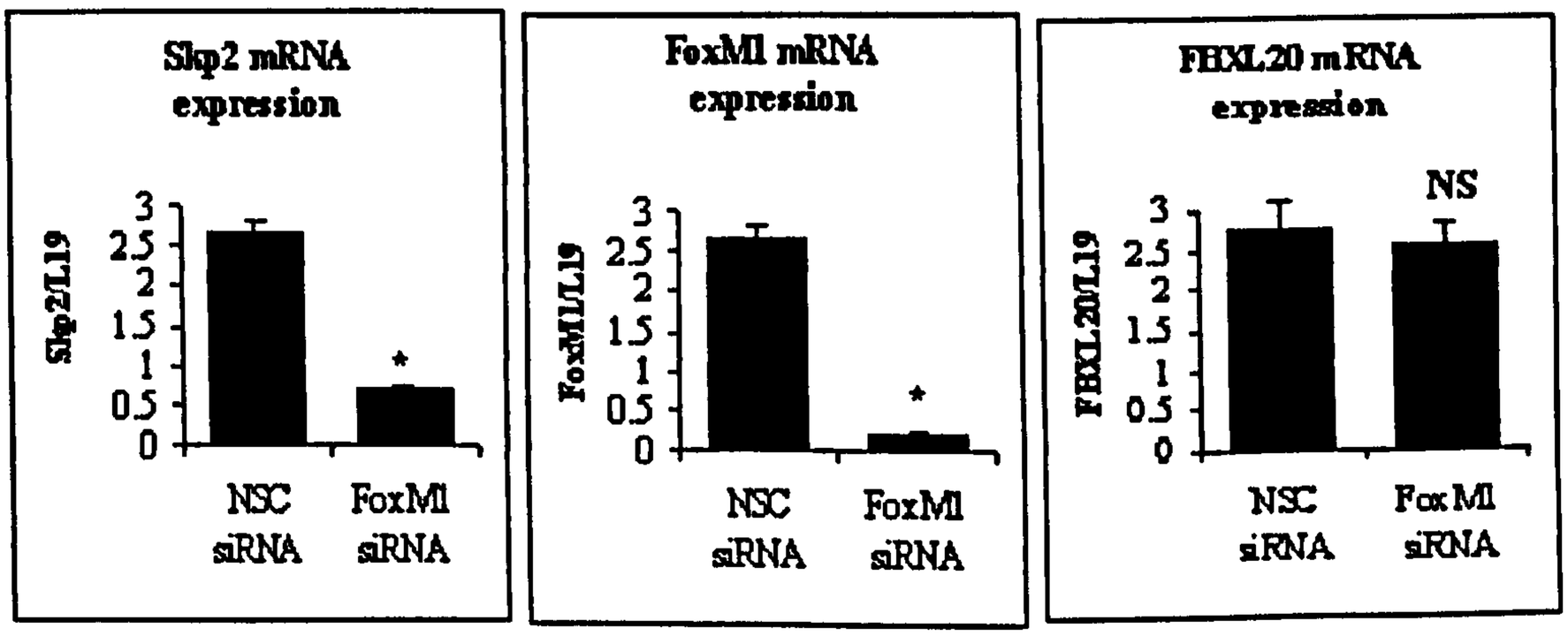


Figure 3.11 FoxM1 regulates *Skp2* but not *FBXL20*. Cells were transfected with siRNA against *FoxM1* and harvested 72h later. A) Lysates were analysed by SDS-PAGE and immunoblotting analysis was performed with antibodies against Skp2 and FoxM1. Tubulin is used as a loading control. Results are representative of three independent experiments. B) cDNA was synthesised and analysed by RT-QPCR. Graph shows the levels of *FBXL20*, *FoxM1* and *Skp2* mRNA normalised by *L19* mRNA levels. Results represent the average ± SD of three independent experiments. Statistical analysis was performed using the Mann-Witney U test *$p<0.05$

III.3 DISCUSSION

In this study, the novel FBXL20 F-Box protein was characterised in the MCF-7 cancer cell line. Sequence analysis revealed that it has 12 LRR repeats that are known to be responsible for recognising and binding target proteins. Furthermore, *FBXL20* in human cells appears to have a splice variant. This transcript appears to lack the exon 7 of the full-length gene, but this deletion does not change the reading frame of the remaining protein. FBL2 splice variants have also been detected in the rat cells (Ilyin et al, 1999).

Comparison of the FBXL20 protein sequence between species showed that FBXL20 is conserved among species. However, the rat expresses only a partial protein compared with that found in humans. Possibly, a mutation in the last codon of exon 10 creates a stop codon, which leads to the production of a truncated protein. Therefore, as the full length protein is expressed in humans and only the truncated protein in the rat, this suggests that human FBXL20 may bind different proteins and have different functions than its rat homolog, since the rat does not express all the LRR repeats found in the human FBXL20.

PCR analysis using cDNA from different cancer cell lines showed that *FBXL20* mRNA appeared to be expressed ubiquitously. Also, as seen with the homolog *FBL2* in rat cells (Ilyin *et al.*, 1999), FBXL20 was mostly expressed in growth arrested cells rather than proliferating cells. This implies that it negatively regulates proteins that promote growth.

This study also showed that FBXL20 is localised within the cytoplasm, predominantly around the nucleus of MCF-7 mammalian breast cancer cells as has been seen with FBL2 in rat cells. Subcellular fractionation followed by immunoblot analyses indicated that Flag-FBXL20 recombinant protein is localised within the cytoplasm. Fluorescence microscopy studies on cells expressing FBXL20-GFP confirmed this result and also revealed that FBXL20 is mainly concentrated around the nucleus of MCF-7 cells. Furthermore, immunofluorescent cytochemical staining of cells expressing the Flag-FBXL20 recombinant vector was also used to provide further evidence of the FBXL20 perinuclear localisation. FBXL20 is targeted to the perinuclear compartment by yet unidentified proteins.

Based on its similarity to other SCF based E3-ligases and its reported interaction with Skp1 in the rat cells (Ilyin et., 1999), it is possible that FBXL20 is part of a novel SCF complex. Immunoprecipitation experiments showed that FBXL20 in human cells binds Skp1, ROC-1 and CUL-1, suggesting that FBXL20 forms the classic tetrameric SCF complex.

Interestingly this study showed that when *FBXL20* is silenced, the expression of Skp2 protein is increased. FBXL20 is very similar in sequence and structure to Skp2 but they differ in their functions. Expression of Skp2 is known to be increased during S phase of the cell cycle (Ang and Wade Harper, 2005). It is localised in the nucleus and is strongly expressed in proliferating cells and downregulated in growth arrested cells. In contrast, my results show FBXL20 to be preferentially expressed in growth-arrested cells and detected in the cytoplasm.

These two proteins seem to exert different functions and bind different substrates. Skp2 is known to target cyclin E and the CDK inhibitor $p27^{Kip1}$ for ubiquitination and subsequent degradation (Carrano et al., 1999; Sutterluty et al., 1999; Zhang et al., 1995). However, FBXL20 does not appear to have the same functions. Therefore, the inverse relationship between Skp2 and FBXL20 could be cell cycle phase mediated. Silencing Skp2 expression leads to a G1/S arrest by inducing the expression of $p27^{Kip1}$ and $p21^{Cip1}$. This arrest can result in the upregulation of FBXL20 levels since FBXL20 appears to be ovexpressed in arrested cells and downregulated in cycling cells. Furthermore, when FBXL20 is silenced Skp2 levels are significantly increased, which suggests that since Skp2 levels are high in proliferating cells, cells acquire a growth advantage upon FBXL20 silencing and Skp2 is increased in order to downregulate proteins such as $p27^{Kip1}$ and lead to the progression of cells from G_1 to S phase. A yet unknown relationship is likely to exist between Skp2 and FBXL20 in MCF-7 cells.

A major regulator of proliferation and the transition of cells from G_1 to S phase and from G_2 to M phase is the FoxM1 trascription factor. This protein has been shown to regulate the transcription of *Skp2* (Wang et al., 2005b). Silencing *FoxM1* leads to the downregulation of Skp2 mRNA and protein levels. Since FBXL20 resembles Skp2, and both their expression is dependent on cell cycle phase, it was thought that FoxM1 could perhaps regulate the expression of *FBXL20*. However, this was not the case as siRNA experiments where *FoxM1* was silenced in MCF-7 cells revealed that there was no significant change in the mRNA expression of FBXL20. Skp2 was significantly downregulated in response to FoxM1 silencing.

Future work

Further studies are required to lead to a better understaning of the role of FBXL20 in cells. The question of the binding partners of FBXL20 remains unanswered and needs to be addressed in further studies. In order to identify its binding partners the RePCA system (Ding et al., 2006) could be used or many other techniques such as GST pulldown, yeast-two hybrid or others. Further experiments using siRNA to silence *FBXL20* expression could then be performed to test its effect on its binding partners.

To be able to study the role, expression and cofactors of FBXL20 the antibody raised against FBXL20 has to be purified and optimised and used in western blot experiments and also in immunohistochemical staining. For example, transformed and non-transformed cells could be compared for their expression of FBXL20 mRNA and protein levels. Also, expression could be compared between cells from low grade and more aggressive, high grade tumours. FBXL20 could play a role in tumourigenesis, apoptosis, proliferation and cancer progression.

Also, the interplay between Skp2 and FBXL20 has to be further investigated. Further experiments could be done to understand the differences between the rat and human FBXL20 protein. FBL2 can be overexpressed and silenced in rat cells to test whether it functions similarly to the full length protein in human cells. Furthermore, the part of FBXL20 that is similar to the rats can be examined for potentially similar functions to the full length protein in human cells. The full-length FBXL20 protein can be expressed in rat cells and the functional differences between the full length and the truncated proteins can be examined.

CHAPTER IV

TSA AND FBXL20

IV.1 BACKGROUND AND OBJECTIVES

HDAC inhibitors bind and inhibit HDACs, leading to an open chromatin structure where transcription factors and other regulatory elements can bind to the DNA and regulate transcription of target genes. They preferentially target transformed rather than non-transformed cells and have been shown to inhibit proliferation of cancer cells and induce cell cycle arrest, differentiation and different kinds of cell death such as autophagy or apoptosis (Johnstone et al., 2002; Narlikar et al., 2002). This chapter studies the mechanism of action of the HDAC inhibitor TSA by characterising its effect on the novel F-Box protein FBXL20. TSA is being used as a benchmark HDACi that is very well studied compared to other HDACi. TSA induces the expression of $p21^{Cip1}$ and the pro-apoptotic protein Bim (Fandy et al, 2006), while it decreases the expression of proteins important for proliferation such as ERα and cyclin D1 (Alao et al., 2004). TSA has been shown to lead to both G_1/S cell cycle arrest and G_2/M arrest dependent on the concentration used (Kim et al., 1999; Li et al., 2006; Rokhlin et al., 2006; Sowa et al., 1999; Yamashita et al., 2003). TSA has been demonstrated to cause G_1/S arrest by repressing ERα and cyclin D1 transcription and inducing ubiquitin dependent proteasomal degradation of cyclin D1 (Alao et al., 2004). Disadvantages of TSA include that it is very toxic and that it is not very specific in targeting only HDACs as it has been reported to directly target a number of proteins like the tumour suppressor p53. This chapter suggests that the novel F-Box protein FBXL20 is crucial for the action of TSA.

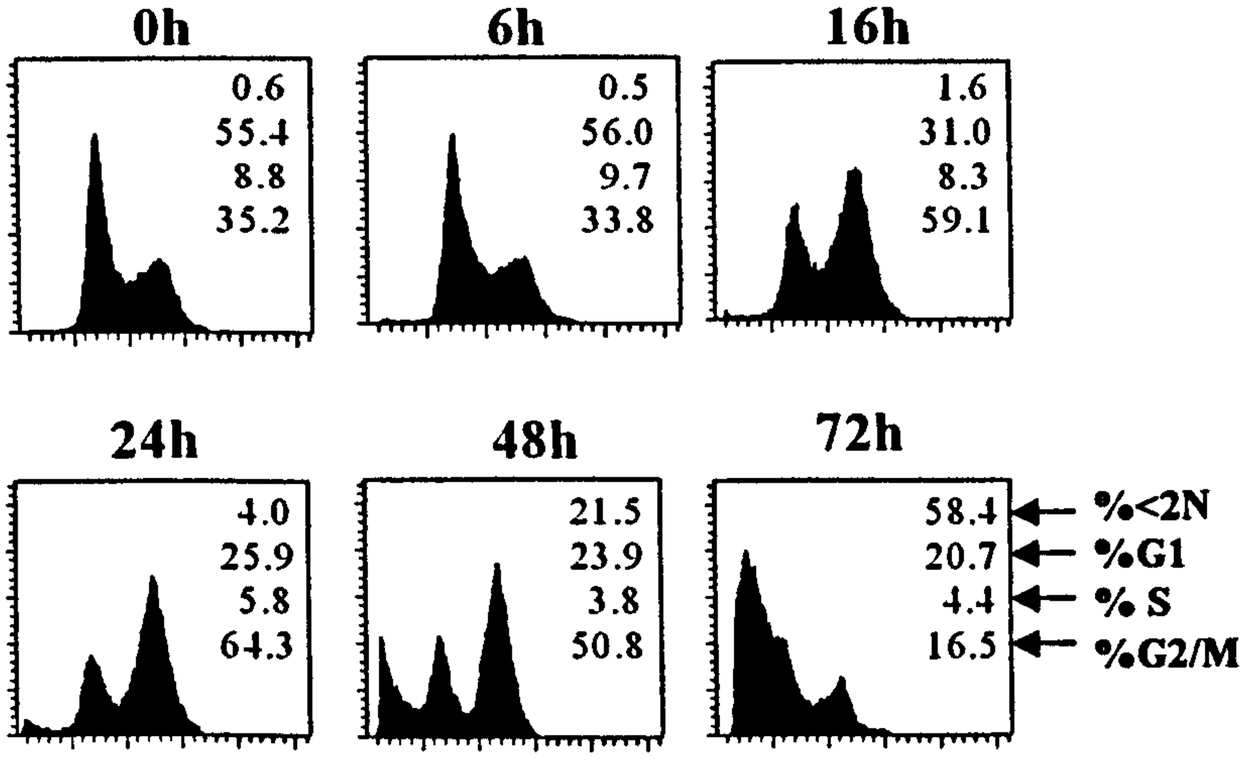
IV.2 RESULTS

TSA causes G_2/M arrest at high concentrations

In order to investigate the mechanism of action of TSA MCF-7 cells were treated with 1μM TSA to study the cell cycle profile of cells after 0, 6, 16, 24, 48, 72 hours. Previous work in our lab has shown that TSA at the concentration of 1μM induces hyper-acetylation of histone H3 and H4 and inhibits proliferation of breast cancer cell lines by 90% (*IC*90) at 48h. Cell cycle analysis showed that after 16h of treatment with 1μM TSA, the majority of cells arrested at the G_2/M phase, whereas a small population arrested at the G_1/S phase and a small percentage accumulated at the sub-G_1 phase. Cells at sub-G_1 have a DNA content of less than 2N, characteristic of apoptotic or necrotic cells. In the later time points, sub-G_1 population was increasing with time and after 72h, 60% of cells were at the sub-G_1 phase (Fig. 4.1A). This concentration was used in further experiments.

The action of TSA on the cell cycle were concentration dependent; as cell cycle analysis of MCF-7 cells treated with 1, 10, 100 and 1000nM TSA showed differential effects. 1nM and 10nM TSA for 48h did not affect the cell cycle distribution, 100nM TSA arrested MCF-7 cells in G_1/S phase and G2/M phase and with 1000nM TSA cells were primarily arrested at the G_2/M phase and the sub-G1 concentration was increased (Fig. 4.1B). However, these observations might only affect the different kinetics of cell cycle arrests by different concentrations of TSA.

A) TSA treatment (1μM)



B) TSA treatment (48h)

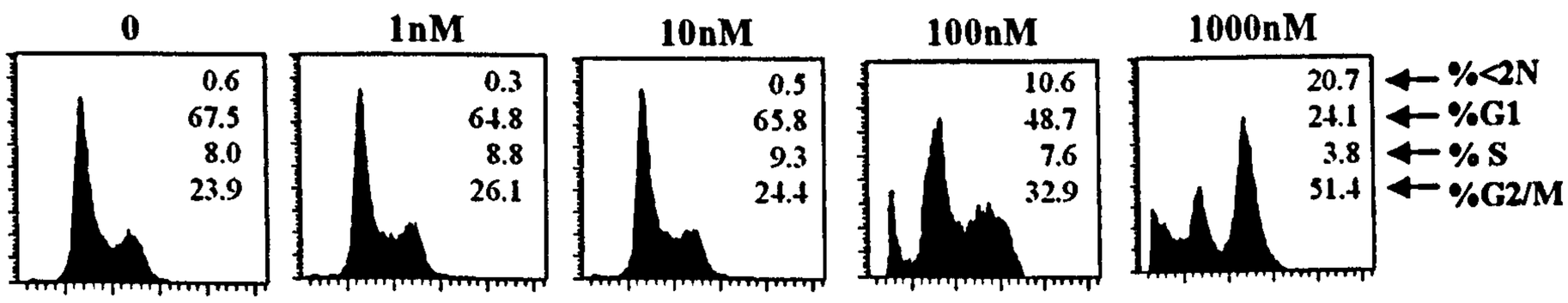


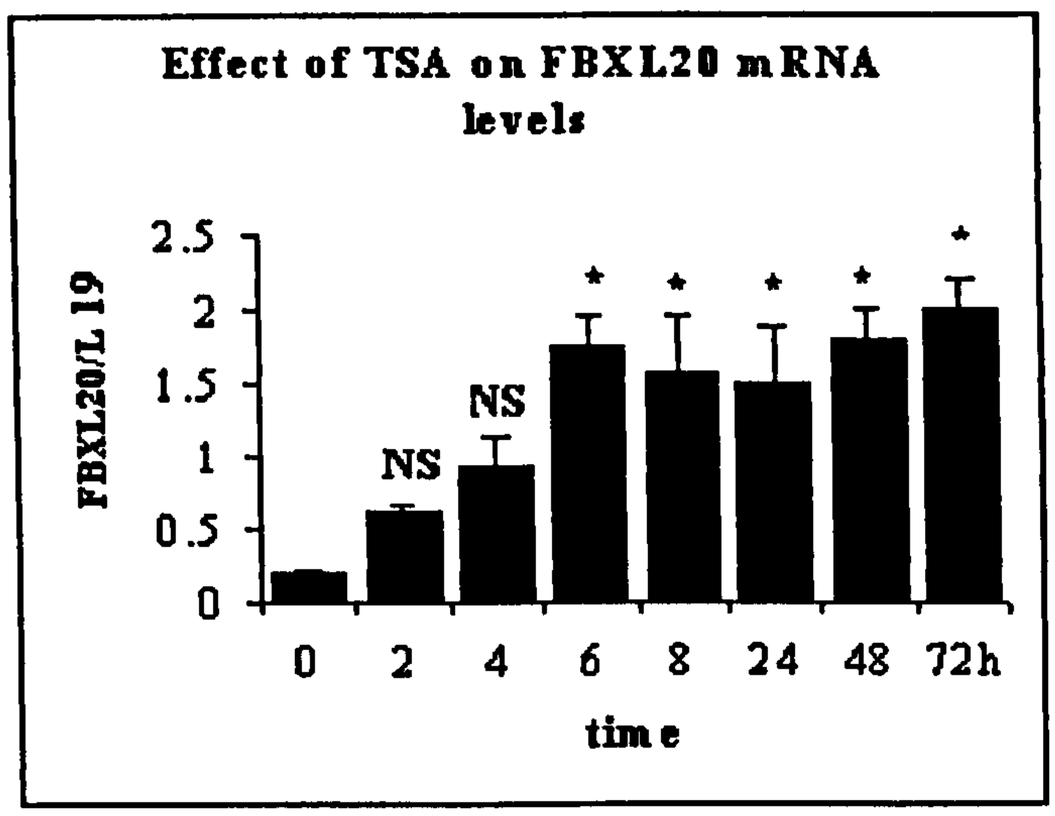
Figure 4.1 TSA causes G_2/M arrest. A) MCF-7 cells were treated with 1μM TSA, and harvested at the indicated times. Cells were fixed in 90% ethanol. DNA content was then analyzed by FACS analysis after propidium iodide staining. The percentages of cells (Y-axis) in each phase of the cell cycle determined by their DNA contents (X-axis) are indicated (<2N, hypo-diploid). B) MCF-7 cells were treated with TSA at the concentrations specified for 48h. Cells were fixed in 90% ethanol. DNA content was then analyzed by FACS analysis after propidium iodide staining. The percentages of cells (Y-axis) in each phase of the cell cycle determined by their DNA contents (X-axis) are indicated (<2N, hypodiploid).

TSA induces the expression of FBXL20 mRNA

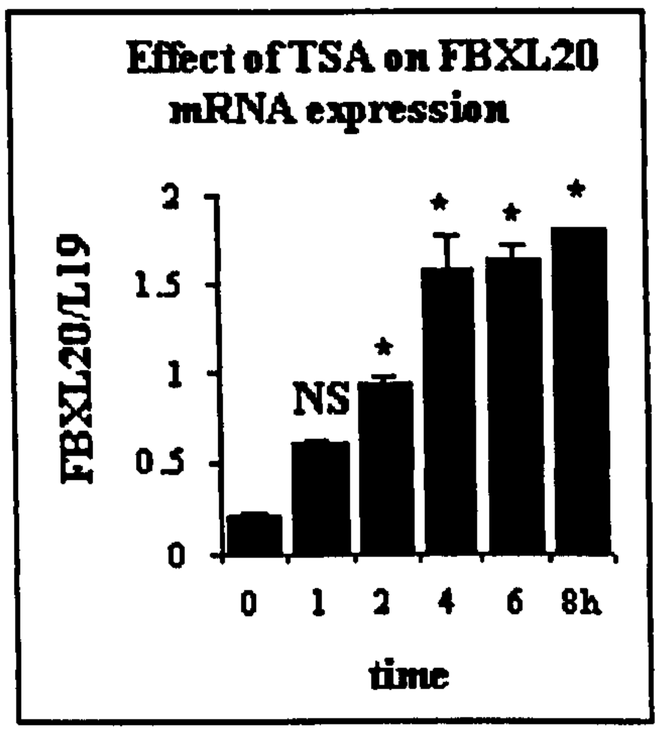
There is no commercially available antibody against FBXL20, and so one was designed against the N-terminal region of FBXL20. However, the antibody was very non-specific and could not be used in further experiments; therefore it was not possible to look at the effect of TSA on FBXL20 protein levels.

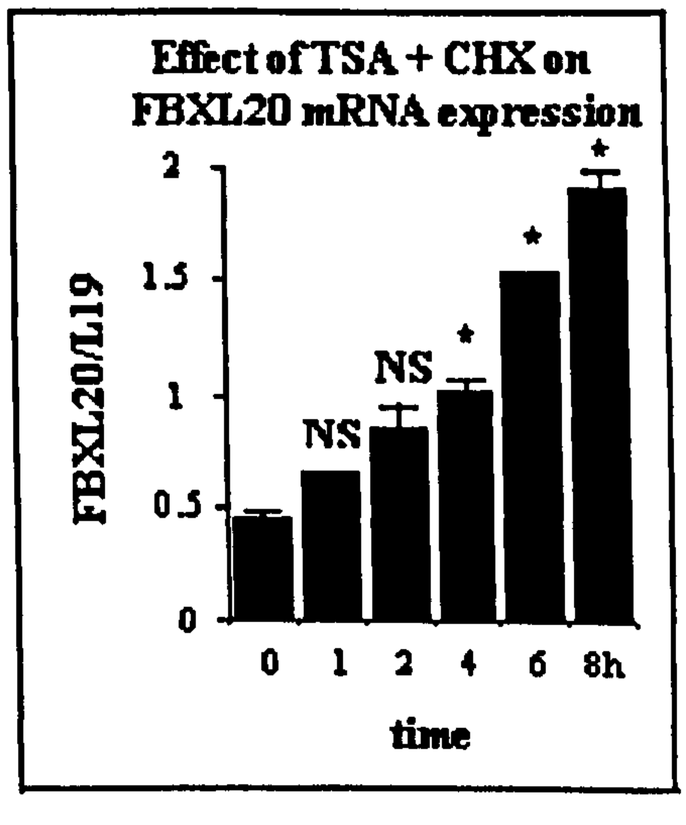
Treatment of cells with 1μM TSA lead to a significant increase in the mRNA levels of FBXL20 (Fig.4.2A). In order to examine whether this is a direct effect, cells were treated with cycloheximide (CHX) alone or the combination of CHX and TSA for 1-8hours in a time-course experiment. RT-QPCR analysis showed that CHX treatment did not alter the mRNA levels of *FBXL20* whereas cotreatment with TSA leads to an induction of FBXL20 expression (Fig. 4.2B). The amount of primers used was optimised for each set of primers.

A)



B)





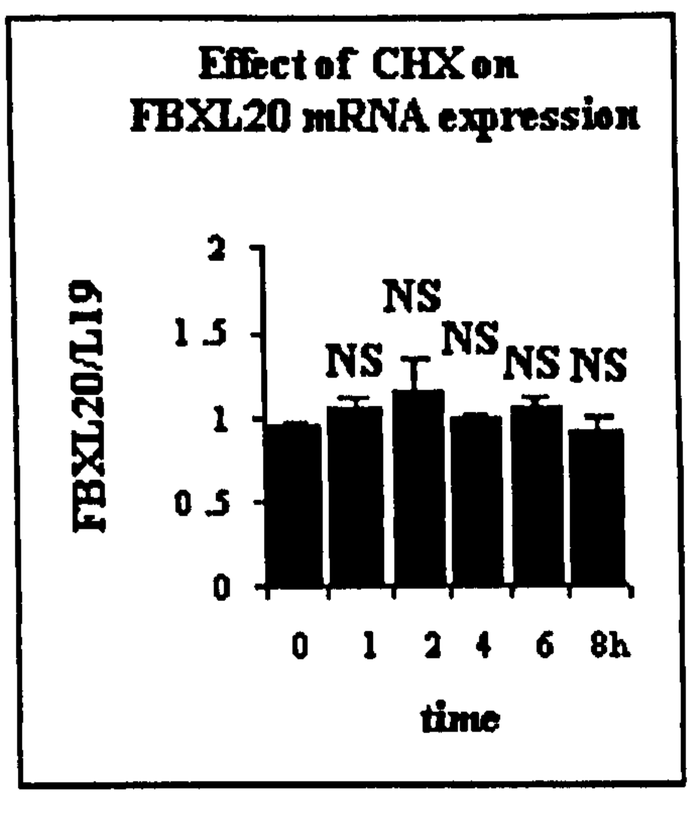


Figure 4.2 TSA directly induces the expression of *FBXL20* mRNA in MCF-7 cells. A) Cells were treated with 1μM TSA and harvested at the indicated times followed by RNA extraction and analysis by RT-QPCR. B) Cells were treated for the indicated times with TSA (1μM), CHX (10μg/μl) or TSA+CHX. When TSA was used in combination with CHX, cells were pre-treated with CHX for 30min, and then treated with TSA and analysed by RT-QPCR for *FBXL20* mRNA levels. Graphs show the levels of *FBXL20* mRNA normalised by L19 and represent the average ±SD of three independent experiments that included 3 replicates each. Statistical analysis was performed using ANOVA with Dunnett's post-hoc analysis for all time points compared to control (0 hr) and *$p<0.05$.

TSA does not affect the localisation of FBXL20

Experiments in the human uterine leiomyosarcoma SK-UT cell line, which has a splice variant of Skp2 retained in the cytoplasm, showed that the Skp2 variant failed to direct cyclin D1 ubiquitination; however expression of full-length Skp2 rescues the cyclin D1 and $p27^{Kip1}$ degradation. Therefore, the absence of the Skp2 from the nucleus of SK-UT-1B cells is the mechanism underlying the ubiquitination defect observed in this cell line (Ganiatsas et al., 2001). This leads to the conclusion that localisation of F-Box proteins is a very important factor affecting their functions in cells. In order to test if TSA affects FBXL20 subcellular localisation and thus potentially change its functions, a sub-cellular fractionation experiment was carried out. Flag-FBXL20 was predominantly detected in the cytoplasm of untreated asynchronously growing MCF-7 cells. Culture with 1μM TSA for 6h resulted in upregulation of Flag-FBXL20 levels but did not alter its localisation. SP1 was used as a control and was detected in the nuclear fraction while tubulin was detected in the cytoplasm (Fig. 4.3).

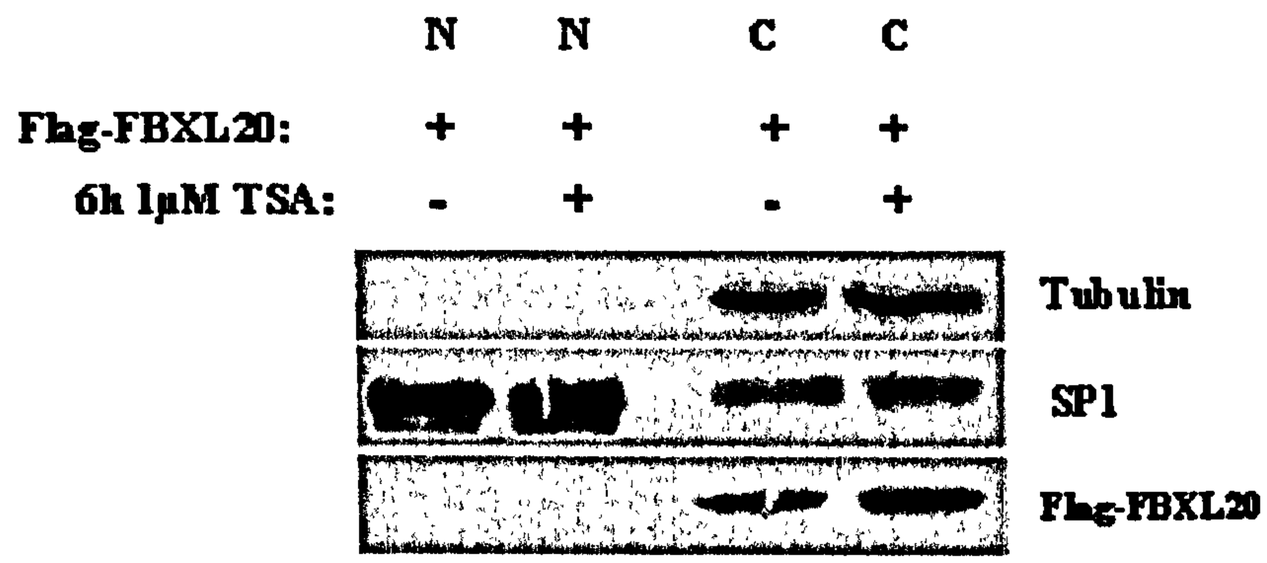
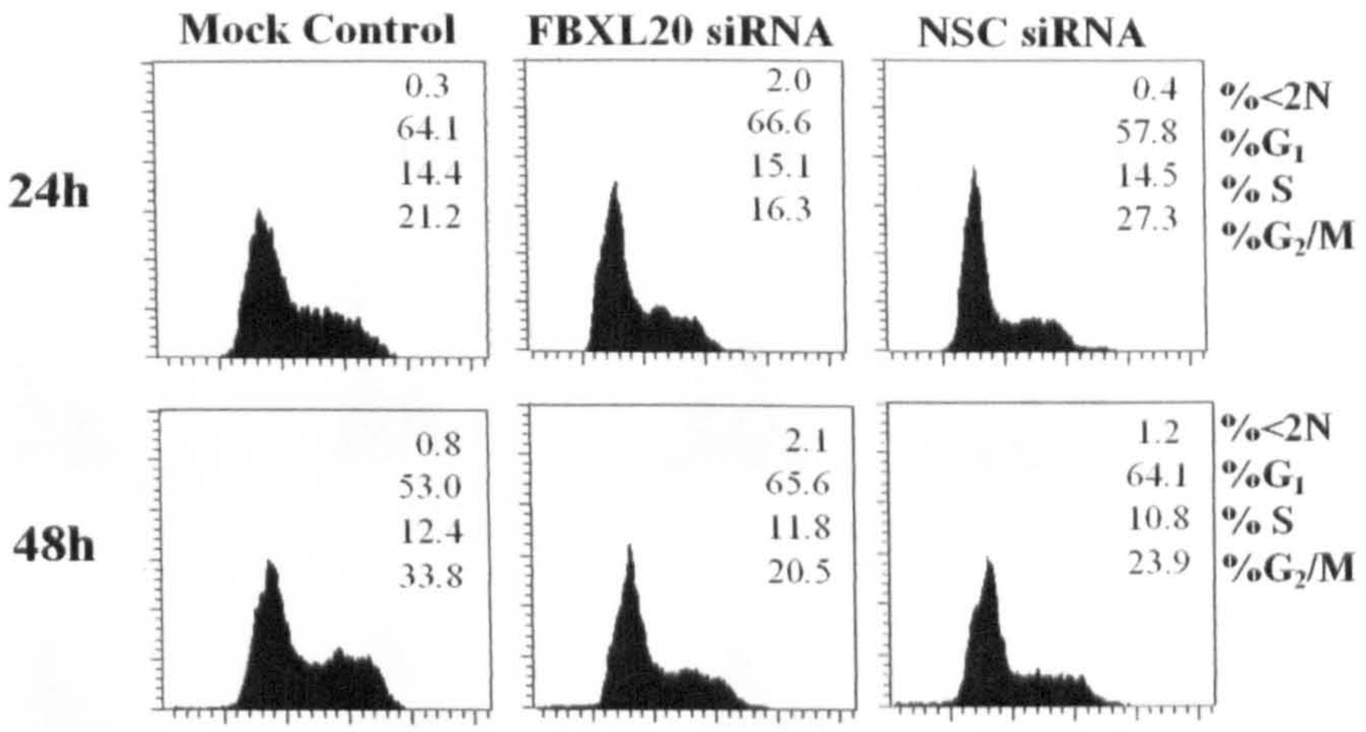


Figure 4.3 TSA does not alter the localisation of FBXL20 in MCF-7 cells. Asynchronously growing cells were treated with and without 1μM TSA for 6h and were then subjected to proteomic fractionation. Nuclear (N) and cytoplasmic (C) fractions of cells were separated. Cell lysates were separated by SDS-PAGE and immunoblot analysis was done using the indicated antibodies Immunoblots against Tubulin (cytoplasmic) and Sp1 (nuclear) served to ensure efficient subcellular fractionation.

Silencing FBXL20 increases the proliferation and abrogates the G_2/M arrest induced by TSA.

In order to examine the effect of silencing *FBXL20* in the cell cycle progression of MCF-7 cells, *FBXL20*-specific or non-specific scrambled siRNA pools were transfected into MCF-7 cells. FACS analysis 24 and 48h after trasfection showed that knockdown *FBXL20* resulted in a slight decrease in the number of cells in the G_2/M phase of the cell cycle (Fig. 4.4A). RT-QPCR confirmed the knockdown of *FBXL20* (Fig 4.4B). Next, I examined the effect of overexpressing Flag-FBXL20 in TSA treated cells on the cell cycle progression of MCF-7 cells. Cells transfected with Flag-FBXL20 showed an increase in apoptosis induced by TSA (Fig 4.5). In a reverse experiment, the functional effects of silencing *FBXL20* gene expression on the MCF-7 cell proliferation in response to TSA were examined. *FBXL20*-specific siRNA pools or scrambled siRNA control pool duplexes were transfected into MCF-7 cells, and cell proliferation was then quantified by SRB assay at 0 and 24h after treatment with 100, 500 and 1000nM TSA (Fig. 4.6A). Knockdown of *FBXL20* expression led to an apparent growth advantage of MCF-7 cells compared to the non-specific control transfected cells. Furthermore, non-specific and *FBXL20*-specific siRNA pools were used to examine whether silencing *FBXL20* changes the cell cycle profile of MCF-7 cells treated with TSA for 24h. FACS analysis showed that after 24h of 1μM TSA treatment there was a decrease in the number of cells in the G_2/M phase compared to the non-specific control transfected cells (Fig. 4.6B). RT-QPCR analysis was used to confirm the knockdown of the *FBXL20* gene expression (Fig. 4.6C).

A)



B)

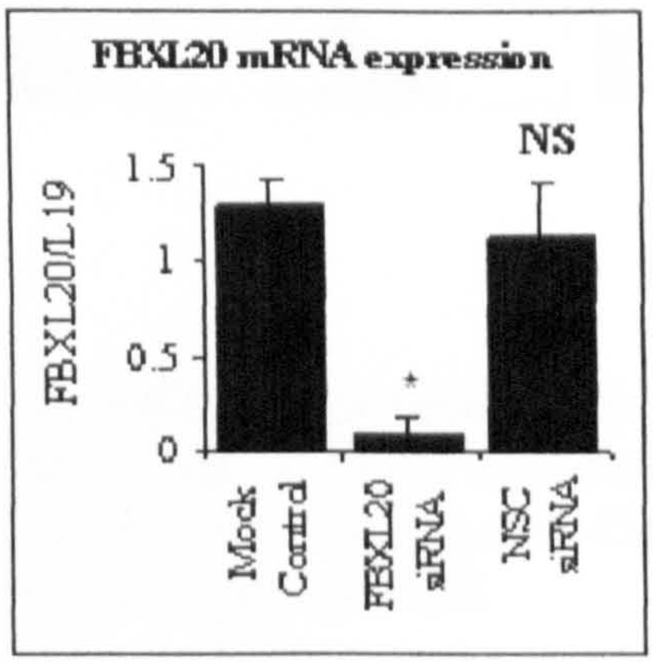


Figure 4.4 siRNA-mediated *FBXL20* knockdown causes a non-significant change in the cell cycle progression of MCF-7 cells. MCF-7 cells were transfected with oligo pools specifically targeting FBXL20 or NSC. A) Cells were then harvested at 24 and 48h after transfection and fixed with 90% ethanol and analysed by FACS. B) RNA from cells transfected in parallel was used in RT-QPCR reaction with primers specific for *FBXL20* to monitor siRNA efficiency.Graph represents the FBXL20 mRNA levels normalised by L19. Statistical analysis was performed by Mann-Witney U test and *$p<0.05$.

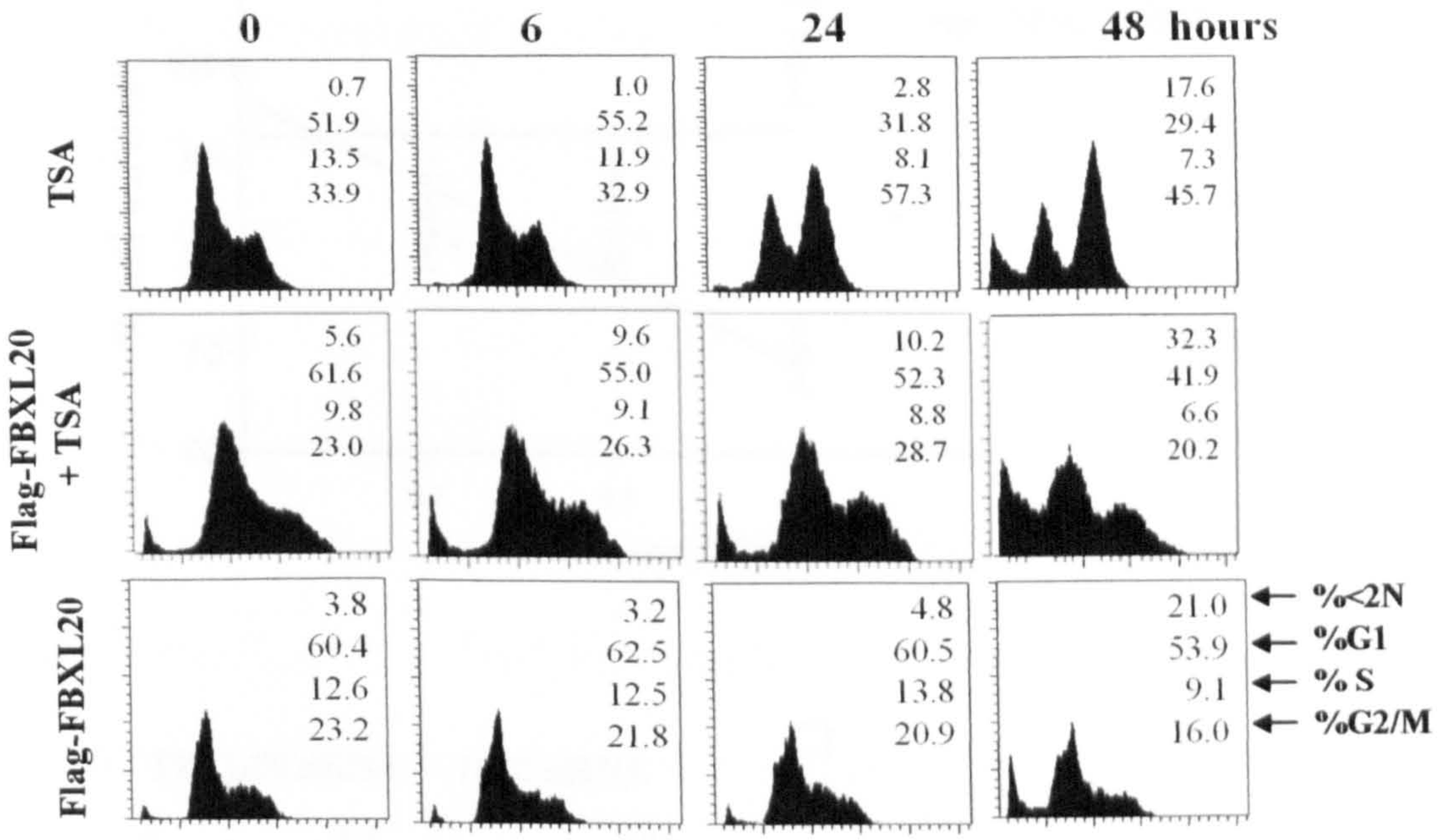


Fig 4.5 Overexpression of Flag-FBXL20 increases the cell death induced by TSA. Cells were transfected with Flag-FBXL20 or remained untransfected and were then treated with 1μM TSA for 0, 6, 24 and 48h. Cells were harvested and fixed with 90% ethanol and then analysed by FACS.

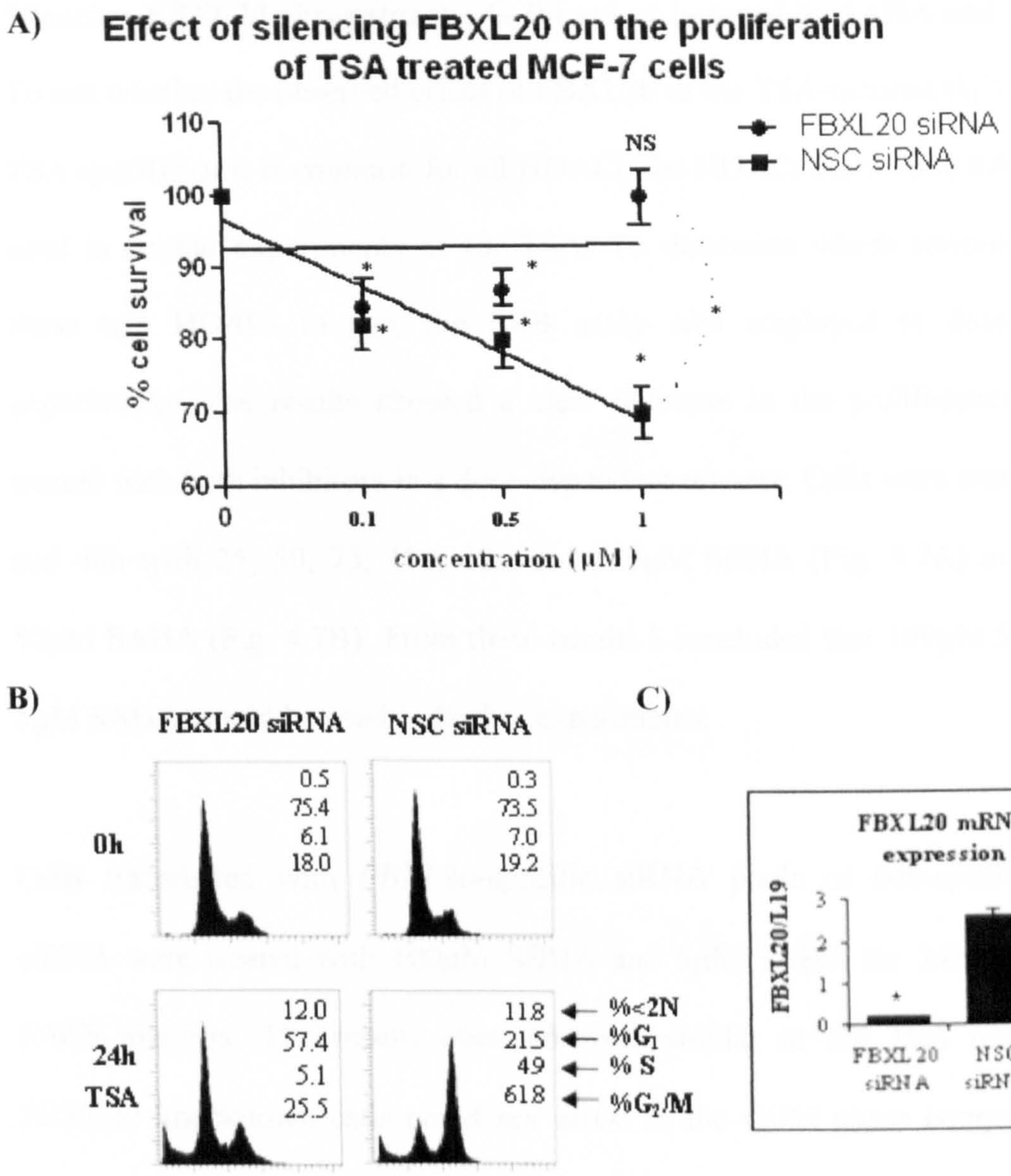


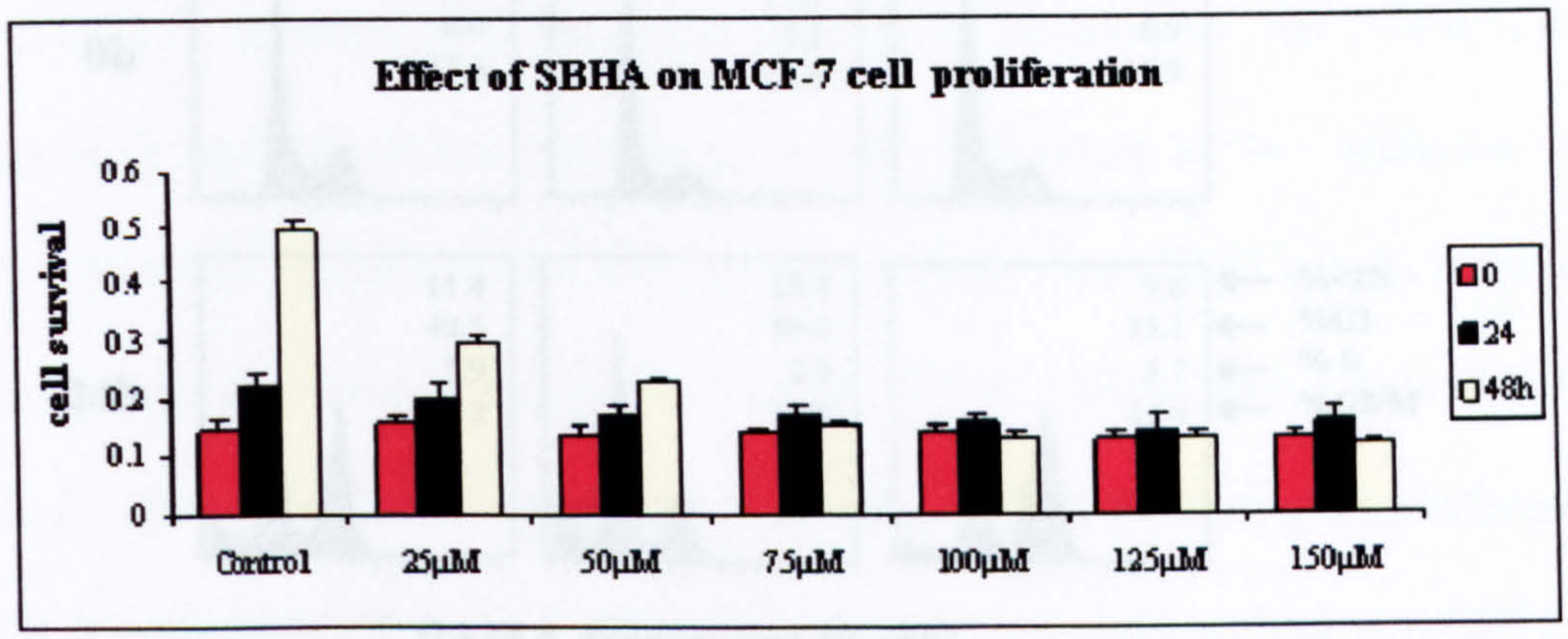
Figure 4.6 Specific knockdown of *FBXL20* attenuates the cytotoxic effect of TSA on MCF-7 cells. A) Cells were transfected with siRNA oligos specific for *FBXL20* and NSC. 24h after transfection cells were harvested and reseeded in 96-well plates and incubated for 24h. Cells were then treated with the indicated concentrations of TSA for 24h and were then analysed by the SRB assay. Results are the average of three independent experiments that included 4 replicates expressed as the percentage of the 0h. Statistical analysis was performed using ANOVA with Bonferroni post-hoc analysis for all points compared to control (0μM) and between FBXL20 siRNA and NSC siRNA samples and *p<0.05 (NS= no significant change). B) Cells were transfected with siRNA oligos specific for *FBXL20* and *NSC* and then treated with 1μM TSA for 24h, harvested and fixed with 90% ethanol and then analysed by FACS. C) RNA from cells transfected in parallel were used in RT-QPCR reaction with primers specific for *FBXL20* to monitor siRNA efficiency. Graph represents FBXL20 mRNA levels normalised by L19 mRNA levels. Statistical analysis was performed using the Mann-Witney U test and *p<0.05.

Silencing *FBXL20* abrogates the G_2/M arrest induced by SAHA and SBHA.

To test whether the observed effect of FBXL20 in the TSA-induced G_2/M arrest is TSA specific or it is common for all HDACi, the HDACi SBHA and SAHA were used in similar experiments as for TSA. To determine which concentration of those two HDACi to use, the SRB assay was employed in dose-response experiments. The results showed a clear decrease in the proliferation of cells treated with both inhibitors in a dose-dependent manner. Cells were treated for 24 and 48h with 25, 50, 75, 100, 125 and 150μM SBHA (Fig. 4.7A) or 1, 5, 10, 50μM SAHA (Fig. 4.7B). From these results I concluded that 100μM SBHA and 5μM SAHA would be used in further experiments.

Cells transfected with *FBXL20*-specific siRNA pools or non-specific (NSC) siRNA were treated with 100μM SBHA and 5μM SAHA for 24h followed by FACS analysis. The results obtained were similar to the TSA treated cells. FBXL20 knockdown cells could not arrest in the G_2/M phase compared to the Mock and NSC control cells (Fig. 4.8A, Fig. 4.8B). Knockdown was again confirmed by RT-QPCR analysis (Fig. 4.8C).

A)



B)

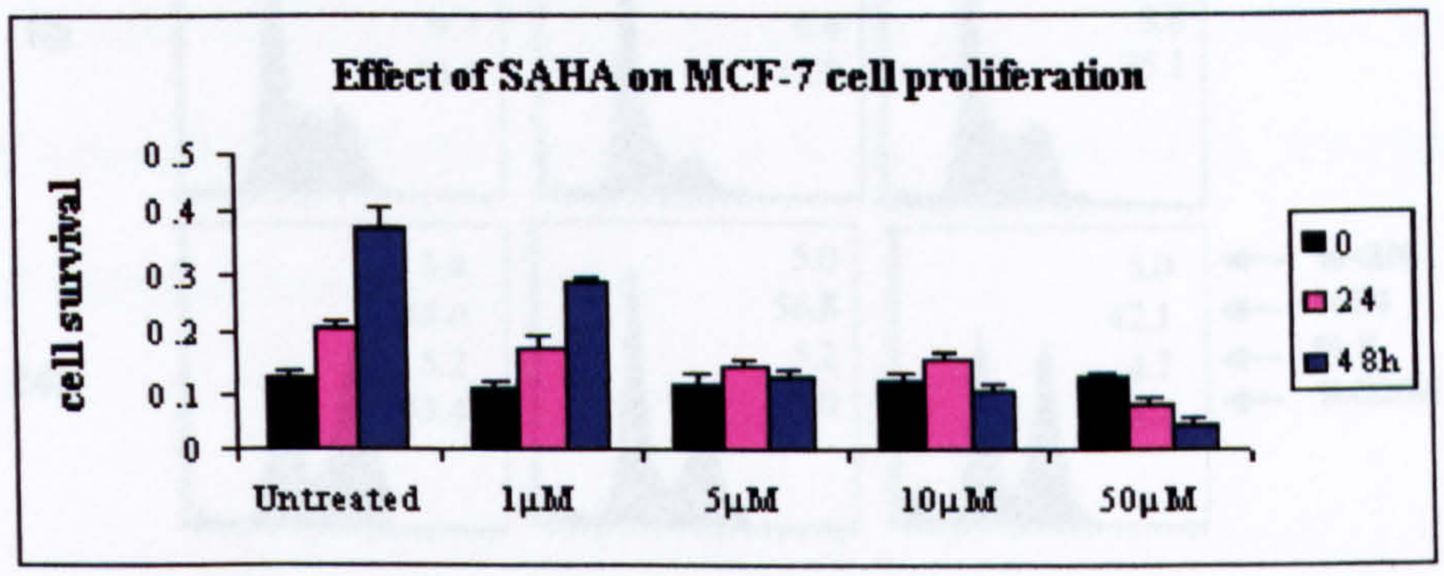
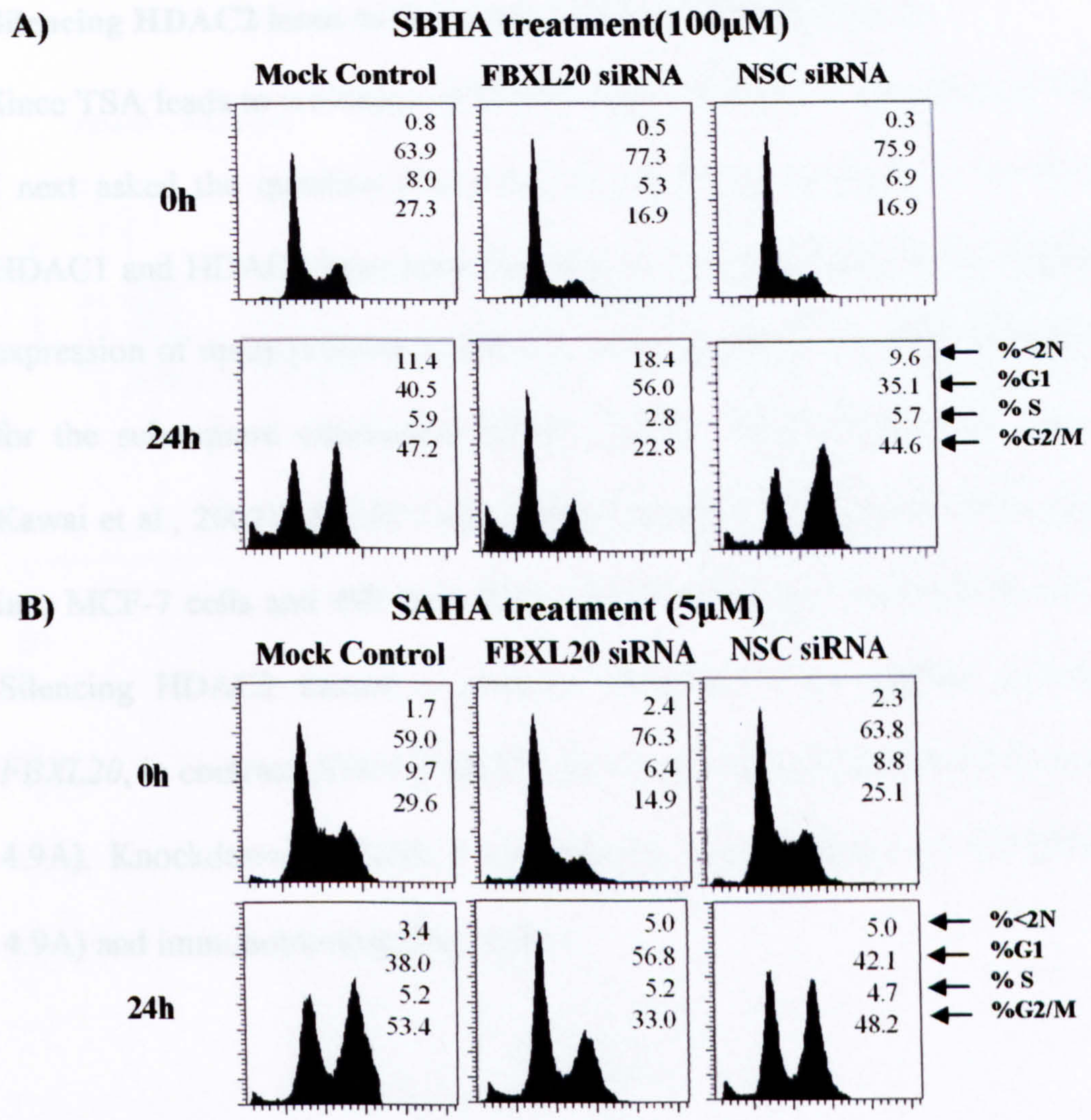


Figure 4.7 Effect of SBHA and SAHA on the proliferation of MCF-7 cells. A) Cells were cultured in 96-well plates with 25-150µM SBHA. Relative cell survival was determined after 24 and 48 h as described in materials and methods section. Results are the average ± SD of three independent experiments that included 4 replicates each. B) MCF-7 cells were cultured in 96-well plates with 1-5µM SAHA. Relative cell survival was determined after 24 and 48h as described in materials and methods section. Results represent the average ± SD of three independent experiments that included 4 replicates each.



C)

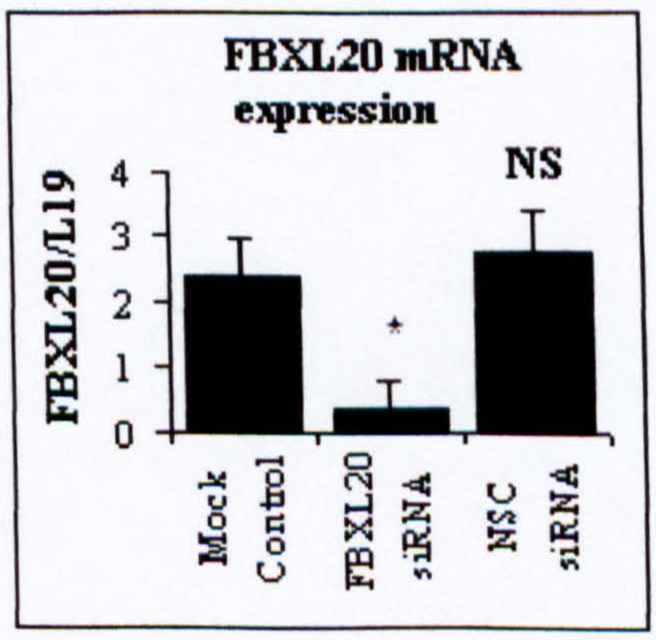
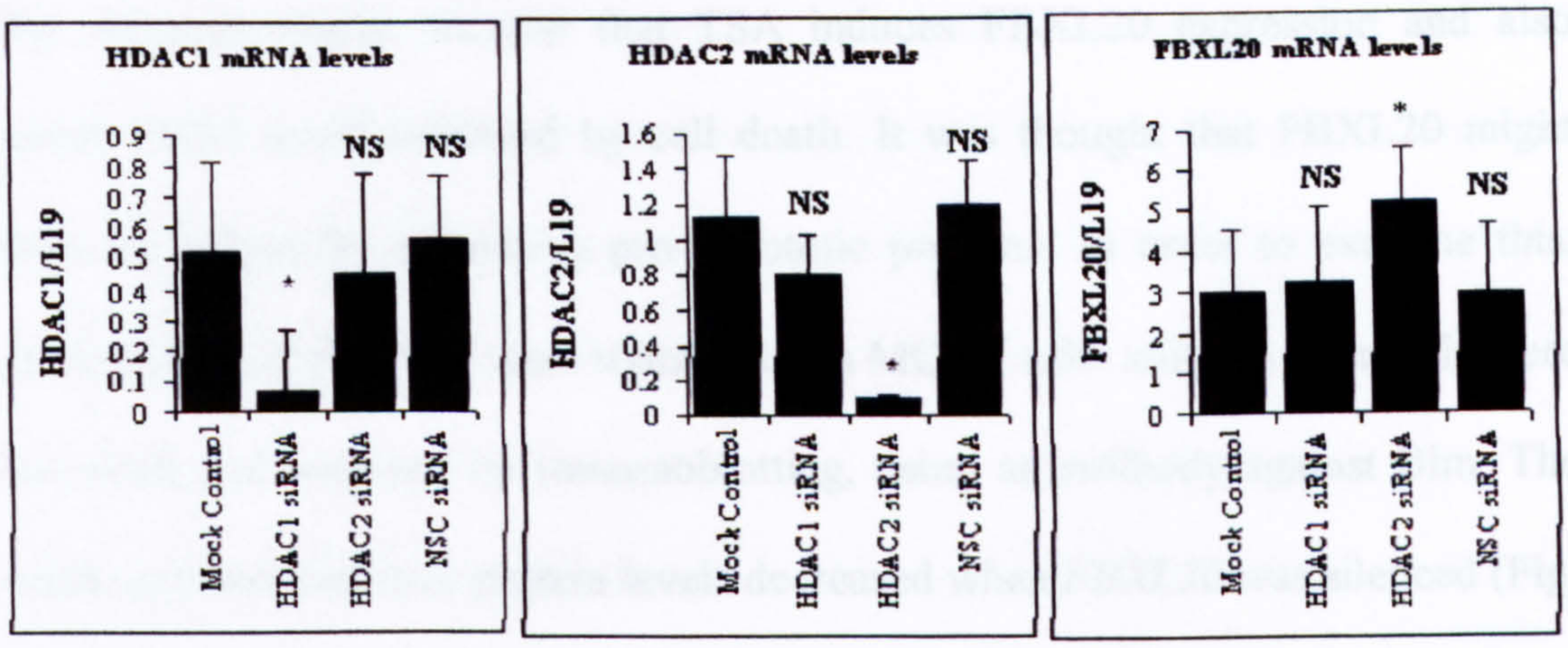


Figure 4.8 siRNA-mediated *FBXL20* knockdown attenuates the cytotoxic effect of SAHA and SBHA on the cell cycle progression of MCF-7 cells. A) Cells were transfected with oligo pools specifically targeting *FBXL20* or *NSC* and 24h later treated with 5μM SAHA (A) or 100μM SBHA (B) for 24h. Cells were then harvested and fixed with 90% ethanol followed by FACS analysis. C) RNA from cells transfected in parallel was used in a RT-QPCR reaction with primers specific for *FBXL20* to monitor siRNA efficiency. Results represent FBXL20 mRNA levels normalised by L19 mRNA levels. Statistical analysis was performed using the Mann-Witney U test and *$p<0.05$.

Silencing HDAC2 leads to induction of FBXL20 mRNA levels

Since TSA leads to inhibition of HDACs and induces the expression of FBXL20, I next asked the question if a particular HDAC is responsible for this effect. HDAC1 and HDAC2 have been shown to be very important in the regulation of expression of many proteins in MCF-7, therefore these two HDACs were chosen for the subsequent experiment (Bicaku et al., 2008; Harms and Chen, 2007; Kawai et al., 2003). *HDAC1* and *HDAC2* specific siRNA pools were transfected into MCF-7 cells and 48h later RNA was extracted and analysed by RT-QPCR. Silencing HDAC2 caused a profound increase in the mRNA expression of *FBXL20*, in contrast, *HDAC1* siRNA did not alter the *FBXL20* mRNA levels (Fig. 4.9A). Knockdown of *HDAC1* and *HDAC2* was confirmed by RT-QPCR (Fig. 4.9A) and immunoblotting (Fig. 4.9B).

A)



B)

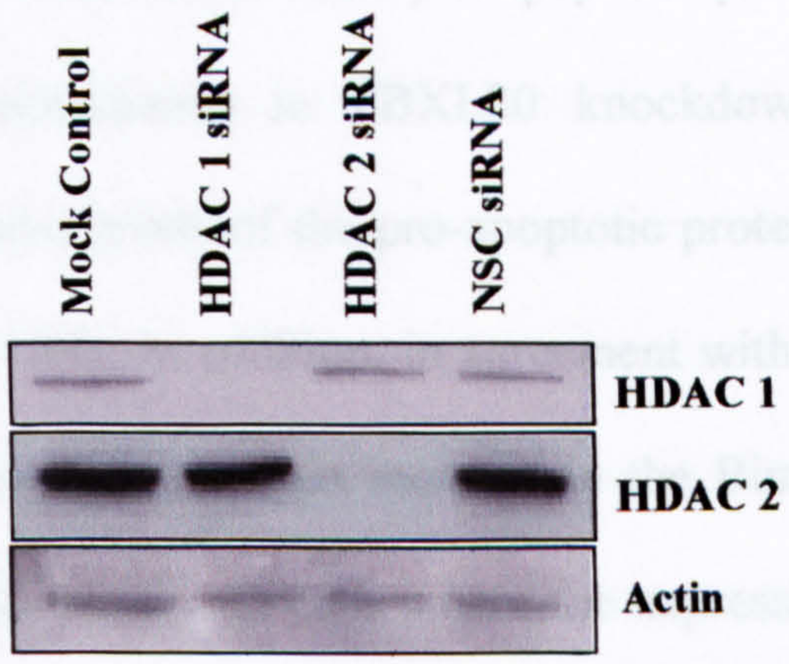


Figure 4.9 Specific knockdown of *HDAC2* induces expression of *FBXL20* mRNA. MCF-7 cells were transfected with oligo pools specifically targeting HDAC1-2 or NSC. 72h after transfection, cells were harvested. A) RNA was extracted followed by cDNA synthesis. *HDAC1*, *HDAC2* and *FBXL20* expression was analysed by RT-QPCR. Graphs represent the indicated levels of mRNA normalised by *L19* mRNA. Results are the mean ± SD of three independent experiments that included 2 replicates each. Statistical analysis was performed using the Mann-Witney U test and $*p<0.05$ B) Lysates were also made and analyzed by SDS-PAGE and immunoblotted with HDAC1 -2 to confirm the silencing in the protein level.

FBXL20 regulates Bim protein levels

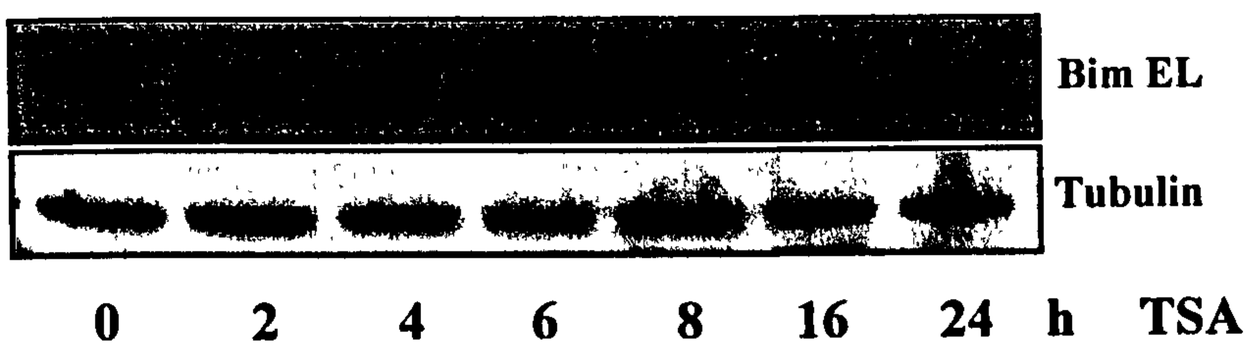
My previous results showed that TSA induces FBXL20 expression and also causes G_2/M arrest followed by cell death. It was thought that FBXL20 might exert its effects by regulating pro-apoptotic proteins. In order to examine this, siRNA pools of *FBXL20* were transfected in MCF-7 cells and 48h later cells were harvested and analysed by immunoblotting, using an antibody against Bim. The results showed that Bim protein levels decreased when *FBXL20* was silenced (Fig. 4.11A) but mRNA levels were unaffected (Fig. 4.12). It was then suggested that silencing FBXL20 may affect other pro-apoptotic proteins as well and therefore immunobloting experiments in FBXL20 knockdown cells were performed. However, the protein levels of the pro-apoptotic proteins Bax and Bad remained unchanged (Fig.4.12B). In addition, in agreement with other studies (Fandy et al, 2006), TSA treatment lead to an increase in the Bim protein (Fig. 4.10A) and mRNA levels (Fig. 4.10B). In cells where the expression of *FBXL20* is silenced, TSA failed to induce the expression of Bim in the protein level as analysed by immunoblotting (Fig. 4.11A), which strongly suggest that TSA-induced Bim upregulation is a FBXL20-dependent event. Because Bim_{EL} was the major form of Bim expressed under these experiments, with only low levels of Bim_L seen, further analysis focused on the regulation of Bim_{EL}. In addition, cells were transfected with Flag-FBXL20 and 24h later cells cell were analysed by immmunoblotting. Bim expression was induced in cells that overexpressed FBXL20 but not mock transfected control cells (Fig. 4.13).

In order to test if FBXL20 binds Bim, cells were transfected with Flag-FBXL20 recombinant vector which was then immunoprecipitated and samples were

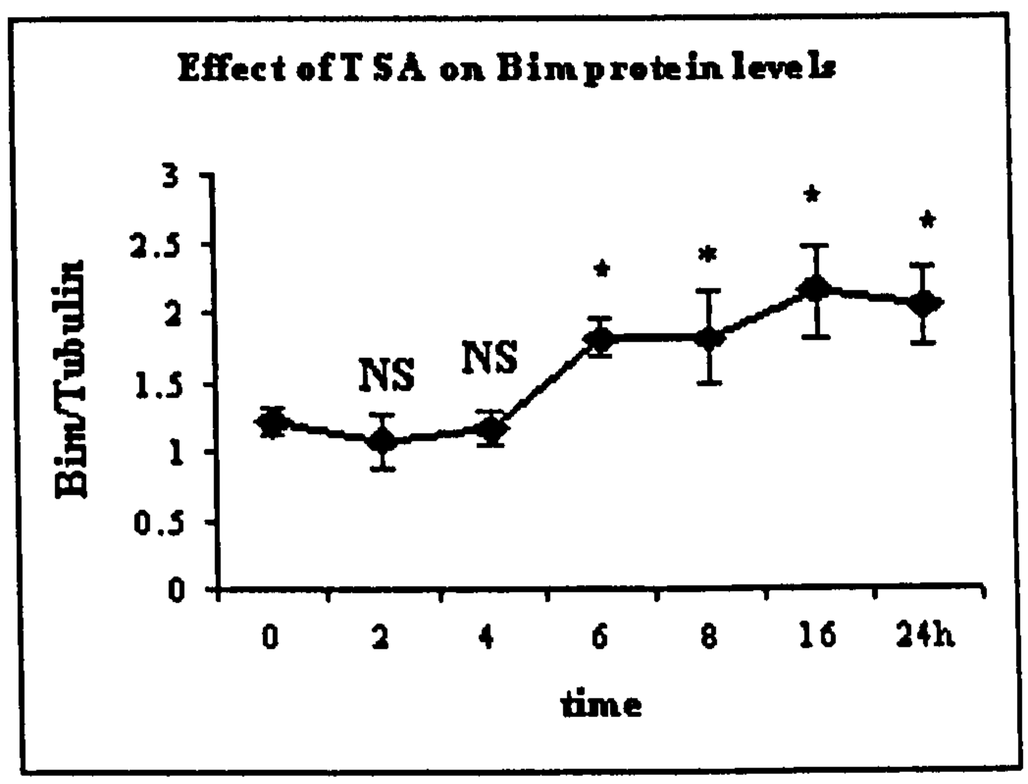
analysed by SDS-PAGE. Immunobloting analysis showed that FBXL20 binds Bim (Fig. 4.14). Skp1, ROC-1 and CUL-1 were also able to bind FBXL20 proving that the immunoprecipitation experiment has worked. As a negative control for the immunoprecipitation, an antibody against ERα was used and showed that ERα does not bind FBXL20.

Cell cycle analysis revealed that when silencing both *FBXL20* and *Bim* in the same cells, cells arrested in the G_2/M phase after treatment with 1μM TSA for 24h, in contrast to cells where only *FBXL20* is silenced (Fig. 4.15A). In cells where only *FBXL20* was silenced, there was also a slight decrease in the number of cells in G_2/M phase before TSA treatment. In cells where Bim was silenced, there were fewer cells in the sub-G_1 phase after TSA, indicating that Bim contributes to protecting cells from the growth inhibition by TSA, as observed in other studies (Donadelli et al, 2007). Knockdown of *FBXL20* was confirmed by RT-QPCR and silencing of Bim was confirmed by SDS-PAGE (Fig. 4.15B).

A)



B)



C)

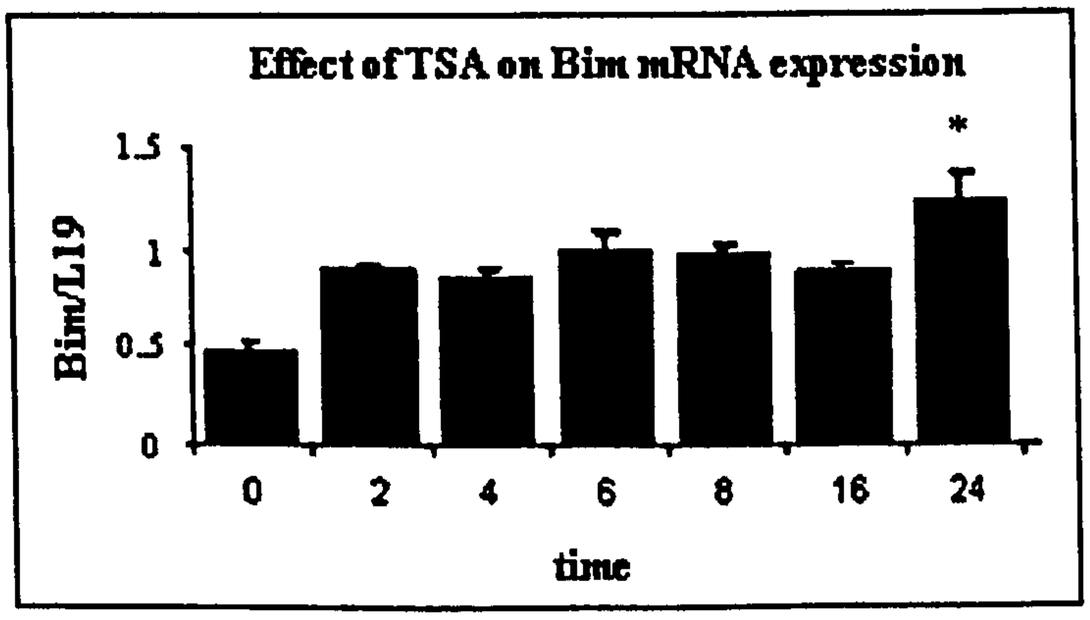
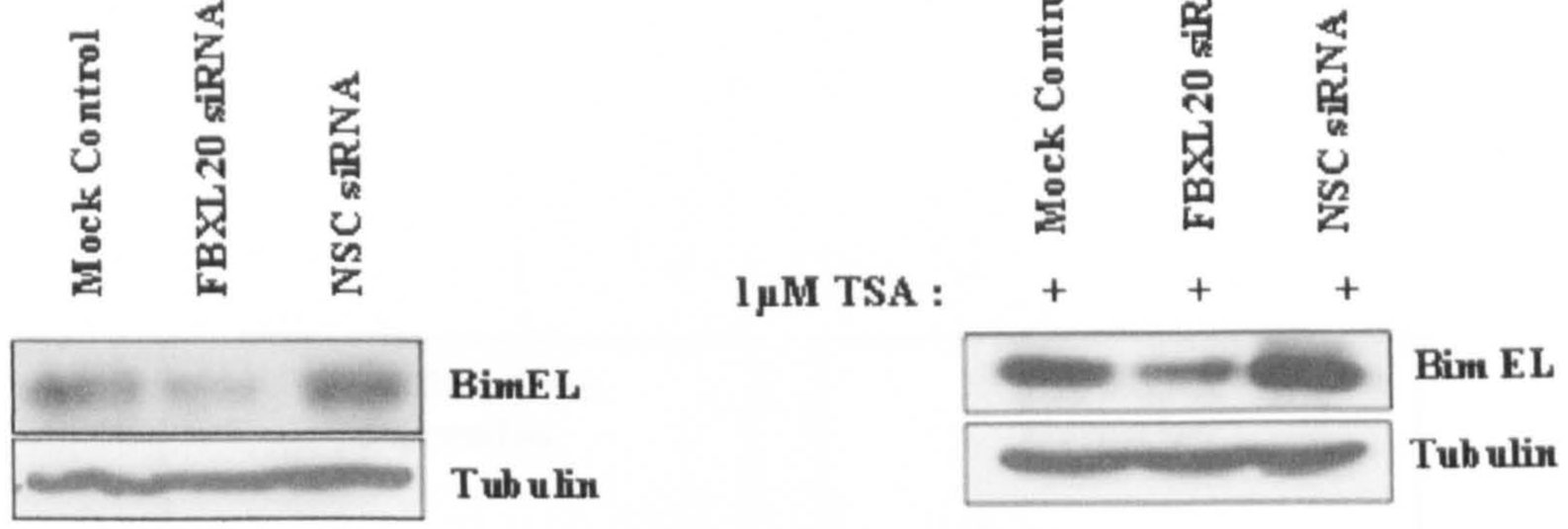
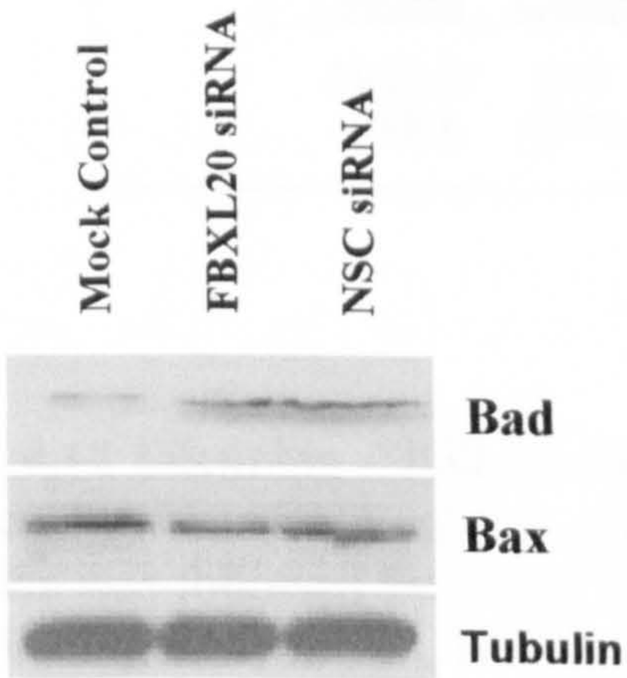


Figure 4.10 TSA induces the expression of *Bim* mRNA and protein. MCF-7 cells were incubated with 1μM TSA for the indicated times. A) Following incubation, the cells were harvested and lysates were resolved by SDS-PAGE. Proteins were detected using the indicated antibodies. Results are representative of three independent experiments. B) Protein concetration of Bim normalised by the concetration of tubulin from cells treated with 1μM TSA Results represent the average of three independent experiments. Statistical analysis was performed using ANOVA with Dunnett's post-hoc analysis for all time points compared to control (0 hr) and *$p<0.05$. C) RNA extraction was followed by cDNA synthesis and finally analysed by RT-QPCR for *Bim* mRNA levels. Graph shows the levels of *Bim* mRNA normalised by *L19* mRNA levels. Statistical analysis was performed using ANOVA with Dunnett's post-hoc analysis for all time points compared to control (0h) and *$p<0.05$.

A)



B)



C)

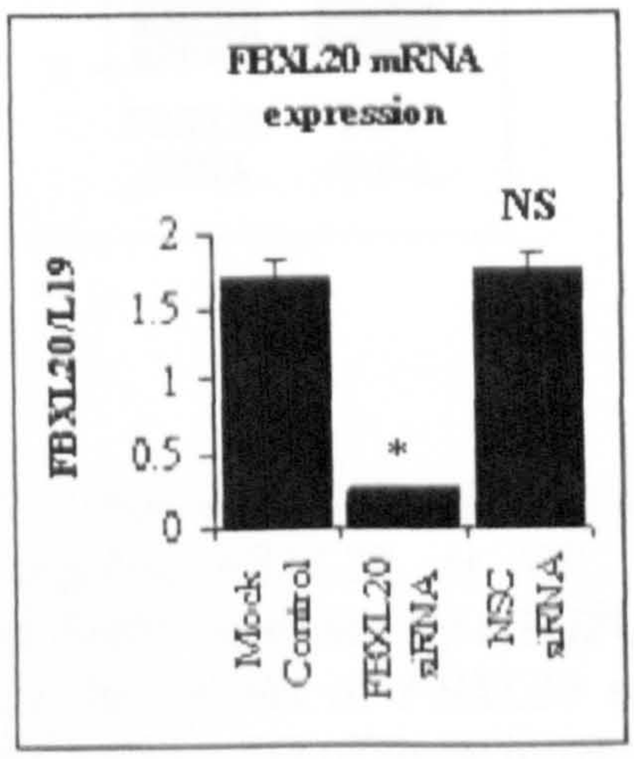


Figure 4.11 Silencing FBXL20 leads to downregulation of Bim protein levels. A) Cells were plated out in 6cm plates and transfected with siRNA oligos specifically targeting FBXL20, or NSC siRNA. Mock cells were not treated with any siRNA. 24h later cells were treated with 1μM TSA or remained untreated. Lysates were then made and analysed by SDS-PAGE and immunobloted by the indicated antibodies. Results are representative of three independent experiments. B) Cells were transfected with siRNA specifically targeting FBXL20 and lysates were analysed by immunoblotting. C) RT-QPCR analysis of cells transfected in parallel were used to confirm *FBXL20* knockdown and the results represent *FBXL20* mRNA levels normalized by *L19* mRNA levels. Statistical analysis was performed using the Mann-Witney U test and *$p<0.05$.

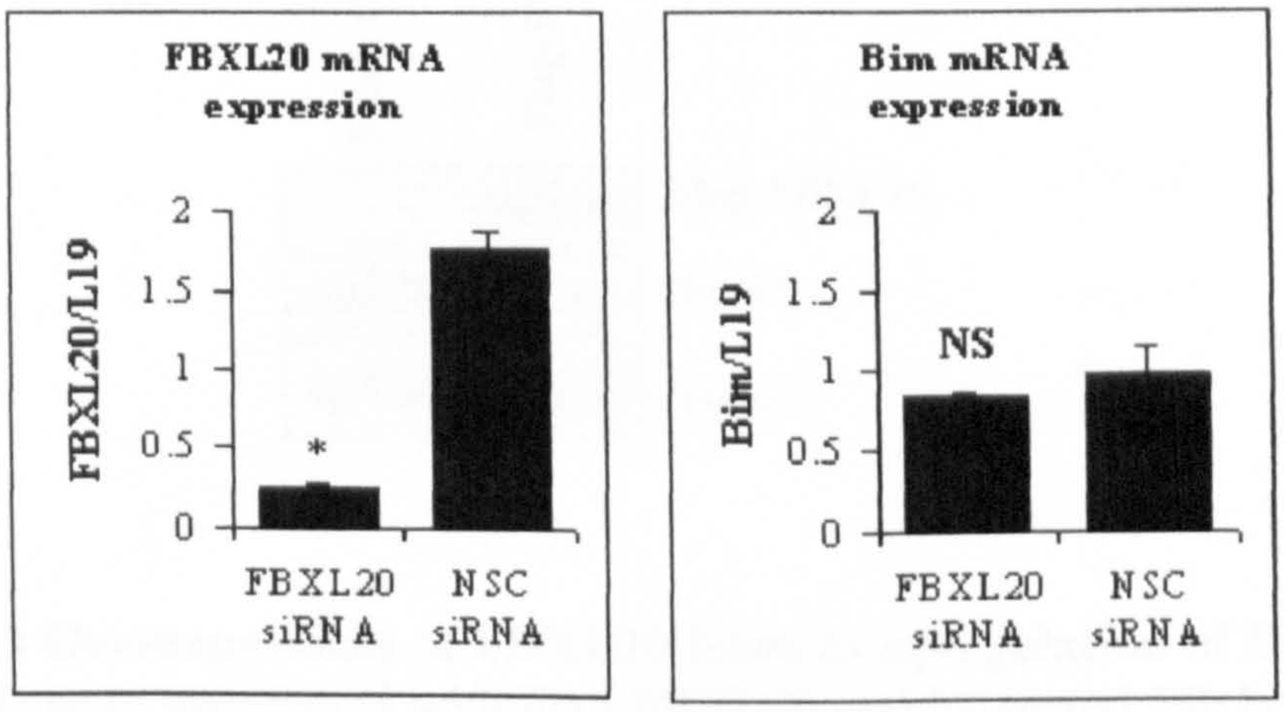


Figure 4.12 Silencing *FBXL20* does not affect *Bim* mRNA levels. Cells were transfected with siRNA oligos specifically targeting *FBXL20*, or *NSC*. RNA extraction was followed by cDNA synthesis and finally analysed by RTQPCR for *FBXL20* and *Bim* mRNA levels. Graphs show the levels of *FBXL20* mRNA normalised by *L19* mRNA levels. Results are the mean ± SD of three independent experiments that included 3 replicates each. Statistical analysis was performed using the Mann-Witney U test and *$p<0.05$.

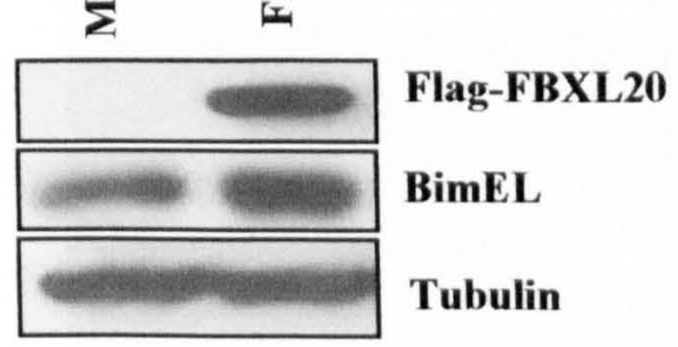


Figure 4.13 Overexpression of FBXL20 leads to upregulation of Bim protein levels. Cells were transfected with Flag-FBXL20 and harvested 24h later. Lysates were made, analysed by SDS-PAGE and immunobloted by the indicated antibodies. Results are representative of three independent experiments.

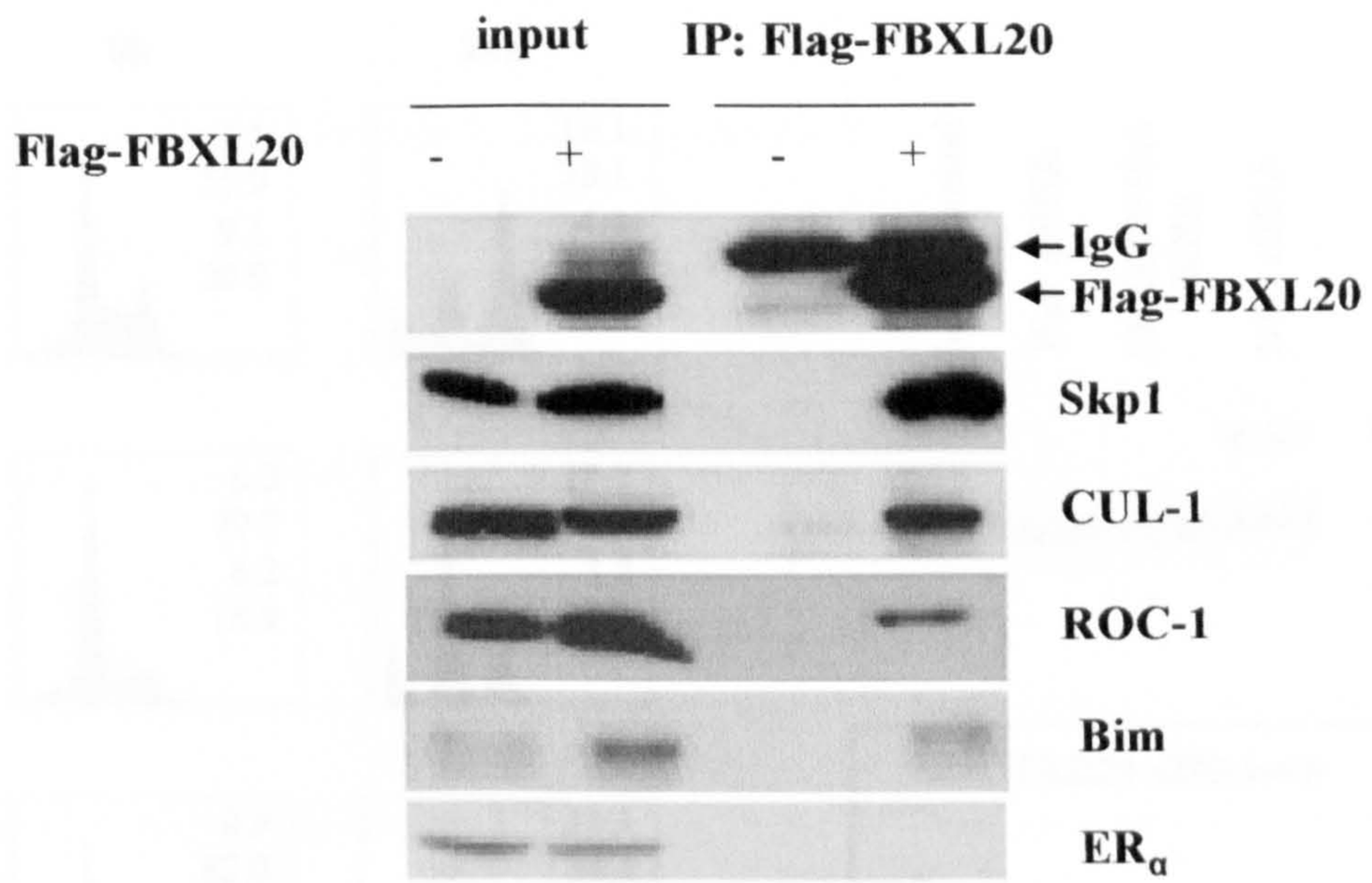


Figure 4.14 FBXL20 binds Bim. MCF-7 cells were transfected with Flag-FBXL20 and harvested 24h later. Whole cell extracts were prepared in lysis buffer and immuprecipitations (IP) were performed using a monoclonal anti-Flag antibody. The IP samples along with samples from the whole cell lysates were then analysed by SDS-PAGE and immunoblotted with the indicated antibodies. Results are representative of three independent experiments.

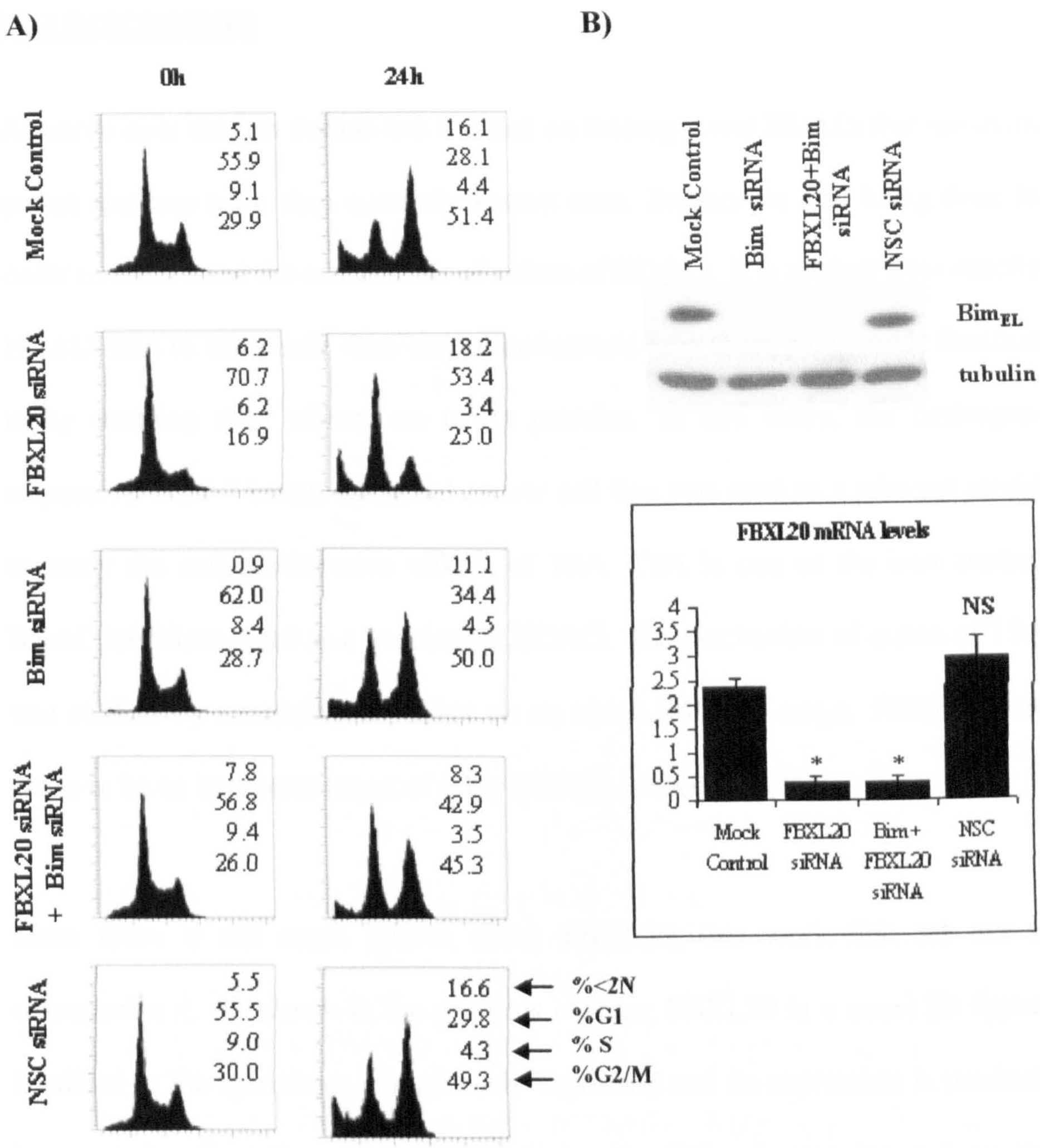


Figure 4.15 Effect of siRNA-mediated FBXL20 and Bim knockdown on the cell cycle progression of MCF-7 cells treated with TSA. A) Cells were transfected with oligo pools specifically targeting *FBXL20*, *Bim*, *FBXL20* and *Bim* together or NSC and 24h later treated with 1μM TSA for 0 and 24h. Cells were then harvested and fixed with 90% ethanol and analysed by FACS analysis. B) RNA from in parallel transfected cells was used in RT-QPCR reaction with primers specific for *FBXL20* to monitor siRNA efficiency. Graphs represent *FBXL20* mRNA levels normalised by *L19* mRNA levels. Statistical analysis was performed using the Mann-Witney U test and *$p<0.05$. Protein from cells transfected in parallel was used in SDS-PAGE experiment to monitor *Bim* siRNA efficiency.

IV.3 DISCUSSION

Research over the last decade has focused on finding novel HDACi that are more potent and less toxic than currently known ones. Studies are also being done in order to understand the mechanism of action of HDACi. It is unclear how exactly HDACi lead to cell death. One way to understand how these compounds function is by studying their effects on target proteins. In this study, the oestrogen-responsive MCF-7 breast epithelial cancer cell line was used as a relevant model to study the anti-proliferative effects of TSA. TSA is one of the best studied HDAC inhibitors, used as a benchmark HDACi. The mechanism of action of TSA was studied by examining its effect on its novel FBXL20 target. FBXL20 may prove to be an important target of other HDACi as well as TSA.

Since there is not much known about FBXL20, this work first set out to characterize it. As shown in the previous chapter, FBXL20 is a novel E3 ligase, localised in the cytoplasm, ubiquitously expressed and its expression is maximal in arrested cells rather than proliferating cells. This chapter focused on the functional role of FBXL20 in MCF-7 cells. Examining the role this protein plays in the TSA-induced effect in cells, I discovered many properties of FBXL20 and also one of its binding partners.

Treatment of MCF-7 cells with 1μM TSA caused a G_2/M arrest after 16h of treatment. Arrest in this phase seems to be an important checkpoint mediated by HDACi in cancer cells. While a lot is known about how the G_1/S arrest occurs at low concetrations of TSA, little is known about how the G_2/M arrest is mediated. TSA has been shown to cause G_1/S arrest by inducing the expression of $p21^{Cip1}$

and downregulating the expression of cyclin D1 and ERα, proteins that are involved in the transition from the G_1 phase to the S phase of the cell cycle (Alao et al., 2004). The results shown in this chapter strongly suggest the involvement of FBXL20 in mediating TSA-induced G_2/M arrest in MCF-7 cells.

TSA caused an upregulation of *FBXL20* mRNA levels. This is a direct effect, since co-treatment with CHX was unable to inhibit the induction of *FBXL20* mRNA. Thus, it is possible that FBXL20 is a direct target of TSA. The best known direct target of TSA is $p21^{Cip1}$. TSA has previously been shown to modulate $p21^{Cip1}$ promoter activity through the proximal Sp1 sites of its promoter region (Han et al, 2000; Margueron et al, 2003; Sowa et al, 1999). It is possible that since *FBXL20* is upregulated upon induction of cell death, it may play a role in degrading proteins that promote cell growth.

TSA led to the upregulation of Flag-FBXL20 protein levels suggesting that TSA may regulate FBXL20 at the protein and mRNA level, since Flag-FBXL20 protein is driven by a different promoter than the endogenous FBXL20. It is possible that the induction of Flag-FBXL20 protein levels is due to decreased degradation of the protein. More work has to be done to understand how TSA regulates FBXL20. Promoter assays have to be performed and the stability of FBXL20 has to be examined. Also the binding partners of FBXL20 have to be identified. Furthermore, the full-length *FBXL20* cDNA was cloned in the Flag-tagged vector without any of the 3' untranslated region of the gene included. This suggests that the action of TSA does not involve the regulation of miRNAs that could subsequently regulate *FBXL20*. miRNAs are known to target the 3'

untranslated region of genes and lead to translational repression of many different mRNAs. In comparison to the well known siRNAs, where the target mRNA is degraded due to their perfect complementarity to their respective siRNA, miRNAs are not perfectly complementary to the corresponding mRNAs (Arenz, 2006).

Silencing *FBXL20* caused a no significant change in the cell cycle profile of MCF-7 cells, as it showed a small decrease in the number of cells in the G_2/M phase. However, upon treatment with TSA, the changes are more significant. Knockdown of *FBXL20* gave a growth advantage to MCF-7 cells in response to TSA, since the proliferation assay (SRB assay) showed an increase in the rate of proliferation in cells where *FBXL20* was silenced compared to the control transfected cells. However, this was seen particularly at the higher concentration of TSA (1μM) where cells are undergoing cell death. At lower concentrations of TSA, where this is not the case, the growth advantage induced by silencing *FBXL20* is not so obvious, indicating that FBXL20 plays a role in mediating cell death. Also, cell cycle analysis of cells transfected with FBXL20 siRNA revealed that knockdown of *FBXL20* and subsequent treatment with TSA led to a reduction in the number of cells at the G_2/M phase compared to the NSC and Mock transfected cells. Moreover, FACS analysis showed that transfection of cells with Flag-FBXL20 and subsequent treatment with TSA, led to an induction of cell death compared to untransfected TSA treated cells. This further suggests that FBXL20 is involved in the induction of cell death. Cell cycle analysis of the Flag-FBXL20 transfected cells also showed that the arrest at the G_2/M phase was abrogated and cells had undergone apoptosis. This could possibly be explained by the induction of Bim caused by overexpressing FBXL20.

The findings that silencing of *FBXL20* expression by siRNA can overcome the G_2/M cell cycle arrest induced by TSA, lead to a growth advantage of cells as it increases their proliferation and the fact that overexpression of FBXL20 led to an induction of cell death, suggest that FBXL20 could act as a tumour suppressor. It is also possible, that FBXL20 plays a role in the G_1/S transition. The similar protein Skp2 is known to contribute to G_1/S transition by degrading $p27^{Kip1}$ (Carrano et al., 1999; Sutterluty et al., 1999; Zhang et al., 1995).

FBXL20 is important for the action of possibly all HDACi and not just TSA, as MCF-7 cells treated with the HDACi SAHA and SBHA showed similar results to those obtained with TSA. Cells where FBXL20 was silenced, failed to arrest in the G_2/M phase. Furthermore, in contrast to *HDAC1*, silencing *HDAC2* caused an increase in the mRNA levels of *FBXL20*, suggesting that this HDAC may play a role in the regulation of FBXL20. It is possible that TSA leads to the downregulation of HDAC2 which might subsequently lead to the induction of FBXL20 mRNA and protein levels.

As shown in other studies (Fandy et al, 2006), TSA induced the expression of Bim at the mRNA and protein level, which plays an important role in TSA-induced apoptosis in cells. This work shows that the TSA induced upregulation of Bim is abrogated when *FBXL20* is silenced. In untreated cells, knockdown of *FBXL20* leads to a decrease in the protein expression of Bim, but no change is observed in the *Bim* mRNA levels. No change was also seen in the protein levels of Bax and Bad therefore FBXL20 does not affect the levels of all pro-apoptotic proteins. Immunoblotting experiments should be done to test the effect of silencing

FBXL20 on other pro-apoptotic proteins as well. Furthermore, overexpression of FBXL20 led to an induction of Bim protein levels. Moreover, immunoprecipitation experiments showed that FBXL20 binds Bim. Taken together these results suggest that FBXL20 does not directly lead to the degradation of Bim. It is likely that FBXL20 actually binds Bim in order to stabilise it, preventing it from being degraded by another E3 ligase. It would be interesting to see whether FBXL20 also binds the smaller Bim isoforms Bim_S and Bim_L. GST-pulldown experiments have to be performed with FBXL20 mutated at different sites to find which region is responsible for binding Bim. Mutation of these sites would inhibit binding of these two proteins. Also, cell cycle analysis showed that in the absence of FBXL20, Bim is required for the abrogation of TSA-induced G_2/M arrest, suggesting that FBXL20 acts through Bim to exert its effect on MCF-7 cells upon TSA treatment. Bim is regulated by ubiquitination and proteasomal degradation. Inhibiting its degradation could lead to the induction of apoptosis in cancer cells. This suggests that a combination of HDACi, such as SAHA, with proteasome inhibitors could be more effective in killing cancer cells.

Collectively, the results from this work suggest that FBXL20 is a target of TSA. Knockdown of FBXL20 causes a change in how TSA exerts its effects on MCF-7 cells, as it leads to an abrogation of TSA-mediated G_2/M arrest. FBXL20 acts through regulating the pro-apoptotic protein Bim.

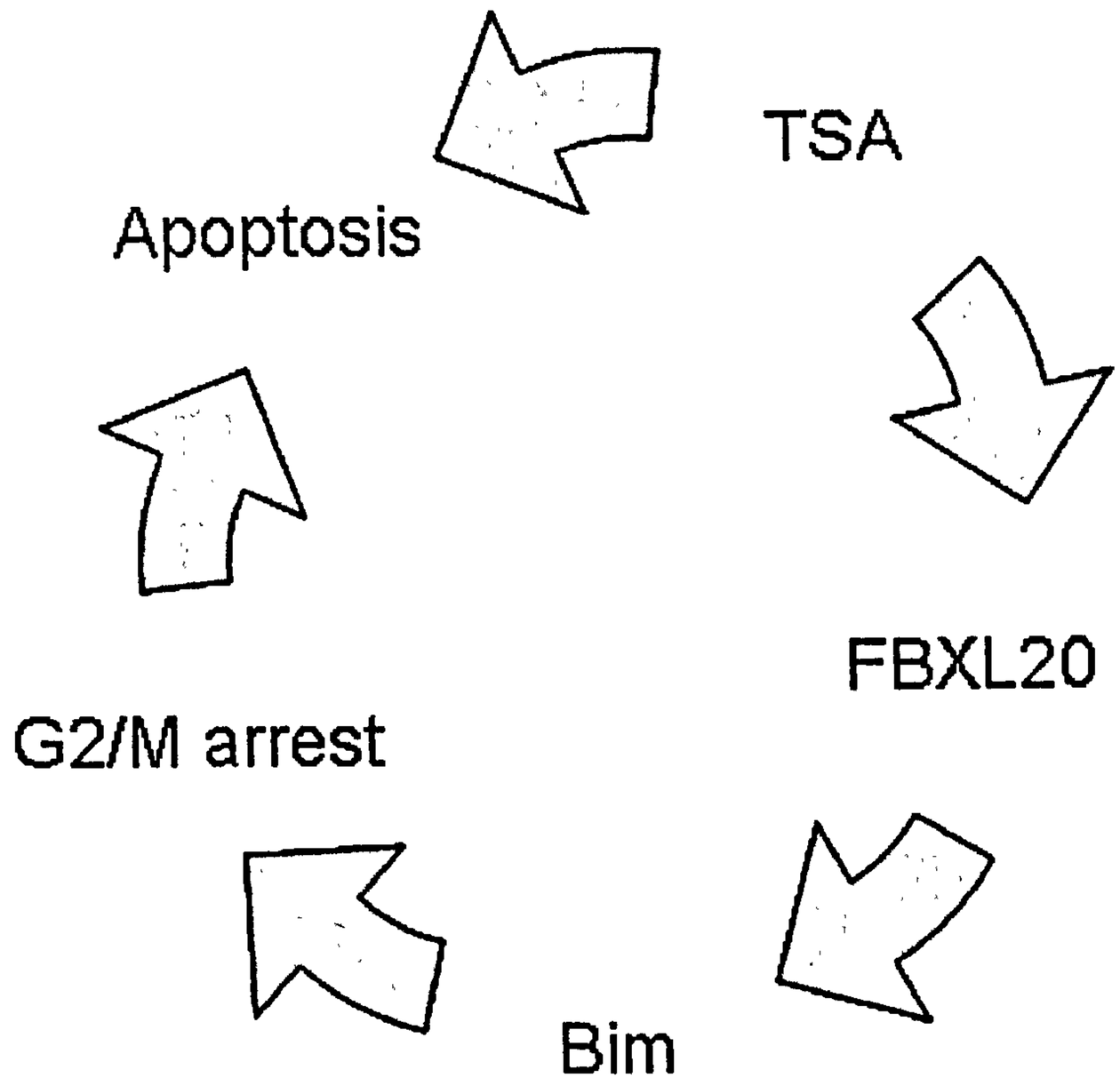


Figure 4.16 Schematic to represent the role of FBXL20 in TSA-induced cell cycle arrest and apoptosis.

Future work

In order to understand the regulation of FBXL20 by TSA at the transcriptional level, the promoter of *FBXL20* could be studied. Analysis of the sequence of the promoter, to see which sites it contains, may help to identify which proteins bind to it. Subsequent cloning of the promoter followed by chromatin immunoprecipitation (ChIP) experiments using antibodies against the proteins thought to bind the particular sequences in the promoter, could be used to determine if these proteins bind the promoter of *FBXL20* in untreated and TSA treated cells. Gene silencing using siRNA technology could be used to silence the expression of these regulators of *FBXL20* expression to characterise their effects

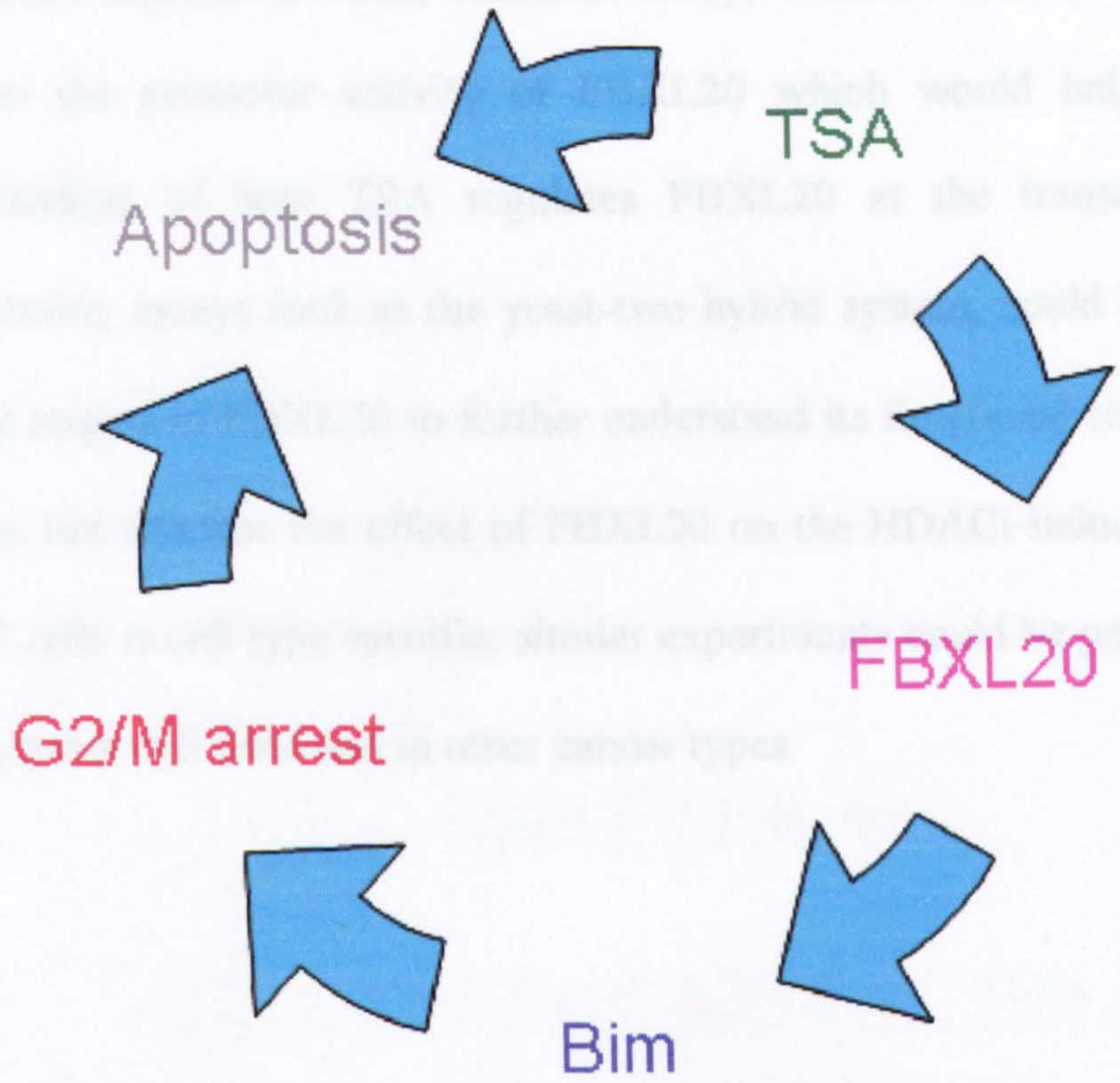


Figure 4.16 Schematic to represent the role of FBXL20 in TSA-induced cell cycle arrest and apoptosis.

Future work

In order to understand the regulation of FBXL20 by TSA at the transcriptional level, the promoter of *FBXL20* could be studied. Analysis of the sequence of the promoter, to see which sites it contains, may help to identify which proteins bind to it. Subsequent cloning of the promoter followed by chromatin immunoprecipitation (ChIP) experiments using antibodies against the proteins thought to bind the particular sequences in the promoter, could be used to determine if these proteins bind the promoter of *FBXL20* in untreated and TSA treated cells. Gene silencing using siRNA technology could be used to silence the expression of these regulators of *FBXL2*0 expression to characterise their effects

on *FBXL20* expression. Also, luciferase assays could be done to test the effect of TSA on the promoter activity of FBXL20 which would help in the better understanding of how TSA regulates FBXL20 at the transcriptional level. Furthermore, assays such as the yeast-two hybrid system, could be performed to find the targets of FBXL20 to further understand its functional role in the cell. In order to test whether the effect of FBXL20 on the HDACi-induced cell death in MCF-7 cells is cell type specific, similar experiments could be performed in other breast cancer cell lines and in other cancer types.

CHAPTER V

ANALYSIS OF NOVEL HDAC INHIBITORS

V.1 BACKGROUND AND OBJECTIVES

The development of HDACi, such as SAHA, has inspired many researchers to search for better inhibitors in the quest for more effective cancer therapy. HDACi have shown promising anti-tumour activity in a variety of cancers. A great advantage of HDACi is that normal cells are relatively more resistant to HDACi-induced cell death than cancer cells (Xu et al., 2007). HDACs deacetylate histones and this eventually leads to repression of transcription as transcription factors are unable to access DNA (Kouzarides, 1999). More precisely, the N-terminal tails of the histones, which are protruding out of the nucleosomes, contain ε-amino groups on their lysine residues and these become deacetylated by HDACs. This deacetylation, catalysed by HDAC enzymes, leads to a compact chromatin structure thus preventing the access of other molecules to DNA, therefore leading to repression of transcription (Strahl and Allis, 2000). HDACi inhibit HDACs, resulting in an increase in acetylation and subsequently transcription of target genes involved in various cellular processes such as proliferation, differentaition and cell death.

Besides histones, HDACi are also known to target other protein substrates, and cause inhibition of proliferation, induce cell cycle arrest, apoptosis and differentiation (Johnstone et al., 2002; Jung et al., 1999; Sambucetti et al., 1999). HDACi are categorised as hydoxamic acids, short chain fatty acids, benzamides and cyclic peptides.

The efficacy of hydroxamic acids depends upon the presence of three domains: a terminal group (in this study it is the hydroxamic acid), a linker unit and an end moiety. The terminal group binds to the zinc in the enzyme's active site which is connected to the linker unit in the channel. This linker is also bound to the end moiety that occupies the external entrance to the channel of the enzyme. This model agrees with structures of histone deacetylase-like protein (HDLP) co-crystallized with either TSA or SAHA (Finnin et al., 1999).

The well known hydroxamic acid SAHA inhibits the class I, II and IV HDACS but not the class III sirtuin family and has been shown to be effective and well tolerated by patients with haematological or solid cancers. However, a number of HDAC inhibitors have toxic side effects at high doses and therefore, are of little use in the clinical setting. Others degrade rapidly, therefore patients will require high dose administration (Warrell et al., 1998). Moreover, HDACi usually cause many non-specific effects affecting other proteins and processes in the cell (Newmark and Young, 1995).

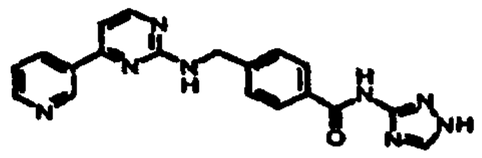
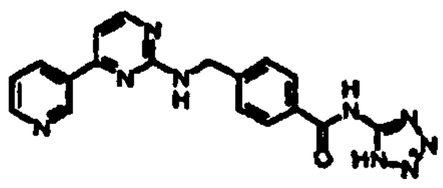
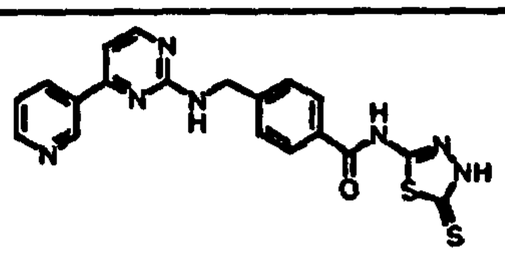
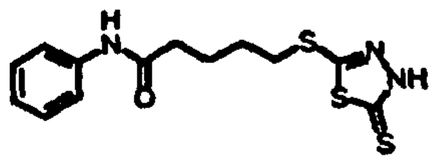
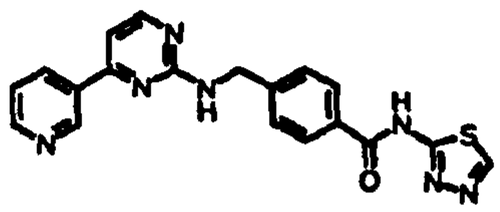
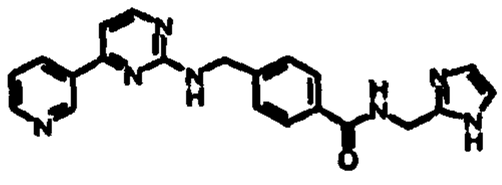
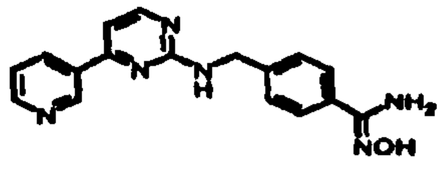
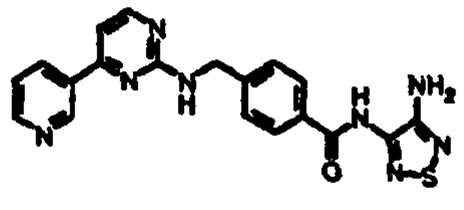
This study focuses on bringing together the knowledge gained from my earlier findings in order to identify a novel hydroxamic acid that shows anti-tumour activities but less toxic and more potent than currently known hydroxamic acids. This work aimed to identify more potent agents by studying their effect on the cell cycle, cell proliferation and deacetylation. The novel compounds were designed and synthesized in collaboration with Prof. Marson's group (UCL University, London).

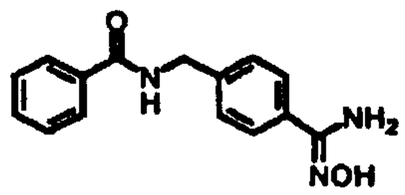
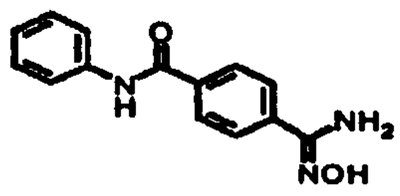
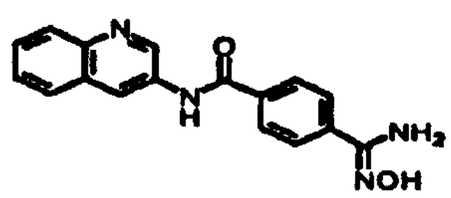
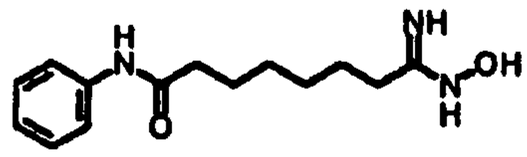
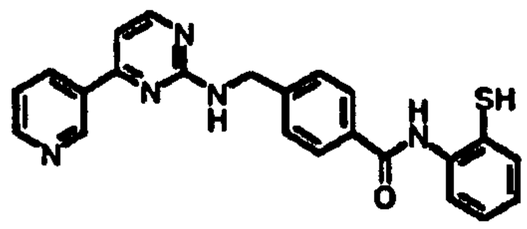
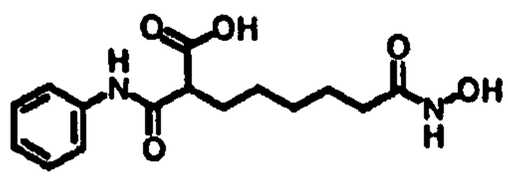
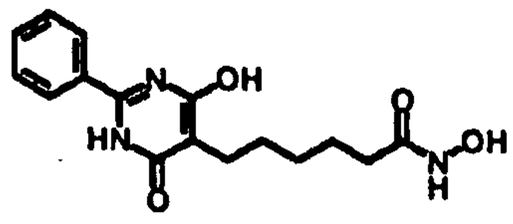
V.2 RESULTS

Compounds 201, 202, 203, 204, 205, 207, 208, 209, 211, 212, 213, 216, 217, 218, 219 do not have a significant effect on MCF-7 cell proliferation

The framework of SAHA was used to design novel HDAC inhibitors which were then analysed by proliferation assays to assay the activity of these agents as has been done in my previous studies with TSA. The SRB proliferation assay was used to test if any of them can inhibit the proliferation of MCF-7 cells. Activities of compounds were compared to SAHA as a benchmark. The concentration used for all compounds in this assay was 5μM as this is the IC_{50} of SAHA in the MCF-7 cell line. TSA was also used as a control. However, it is a much more toxic compound and as a consequence the lower concentration of 1μM was used in all experiments and was enough to inhibit the growth of cells. Results showed that SAHA and TSA decreased the proliferation of cells but none of the novel compounds (201, 202, 203, 204, 205, 207, 208, 209, 216, 217, 218, 219) had any significant effect (Fig. 5.2A, B). The chemical structures of these compounds are shown in figure 5.1A. These compounds were thus considered having little anti-tumour properties and were not analysed in further experiments. Compounds 211, 212 and 213 caused a small decrease in the proliferation but were not as good as SAHA and were therefore not considered as good compounds.

A)

Compound name	Structure	IC_{50} **Cell proliferation**
201		> 10μM
202		> 10μM
203		>10μM
204		>10μM
205		>10μM
207		>10μM
208		>10μM
209		>10μM
210		>10μM

Compound name	Structure	IC_{50} **Cell proliferation**
211		>10μM
212		>10μM
213		>10μM
216		>10μM
217		>10μM
218		>10μM
219		>10μM

B)

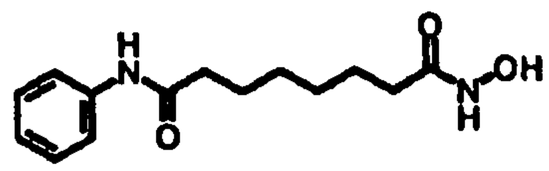
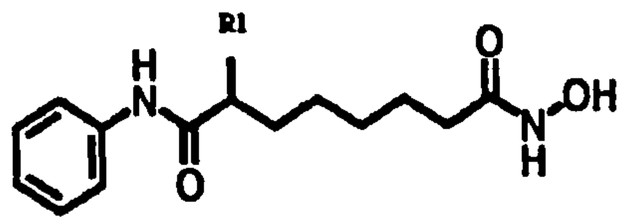
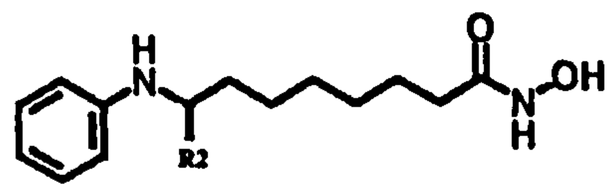
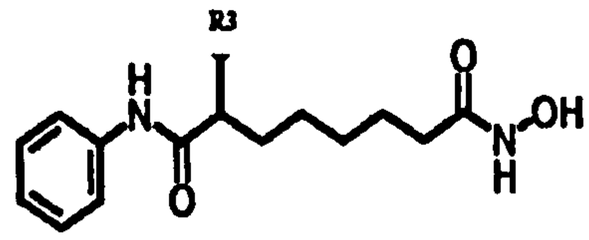
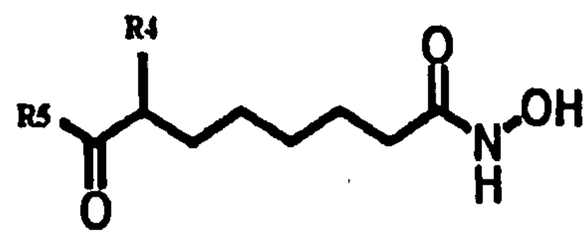
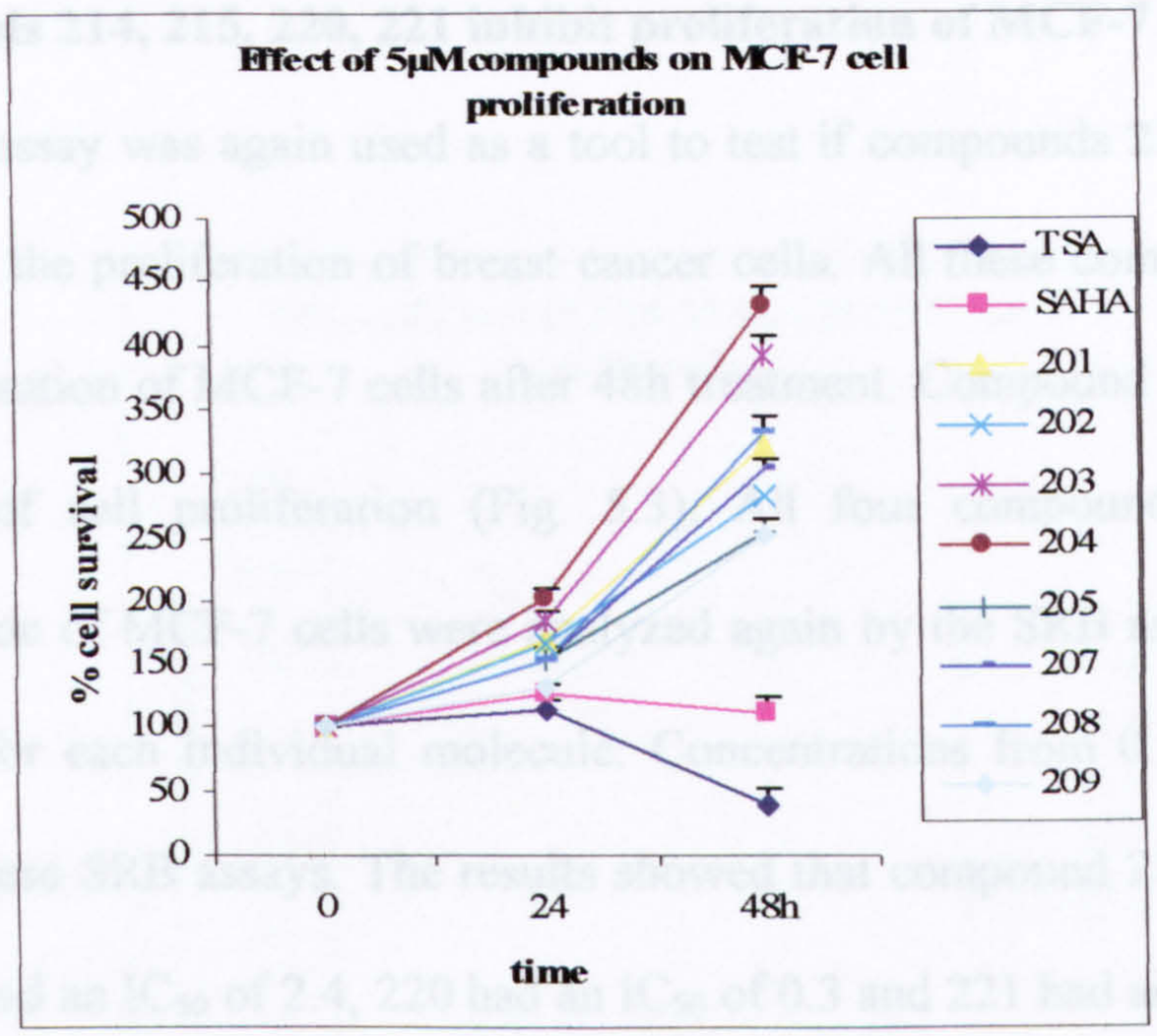
Compound name	Structure	IC_{50} **Cell proliferation**
SAHA		2.5μM
214		2.4μM
215		2.3μM
220		0.3μM
221		2.3μM

Figure 5.1 Representation of the chemical structures of all the compounds synthesized in this work. A) Chemical structures of all inactive compounds B) Chemical structures of all the active compounds in comparison to SAHA. R1, R2, R3, R4 and R5 represent the active moiety attached to the carbon atom shown. The complete structures of the active compounds are not shown in this thesis as patents are being sought to cover the intellectual properties arising from these findings.

A)



B)

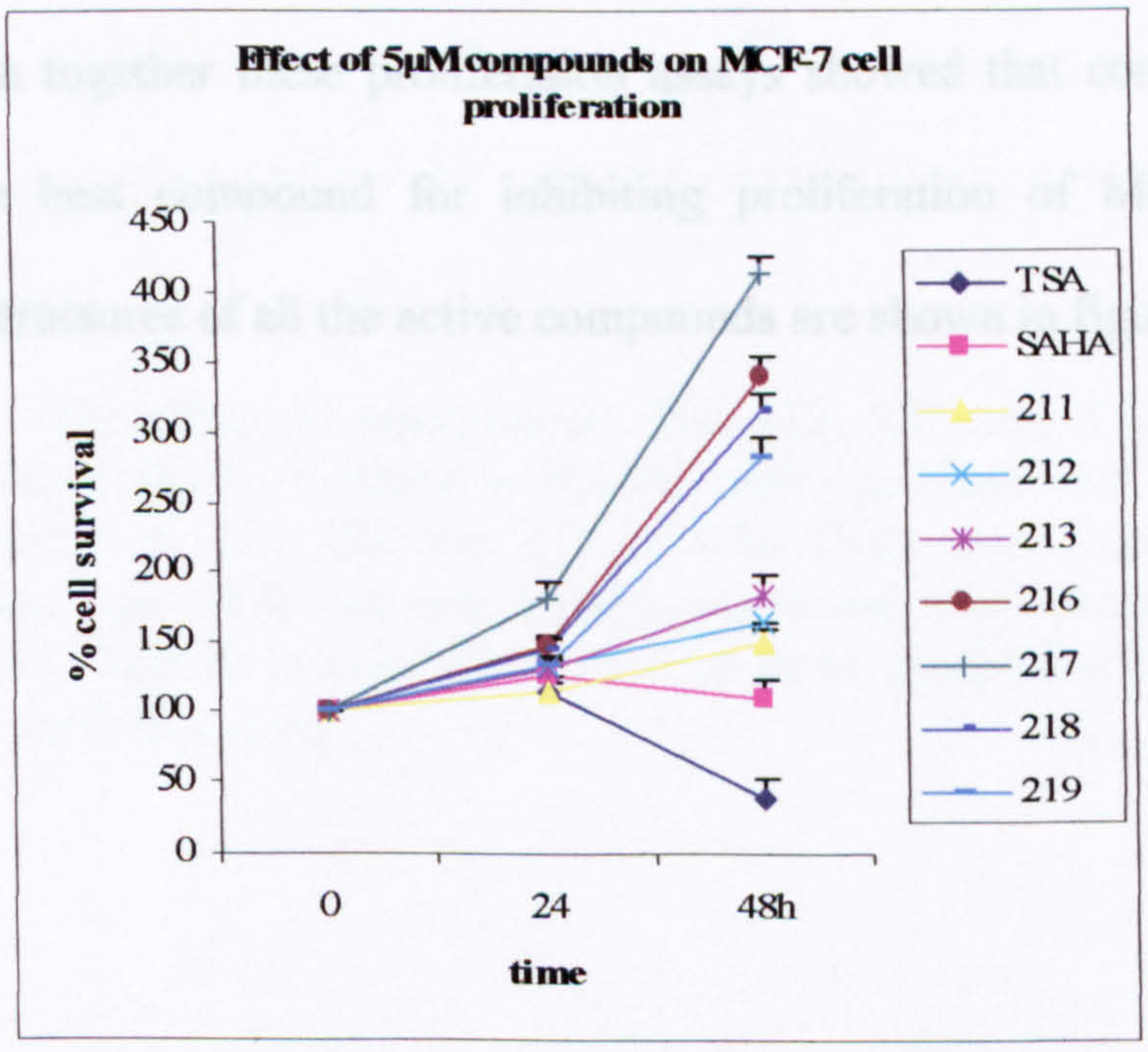


Figure 5.2 Compounds do not affect the proliferation of MCF-7 cells. MCF-7cells were cultured in 96-well plates with 5μM SAHA, 1μM TSA and 5μM of each compound A) 201, 202, 203, 204, 205, 207, 208 and 209. B) 211, 212, 213, 216, 217, 218, 219. Relative cell survival was determined after 24 and 48h using the SRB assay as described in the materials and methods section. Results are the mean ± SD of three independent experiments that included 4 replicates each.

Compounds 214, 215, 220, 221 inhibit proliferation of MCF-7 cells

The SRB assay was again used as a tool to test if compounds 214, 215, 220 and 221 affect the proliferation of breast cancer cells. All these compounds inhibited the proliferation of MCF-7 cells after 48h treatment. Compound 220 was the best inhibitor of cell proliferation (Fig. 5.3). All four compounds that inhibited proliferation of MCF-7 cells were analyzed again by the SRB assay to determine the IC_{50} for each individual molecule. Concentrations from 0.5 to 10μM were used in these SRB assays. The results showed that compound 214 had an IC_{50} of 2.3, 215 had an IC_{50} of 2.4, 220 had an IC_{50} of 0.3 and 221 had an IC_{50} of 2.4 (Fig. 5.4). Taken together these proliferation assays showed that compound 220 was indeed the best compound for inhibiting proliferation of MCF-7 cells. The chemical structures of all the active compounds are shown in figure 5.1B.

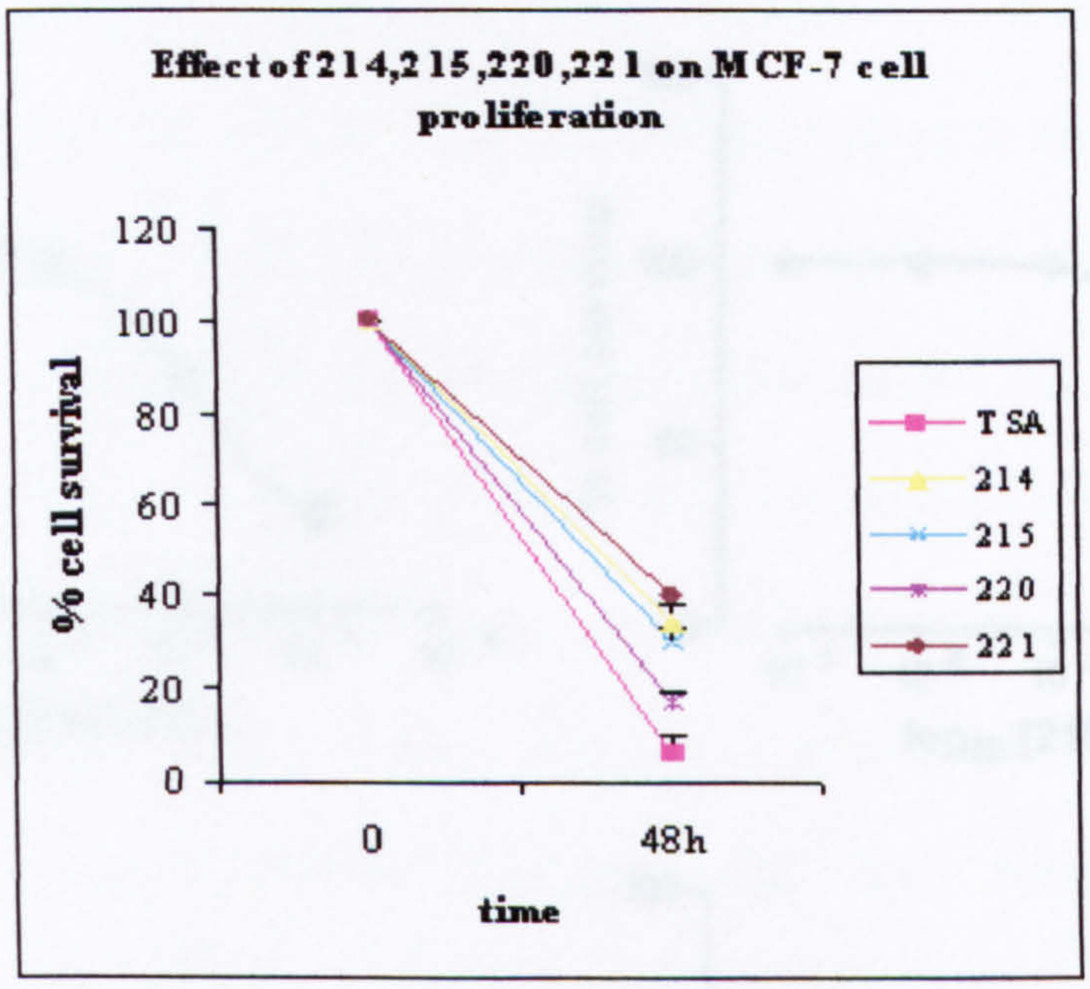


Figure 5.3 The effect of compounds 214, 215, 220 and 221 on MCF-7 cell proliferation. Cells were plated in 96-well plates and 24h later treated with 1μM TSA or 5μM 214, 215, 220 and 221 for 48h. Cells were then fixed with 40% TCA, stained with SRB, and cell density was measured as described in materials and methods. Results are the mean ±SD of three independent experiments that included 4 replicates each.

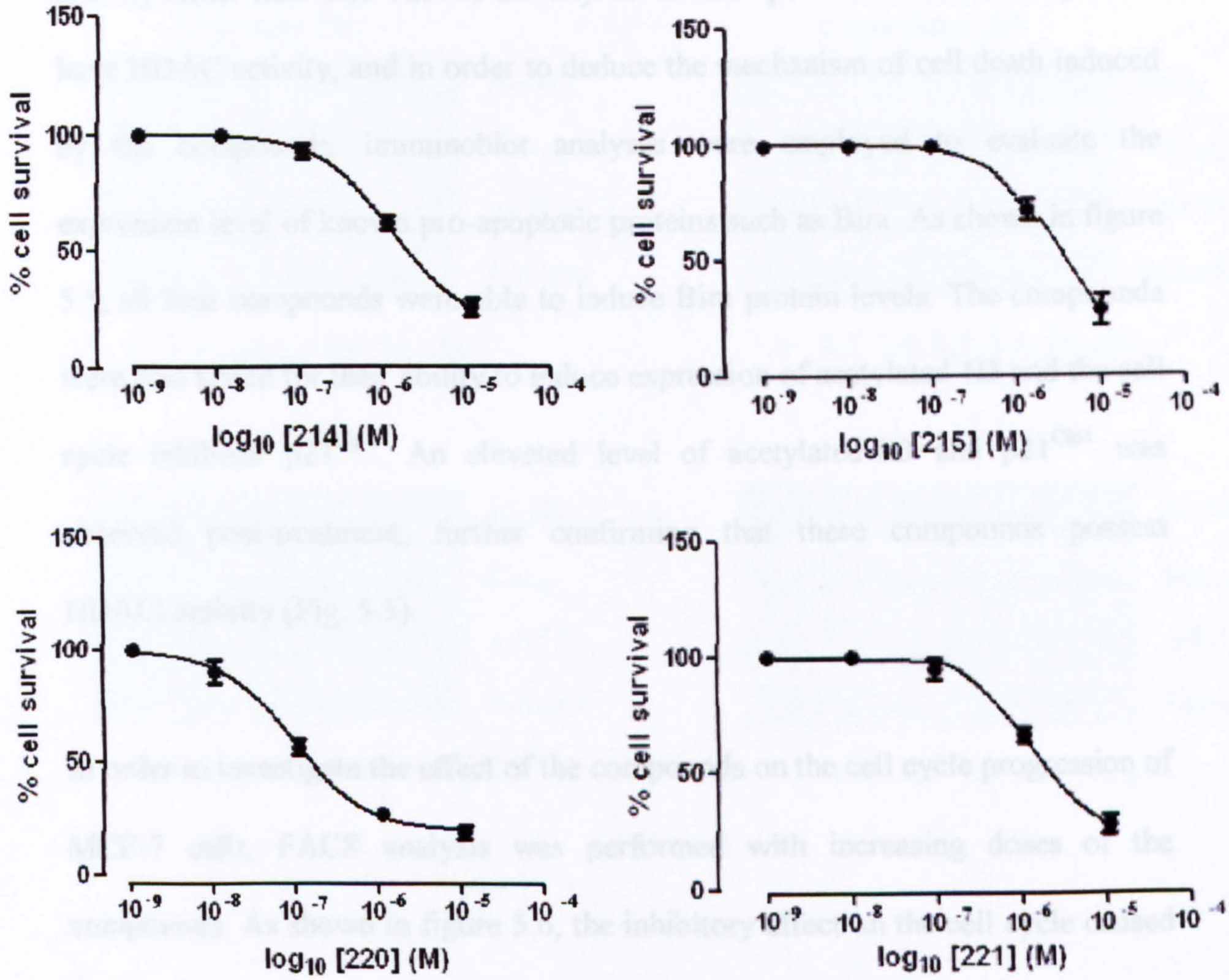


Figure 5.4 Concentration response curves for the impact of selected HDACi on cell survival.. Cells were plated in 96 well plates and 24h later treated with the indicated amounts of 214, 215, 220 and 221 for 48h. Cells were then fixed with 40% TCA, stained with SRB, and cell density was measured as described in materials and methods.Graphs were plotted using Prism and represent the mean ± SD of three independent experiments that included 4 replicates expressed as the percentage of the control value in vehicle treated cells.

Compounds 214, 215, 220, 221 induce expression of Ac-H3, Bim and p21^{Cip1}

It is likely that these novel compounds could cause proliferation arrest due to their toxicity rather than their HDAC activity. In an attempt to test if these compounds have HDAC activity, and in order to deduce the mechanism of cell death induced by the compounds, immunoblot analyses were employed to evaluate the expression level of known pro-apoptotic proteins such as Bim. As shown in figure 5.5, all four compounds were able to induce Bim protein levels. The compounds were also tested for their ability to induce expression of acetylated-H3 and the cell cycle inhibitor p21^{Cip1}. An eleveted level of acetylated-H3 and p21^{Cip1} was observed post-treatment, further confirming that these compounds possess HDACi activity (Fig. 5.5).

In order to investigate the effect of the compounds on the cell cycle progression of MCF-7 cells, FACS analysis was performed with increasing doses of the compounds. As shown in figure 5.6, the inhibitory effect on the cell cycle caused by the compounds was clearly concentration dependent. All four compounds induced G_1/S arrest at low concentrations, and G_2/M arrest and an increase in sub-G1 population at the higher concentrations as has been shown for SAHA, TSA and other HDAC inhibitors (Fig. 5.6).

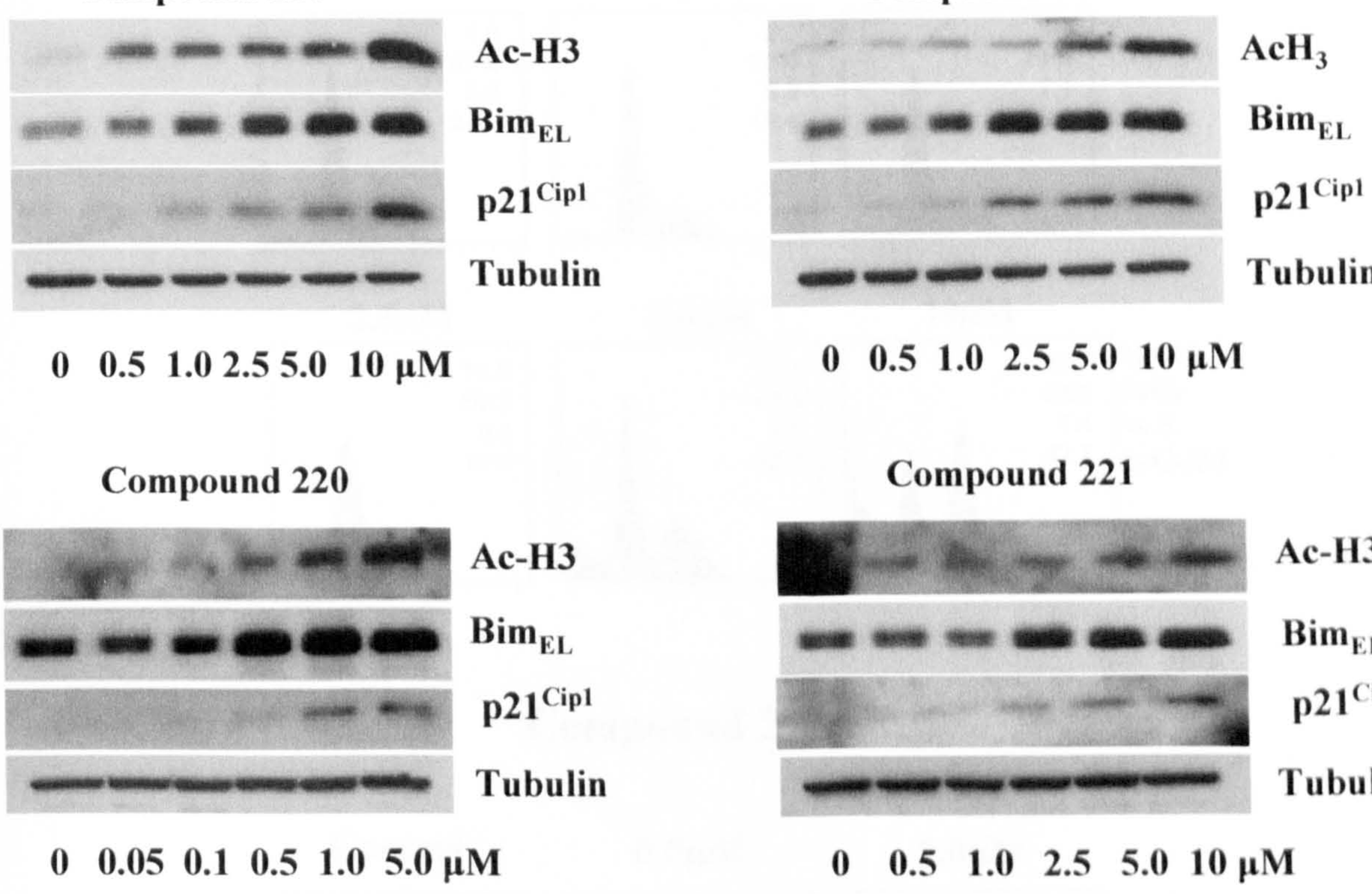


Figure 5.5 214, 215, 220, 221 induce expression of acetylated H3 (Ac-H3), Bim$_{EL}$ and p21^{Cip1}. Cells were treated with the indicated amounts of 214, 215, 220 and 221 for 48h, harvested, lysed and analysed by SDS-PAGE, using antibodies against Bim, p21^{Cip1}, Ac-H3. Tubulin was used as a loading control. Results are representative of three independent experiments.

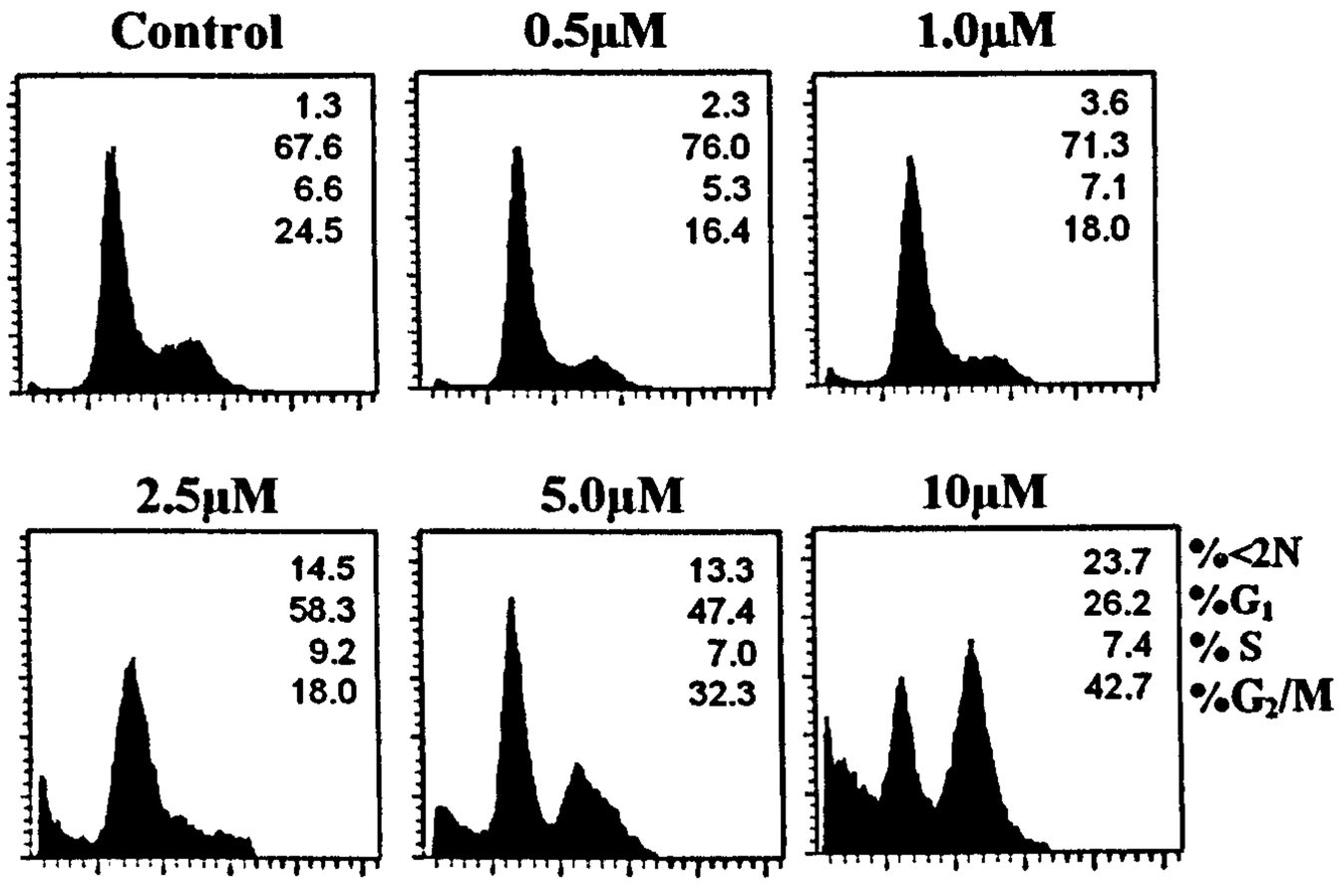
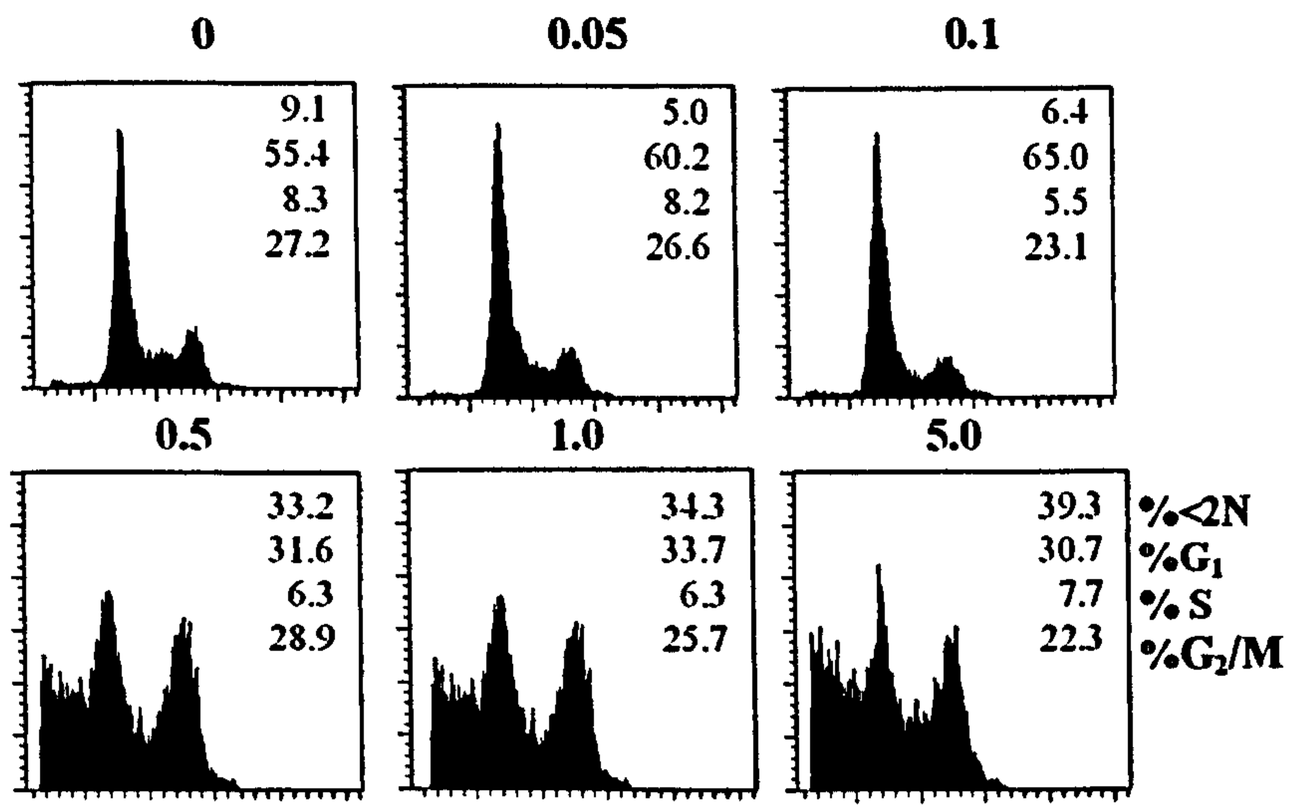


Figure 5.6 Cell cycle profiles of cells treated with 214, 215, 220 and 221. Cells were treated with 214, 215, 220, 221 at the concentrations specified for 48h. Cells were then fixed in 90% ethanol and analysed by FACS after propidium iodide staining.



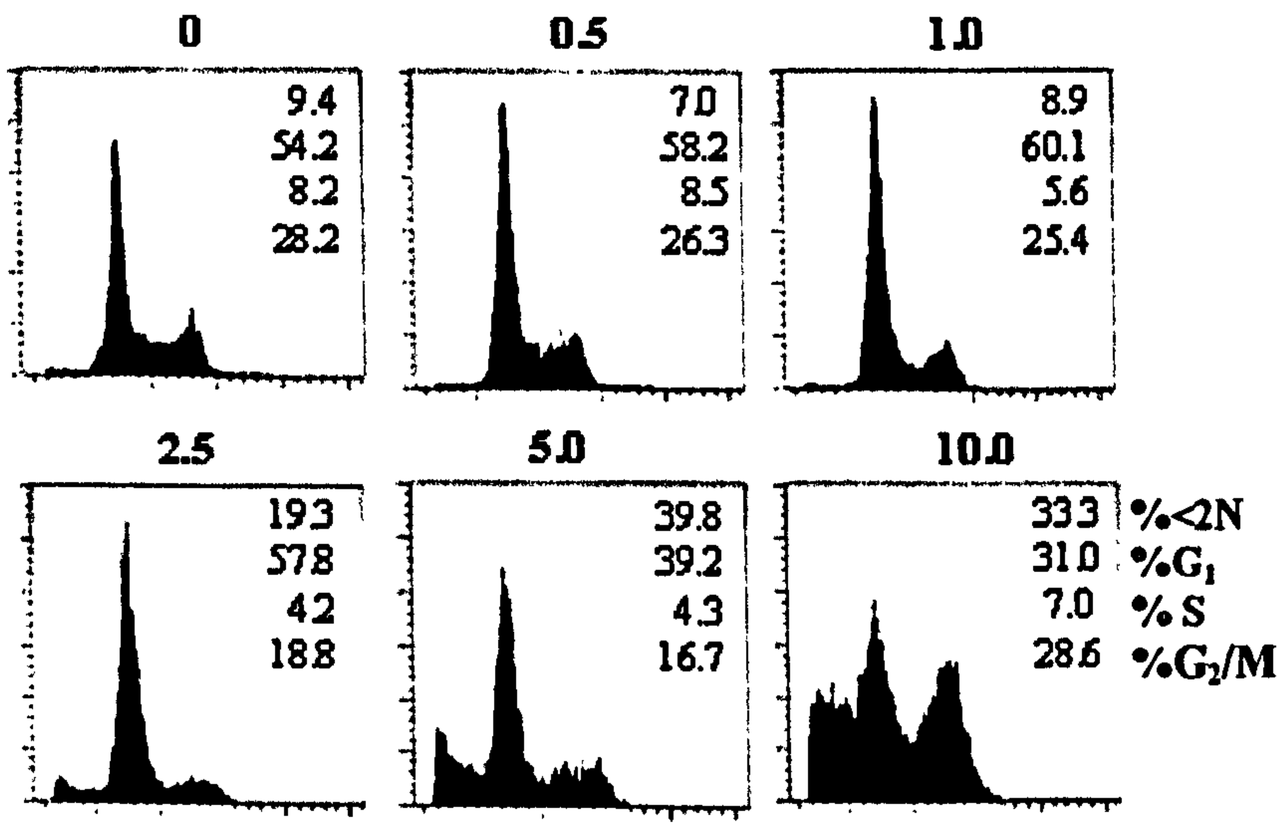
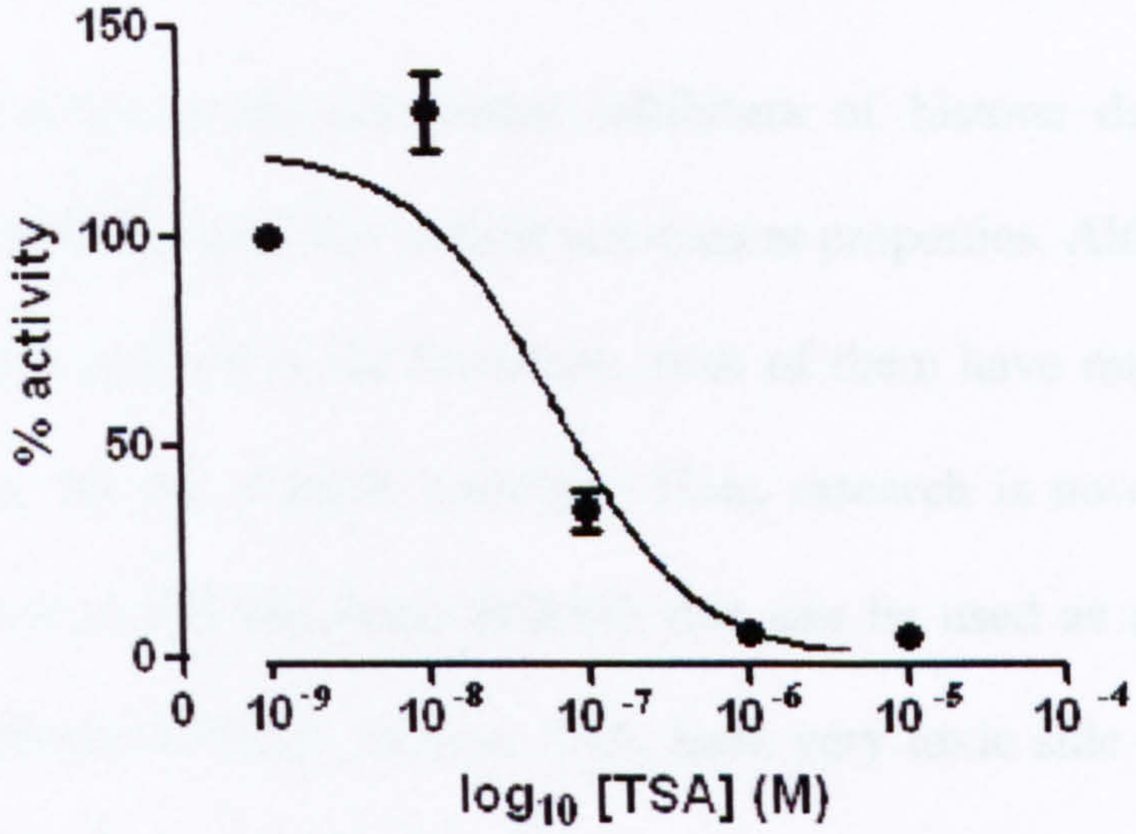


Figure 5.6 Cell cycle profiles of cells treated with compounds 214, 215, 220 and 221. Cells were treated with 214, 215, 220, 221 at the μM concentrations specified for 48h. Cells were then fixed in 90% ethanol and analysed by FACS after propidium iodide staining.

Compound 220 inhibits HDACs

The most potent compound tested so far is 220, and therefore it was decided that more compounds would be synthesized that resemble its structure and also more experiments would be done to understand its mechanism of action. In order to measure the HDAC inhibitory activity of cells treated with the compound 220 and to verify that this compound is indeed targeting HDACs, the HDAC Fluorimetric Assay/Drug kit was used. To determine the HDAC inhibitory activity of compound 220 treatment with different concentrations of 220 for 20 min resulted in a decrease in HDAC activity. This decrease in HDAC activity was associated with increasing amounts of compound 220. The IC_{50} of compound 220 was calculated to be approximately 0.3μM. The control TSA showed a clear inhibition of HDAC activity as reported in other studies (Fig. 5.7).



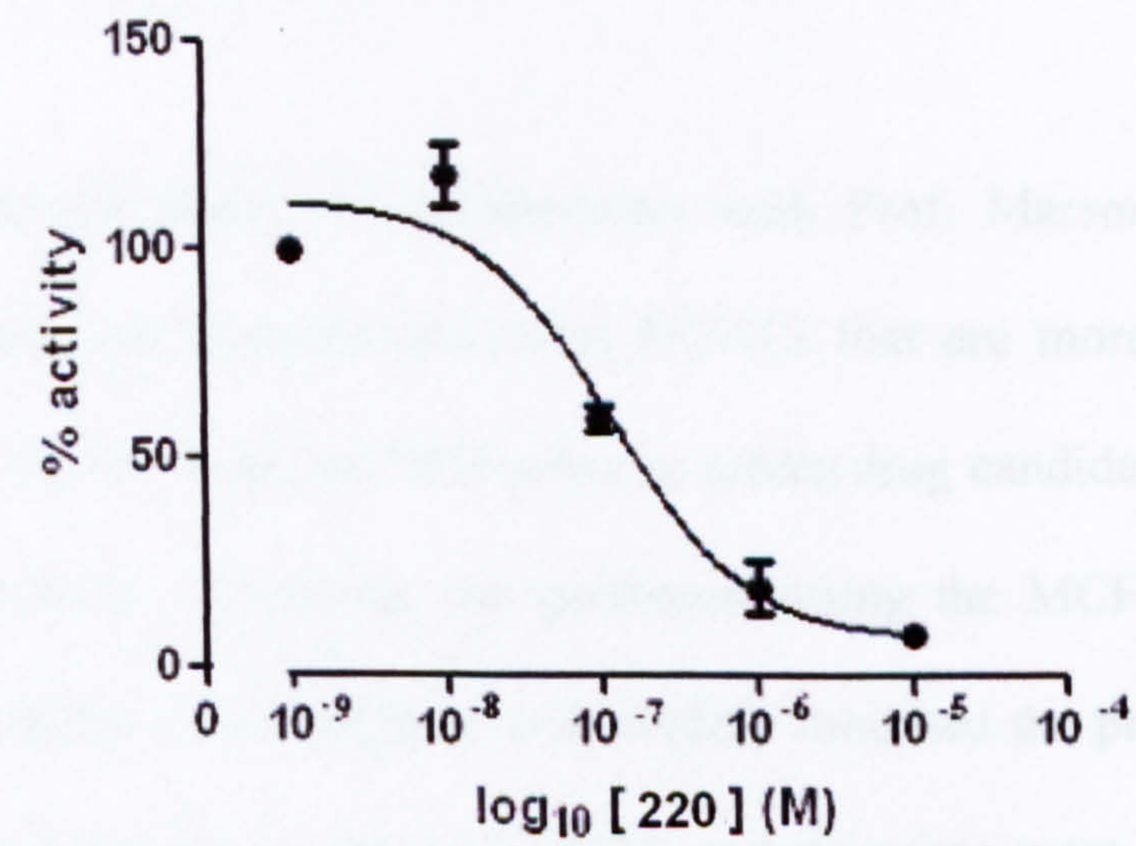


Figure 5.7 Compound 220 inhibits HDAC activity. HeLa Nuclear Extract (0.5µl/well) were incubated (25°C) with 116µM substrate and the indicated concentrations of 220 or TSA as a control. Reactions were stopped after 20min with the Fluor de Lys™ developer and fluorescence was measured on a fluorometric plate reader (460nm). Graphs were plotted using Prism.

V.3 DISCUSSION

The hydroxamic acids are potent inhibitors of histone deacetylase and have attracted much interest due to their anti-cancer properties. Although many HDACi have been described in the literature, most of them have many disadvantages in the clinical setting, namely toxicity. Thus, research is now focused on finding more effective and less toxic HDACi that can be used as anti-tumour drugs in cancer patients. HDACi, such as TSA, have very toxic side effects at high doses and therefore are of limited therapeutic use. For example, depsipeptide was withdrawn from clinical trials due to its cardiovascular toxicity (Lin et al., 2006).

In the present study, in collaboration with Prof. Marson at UCL, we have synthesised and characterised novel HDACi that are more potent than SAHA (figure 5.1). We used the SRB assay to screen drug candidates for potential anti-tumour activity. Screening was performed using the MCF-7 breast cancer cell line. A number of compounds only slightly inhibited the proliferation of MCF-7 cells, but were not as good as SAHA and therefore were not analysed further. However, four of them, compounds 214, 215, 220 and 221 were able to inhibit the proliferation of MCF-7 cells. Compounds 214, 215 and 221 had similar IC_{50} of around 2.3μM, slightly less than SAHA. The complete structures of these compounds are not shown in this thesis as patents are being sought to cover the intellectual properties arising from these findings. Also, compounds 214, 215 and 221 caused a G_2/M arrest at higher concentrations, and were able to induce the expression of Ac-H3, Bim and $p21^{Cip1}$. The induction of Bim suggests that cells die by apoptosis rather than necrosis, since this Bcl2- family member is a well

known pro-apoptotic protein. Furthermore, the induction of acetylated-H3 further confirms that these compounds are actually HDAC inhibitors and their effects in cells are not due to non-specific cytotoxic events. The induction of the cell cycle inhibitor $p21^{Cip1}$ agrees with other studies performed with similar compounds, such as TSA, that have shown that $p21^{Cip1}$ is an important target of HDACi. Also, it suggests that the G_1/S arrest caused by the compounds could be due to the induction of $p21^{Cip1}$. These characteristics make these HDACi good anti-cancer drug candidates. Although there are seemingly small differences in the chemical structures of compounds 214, 215 and 221, it was found that these structural changes had a significant effect on biological activity.

As judged by the results presented in this chapther, compound 220 is a more potent inhibitor than SAHA but less potent than TSA. Compound 220 caused cell cycle arrest with apoptosis occuring after 48h of treatment. An extra group ("G") attached to the SAHA molecule therefore appears to increase the potency of the drug and is thought to be responsible for the increased inhibition of proliferation of MCF-7 cells. Variation of the groups fused to this key carbon atom in the SAHA molecule, where the "G" group binds, results in a marked difference in potency. Cell cycle analysis revealed that compound 220 induces G_1/S arrest at low concentrations (0.1μM) and G_2/M arrest at higher and more cytotoxic concentrations (0.5μM). This is consistent with other findings were HDACi, such as TSA, induce similar cell cycle profiles in many cancer cell types (Kim et al., 1999; Li et al., 2006; Rokhlin et al., 2006; Sowa et al., 1999; Yamashita et al., 2003). Interestingly, the SRB assay and the HDAC assay gave consistent results. Compound 220 gave an *in vitro* and *in vivo* IC_{50} of approximately 0.3μM

compared to the 2.5μM of SAHA. Also, compound 220 was able to induce the expression of Bim_{EL}, $p21^{Cip1}$ and acetylated-H3, proving that this compound has HDAC inhibitory activity and probably induces apoptosis in MCF-7 cells. Compound 220 was chosen for further studies in order to validate its potential properties as an anti-cancer drug.

Besides cancer, HDACi can be used for the treatment of other diseases also. HDACi such as valproic acid have also been used for the treatment of neurodegenerative diseases like epilepsy. This is partly due to the fact that HDACi induce the expression of various neuroprotective proteins (Nau et al., 1991). Moreover, some HDACi have been shown to reduce graft-versus-host disease in patients that have had bone marrow transplantation by suppressing pro-inflammatory cytokines (Leng et al., 2006).

Future work

Further studies on the effects of these HDACi on other types of transformed cancer cells will need to be done. Also, the effect of these HDACi on non-transformed cells has to be examined. TSA has been shown to have a much greater effect on transformed rather than non-transformed cells. It will be very interesting to see if the same happens with the novel HDACi discussed in this work. In addition, it will be important to see if there is a difference on the effect of HDACi between low grade and more aggressive tumour types.

Clearly other factors will have to be considered before this drug can be used in clinical trials. Studies will be done to test the solubility and perhaps improve it so

that it potentially improves the efficacy of the HDACi. Accordingly, efforts are currently under way to more thoroughly evaluate the efficacy and toxicity profiles of these and other HDACi and to optimize their potency through synthesis of further derivatives. Moreover, the metabolism of compounds has to be examined before further studies can be done. TSA and other known HDACi compounds such as butyrate and phenylbutyrate show high biotransformation; therefore patients require high dose administration (Warrell et al., 1998). Studies have shown that TSA converts to its corresponding metabolites after only 20min of exposure therefore causing a very short exposure to the pharmacologically active parent compound. This is a limiting factor for use as a therapeutic agent (Elaut et al., 2002).

This study was mainly performed in MCF-7 cells so it has to be extended in other breast cancer cell lines and other cancer types to verify it. Furthermore, studies would need to be done in primary patient samples as results from cell lines may not apply to primary cells. Another factor that could be addressed in further studies is the specificity of each compound. Most HDACi are known to target more than one HDAC. Very few HDACi are known to be able to specifically target one HDAC. For example, tubacin selectivily inhibits HDAC6 and causes accumulation of acetylated α-tubulin but fails to inhibit proliferation of cells (Haggarty et al., 2003; Kim et al., 2003a).

Compound 220 was selected for further study to determine its *in vivo* efficacy in xenograft mouse models because of its favorable toxicity profile. Based on further examination of this compound to evaluate its solubility, toxicity, metabolic

properties and its ability to decrease tumour growth in mouse models, the compound could lead to a phase I clinical trial in humans.

All the data accumulated thus far are consistent with an epigenetic effect of these HDAC inhibitors. The precise mechanism of induction of cell death remains unknown and needs to be addressed in future studies.

CHAPTER VI

DISCUSSION

Research performed over the last decade has highlighted the role of HDACi as a potential new class of therapeutic agents. One of the best-studied HDAC inhibitors, called TSA, has been shown to exhibit potent anti-proliferative properties, therefore studying its mechanism of action allows us to determine a role for its use in the future as a cancer therapeutic agent (Johnstone et al., 2002; Narlikar et al., 2002). HDAC inhibitors inhibit HDACs, leading to a less condensed chromatin structure by increasing acetylation. The first HDACi approved by the FDA was SAHA. SAHA is used for the treatment of cutaneous T-cell lymphoma and is well tolerated by humans (Kelly et al., 2005). However, most HDACi are very toxic to humans and cannot be used in the clinical setting. Research is now focused on studying the biology and structure of HDACi in order to identify novel HDACi that can be used as drugs in humans with diseases such as cancer.

One way to study the mechanism of action of various anti-cancer drugs is to study their effects on their targets. Studies have shown that the expression of 7-10% of genes is altered in response to treatment with various HDACi (Chambers et al., 2003; Glaser et al., 2003; Mitsiades et al., 2004; Peart et al., 2005; Sasakawa et al., 2005). Therefore, despite the fact that HDACi are non-specific and toxic, they actually affect only a small number of genes. The targets of most HDACi still remain unknown. The best characterised target of TSA is the cell cycle inhibitor $p21^{Cip1}$ (Kim et al., 1999). In chapter III, the F-Box protein FBXL20 was identified as an important TSA target. The identification of this novel F-Box protein stemmed from previous work in our laboratory in finding Skp2 homologues that could be involved in the regulation of cyclin D1. FBXL20 was

not shown to regulate cyclin D1. In chapter IV, FBXL20 was shown to be a direct target of TSA, as induction of its mRNA levels by TSA was not blocked by the protein synthesis inhibitor CHX and therefore *de novo* protein synthesis is not required. Since there are no known data characterising the role and function of FBXL20 in human cells, this work initially focused on characterising FBXL20 and subsequently examining its role in the TSA-induced effects in MCF-7 cells.

Previous research performed on the FBXL20 homologue FBL2 in rat cells showed that FBL2 is ubiquitously expressed, able to bind Skp1, localised in the perinuclear compartment of cells and overexpressed in growth arrested hepatocytes (Ilyin et al., 1999). Similar results were obtained for FBXL20 in human MCF-7 breast cancer cells. PCR analysis showed that it is expressed in many cancer cell lines. Interestingly, the rat expresses only part of the protein found in humans. This is likely to be due to a mutation that leads to the formation of a translational stop codon, which subsequently leads to a truncated protein in rats. This suggests that the human FBXL20 may bind different proteins and have different functions than its rat homologue i.e the C-terminal region which is not expressed in rat cells may have additional functions in the human. Consistent with other studies, where a number of FBL2 splice variants were shown in the rat cells (Ilyin et al., 1999), FBXL20 was shown to have a splice variant in MCF-7 cells that lacks exon 7.

Subcellular localisation studies in human cells, similar to the rats, showed that FBXL20 localises in the cytoplasm, concentrated mainly around the nucleus. In addition, in agreement with other classical SCF E3 ligases, where F-Box proteins

such as Skp2 are able to bind Skp1, ROC-1 and CUL-1 (Zhang et al., 1995), FBXL20 was shown to bind all three proteins, suggesting that FBXL20 is a novel E3 ligase that leads to the degradation of yet unknown proteins.

Due to its similarity to Skp2, FBL2 has been compared to Skp2 in rat cells in other studies (Ilyin et al., 1999). In agreement with these studies, this work has shown that, despite the similarities between Skp2 and FBXL20, they have distinct functions. The reason for this remains unclear. Skp2 expression is mainly increased during S-phase, leading to the degradation of the G_1/S phase inhibitor $p27^{Kip1}$(Carrano et al., 1999). This allows progression of cells through the cell cycle. However, this study showed that FBXL20 is mainly expressed in growth arrested cells, which suggests that it may play a role in the G_0/G_1 transition. Moreover, when *FBXL20* is silenced, the expression of Skp2 protein is increased and vice versa. This inverse relationship between Skp2 and FBXL20 expression could be cell cycle phase mediated. Silencing Skp2 expression leads to a G_1/S arrest, which may indirectly lead to the upregulation of FBXL20. Conversely, when FBXL20 is silenced, Skp2 levels increase, which suggests that since Skp2 levels are high in cycling cells, silencing FBXL20 gives cells a growth advantage and Skp2 levels increase in order to mediate cell cycle progression. The relationship between these two proteins remains unclear. Furthermore, the transcription of *Skp2* has been shown to be regulated by the FoxM1 transcription factor but this is not the case with FBXL20, as silencing *FoxM1* had no effect on the mRNA levels of *FBXL20*. These data together show that FBXL20 is a novel E3 ligase that is ubiquitously expressed, localised in the cytoplasm and its expression is induced during cell death and growth arrest.

The work in chapter IV also demonstrated that TSA caused G_1/S arrest at low concentrations and G_2/M arrest at higher concentrations (Li et al., 2006; Rokhlin et al., 2006; Yamashita et al., 2003). Knockdown of FBXL20 gave a growth advantage to MCF-7 cells in response to TSA. Cell cycle analysis showed that knockdown of *FBXL20* and subsequent treatment with TSA leads to a reduction in the number of cells in the G_2/M phase of the cell cycle compared to the NSC transfected cells. This implies that *FBXL20* may cause the degradation of a protein or proteins involved in the G_2/M transition. Furthermore, overexpression of FBXL20 in TSA treated cells led to an induction in apoptotic cell death compared to non-transfected cells. My data indicates that the novel FBXL20 F-Box protein plays an important role in TSA-induced G_2/M arrest and apoptosis in MCF-7 cells. Similar results were also obtained when cells were treated with SAHA and SBHA. This is very important as it suggests that FBXL20 is a target of all HDACi and not only TSA.

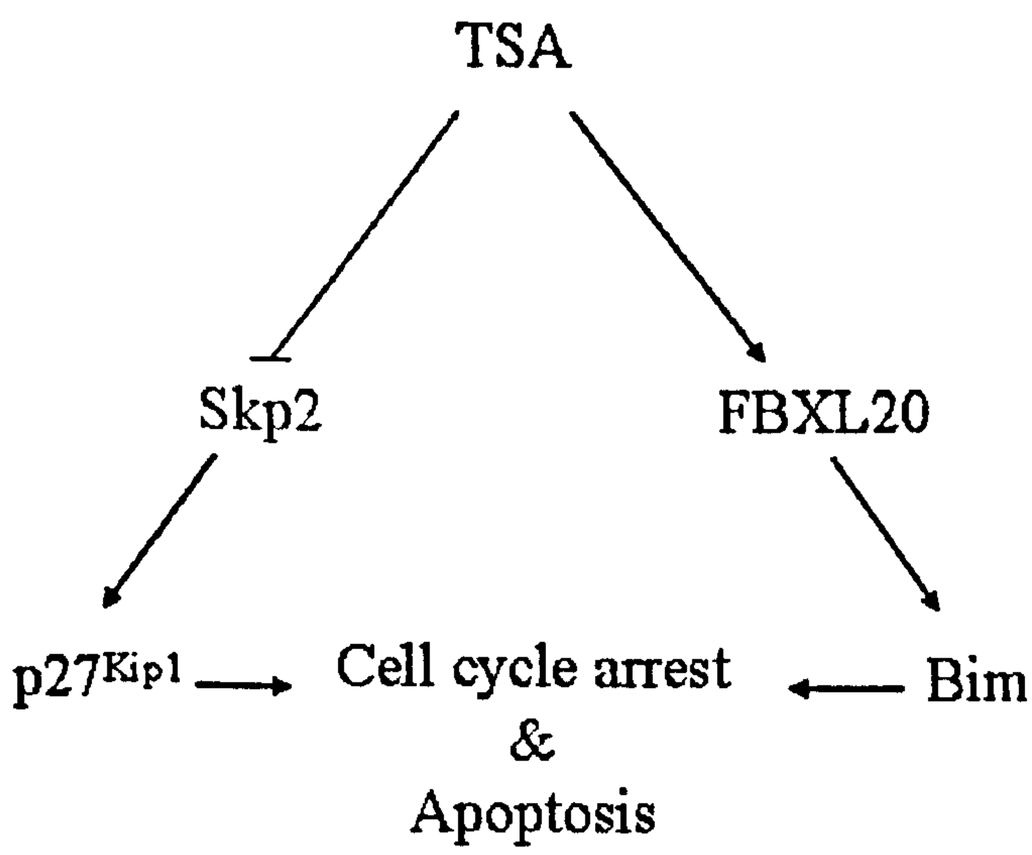


Figure 6.1 Schematic to represent the role of FBXL20 and Skp2 in TSA-induced cell cycle arrest and apoptosis.

It is still unclear exactly how TSA regulates FBXL20. It is possible that TSA affects FBXL20 through HDAC2, since silencing *HDAC2* caused an increase in the mRNA levels of *FBXL20*. Research in our laboratory has suggested that HDAC2 is the predominant HDAC in MCF-7 cells and that is why I decided to examine its possible role in regulating FBXL20. In contrast, HDAC1 did not seem to regulate the expression of FBXL20 as its knockdown in MCF-7 cells did not affect the levels of FBXL20 mRNA. Other HDACs could also potentially regulate FBXL20 but have not been tested in this study. Future studies could focus on finding which HDACs could regulate FBXL20 using techniques such as RNAi in order to silence the expression of all HDACs and then test the expression of FBXL20.

Also, it is uncertain if TSA regulates FBXL20 only at the transcriptional level, since TSA induced the expression of the recombinant protein Flag-FBXL20 which is regulated by a different promoter than the endogenous FBXL20. TSA probably regulates FBXL20 in two different ways, at the transcriptional and translational level. However, the induction of the protein levels of Flag-FBXL20 could de due to decreased degradation of the protein. If this is the case, then TSA regulates FBXL20 only at the transcriptional level. The promoter and the stability of FBXL20 have to be examined further in order to understand how TSA regulates FBXL20.

In chapter IV the function of FBXL20 was explored through identifying one of its downstream targets. FBXL20 was shown to function by regulating the pro-apoptotic protein Bim. The induction of Bim expression by TSA is abrogated

when *FBXL20* is silenced. Also, knockdown of FBXL20 leads to a decrease in the protein expression of Bim. This is unlikely to be mediated at the transcriptional level since silencing of FBXL20 did not significantly alter *Bim* mRNA levels. Cell cycle analysis also showed that when *FBXL20* is silenced, Bim is required for the abrogation of TSA-induced G_2/M arrest. As discussed in chapter IV, FBXL20 was able to bind Bim and its overexpression led to the overexpression of Bim protein levels. It is unlikely that FBXL20 is responsible for the degradation of Bim as silencing FBXL20 should lead to an increase in the protein levels of Bim. This is not the case and thus it is possible that FBXL20 binds Bim and prevents it from binding another E3 ligase that is responsible for its degradation. More work has to be done to understand how FBXL20 regulates Bim. Mutations in FBXL20 and further GST-pulldowns of the constructs could lead to the identification of the site that is responsible for binding Bim. Other binding partners of FBXL20 also have to be identified. Moreover, FBXL20 could be tested for its potential binding of Bim_L and Bim_S.

Current research focuses on the design of drugs that specifically target molecular alterations found only in transformed cells and not in normal cells. HDACi have been shown to be very promising in this respect and therefore there has been a lot of effort to market HDACi as treatment for all major solid and haematologic cancers, either as a single therapy or in combination. Researchers are trying to associate specific tumour types with specific gene expression profiles and thus identify the changes that occur in normal cells that lead them to become cancerous.

In chapter V, a series of compounds showed promising anti-tumour properties. Compounds 214, 215, 220 and 221 inhibited proliferation of MCF-7 cells. The most potent so far, compound 220, when used at a dose of 500nM, caused accumulation of acetylated histone H3, inhibition of cell proliferation and G_2/M cell cycle arrest. This was accompanied by an increase of $p21^{Cip1}$ and Bim in MCF-7 cells. This compound does indeed target HDACs, as an HDAC assay revealed that there is a decrease in HDAC activity upon treatment with compound 220. This is a very promising anti-tumour agent and shows greater potency than SAHA. The relationship of the antitumour effects of this compound to its pharmacodynamic and pharmacokinetic properties in vivo is yet unknown but will be examined in future studies. However the IC_{50} of 220 is still high and could cause side effects when used in humans. It is possible that compounds like 220 would have a better therapeutic effect when used in combination with chemotherapy as has been shown with the combination of other HDACi with DNA topoisomerase II inhibitors (Marchion et al., 2004), doxorubicin (Catalano et al., 2006), taxanes (Dowdy et al., 2006) and imatinib (Nimmanapalli et al., 2003). Using these combination treatments, HDACi increase the efficacy of chemotherapeutic drugs in treating many cancer types, possibly by offering improved access for these agents to target DNA/protein complexes.

A number of HDACi are now in clinical trials for the treatment of many types of cancer including breast, lung, renal, pancreatic and bladder cancer (Paris et al., 2008). Development of novel HDACi is an extensive area of research. However, most HDACi developed have shown significant levels of toxicity. For some inhibitors, it is possible that their increased binding time is responsible for this

increased in vivo toxicity, which is why less potent inhibitors such as SAHA may have better therapeutic properties. Also, HDACi are non-specific and thus can target a number of different cell death pathways, making them very effective anti-tumour agents. A number of studies are now being carried out to develop HDACi that have more selective inhibitory properties. HDACi that target a specific HDAC are not yet available due to the fact that there is a high degree of homology between their catalytic sites. Also, HDACs function by being part of large protein complexes and this makes the discovery of an isotype specific drug an even harder task. However it is not clear how efficient these drugs will be in killing cancer cells. Efficacy may decrease considerably as these HDACi will only target a single HDAC. More selective inhibitors may however be beneficial in lowering the tendency of tumours to become HDACi resistant and thus increase their efficacy. Isotype specific HDACi would certainly be very useful in understanding better the biology and pharmacology of HDACs. Up to now, the RNAi technique has been used as a tool to study the functions of a specific HDAC.

An important factor that has to be considered when using these drugs in clinical trials is that cardiac toxicity has sometimes been observed as a side effect of treatment (Paris et al., 2008). This includes conduction problems and also cardiac muscle hypertrophy. Some studies suggest that these toxicities may be HDAC class specific, while others think that it is due to the chemical structure of the compound under study. This of course should not stop the development of these drugs. The exact mechanism of action of these drugs remains unknown and the mode of action of one inhibitor may differ considerably from another due to their chemical structure or pharmacokinetic profile. Therefore, there is a strong need

for identifying more targets that are common for all compounds, shedding some light on the general mechanism of action of these drugs.

HDACi could not only be used for the treatment of cancer but also for other diseases such as epilepsy, as has been shown with the HDACi valproic acid (Nau et al., 1991). Moreover, some HDACi have been shown to reduce graft-versus-host disease in patients that have had bone marrow transplantation by suppressing pro-inflammatory cytokines (Leng et al., 2006). Also, HDACi have shown a promising therapeutic role in the treatment of Huntington's disease (Sadri-Vakili and Cha, 2006). They have also emerged as potent alternatives to anti-inflammatory drugs, offering a novel approach for the treatment of rheumatoid arthritis or lupus erythematosus (Blanchard and Chipoy, 2005). Furthermore, a novel HDACi inhibitor named MGD0103 has shown potential for the treatment of high-risk myelodysplastic syndrome (MDS)(Garcia-Manero et al., 2008). The variety of diseases that HDACi can target highlights even more how important it is to discover novel HDACi that can be more potent, less toxic and cause less side effects than already known ones.

The characterisation of the role and function of FBXL20 is important as it appears to be a target of all HDACi. This will allow a greater understanding of how HDACi work. Moreover, FBXL20 may be considered a tumour suppressor and therefore its overexpression may be used for potential therapeutic benefit. The function of a single gene is insufficient to explain how HDACi work but, along with other targets, it helps in elucidating the mechanism of action of HDACi in different cells.

In summary, this work has shed some light on how HDACi exert their effects on cells by identifying the FBXL20 protein as an important target of the HDAC inhibitor TSA. FBXL20 was shown to be a novel E3 ligase that mediates its functions through regulating the pro-apoptotic BCL-2 member Bim. This novel finding could have therapeutic implications as HDACi such as SAHA have been used in clinical trials and targeting FBXL20 could synergise with conventional chemotherapeutic drugs or HDACi to promote cell cycle arrest and/or cell death in breast cancer cells. Lastly, this study has set the parameters for testing novel HDAC inhibitors by examining their effect on the cell cycle, proliferation and their effect on deacetylation.

REFERENCES

Akimoto, T. (2004). [Potentiation of radiation-induced cell killing by histone deacetylase inhibitor]. Nippon Rinsho *62*, 1348-1354.

Alao, J. P., Lam, E. W., Ali, S., Buluwela, L., Bordogna, W., Lockey, P., Varshochi, R., Stavropoulou, A. V., Coombes, R. C., and Vigushin, D. M. (2004). Histone deacetylase inhibitor trichostatin A represses estrogen receptor alpha-dependent transcription and promotes proteasomal degradation of cyclin D1 in human breast carcinoma cell lines. Clin Cancer Res *10*, 8094-8104.

Alberts, B., Dennis, B., Lewis, J., Raff, M., Roberts, K., Watson, J.D. (1994) Molecular biology of the cell, pg. 863-870

Ali, S., and Coombes, R. C. (2002). Endocrine-responsive breast cancer and strategies for combating resistance. Nat Rev Cancer *2*, 101-112.

Alland, L., Muhle, R., Hou, H., Jr., Potes, J., Chin, L., Schreiber-Agus, N., and DePinho, R. A. (1997). Role for N-CoR and histone deacetylase in Sin3-mediated transcriptional repression. Nature *387*, 49-55.

Ang, X. L., and Wade Harper, J. (2005). SCF-mediated protein degradation and cell cycle control. Oncogene *24*, 2860-2870.

Aranda, A., and Pascual, A. (2001). Nuclear hormone receptors and gene expression. Physiol Rev *81*, 1269-1304.

Arenz, C. (2006). MicroRNAs--future drug targets? Angew Chem Int Ed Engl *45*, 5048-5050.

Azambuja, E., Durbecq, V., Rosa, D. D., Colozza, M., Larsimont, D., Piccart-Gebhart, M., and Cardoso, F. (2008). HER-2 overexpression/amplification and its interaction with taxane-based therapy in breast cancer. Ann Oncol *19*, 223-232.

Bai, C., Sen, P., Hofmann, K., Ma, L., Goebl, M., Harper, J. W., and Elledge, S. J. (1996). SKP1 connects cell cycle regulators to the ubiquitin proteolysis machinery through a novel motif, the F-box. Cell *86*, 263-274.

Bakin, R. E., and Jung, M. O. (2004). Cytoplasmic sequestration of HDAC7 from mitochondrial and nuclear compartments upon initiation of apoptosis. J Biol Chem *279*, 51218-51225.

Baldin, V., Lukas, J., Marcote, M. J., Pagano, M., and Draetta, G. (1993). Cyclin D1 is a nuclear protein required for cell cycle progression in G1. Genes Dev *7*, 812-821.

Barber, G. N. (2000). The interferons and cell death: guardians of the cell or accomplices of apoptosis? Semin Cancer Biol *10*, 103-111.

Barlev, N. A., Liu, L., Chehab, N. H., Mansfield, K., Harris, K. G., Halazonetis, T. D., and Berger, S. L. (2001). Acetylation of p53 activates transcription through recruitment of coactivators/histone acetyltransferases. Mol Cell *8*, 1243-1254.

Barnes, D. M., and Gillett, C. E. (1998). Cyclin D1 in breast cancer. Breast Cancer Res Treat *52*, 1-15.

Bertos, N. R., Wang, A. H., and Yang, X. J. (2001). Class II histone deacetylases: structure, function, and regulation. Biochem Cell Biol *79*, 243-252.

Bicaku, E., Marchion, D. C., Schmitt, M. L., and Munster, P. N. (2008). Selective inhibition of histone deacetylase 2 silences progesterone receptor-mediated signaling. Cancer Res *68*, 1513-1519.

Bilancia, D., Rosati, G., Dinota, A., Germano, D., Romano, R., and Manzione, L. (2007). Lapatinib in breast cancer. Ann Oncol *18 Suppl 6*, vi26-30.

Bird, A. (2002). DNA methylation patterns and epigenetic memory. Genes Dev *16*, 6-21.

Blanchard, F., and Chipoy, C. (2005). Histone deacetylase inhibitors: new drugs for the treatment of inflammatory diseases? Drug Discov Today *10*, 197-204.

Bolden, J. E., Peart, M. J., and Johnstone, R. W. (2006). Anticancer activities of histone deacetylase inhibitors. Nat Rev Drug Discov *5*, 769-784.

Bouck, D., and Bloom, K. (2005). The role of centromere-binding factor 3 (CBF3) in spindle stability, cytokinesis, and kinetochore attachment. Biochem Cell Biol *83*, 696-702.

Brehm, A., Miska, E. A., McCance, D. J., Reid, J. L., Bannister, A. J., and Kouzarides, T. (1998). Retinoblastoma protein recruits histone deacetylase to repress transcription. Nature *391*, 597-601.

Broker, L. E., Kruyt, F. A., and Giaccone, G. (2005). Cell death independent of caspases: a review. Clin Cancer Res *11*, 3155-3162.

Buzdar, A. U., Coombes, R. C., Goss, P. E., and Winer, E. P. (2007). Summary of aromatase inhibitor clinical trials in postmenopausal women with early breast cancer. Cancer *112*, 700-709.

Caron, C., Boyault, C., and Khochbin, S. (2005). Regulatory cross-talk between lysine acetylation and ubiquitination: role in the control of protein stability. Bioessays *27*, 408-415.

Carrano, A. C., Eytan, E., Hershko, A., and Pagano, M. (1999). SKP2 is required for ubiquitin-mediated degradation of the CDK inhibitor p27. Nat Cell Biol *1*, 193-199.

Castedo, M., Perfettini, J. L., Roumier, T., Andreau, K., Medema, R., and Kroemer, G. (2004). Cell death by mitotic catastrophe: a molecular definition. Oncogene *23*, 2825-2837.

Catalano, M. G., Fortunati, N., Pugliese, M., Poli, R., Bosco, O., Mastrocola, R., Aragno, M., and Boccuzzi, G. (2006). Valproic acid, a histone deacetylase inhibitor, enhances sensitivity to doxorubicin in anaplastic thyroid cancer cells. J Endocrinol *191*, 465-472.

Chambers, A. E., Banerjee, S., Chaplin, T., Dunne, J., Debernardi, S., Joel, S. P., and Young, B. D. (2003). Histone acetylation-mediated regulation of genes in leukaemic cells. Eur J Cancer *39*, 1165-1175.

Chang, B. D., Broude, E. V., Dokmanovic, M., Zhu, H., Ruth, A., Xuan, Y., Kandel, E. S., Lausch, E., Christov, K., and Roninson, I. B. (1999). A senescence-like phenotype distinguishes tumor cells that undergo terminal proliferation arrest after exposure to anticancer agents. Cancer Res *59*, 3761-3767.

Chen, G., Fernandez, J., Mische, S., and Courey, A. J. (1999). A functional interaction between the histone deacetylase Rpd3 and the corepressor groucho in Drosophila development. Genes Dev *13*, 2218-2230.

Chen, J. D., and Evans, R. M. (1995). A transcriptional co-repressor that interacts with nuclear hormone receptors. Nature *377*, 454-457.

Chen, L. C., Manjeshwar, S., Lu, Y., Moore, D., Ljung, B. M., Kuo, W. L., Dairkee, S. H., Wernick, M., Collins, C., and Smith, H. S. (1998). The human homologue for the Caenorhabditis elegans cul-4 gene is amplified and overexpressed in primary breast cancers. Cancer Res *58*, 3677-3683.

Choudhary, S., and Wang, H. C. (2007). Pro-apoptotic activity of oncogenic H-Ras for histone deacetylase inhibitor to induce apoptosis of human cancer HT29 cells. J Cancer Res Clin Oncol *133*, 725-739.

Ciechanover, A., Orian, A., and Schwartz, A. L. (2000). The ubiquitin-mediated proteolytic pathway: mode of action and clinical implications. J Cell Biochem Suppl *34*, 40-51.

Coradini, D., Zorzet, S., Rossin, R., Scarlata, I., Pellizzaro, C., Turrin, C., Bello, M., Cantoni, S., Speranza, A., Sava, G., *et al.* (2004). Inhibition of hepatocellular carcinomas in vitro and hepatic metastases in vivo in mice by the histone deacetylase inhibitor HA-But. Clin Cancer Res *10*, 4822-4830.

Costa, R. H. (2005). FoxM1 dances with mitosis. Nat Cell Biol *7*, 108-110.
Coultas, L., and Strasser, A. (2003). The role of the Bcl-2 protein family in cancer. Semin Cancer Biol *13*, 115-123.

Couse, J. F., and Korach, K. S. (1999). Estrogen receptor null mice: what have we learned and where will they lead us? Endocr Rev *20*, 358-417.

Cress, W. D., and Seto, E. (2000). Histone deacetylases, transcriptional control, and cancer. J Cell Physiol *184*, 1-16.

Datta, S. R., Brunet, A., and Greenberg, M. E. (1999). Cellular survival: a play in three Akts. Genes Dev *13*, 2905-2927.

de Ruijter, A. J., van Gennip, A. H., Caron, H. N., Kemp, S., and van Kuilenburg, A. B. (2003). Histone deacetylases (HDACs): characterization of the classical HDAC family. Biochem J *370*, 737-749.

Ding, Z., Liang, J., Lu, Y., Yu, Q., Songyang, Z., Lin, S. Y., and Mills, G. B. (2006). A retrovirus-based protein complementation assay screen reveals functional AKT1-binding partners. Proc Natl Acad Sci U S A *103*, 15014-15019.

Dowdy, S. C., Jiang, S., Zhou, X. C., Hou, X., Jin, F., Podratz, K. C., and Jiang, S. W. (2006). Histone deacetylase inhibitors and paclitaxel cause synergistic effects on apoptosis and microtubule stabilization in papillary serous endometrial cancer cells. Mol Cancer Ther *5*, 2767-2776.

Dowling, M., Voong, K. R., Kim, M., Keutmann, M. K., Harris, E., and Kao, G. D. (2005). Mitotic spindle checkpoint inactivation by trichostatin a defines a mechanism for increasing cancer cell killing by microtubule-disrupting agents. Cancer Biol Ther *4*, 197-206.

Dutta, U., and Pant, K. (2007). Aromatase inhibitors: past, present and future in breast cancer therapy. Med Oncol.

Dyer, E. S., Paulsen, M. T., Markwart, S. M., Goh, M., Livant, D. L., and Ljungman, M. (2002). Phenylbutyrate inhibits the invasive properties of prostate and breast cancer cell lines in the sea urchin embryo basement membrane invasion assay. Int J Cancer *101*, 496-499.

Elaut, G., Torok, G., Vinken, M., Laus, G., Papeleu, P., Tourwe, D., and Rogiers, V. (2002). Major phase I biotransformation pathways of Trichostatin a in rat hepatocytes and in rat and human liver microsomes. Drug Metab Dispos *30*, 1320-1328.

Engel, R. H., and Kaklamani, V. G. (2007). HER2-positive breast cancer: current and future treatment strategies. Drugs *67*, 1329-1341.

Eyupoglu, I. Y., Hahnen, E., Buslei, R., Siebzehnrubl, F. A., Savaskan, N. E., Luders, M., Trankle, C., Wick, W., Weller, M., Fahlbusch, R., and Blumcke, I. (2005). Suberoylanilide hydroxamic acid (SAHA) has potent anti-glioma properties in vitro, ex vivo and in vivo. J Neurochem *93*, 992-999.

Feldman, R. M., Correll, C. C., Kaplan, K. B., and Deshaies, R. J. (1997). A complex of Cdc4p, Skp1p, and Cdc53p/cullin catalyzes ubiquitination of the phosphorylated CDK inhibitor Sic1p. Cell *91*, 221-230.

Fesik, S. W. (2000). Insights into programmed cell death through structural biology. Cell *103*, 273-282.

Finnin, M. S., Donigian, J. R., Cohen, A., Richon, V. M., Rifkind, R. A., Marks, P. A., Breslow, R., and Pavletich, N. P. (1999). Structures of a histone deacetylase homologue bound to the TSA and SAHA inhibitors. Nature *401*, 188-193.

Forbes, J. F., Cuzick, J., Buzdar, A., Howell, A., Tobias, J. S., and Baum, M. (2008). Effect of anastrozole and tamoxifen as adjuvant treatment for early-stage breast cancer: 100-month analysis of the ATAC trial. Lancet Oncol *9*, 45-53.

Friedrichs, K., Holzel, F., and Janicke, F. (2002). Combination of taxanes and anthracyclines in first-line chemotherapy of metastatic breast cancer: an interim report. Eur J Cancer *38*, 1730-1738.

Fujita, N., Takebayashi, S., Okumura, K., Kudo, S., Chiba, T., Saya, H., and Nakao, M. (1999). Methylation-mediated transcriptional silencing in euchromatin by methyl-CpG binding protein MBD1 isoforms. Mol Cell Biol *19*, 6415-6426.

Gallinari, P., Di Marco, S., Jones, P., Pallaoro, M., and Steinkuhler, C. (2007). HDACs, histone deacetylation and gene transcription: from molecular biology to cancer therapeutics. Cell Res *17*, 195-211.

Ganiatsas, S., Dow, R., Thompson, A., Schulman, B., and Germain, D. (2001). A splice variant of Skp2 is retained in the cytoplasm and fails to direct cyclin D1 ubiquitination in the uterine cancer cell line SK-UT. Oncogene *20*, 3641-3650.

Gao, L., Cueto, M. A., Asselbergs, F., and Atadja, P. (2002). Cloning and functional characterization of HDAC11, a novel member of the human histone deacetylase family. J Biol Chem *277*, 25748-25755.

Garcia-Manero, G., Assouline, S., Cortes, J., Estrov, Z., Kantarjian, H., Yang, H., Newsome, W. M., Miller, W. H., Jr., Rousseau, C., Kalita, A., *et al.* (2008). Phase I study of the oral isotype specific histone deacetylase inhibitor MGCD0103 in leukemia. Blood.

Glaser, K. B., Staver, M. J., Waring, J. F., Stender, J., Ulrich, R. G., and Davidsen, S. K. (2003). Gene expression profiling of multiple histone deacetylase (HDAC) inhibitors: defining a common gene set produced by HDAC inhibition in T24 and MDA carcinoma cell lines. Mol Cancer Ther *2*, 151-163.

Goodlett, C. R., and Horn, K. H. (2001). Mechanisms of alcohol-induced damage to the developing nervous system. Alcohol Res Health *25*, 175-184.

Grangeasse, C., Cozzone,AJ, Deutscher,J, Mijakovic,I (2007). Tyrosine phosphorylation: an emerging regulatory device of bacterial physiology. Trends in Biochemical Sciences *32*.

Greer, E. L., and Brunet, A. (2005). FOXO transcription factors at the interface between longevity and tumor suppression. Oncogene *24*, 7410-7425.

Gross, A., McDonnell, J. M., and Korsmeyer, S. J. (1999). BCL-2 family members and the mitochondria in apoptosis. Genes Dev *13*, 1899-1911.

Gu, W., and Roeder, R. G. (1997). Activation of p53 sequence-specific DNA binding by acetylation of the p53 C-terminal domain. Cell *90*, 595-606.

Guan, K. L., Jenkins, C. W., Li, Y., Nichols, M. A., Wu, X., O'Keefe, C. L., Matera, A. G., and Xiong, Y. (1994). Growth suppression by p18, a p16INK4/MTS1- and p14INK4B/MTS2-related CDK6 inhibitor, correlates with wild-type pRb function. Genes Dev *8*, 2939-2952.

Haggarty, S. J., Koeller, K. M., Wong, J. C., Grozinger, C. M., and Schreiber, S. L. (2003). Domain-selective small-molecule inhibitor of histone deacetylase 6 (HDAC6)-mediated tubulin deacetylation. Proc Natl Acad Sci U S A *100*, 4389-4394.

Harms, K. L., and Chen, X. (2007). Histone deacetylase 2 modulates p53 transcriptional activities through regulation of p53-DNA binding activity. Cancer Res *67*, 3145-3152.

Hashizume, R., Fukuda, M., Maeda, I., Nishikawa, H., Oyake, D., Yabuki, Y., Ogata, H., and Ohta, T. (2001). The RING heterodimer BRCA1-BARD1 is a ubiquitin ligase inactivated by a breast cancer-derived mutation. J Biol Chem *276*, 14537-14540.

Hatakeyama, S., Yada, M., Matsumoto, M., Ishida, N., and Nakayama, K. I. (2001). U box proteins as a new family of ubiquitin-protein ligases. J Biol Chem *276*, 33111-33120.

Hayes, D. F. (2004). Tamoxifen: Dr. Jekyll and Mr. Hyde? J Natl Cancer Inst *96*, 895-897.

Heinzel, T., Lavinsky, R. M., Mullen, T. M., Soderstrom, M., Laherty, C. D., Torchia, J., Yang, W. M., Brard, G., Ngo, S. D., Davie, J. R., *et al.* (1997). A complex containing N-CoR, mSin3 and histone deacetylase mediates transcriptional repression. Nature *387*, 43-48.

Hermand, D. (2006). F-box proteins: more than baits for the SCF? Cell Div *1*, 30.
Hess-Stumpp, H. (2005). Histone deacetylase inhibitors and cancer: from cell biology to the clinic. Eur J Cell Biol *84*, 109-121.

Hicke, L. (2001). Protein regulation by monoubiquitin. Nat Rev Mol Cell Biol *2*, 195-201.

Hildmann, C., Wegener, D., Riester, D., Hempel, R., Schober, A., Merana, J., Giurato, L., Guccione, S., Nielsen, T. K., Ficner, R., and Schwienhorst, A. (2006). Substrate and inhibitor specificity of class 1 and class 2 histone deacetylases. J Biotechnol *124*, 258-270.

Hitomi, T., Matsuzaki, Y., Yokota, T., Takaoka, Y., and Sakai, T. (2003). p15(INK4b) in HDAC inhibitor-induced growth arrest. FEBS Lett *554*, 347-350.

Ho, M. S., Tsai, P. I., and Chien, C. T. (2006). F-box proteins: the key to protein degradation. J Biomed Sci *13*, 181-191.

Hodges-Gallagher, L., Valentine, C. D., Bader, S. E., and Kushner, P. J. (2007). Inhibition of histone deacetylase enhances the anti-proliferative action of antiestrogens on breast cancer cells and blocks tamoxifen-induced proliferation of uterine cells. Breast Cancer Res Treat *105*, 297-309.

Horlein, A. J., Naar, A. M., Heinzel, T., Torchia, J., Gloss, B., Kurokawa, R., Ryan, A., Kamei, Y., Soderstrom, M., Glass, C. K., and et al. (1995). Ligand-independent repression by the thyroid hormone receptor mediated by a nuclear receptor co-repressor. Nature *377*, 397-404.

Horwitz, K. B., and McGuire, W. L. (1980). Studies on mechanisms of estrogen and antiestrogen action in human breast cancer. Recent Results Cancer Res *71*, 45-58.

Howell, A., and Dowsett, M. (1997). Recent advances in endocrine therapy of breast cancer. Bmj *315*, 863-866.

Huang, H., Regan, K. M., Wang, F., Wang, D., Smith, D. I., van Deursen, J. M., and Tindall, D. J. (2005). Skp2 inhibits FOXO1 in tumor suppression through ubiquitin-mediated degradation. Proc Natl Acad Sci U S A *102*, 1649-1654.

Ilyin, G. P., Rialland, M., Glaise, D., and Guguen-Guillouzo, C. (1999). Identification of a novel Skp2-like mammalian protein containing F-box and leucine-rich repeats. FEBS Lett *459*, 75-79.

Ilyin, G. P., Serandour, A. L., Pigeon, C., Rialland, M., Glaise, D., and Guguen-Guillouzo, C. (2002). A new subfamily of structurally related human F-box proteins. Gene *296*, 11-20.

Ito, A., Kawaguchi, Y., Lai, C. H., Kovacs, J. J., Higashimoto, Y., Appella, E., and Yao, T. P. (2002). MDM2-HDAC1-mediated deacetylation of p53 is required for its degradation. Embo J *21*, 6236-6245.

Jackson, P. K., Eldridge, A. G., Freed, E., Furstenthal, L., Hsu, J. Y., Kaiser, B. K., and Reimann, J. D. (2000). The lore of the RINGs: substrate recognition and catalysis by ubiquitin ligases. Trends Cell Biol *10*, 429-439.

Jang, E. R., Lim, S. J., Lee, E. S., Jeong, G., Kim, T. Y., Bang, Y. J., and Lee, J. S. (2004). The histone deacetylase inhibitor trichostatin A sensitizes estrogen receptor alpha-negative breast cancer cells to tamoxifen. Oncogene *23*, 1724-1736.

Jarvinen, T. A., Pelto-Huikko, M., Holli, K., and Isola, J. (2000). Estrogen receptor beta is coexpressed with ERalpha and PR and associated with nodal status, grade, and proliferation rate in breast cancer. Am J Pathol *156*, 29-35.

Jin, Y. H., Jeon, E. J., Li, Q. L., Lee, Y. H., Choi, J. K., Kim, W. J., Lee, K. Y., and Bae, S. C. (2004). Transforming growth factor-beta stimulates p300-dependent RUNX3 acetylation, which inhibits ubiquitination-mediated degradation. J Biol Chem *279*, 29409-29417.

Johnstone, R. W., Ruefli, A. A., and Lowe, S. W. (2002). Apoptosis: a link between cancer genetics and chemotherapy. Cell *108*, 153-164.

Jung, M., Brosch, G., Kolle, D., Scherf, H., Gerhauser, C., and Loidl, P. (1999). Amide analogues of trichostatin A as inhibitors of histone deacetylase and inducers of terminal cell differentiation. J Med Chem *42*, 4669-4679.

Kajava, A. V., Vassart, G., and Wodak, S. J. (1995). Modeling of the three-dimensional structure of proteins with the typical leucine-rich repeats. Structure *3*, 867-877.

Kamura, T., Koepp, D. M., Conrad, M. N., Skowyra, D., Moreland, R. J., Iliopoulos, O., Lane, W. S., Kaelin, W. G., Jr., Elledge, S. J., Conaway, R. C., *et al.* (1999). Rbx1, a component of the VHL tumor suppressor complex and SCF ubiquitin ligase. Science *284*, 657-661.

Karagiannis, T. C., and El-Osta, A. (2006). Clinical potential of histone deacetylase inhibitors as stand alone therapeutics and in combination with other chemotherapeutics or radiotherapy for cancer. Epigenetics *1*, 121-126.

Kawai, H., Li, H., Avraham, S., Jiang, S., and Avraham, H. K. (2003). Overexpression of histone deacetylase HDAC1 modulates breast cancer progression by negative regulation of estrogen receptor alpha. Int J Cancer *107*, 353-358.

Kelly, W. K., O'Connor, O. A., Krug, L. M., Chiao, J. H., Heaney, M., Curley, T., MacGregore-Cortelli, B., Tong, W., Secrist, J. P., Schwartz, L., *et al.* (2005). Phase I study of an oral histone deacetylase inhibitor, suberoylanilide hydroxamic acid, in patients with advanced cancer. J Clin Oncol *23*, 3923-3931.

Kelly, W. K., Richon, V. M., O'Connor, O., Curley, T., MacGregor-Curtelli, B., Tong, W., Klang, M., Schwartz, L., Richardson, S., Rosa, E., *et al.* (2003). Phase I clinical trial of histone deacetylase inhibitor: suberoylanilide hydroxamic acid administered intravenously. Clin Cancer Res *9*, 3578-3588.

Kerr, J. F. (2002). History of the events leading to the formulation of the apoptosis concept. Toxicology *181-182*, 471-474.

Kerr, J. F., Wyllie, A. H., and Currie, A. R. (1972). Apoptosis: a basic biological phenomenon with wide-ranging implications in tissue kinetics. Br J Cancer *26*, 239-257.

Khan, S. B., Maududi, T., Barton, K., Ayers, J., and Alkan, S. (2004). Analysis of histone deacetylase inhibitor, depsipeptide (FR901228), effect on multiple myeloma. Br J Haematol *125*, 156-161.

Khaw, A. K., Silasudjana, M., Banerjee, B., Suzuki, M., Baskar, R., and Hande, M. P. (2007). Inhibition of telomerase activity and human telomerase reverse transcriptase gene expression by histone deacetylase inhibitor in human brain cancer cells. Mutat Res *625*, 134-144.

Kim, D. K., Lee, J. Y., Kim, J. S., Ryu, J. H., Choi, J. Y., Lee, J. W., Im, G. J., Kim, T. K., Seo, J. W., Park, H. J., *et al.* (2003a). Synthesis and biological evaluation of 3-(4-substituted-phenyl)-N-hydroxy-2-propenamides, a new class of histone deacetylase inhibitors. J Med Chem *46*, 5745-5751.

Kim, J. H., Choi, H. J., Kim, B., Kim, M. H., Lee, J. M., Kim, I. S., Lee, M. H., Choi, S. J., Kim, K. I., Kim, S. I., *et al.* (2006). Roles of sumoylation of a reptin chromatin-remodelling complex in cancer metastasis. Nat Cell Biol *8*, 631-639.

Kim, S. H., Ahn, S., Han, J. W., Lee, H. W., Lee, H. Y., Lee, Y. W., Kim, M. R., Kim, K. W., Kim, W. B., and Hong, S. (2004). Apicidin is a histone deacetylase inhibitor with anti-invasive and anti-angiogenic potentials. Biochem Biophys Res Commun *315*, 964-970.

Kim, S. Y., Herbst, A., Tworkowski, K. A., Salghetti, S. E., and Tansey, W. P. (2003b). Skp2 regulates Myc protein stability and activity. Mol Cell *11*, 1177-1188.

Kim, Y. B., Yoshida, M., and Horinouchi, S. (1999). Selective induction of cyclin-dependent kinase inhibitors and their roles in cell cycle arrest caused by trichostatin A, an inhibitor of histone deacetylase. Ann N Y Acad Sci *886*, 200-203.

Kinloch, R. A., Treherne, J. M., Furness, L. M., and Hajimohamadreza, I. (1999). The pharmacology of apoptosis. Trends Pharmacol Sci *20*, 35-42.

Kipreos, E. T., and Pagano, M. (2000). The F-box protein family. Genome Biol *1*, REVIEWS3002.

Kirsh, O., Seeler, J. S., Pichler, A., Gast, A., Muller, S., Miska, E., Mathieu, M., Harel-Bellan, A., Kouzarides, T., Melchior, F., and Dejean, A. (2002). The SUMO E3 ligase RanBP2 promotes modification of the HDAC4 deacetylase. Embo J *21*, 2682-2691.

Kitagawa, K., Skowyra, D., Elledge, S. J., Harper, J. W., and Hieter, P. (1999). SGT1 encodes an essential component of the yeast kinetochore assembly pathway and a novel subunit of the SCF ubiquitin ligase complex. Mol Cell *4*, 21-33.

Kondo, Y., and Kondo, S. (2006). Autophagy and cancer therapy. Autophagy *2*, 85-90.

Kouzarides, T. (1999). Histone acetylases and deacetylases in cell proliferation. Curr Opin Genet Dev *9*, 40-48.

Krege, J. H., Hodgin, J. B., Couse, J. F., Enmark, E., Warner, M., Mahler, J. F., Sar, M., Korach, K. S., Gustafsson, J. A., and Smithies, O. (1998). Generation and reproductive phenotypes of mice lacking estrogen receptor beta. Proc Natl Acad Sci U S A *95*, 15677-15682.

Kukuruzinska, M. A., and Lennon, K. (1998). Protein N-glycosylation: molecular genetics and functional significance. Crit Rev Oral Biol Med *9*, 415-448.

Kuljaca, S., Liu, T., Tee, A. E., Haber, M., Norris, M. D., Dwarte, T., and Marshall, G. M. (2007). Enhancing the anti-angiogenic action of histone deacetylase inhibitors. Mol Cancer *6*, 68.

Kumagai, T., Wakimoto, N., Yin, D., Gery, S., Kawamata, N., Takai, N., Komatsu, N., Chumakov, A., Imai, Y., and Koeffler, H. P. (2007). Histone deacetylase inhibitor, suberoylanilide hydroxamic acid (Vorinostat, SAHA) profoundly inhibits the growth of human pancreatic cancer cells. Int J Cancer *121*, 656-665.

Kumar, R., Neilsen, P. M., Crawford, J., McKirdy, R., Lee, J., Powell, J. A., Saif, Z., Martin, J. M., Lombaerts, M., Cornelisse, C. J., *et al.* (2005). FBXO31 is the chromosome 16q24.3 senescence gene, a candidate breast tumor suppressor, and a component of an SCF complex. Cancer Res *65*, 11304-11313.

Kurokawa, R., Soderstrom, M., Horlein, A., Halachmi, S., Brown, M., Rosenfeld, M. G., and Glass, C. K. (1995). Polarity-specific activities of retinoic acid receptors determined by a co-repressor. Nature *377*, 451-454.

Kwon, H. J., Kim, M. S., Kim, M. J., Nakajima, H., and Kim, K. W. (2002a). Histone deacetylase inhibitor FK228 inhibits tumor angiogenesis. Int J Cancer *97*, 290-296.

Kwon, S. H., Ahn, S. H., Kim, Y. K., Bae, G. U., Yoon, J. W., Hong, S., Lee, H. Y., Lee, Y. W., Lee, H. W., and Han, J. W. (2002b). Apicidin, a histone deacetylase inhibitor, induces apoptosis and Fas/Fas ligand expression in human acute promyelocytic leukemia cells. J Biol Chem *277*, 2073-2080.

Lammer, D., Mathias, N., Laplaza, J. M., Jiang, W., Liu, Y., Callis, J., Goebl, M., and Estelle, M. (1998). Modification of yeast Cdc53p by the ubiquitin-related protein rub1p affects function of the SCFCdc4 complex. Genes Dev *12*, 914-926.

Laoukili, J., Kooistra, M. R., Bras, A., Kauw, J., Kerkhoven, R. M., Morrison, A., Clevers, H., and Medema, R. H. (2005). FoxM1 is required for execution of the mitotic programme and chromosome stability. Nat Cell Biol *7*, 126-136.

Lee, J. W., Bae, S. H., Jeong, J. W., Kim, S. H., and Kim, K. W. (2004). Hypoxia-inducible factor (HIF-1)alpha: its protein stability and biological functions. Exp Mol Med *36*, 1-12.

Lei, K., Nimnual, A., Zong, W. X., Kennedy, N. J., Flavell, R. A., Thompson, C. B., Bar-Sagi, D., and Davis, R. J. (2002). The Bax subfamily of Bcl2-related proteins is essential for apoptotic signal transduction by c-Jun NH(2)-terminal kinase. Mol Cell Biol *22*, 4929-4942.

Leng, C., Gries, M., Ziegler, J., Lokshin, A., Mascagni, P., Lentzsch, S., and Mapara, M. Y. (2006). Reduction of graft-versus-host disease by histone deacetylase inhibitor suberonylanilide hydroxamic acid is associated with modulation of inflammatory cytokine milieu and involves inhibition of STAT1. Exp Hematol *34*, 776-787.

Lewin, B. (2000) Genes VII, chapter 27

Ley, R., Balmanno, K., Hadfield, K., Weston, C., and Cook, S. J. (2003). Activation of the ERK1/2 signaling pathway promotes phosphorylation and proteasome-dependent degradation of the BH3-only protein, Bim. J Biol Chem *278*, 18811-18816.

Li, G. C., Zhang, X., Pan, T. J., Chen, Z., and Ye, Z. Q. (2006). Histone deacetylase inhibitor trichostatin A inhibits the growth of bladder cancer cells through induction of p21WAF1 and G1 cell cycle arrest. Int J Urol *13*, 581-586.

Lin, H. Y., Chen, C. S., Lin, S. P., Weng, J. R., and Chen, C. S. (2006). Targeting histone deacetylase in cancer therapy. Med Res Rev *26*, 397-413.

Lisztwan, J., Marti, A., Sutterluty, H., Gstaiger, M., Wirbelauer, C., and Krek, W. (1998). Association of human CUL-1 and ubiquitin-conjugating enzyme CDC34 with the F-box protein p45(SKP2): evidence for evolutionary conservation in the subunit composition of the CDC34-SCF pathway. Embo J *17*, 368-383.

Liu, T., Kuljaca, S., Tee, A., and Marshall, G. M. (2006). Histone deacetylase inhibitors: multifunctional anticancer agents. Cancer Treat Rev *32*, 157-165.

Lucas, D. M., Davis, M. E., Parthun, M. R., Mone, A. P., Kitada, S., Cunningham, K. D., Flax, E. L., Wickham, J., Reed, J. C., Byrd, J. C., and Grever, M. R. (2004). The histone deacetylase inhibitor MS-275 induces caspase-dependent apoptosis in B-cell chronic lymphocytic leukemia cells. Leukemia *18*, 1207-1214.

Luo, R. X., Postigo, A. A., and Dean, D. C. (1998). Rb interacts with histone deacetylase to repress transcription. Cell *92*, 463-473.

Lyapina, S. A., Correll, C. C., Kipreos, E. T., and Deshaies, R. J. (1998). Human CUL1 forms an evolutionarily conserved ubiquitin ligase complex (SCF) with SKP1 and an F-box protein. Proc Natl Acad Sci U S A *95*, 7451-7456.

Lynch, H. T., Silva, E., Snyder, C., and Lynch, J. F. (2008). Hereditary breast cancer: part I. Diagnosing hereditary breast cancer syndromes. Breast J *14*, 3-13.

Ma, R. Y., Tong, T. H., Cheung, A. M., Tsang, A. C., Leung, W. Y., and Yao, K. M. (2005). Raf/MEK/MAPK signaling stimulates the nuclear translocation and transactivating activity of FOXM1c. J Cell Sci *118*, 795-806.

Maggio, S. C., Rosato, R. R., Kramer, L. B., Dai, Y., Rahmani, M., Paik, D. S., Czarnik, A. C., Payne, S. G., Spiegel, S., and Grant, S. (2004). The histone deacetylase inhibitor MS-275 interacts synergistically with fludarabine to induce apoptosis in human leukemia cells. Cancer Res *64*, 2590-2600.

Majno, G., and Joris, I. (1995). Apoptosis, oncosis, and necrosis. An overview of cell death. Am J Pathol *146*, 3-15.

Mansilla, S., Priebe, W., and Portugal, J. (2006). Mitotic catastrophe results in cell death by caspase-dependent and caspase-independent mechanisms. Cell Cycle *5*, 53-60.

Marchion, D. C., Bicaku, E., Daud, A. I., Richon, V., Sullivan, D. M., and Munster, P. N. (2004). Sequence-specific potentiation of topoisomerase II inhibitors by the histone deacetylase inhibitor suberoylanilide hydroxamic acid. J Cell Biochem *92*, 223-237.

Margueron, R., Licznar, A., Lazennec, G., Vignon, F., and Cavailles, V. (2003). Oestrogen receptor alpha increases p21(WAF1/CIP1) gene expression and the antiproliferative activity of histone deacetylase inhibitors in human breast cancer cells. J Endocrinol *179*, 41-53.

Marks, P. A., Richon, V. M., and Rifkind, R. A. (2000). Histone deacetylase inhibitors: inducers of differentiation or apoptosis of transformed cells. J Natl Cancer Inst *92*, 1210-1216.

Masumoto, H., Hawke, D., Kobayashi, R., and Verreault, A. (2005). A role for cell-cycle-regulated histone H3 lysine 56 acetylation in the DNA damage response. Nature *436*, 294-298.

McGarry, L. C., Winnie, J. N., and Ozanne, B. W. (2004). Invasion of v-Fos(FBR)-transformed cells is dependent upon histone deacetylase activity and suppression of histone deacetylase regulated genes. Oncogene *23*, 5284-5292.

Meraldi, P., Honda, R., and Nigg, E. A. (2004). Aurora kinases link chromosome segregation and cell division to cancer susceptibility. Curr Opin Genet Dev *14*, 29-36.

Miki, Y., Swensen, J., Shattuck-Eidens, D., Futreal, P. A., Harshman, K., Tavtigian, S., Liu, Q., Cochran, C., Bennett, L. M., Ding, W., and et al. (1994). A strong candidate for the breast and ovarian cancer susceptibility gene BRCA1. Science *266*, 66-71.

Minucci, S., and Pelicci, P. G. (2006). Histone deacetylase inhibitors and the promise of epigenetic (and more) treatments for cancer. Nat Rev Cancer *6*, 38-51.

Mitsiades, C. S., Mitsiades, N., Poulaki, V., Schlossman, R., Akiyama, M., Chauhan, D., Hideshima, T., Treon, S. P., Munshi, N. C., Richardson, P. G., and Anderson, K. C. (2002a). Activation of NF-kappaB and upregulation of intracellular anti-apoptotic proteins via the IGF-1/Akt signaling in human multiple myeloma cells: therapeutic implications. Oncogene *21*, 5673-5683.

Mitsiades, C. S., Mitsiades, N. S., McMullan, C. J., Poulaki, V., Shringarpure, R., Hideshima, T., Akiyama, M., Chauhan, D., Munshi, N., Gu, X., *et al.* (2004). Transcriptional signature of histone deacetylase inhibition in multiple myeloma: biological and clinical implications. Proc Natl Acad Sci U S A *101*, 540-545.

Mitsiades, N., Mitsiades, C. S., Poulaki, V., Chauhan, D., Fanourakis, G., Gu, X., Bailey, C., Joseph, M., Libermann, T. A., Treon, S. P., *et al.* (2002b). Molecular sequelae of proteasome inhibition in human multiple myeloma cells. Proc Natl Acad Sci U S A *99*, 14374-14379.

Mukhopadhyay, N. K., Weisberg, E., Gilchrist, D., Bueno, R., Sugarbaker, D. J., and Jaklitsch, M. T. (2006). Effectiveness of trichostatin A as a potential candidate for anticancer therapy in non-small-cell lung cancer. Ann Thorac Surg *81*, 1034-1042.

Munshi, A., Tanaka, T., Hobbs, M. L., Tucker, S. L., Richon, V. M., and Meyn, R. E. (2006). Vorinostat, a histone deacetylase inhibitor, enhances the response of human tumor cells to ionizing radiation through prolongation of gamma-H2AX foci. Mol Cancer Ther *5*, 1967-1974.

Narlikar, G. J., Fan, H. Y., and Kingston, R. E. (2002). Cooperation between complexes that regulate chromatin structure and transcription. Cell *108*, 475-487.

Nash, P., Tang, X., Orlicky, S., Chen, Q., Gertler, F. B., Mendenhall, M. D., Sicheri, F., Pawson, T., and Tyers, M. (2001). Multisite phosphorylation of a CDK inhibitor sets a threshold for the onset of DNA replication. Nature *414*, 514-521.

Nau, H., Hauck, R. S., and Ehlers, K. (1991). Valproic acid-induced neural tube defects in mouse and human: aspects of chirality, alternative drug development, pharmacokinetics and possible mechanisms. Pharmacol Toxicol *69*, 310-321.

Nebbioso, A., Clarke, N., Voltz, E., Germain, E., Ambrosino, C., Bontempo, P., Alvarez, R., Schiavone, E. M., Ferrara, F., Bresciani, F., *et al.* (2005). Tumor-selective action of HDAC inhibitors involves TRAIL induction in acute myeloid leukemia cells. Nat Med *11*, 77-84.

Nelson, R. F., Glenn, K. A., Zhang, Y., Wen, H., Knutson, T., Gouvion, C. M., Robinson, B. K., Zhou, Z., Yang, B., Smith, R. J., and Paulson, H. L. (2007). Selective cochlear degeneration in mice lacking the F-box protein, Fbx2, a glycoprotein-specific ubiquitin ligase subunit. J Neurosci *27*, 5163-5171.

Newmark, H. L., and Young, C. W. (1995). Butyrate and phenylacetate as differentiating agents: practical problems and opportunities. J Cell Biochem Suppl *22*, 247-253.

Nielsen, T. K., Hildmann, C., Dickmanns, A., Schwienhorst, A., and Ficner, R. (2005). Crystal structure of a bacterial class 2 histone deacetylase homologue. J Mol Biol *354*, 107-120.

Nimmanapalli, R., Fuino, L., Stobaugh, C., Richon, V., and Bhalla, K. (2003). Cotreatment with the histone deacetylase inhibitor suberoylanilide hydroxamic acid (SAHA) enhances imatinib-induced apoptosis of Bcr-Abl-positive human acute leukemia cells. Blood *101*, 3236-3239.

Ohta, T., and Fukuda, M. (2004). Ubiquitin and breast cancer. Oncogene *23*, 2079-2088.

Ohta, T., Michel, J. J., Schottelius, A. J., and Xiong, Y. (1999). ROC1, a homolog of APC11, represents a family of cullin partners with an associated ubiquitin ligase activity. Mol Cell *3*, 535-541.

Orlicky, S., Tang, X., Willems, A., Tyers, M., and Sicheri, F. (2003). Structural basis for phosphodependent substrate selection and orientation by the SCFCdc4 ubiquitin ligase. Cell *112*, 243-256.

Pan, L. N., Lu, J., and Huang, B. (2007). HDAC inhibitors: a potential new category of anti-tumor agents. Cell Mol Immunol *4*, 337-343.

Paris, M., Porcelloni, M., Binaschi, M., and Fattori, D. (2008). Histone deacetylase inhibitors: from bench to clinic. J Med Chem *51*, 1505-1529.

Paruthiyil, S., Parmar, H., Kerekatte, V., Cunha, G. R., Firestone, G. L., and Leitman, D. C. (2004). Estrogen receptor beta inhibits human breast cancer cell proliferation and tumor formation by causing a G2 cell cycle arrest. Cancer Res *64*, 423-428.

Pawson, T., Scott, JD (2005). Protein phosphorylation in signalling-50 years and counting. Trends in Biochemical Sciences *30*.

Peart, M. J., Smyth, G. K., van Laar, R. K., Bowtell, D. D., Richon, V. M., Marks, P. A., Holloway, A. J., and Johnstone, R. W. (2005). Identification and functional significance of genes regulated by structurally different histone deacetylase inhibitors. Proc Natl Acad Sci U S A *102*, 3697-3702.

Piekarz, R. L., Robey, R., Sandor, V., Bakke, S., Wilson, W. H., Dahmoush, L., Kingma, D. M., Turner, M. L., Altemus, R., and Bates, S. E. (2001). Inhibitor of histone deacetylation, depsipeptide (FR901228), in the treatment of peripheral and cutaneous T-cell lymphoma: a case report. Blood *98*, 2865-2868.

Pietras, R. J., and Szego, C. M. (1977). Specific binding sites for oestrogen at the outer surfaces of isolated endometrial cells. Nature *265*, 69-72.

Pines, J., and Lindon, C. (2005). Proteolysis: anytime, any place, anywhere? Nat Cell Biol *7*, 731-735.

Platta, C. S., Greenblatt, D. Y., Kunnimalaiyaan, M., and Chen, H. (2007). The HDAC inhibitor trichostatin A inhibits growth of small cell lung cancer cells. J Surg Res *142*, 219-226.

Puthalakath, H., Villunger, A., O'Reilly, L. A., Beaumont, J. G., Coultas, L., Cheney, R. E., Huang, D. C., and Strasser, A. (2001). Bmf: a proapoptotic BH3-only protein regulated by interaction with the myosin V actin motor complex, activated by anoikis. Science *293*, 1829-1832.

Qian, D. Z., Wei, Y. F., Wang, X., Kato, Y., Cheng, L., and Pili, R. (2007). Antitumor activity of the histone deacetylase inhibitor MS-275 in prostate cancer models. Prostate *67*, 1182-1193.

Radhakrishnan, V., Song, Y. S., and Thiruvengadam, D. (2007). Romidepsin (depsipeptide) induced cell cycle arrest, apoptosis and histone hyperacetylation in lung carcinoma cells (A549) are associated with increase in p21 and hypophosphorylated retinoblastoma proteins expression. Biomed Pharmacother.

Rajkumar, S. V., Richardson, P. G., Hideshima, T., and Anderson, K. C. (2005). Proteasome inhibition as a novel therapeutic target in human cancer. J Clin Oncol *23*, 630-639.

Razandi, M., Pedram, A., Greene, G. L., and Levin, E. R. (1999). Cell membrane and nuclear estrogen receptors (ERs) originate from a single transcript: studies of ERalpha and ERbeta expressed in Chinese hamster ovary cells. Mol Endocrinol *13*, 307-319.

Richon, V. M., Sandhoff, T. W., Rifkind, R. A., and Marks, P. A. (2000). Histone deacetylase inhibitor selectively induces p21WAF1 expression and gene-associated histone acetylation. Proc Natl Acad Sci U S A *97*, 10014-10019.

Roberts, E. C., Shapiro, P. S., Nahreini, T. S., Pages, G., Pouyssegur, J., and Ahn, N. G. (2002). Distinct cell cycle timing requirements for extracellular signal-regulated kinase and phosphoinositide 3-kinase signaling pathways in somatic cell mitosis. Mol Cell Biol *22*, 7226-7241.

Roger, P., Sahla, M. E., Makela, S., Gustafsson, J. A., Baldet, P., and Rochefort, H. (2001). Decreased expression of estrogen receptor beta protein in proliferative preinvasive mammary tumors. Cancer Res *61*, 2537-2541.

Rokhlin, O. W., Glover, R. B., Guseva, N. V., Taghiyev, A. F., Kohlgraf, K. G., and Cohen, M. B. (2006). Mechanisms of cell death induced by histone deacetylase inhibitors in androgen receptor-positive prostate cancer cells. Mol Cancer Res *4*, 113-123.

Roninson, I. B. (2003). Tumor cell senescence in cancer treatment. Cancer Res *63*, 2705-2715.

Ropero, S., Fraga, M. F., Ballestar, E., Hamelin, R., Yamamoto, H., Boix-Chornet, M., Caballero, R., Alaminos, M., Setien, F., Paz, M. F., *et al.* (2006). A truncating mutation of HDAC2 in human cancers confers resistance to histone deacetylase inhibition. Nat Genet *38*, 566-569.

Rosato, R. R., Almenara, J. A., and Grant, S. (2003). The histone deacetylase inhibitor MS-275 promotes differentiation or apoptosis in human leukemia cells through a process regulated by generation of reactive oxygen species and induction of p21CIP1/WAF1 1. Cancer Res *63*, 3637-3645.

Roy, D., Cai, Q., Felty, Q., and Narayan, S. (2007). Estrogen-induced generation of reactive oxygen and nitrogen species, gene damage, and estrogen-dependent cancers. J Toxicol Environ Health B Crit Rev *10*, 235-257.

Ruefli, A. A., Ausserlechner, M. J., Bernhard, D., Sutton, V. R., Tainton, K. M., Kofler, R., Smyth, M. J., and Johnstone, R. W. (2001). The histone deacetylase inhibitor and chemotherapeutic agent suberoylanilide hydroxamic acid (SAHA) induces a cell-death pathway characterized by cleavage of Bid and production of reactive oxygen species. Proc Natl Acad Sci U S A *98*, 10833-10838.

Sadri-Vakili, G., and Cha, J. H. (2006). Histone deacetylase inhibitors: a novel therapeutic approach to Huntington's disease (complex mechanism of neuronal death). Curr Alzheimer Res *3*, 403-408.

Sambucetti, L. C., Fischer, D. D., Zabludoff, S., Kwon, P. O., Chamberlin, H., Trogani, N., Xu, H., and Cohen, D. (1999). Histone deacetylase inhibition selectively alters the activity and expression of cell cycle proteins leading to specific chromatin acetylation and antiproliferative effects. J Biol Chem *274*, 34940-34947.

Samuels, Y., Diaz, L. A., Jr., Schmidt-Kittler, O., Cummins, J. M., Delong, L., Cheong, I., Rago, C., Huso, D. L., Lengauer, C., Kinzler, K. W., *et al.* (2005). Mutant PIK3CA promotes cell growth and invasion of human cancer cells. Cancer Cell *7*, 561-573.

Sasakawa, Y., Naoe, Y., Noto, T., Inoue, T., Sasakawa, T., Matsuo, M., Manda, T., and Mutoh, S. (2003). Antitumor efficacy of FK228, a novel histone deacetylase inhibitor, depends on the effect on expression of angiogenesis factors. Biochem Pharmacol *66*, 897-906.

Sasakawa, Y., Naoe, Y., Sogo, N., Inoue, T., Sasakawa, T., Matsuo, M., Manda, T., and Mutoh, S. (2005). Marker genes to predict sensitivity to FK228, a histone deacetylase inhibitor. Biochem Pharmacol *69*, 603-616.

Sawa, H., Murakami, H., Ohshima, Y., Murakami, M., Yamazaki, I., Tamura, Y., Mima, T., Satone, A., Ide, W., Hashimoto, I., and Kamada, H. (2002). Histone deacetylase inhibitors such as sodium butyrate and trichostatin A inhibit vascular endothelial growth factor (VEGF) secretion from human glioblastoma cells. Brain Tumor Pathol *19*, 77-81.

Schafer, K. A. (1998). The cell cycle: a review. Vet Pathol *35*, 461-478.
Schwarz, D. S., Hutvagner, G., Haley, B., and Zamore, P. D. (2002). Evidence that siRNAs function as guides, not primers, in the Drosophila and human RNAi pathways. Mol Cell *10*, 537-548.

Sengupta, P. P., Northfelt, D. W., Gentile, F., Zamorano, J. L., and Khandheria, B. K. (2008). Trastuzumab-induced cardiotoxicity: heart failure at the crossroads. Mayo Clin Proc *83*, 197-203.

Shao, Y., Gao, Z., Marks, P. A., and Jiang, X. (2004). Apoptotic and autophagic cell death induced by histone deacetylase inhibitors. Proc Natl Acad Sci U S A *101*, 18030-18035.

Siddiqui, H., Solomon, D. A., Gunawardena, R. W., Wang, Y., and Knudsen, E. S. (2003). Histone deacetylation of RB-responsive promoters: requisite for specific gene repression but dispensable for cell cycle inhibition. Mol Cell Biol *23*, 7719-7731.

Signoretti, S., Di Marcotullio, L., Richardson, A., Ramaswamy, S., Isaac, B., Rue, M., Monti, F., Loda, M., and Pagano, M. (2002). Oncogenic role of the ubiquitin ligase subunit Skp2 in human breast cancer. J Clin Invest *110*, 633-641.

Skliris, G. P., Carder, P. J., Lansdown, M. R., and Speirs, V. (2001). Immunohistochemical detection of ERbeta in breast cancer: towards more detailed receptor profiling? Br J Cancer *84*, 1095-1098.

Skorski, T. (2002). Oncogenic tyrosine kinases and the DNA-damage response. Nat Rev Cancer *2*, 351-360.

Skowyra, D., Craig, K. L., Tyers, M., Elledge, S. J., and Harper, J. W. (1997). F-box proteins are receptors that recruit phosphorylated substrates to the SCF ubiquitin-ligase complex. Cell *91*, 209-219.

Slamon, D. J., Leyland-Jones, B., Shak, S., Fuchs, H., Paton, V., Bajamonde, A., Fleming, T., Eiermann, W., Wolter, J., Pegram, M., *et al.* (2001). Use of chemotherapy plus a monoclonal antibody against HER2 for metastatic breast cancer that overexpresses HER2. N Engl J Med *344*, 783-792.

Smith, I., and Chua, S. (2006a). Medical treatment of early breast cancer. I: adjuvant treatment. Bmj *332*, 34-37.

Smith, I., and Chua, S. (2006b). Medical treatment of early breast cancer. II: endocrine therapy. Bmj *332*, 101-103.

Smith, I., and Chua, S. (2006c). Medical treatment of early breast cancer. III: chemotherapy. Bmj *332*, 161-162.

Smith, I., and Chua, S. (2006d). Medical treatment of early breast cancer. IV: neoadjuvant treatment. Bmj *332*, 223-224.

Sommer, S., and Fuqua, S. A. (2001). Estrogen receptor and breast cancer. Semin Cancer Biol *11*, 339-352.

Somoza, J. R., Skene, R. J., Katz, B. A., Mol, C., Ho, J. D., Jennings, A. J., Luong, C., Arvai, A., Buggy, J. J., Chi, E., *et al.* (2004). Structural snapshots of human HDAC8 provide insights into the class I histone deacetylases. Structure *12*, 1325-1334.

Song, Z., and Steller, H. (1999). Death by design: mechanism and control of apoptosis. Trends Cell Biol *9*, M49-52.

Sowa, Y., Orita, T., Hiranabe-Minamikawa, S., Nakano, K., Mizuno, T., Nomura, H., and Sakai, T. (1999). Histone deacetylase inhibitor activates the p21/WAF1/Cip1 gene promoter through the Sp1 sites. Ann N Y Acad Sci *886*, 195-199.

Spigel, D. R., and Burstein, H. J. (2002). HER2 overexpressing metastatic breast cancer. Curr Treat Options Oncol *3*, 163-174.

Stern, D. F. (2000). Tyrosine kinase signalling in breast cancer: ErbB family receptor tyrosine kinases. Breast Cancer Res *2*, 176-183.

Strahl, B. D., and Allis, C. D. (2000). The language of covalent histone modifications. Nature *403*, 41-45.

Strait, K. A., Dabbas, B., Hammond, E. H., Warnick, C. T., Iistrup, S. J., and Ford, C. D. (2002). Cell cycle blockade and differentiation of ovarian cancer cells by the histone deacetylase inhibitor trichostatin A are associated with changes in p21, Rb, and Id proteins. Mol Cancer Ther *1*, 1181-1190.

Sunters, A., Fernandez de Mattos, S., Stahl, M., Brosens, J. J., Zoumpoulidou, G., Saunders, C. A., Coffer, P. J., Medema, R. H., Coombes, R. C., and Lam, E. W. (2003). FoxO3a transcriptional regulation of Bim controls apoptosis in paclitaxel-treated breast cancer cell lines. J Biol Chem *278*, 49795-49805.

Sutterluty, H., Chatelain, E., Marti, A., Wirbelauer, C., Senften, M., Muller, U., and Krek, W. (1999). p45SKP2 promotes p27Kip1 degradation and induces S phase in quiescent cells. Nat Cell Biol *1*, 207-214.

Takai, D., and Jones, P. A. (2002). Comprehensive analysis of CpG islands in human chromosomes 21 and 22. Proc Natl Acad Sci U S A *99*, 3740-3745.

Tan, P., Fuchs, S. Y., Chen, A., Wu, K., Gomez, C., Ronai, Z., and Pan, Z. Q. (1999). Recruitment of a ROC1-CUL1 ubiquitin ligase by Skp1 and HOS to catalyze the ubiquitination of I kappa B alpha. Mol Cell *3*, 527-533.

Tang, X. X., Robinson, M. E., Riceberg, J. S., Kim, D. Y., Kung, B., Titus, T. B., Hayashi, S., Flake, A. W., Carpentieri, D., and Ikegaki, N. (2004). Favorable

neuroblastoma genes and molecular therapeutics of neuroblastoma. Clin Cancer Res *10*, 5837-5844.
Thai, T. H., Du, F., Tsan, J. T., Jin, Y., Phung, A., Spillman, M. A., Massa, H. F., Muller, C. Y., Ashfaq, R., Mathis, J. M., *et al.* (1998). Mutations in the BRCA1-associated RING domain (BARD1) gene in primary breast, ovarian and uterine cancers. Hum Mol Genet *7*, 195-202.

Thompson, C. B. (1995). Apoptosis in the pathogenesis and treatment of disease. Science *267*, 1456-1462.

Thornberry, N. A., and Lazebnik, Y. (1998). Caspases: enemies within. Science *281*, 1312-1316.

Tominaga, K., Olgun, A., Smith, J. R., and Pereira-Smith, O. M. (2002). Genetics of cellular senescence. Mech Ageing Dev *123*, 927-936.

Tuschl, T., and Borkhardt, A. (2002). Small interfering RNAs: a revolutionary tool for the analysis of gene function and gene therapy. Mol Interv *2*, 158-167.

Ulrich, H. D. (2005). Mutual interactions between the SUMO and ubiquitin systems: a plea of no contest. TRENDS in Cell Biology *15*.

Ungerstedt, J. S., Sowa, Y., Xu, W. S., Shao, Y., Dokmanovic, M., Perez, G., Ngo, L., Holmgren, A., Jiang, X., and Marks, P. A. (2005). Role of thioredoxin in the response of normal and transformed cells to histone deacetylase inhibitors. Proc Natl Acad Sci U S A *102*, 673-678.

Vannini, A., Volpari, C., Filocamo, G., Casavola, E. C., Brunetti, M., Renzoni, D., Chakravarty, P., Paolini, C., De Francesco, R., Gallinari, P., *et al.* (2004). Crystal structure of a eukaryotic zinc-dependent histone deacetylase, human HDAC8, complexed with a hydroxamic acid inhibitor. Proc Natl Acad Sci U S A *101*, 15064-15069.

Vermeulen, K., Van Bockstaele, D. R., and Berneman, Z. N. (2003). The cell cycle: a review of regulation, deregulation and therapeutic targets in cancer. Cell Prolif *36*, 131-149.

Vigushin, D. M., and Coombes, R. C. (2002). Histone deacetylase inhibitors in cancer treatment. Anticancer Drugs *13*, 1-13.

Wang, C., Gale, M., Jr., Keller, B. C., Huang, H., Brown, M. S., Goldstein, J. L., and Ye, J. (2005a). Identification of FBL2 as a geranylgeranylated cellular protein required for hepatitis C virus RNA replication. Mol Cell *18*, 425-434.

Wang, I. C., Chen, Y. J., Hughes, D., Petrovic, V., Major, M. L., Park, H. J., Tan, Y., Ackerson, T., and Costa, R. H. (2005b). Forkhead box M1 regulates the transcriptional network of genes essential for mitotic progression and genes encoding the SCF (Skp2-Cks1) ubiquitin ligase. Mol Cell Biol *25*, 10875-10894.

Wang, W., Ungermannova, D., Chen, L., and Liu, X. (2004). Molecular and biochemical characterization of the Skp2-Cks1 binding interface. J Biol Chem *279*, 51362-51369.

Warrell, R. P., Jr., He, L. Z., Richon, V., Calleja, E., and Pandolfi, P. P. (1998). Therapeutic targeting of transcription in acute promyelocytic leukemia by use of an inhibitor of histone deacetylase. J Natl Cancer Inst *90*, 1621-1625.

Wei, W., Ayad, N. G., Wan, Y., Zhang, G. J., Kirschner, M. W., and Kaelin, W. G., Jr. (2004). Degradation of the SCF component Skp2 in cell-cycle phase G1 by the anaphase-promoting complex. Nature *428*, 194-198.

Weissman, A. M. (2001). Themes and variations on ubiquitylation. Nat Rev Mol Cell Biol *2*, 169-178.

Welcker, M., Orian, A., Jin, J., Grim, J. E., Harper, J. W., Eisenman, R. N., and Clurman, B. E. (2004). The Fbw7 tumor suppressor regulates glycogen synthase kinase 3 phosphorylation-dependent c-Myc protein degradation. Proc Natl Acad Sci U S A *101*, 9085-9090.

Wiggins, C. M., Band, H., and Cook, S. J. (2007). c-Cbl is not required for ERK1/2-dependent degradation of BimEL. Cell Signal *19*, 2605-2611.

Wood, E. R., Truesdale, A. T., McDonald, O. B., Yuan, D., Hassell, A., Dickerson, S. H., Ellis, B., Pennisi, C., Horne, E., Lackey, K., *et al.* (2004). A unique structure for epidermal growth factor receptor bound to GW572016 (Lapatinib): relationships among protein conformation, inhibitor off-rate, and receptor activity in tumor cells. Cancer Res *64*, 6652-6659.

Woodgett, J. R. (2005). Recent advances in the protein kinase B signaling pathway. Curr Opin Cell Biol *17*, 150-157.

Wooster, R., Bignell, G., Lancaster, J., Swift, S., Seal, S., Mangion, J., Collins, N., Gregory, S., Gumbs, C., and Micklem, G. (1995). Identification of the breast cancer susceptibility gene BRCA2. Nature *378*, 789-792.

Wright, J. H., Munar, E., Jameson, D. R., Andreassen, P. R., Margolis, R. L., Seger, R., and Krebs, E. G. (1999). Mitogen-activated protein kinase kinase activity is required for the G(2)/M transition of the cell cycle in mammalian fibroblasts. Proc Natl Acad Sci U S A *96*, 11335-11340.

Wu, Z. Q., Zhang, R., Chao, C., Zhang, J. F., and Zhang, Y. Q. (2007). Histone deacetylase inhibitor trichostatin A induced caspase-independent apoptosis in human gastric cancer cell. Chin Med J (Engl) *120*, 2112-2118.

Xu, W., Ngo, L., Perez, G., Dokmanovic, M., and Marks, P. A. (2006). Intrinsic apoptotic and thioredoxin pathways in human prostate cancer cell response to histone deacetylase inhibitor. Proc Natl Acad Sci U S A *103*, 15540-15545.

Xu, W. S., Parmigiani, R. B., and Marks, P. A. (2007). Histone deacetylase inhibitors: molecular mechanisms of action. Oncogene *26*, 5541-5552.

Yada, M., Hatakeyama, S., Kamura, T., Nishiyama, M., Tsunematsu, R., Imaki, H., Ishida, N., Okumura, F., Nakayama, K., and Nakayama, K. I. (2004). Phosphorylation-dependent degradation of c-Myc is mediated by the F-box protein Fbw7. Embo J *23*, 2116-2125.

Yamashita, Y., Shimada, M., Harimoto, N., Rikimaru, T., Shirabe, K., Tanaka, S., and Sugimachi, K. (2003). Histone deacetylase inhibitor trichostatin A induces cell-cycle arrest/apoptosis and hepatocyte differentiation in human hepatoma cells. Int J Cancer *103*, 572-576.

Yang, W. M., Inouye, C., Zeng, Y., Bearss, D., and Seto, E. (1996). Transcriptional repression by YY1 is mediated by interaction with a mammalian homolog of the yeast global regulator RPD3. Proc Natl Acad Sci U S A *93*, 12845-12850.

Yang, W. M., Tsai, S. C., Wen, Y. D., Fejer, G., and Seto, E. (2002). Functional domains of histone deacetylase-3. J Biol Chem *277*, 9447-9454.

Yang, X. J., and Seto, E. (2007). HATs and HDACs: from structure, function and regulation to novel strategies for therapy and prevention. Oncogene *26*, 5310-5318.

Ylisastigui, L., Archin, N. M., Lehrman, G., Bosch, R. J., and Margolis, D. M. (2004). Coaxing HIV-1 from resting CD4 T cells: histone deacetylase inhibition allows latent viral expression. Aids *18*, 1101-1108.

Yoo, C. B., and Jones, P. A. (2006). Epigenetic therapy of cancer: past, present and future. Nat Rev Drug Discov *5*, 37-50.

Yoshida, M., Kijima, M., Akita, M., and Beppu, T. (1990). Potent and specific inhibition of mammalian histone deacetylase both in vivo and in vitro by trichostatin A. J Biol Chem *265*, 17174-17179.

Yu, X. D., Wang, S. Y., Chen, G. A., Hou, C. M., Zhao, M., Hong, J. A., Nguyen, D. M., and Schrump, D. S. (2007). Apoptosis induced by depsipeptide FK228 coincides with inhibition of survival signaling in lung cancer cells. Cancer J *13*, 105-113.

Yuan, Z. L., Guan, Y. J., Chatterjee, D., and Chin, Y. E. (2005). Stat3 dimerization regulated by reversible acetylation of a single lysine residue. Science *307*, 269-273.

Zamir, I., Harding, H. P., Atkins, G. B., Horlein, A., Glass, C. K., Rosenfeld, M. G., and Lazar, M. A. (1996). A nuclear hormone receptor corepressor mediates transcriptional silencing by receptors with distinct repression domains. Mol Cell Biol *16*, 5458-5465.

BIBL. LONDON UNIV.

Zgouras, D., Becker, U., Loitsch, S., and Stein, J. (2004). Modulation of angiogenesis-related protein synthesis by valproic acid. Biochem Biophys Res Commun *316*, 693-697.
Zgouras, D., Wachtershauser, A., Frings, D., and Stein, J. (2003). Butyrate impairs intestinal tumor cell-induced angiogenesis by inhibiting HIF-1alpha nuclear translocation. Biochem Biophys Res Commun *300*, 832-838.

Zhang, H., Kobayashi, R., Galaktionov, K., and Beach, D. (1995). p19Skp1 and p45Skp2 are essential elements of the cyclin A-CDK2 S phase kinase. Cell *82*, 915-925.

Zhang, X. D., Gillespie, S. K., Borrow, J. M., and Hersey, P. (2004). The histone deacetylase inhibitor suberic bishydroxamate regulates the expression of multiple apoptotic mediators and induces mitochondria-dependent apoptosis of melanoma cells. Mol Cancer Ther *3*, 425-435.

Zhang, Y., Carr, T., Dimtchev, A., Zaer, N., Dritschilo, A., and Jung, M. (2007). Attenuated DNA damage repair by trichostatin A through BRCA1 suppression. Radiat Res *168*, 115-124.

Zielke, N., Querings, S., Grosskortenhaus, R., Reis, T., and Sprenger, F. (2006). Molecular dissection of the APC/C inhibitor Rca1 shows a novel F-box-dependent function. EMBO Rep *7*, 1266-1272.

Zong, W. X., Ditsworth, D., Bauer, D. E., Wang, Z. Q., and Thompson, C. B. (2004). Alkylating DNA damage stimulates a regulated form of necrotic cell death. Genes Dev *18*, 1272-1282.

Zong, W. X., and Thompson, C. B. (2006). Necrotic death as a cell fate. Genes Dev *20*, 1-15.